FACULTY OF SCIENCE
UNIVERSITY OF COPENHAGEN

The Effects of Interactions in Topological Quantum Systems

Peter Røhr Beresford Tunstall

Master's Thesis in Physics

Supervisor: Prof. Karsten Flensberg

Niels Bohr Institute

University of Copenhagen

Date: November 2, 2018

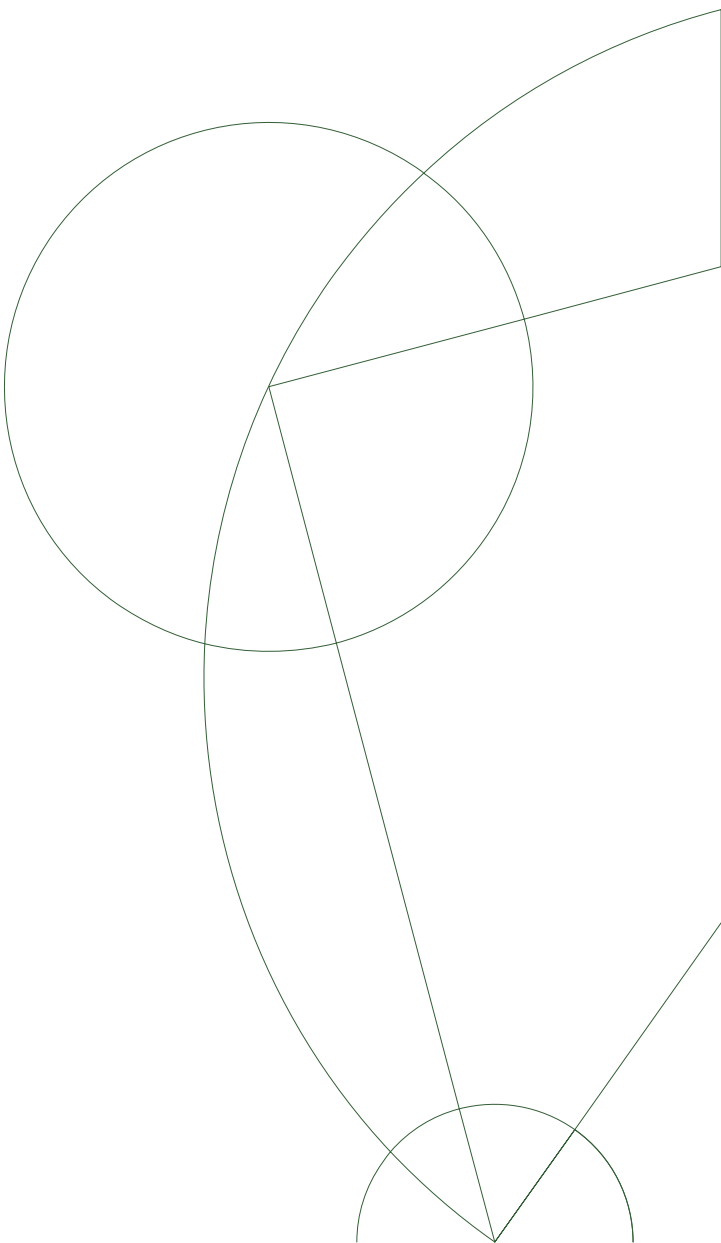

ABSTRACT

In this thesis, we review the process of translating the classification of non-interacting Topological Quantum Systems to the interacting case, by working with the Kitaev model for a 1D p-wave superconducting wire as an example. The model is introduced, the existence of boundary Majorana zero modes is demonstrated, and their properties are analysed using both the Hamiltonian and the Green's function. This analysis is performed analytically both at the symmetric point $\mu = 0, \Delta = t$, and with general parameters in an infinitely long wire. These findings were compared to the numerically computed results for a finite sized system. The concepts of symmetry classes, Topological Invariants and the Bulk-Boundary correspondence, are translated to interacting systems, where the full many-body Green's function is the key ingredient. The inclusion of two kinds of interactions is presented, namely bosonic charge fluctuations and a nearest neighbour repulsive electron-electron interaction. The bosonic interactions, resultant from coupling the wire to a capacitive gate, are included via a Perturbation Theory calculation, and a low order self-energy diagram is computed. The characteristics of the full local spectral function are investigated, where the imaginary part of the self-energy resulted in a broadening of the zero bias peaks, but the decay rate of the zero mode coherence into the bulk was unaffected. Motivated by recent literature, we consider a local two-body interaction between the electrons controlled by the interaction strength W. By a Jordan-Wigner transformation, the system is then mapped to an XYZ spin chain model, and parts of the phase diagram is explored for $\Delta = t$. The specific region of parameter space given by $\mu = \sqrt{(W+t)^2 - \Delta^2}$ defines an exactly solvable case, where the many-body ground state is calculated. For small chain sizes the ground state energies are compared with results from an Exact Diagonalization procedure, and they are shown to be a perfect match. A self-energy term in the perturbation theory is also calculated for this kind of interaction, and the local spectral function is determined numerically for various temperatures and interaction strengths. To make a connection with preceding calculations, the symmetry properties of the Green's function are shown to be preserved when adding interactions.

ACKNOWLEDGEMENTS

I would like to thank my supervisor Karsten Flensberg for being a great mentor throughout my thesis. His advice and help during the process has been much appreciated.
Thank you to the entire CMT group for the great company this last year, it has been a pleasure working side by side with you.
Mads Kruse, Abdurrahman Barzinji, Stefan Hasselgren and Marieke van Beest were incredibly generous with their time and patience in reading some of my thesis, and their corrections and feedback has been priceless.
To Mathias Nesheim, you have been a true brother in arms for the past ten years. Thank you for your unending reservoir of great spirit and good humour.
Special thanks to my treasured partner, in physics and everything else, Marieke van Beest. I cannot be grateful enough for her unyielding support and limitless love.
Lastly, I would like to thank my Grandpa, for buying me that first science book when I was 9.

CONTENTS

1

INTRODUCTION

In the recent decades of condensed matter research there has been a great effort to consolidate all knowledge about topological quantum phase transitions into a general classification scheme. This has resulted in a description of topological systems called *the ten-fold way*, where all non-interacting Hamiltonians fall into ten symmetry classes. This, together with the dimensionality of the system, determines the topological classification [28]. An example of such exotic phases is the Integer Quantum Hall Effect, where the transverse electrical conductance $\sigma_{xy} = \nu \frac{e^2}{h}$ is quantized in integer steps, ν being a topological invariant that cannot change by adiabatically changing the parameters of the system. In more recent studies the attention has been focused on generalising the free classification of topological quantum systems to cases where interactions and disorder are present [10][11][12][15]. The main difficulties and advances in such a mission will be the topic of this thesis. As a preamble to this analysis, some facts about topological systems, superconductivity and Interacting topological phases will be introduced.

The Landau theory of phase transitions is one of the hallmarks of condensed matter physics in the 20th century. It turned out that all phase transitions observed in nature, like water freezing to ice and metals acquiring magnetic ordering, could be described using one simple framework of spontaneous symmetry breaking [3]. What separates the different phases in these classical systems is a transition point in temperature T_c, below which the symmetries of the system are spontaneously broken and a corresponding order parameter acquires a non-zero value.

In addition to these normal phases of matter, there also exists quantum phases that are ordered states at zero temperature. For these systems the transition point is not at a critical temperature, but is instead determined by critical values of the parameters in the Hamiltonian. Topological phases cannot be described by any local order parameter, but are instead characterised by non-trivial bulk topological invariants, i.e. integer numbers that cannot be changed by continuously varying the parameters of the theory[17]. A topological phase is in this sense a phase that cannot be connected adiabatically to the trivial phase. Every phase will have its own topological number, and they are separated by topological phase transitions, at which the energy spectrum becomes gapless.

If one introduces a boundary in a system with non-trivial topology, there will be a state which lives on the boundary. The properties of this state is dependant on which system we consider, but they can include exotic attributes, such as fractional charges, non-Abelian exchange statistics etc., the existence of which has not been observed outside of condensed matter [1][21]. This is one of the reasons why the study of topological phases has become a focal point for modern research. The one-to-one relation between bulk topology and boundary excitations is called the *Bulk-Boundary correspondence*. Recent research suggests that this is one of the facts that will have to be modified in the presence of interactions [10]. A visualization of

a topological phase transition is shown in figure 1 together with an example of an imagined consequence when adding interactions.

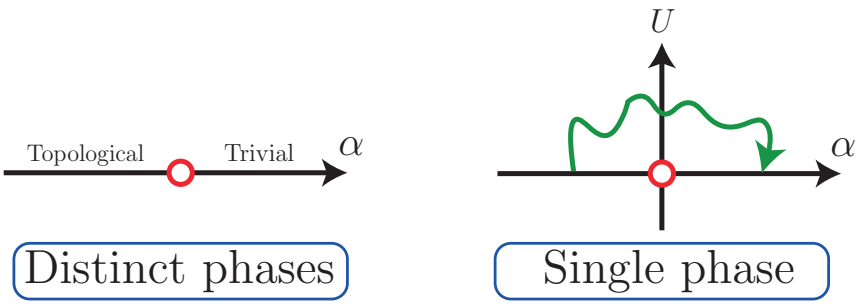

Figure 1: Illustration of some aspects of the topological phase transitions. A parameter of the system α is varied smoothly, but at the point shown as a red circle, the energy gap closes which marks the topological phase transition. The topological phase is thus different from the trivial phase. An imagined effect of adding interactions (shown on the right) by the adding new axis U, is that the two different phases can now be connected adiabatically, by changing the values along the green line in parameter space. Along this curve, there is no gap closing, and we then conclude that the two phases now become topologically equivalent.

In some condensed matter systems like superfluid or superconducting states, it is possible for fermions to condense and develop long-range correlations. In a Hamiltonian describing such a circumstance with bosonic or fermionic degrees of freedom, we can have anomalous quadratic terms in creation/annihilation operators of the form $c^\dagger c^\dagger$ and cc, which stem from a mean-field analysis. There, a quartic interaction (4 electron operators) has been reduced to a quadratic term by coupling the electrons to an auxiliary bosonic pairing field Δ[2]. Under the transition temperature T_c, this field will then condense to a non-zero value, where Δ is associated with the density of superconducting electrons and the size of the gap in the density of states. Electrons in this superconducting phase will form *Cooper pairs*, consisting of two time-reversed electrons that attract each other via quantum fluctuations of the crystal lattice called *Phonons*.

To solve the resulting system, assuming translational invariance, one introduces a quasi-particle momentum space operator $\alpha_{k\uparrow} = u_k c_{k\uparrow} + v_k c^\dagger_{-k\downarrow}$ defining the annihilation operator for the *Bogoliubon* particle, which is a superposition of an electron and a hole. Written in terms of these operators, the Hamiltonian is diagonal, and the many-body ground state is the vacuum of Bogoliubons $\alpha_{k\uparrow}|\psi_0\rangle = 0$. Now, one may ask, what happens if we combine the notions of topological quantum systems, with the theory of superconductivity?

A prime example of a topological superconductor, was proposed by Kitaev [19]. He considered a simple toy model for a 1D p-wave superconductor with spinless electrons, where the boundary excitations exhibit novel phenomena that are interesting from both theoretical and practical perspectives. The edge states in this system

are Bogoliubov type quasi-particles called Majorana zero modes, which are equal weight electron and hole $\gamma = c^\dagger + c$. In this sense, they are their own antiparticles, i.e. their 2nd quantized operators are Hermitian $\gamma = \gamma^\dagger$. The ground-state of the system spans a degenerate subspace, resulting in the Majoranas obeying non-Abelian exchange statistics. This means that the Berry phases picked up by exchange is not described by a number, but instead a matrix, thereby changing the wave-functions. This is a property that is hoped to be utilized in building a fault tolerant quantum computer, since a system of 4 or more Majoranas can define a Quantum bit [21]. The fact that the Majoranas are localized on the edges of a wire means that the information stored in both ends will be protected from local fluctuations.

Adding interactions may have several effects on these topological systems. They might enlarge a range in the phase diagram where topological order exists, or they might change the topological classification altogether as shown in figure 1. An important result in the research of topological quantum systems, where the effect of interactions was included, was shown by Fidkowski and Kitaev [11]. They showed that a system consisting of 8 Kitaev chains, with one Majorana per edge, all interacting with each other, exists in a phase that is connected to the trivial state. Thereby exhibiting a reduction of the topological classification from $\mathcal{Z}$ (integer) to $\mathcal{Z}_8$ (integers modulo 8). In order to tackle the problem of generalising results from non-interacting systems to the interacting counterparts, work must be done to translate concepts from one to the other. The description of symmetry classes, topological invariants, bulk-boundary correspondence etc. must consistently be translated from non-interacting to interacting cases, and this will be the main focus of this thesis. To make matters more concrete, we will work with the Kitaev model as a reference point in this inquiry.

The outline of this thesis is as follows. Chapter 2 introduces the non-interacting Kitaev chain with open boundary conditions and shows the existence of Majorana zero modes. Then concepts of momentum space topology of the closed translational invariant system is analysed, the symmetry class is determined and the Topological Invariant (TI) is calculated. After this, the exact zero modes will be found in the limit of an infinitely long wire, and then the full system will be diagonalized numerically. The Green's function (GF) of the Kitaev model is found, and used to show the relation between the Bogoliubov-De Gennes wavefunction and the local spectral function. Symmetry classes and TI's are then generalized to include interacting systems. Chapter 3 covers the inclusion of bosonic interactions in the Hamiltonian, motivated by an experimental realisation where the wire is coupled to a capacitive gate. Details of the development of a perturbation series is shown, and the full spectral function is then found using a low order self-energy diagram. In chapter 4 we instead include a nearest neighbour electron-electron interaction, and explore the phase-diagram described in recent literature[18][22][24]. Again, a self-energy diagram is calculated and inserted in the full spectral function, allowing us to see how the interactions affect the Majorana zero modes, and to compare symmetries of the GF with those found in chapter 2.

2

THE NON-INTERACTING KITAEV CHAIN

2.1 HAMILTONIAN DESCRIPTION

In this chapter we will investigate the Kitaev chain in the non-interacting case, and show that majorana zero modes exist on the edges of a 1D wire, when the system is in the topologically non-trivial phase [21]. The model describes spinless fermions, subject to nearest-neighbour hopping t and superconducting pairing Δ. The system has N sites, and is assumed to have open boundary conditions, for which the Hamiltonian is

$$H = -\mu \sum_{n=1}^{N} c_n^\dagger c_n - \frac{t}{2} \sum_{n=1}^{N-1} \left(c_n^\dagger c_{n+1} + c_{n+1}^\dagger c_n \right) + \frac{|\Delta|}{2} \sum_{n=1}^{N-1} \left(e^{i\varphi} c_n c_{n+1} + e^{-i\varphi} c_{n+1}^\dagger c_n^\dagger \right) \tag{2.1}$$

where $c_n^\dagger$ creates an electron at site n, μ is the chemical potential, t the hopping amplitude and $|\Delta| e^{i\varphi}$ is the superconducting pairing function. This can be assumed real, since the phase factor can be removed by the global gauge transformation $c_n \to c_n e^{-i\frac{\varphi}{2}}$, so the notation for the pairing function $|\Delta| \to \Delta$ will be used in further calculations. Interestingly, this Hamiltonian does not conserve the total particle number $F = \sum_n c_n^\dagger c_n$ due to the anomalous pairing term, $\left[H, c_n^\dagger c_n\right] \neq 0$, but parity, defined as total particle number F modulo 2, is a conserved quantity, i.e. $\left[H, (-1)^F\right] = 0$.

2.1.1 *Zero energy edge states*

To analyze the model described by the Hamiltonian in eq. (2.1) one can introduce the Majorana operators

$$\begin{aligned} \gamma_{A,n} &= \left(c_n^\dagger + c_n \right) & c_n &= \frac{1}{2} \left(\gamma_{A,n} + i\gamma_{B,n} \right) \\ \gamma_{B,n} &= i \left(c_n^\dagger - c_n \right) & c_n^\dagger &= \frac{1}{2} \left(\gamma_{A,n} - i\gamma_{B,n} \right) \end{aligned} \tag{2.2}$$

which is essentially a division of the electronic operators into their real and imaginary part. The γ operators obey the Majorana condition $\gamma_{\alpha,n} = \gamma_{\alpha,n}^\dagger$ and the anti-

commutator relation $\{\gamma_{\alpha,n}, \gamma_{\alpha',n'}\} = 2\delta_{\alpha,\alpha'}\delta_{n,n'}$. Inserting these into the Hamiltonian in eq. (2.1) yields

$$\begin{aligned} H = &-\frac{\mu}{4}\sum_{n=1}^{N}\left(\gamma_{A,n} - i\gamma_{B,n}\right)\left(\gamma_{A,n} + i\gamma_{B,n}\right) \\ &-\frac{t}{8}\sum_{n=1}^{N-1}\left[\left(\gamma_{A,n} - i\gamma_{B,n}\right)\left(\gamma_{A,n+1} + i\gamma_{B,n+1}\right) + \left(\gamma_{A,n+1} - i\gamma_{B,n+1}\right)\left(\gamma_{A,n} + i\gamma_{B,n}\right)\right] \\ &+\frac{\Delta}{8}\sum_{n=1}^{N-1}\left[\left(\gamma_{A,n} + i\gamma_{B,n}\right)\left(\gamma_{A,n+1} + i\gamma_{B,n+1}\right) + \left(\gamma_{A,n+1} - i\gamma_{B,n+1}\right)\left(\gamma_{A,n} - i\gamma_{B,n}\right)\right] \\ = &-\frac{\mu}{2}\sum_{n=1}^{N}\left(1 + i\gamma_{A,n}\gamma_{B,n}\right) - \frac{i}{4}\sum_{n=1}^{N-1}\left[\left(t+\Delta\right)\gamma_{A,n+1}\gamma_{B,n} + \left(t-\Delta\right)\gamma_{A,n}\gamma_{B,n+1}\right] \end{aligned} \tag{2.3}$$

Were the anti-commutation relation is used to commute Majorana operators, and to conclude $\gamma_{\alpha,n}^2 = 1$. In the case $\mu < 0, \Delta = t = 0$, there is only coupling between Majoranas on the same site, so the system is fully dimerized as depicted in the top of figure 2. In this case, the many-body ground state (GS) will just be the vacuum of fermions $|\psi\rangle = |0\rangle$. The system is in the trivial phase, and has a gap of size $|\mu|$ corresponding to the energy cost of adding an electron. Another simple case, though more interesting, is the *symmetric point* with $\mu = 0, \Delta = t$, where the Hamiltonian greatly reduces to

$$H = \frac{it}{2}\sum_{n=1}^{N-1}\gamma_{B,n}\gamma_{A,n+1} \tag{2.4}$$

Which indicates that $\gamma_{B,n}$ is coupled to $\gamma_{A,n+1}$ as shown in figure 2.

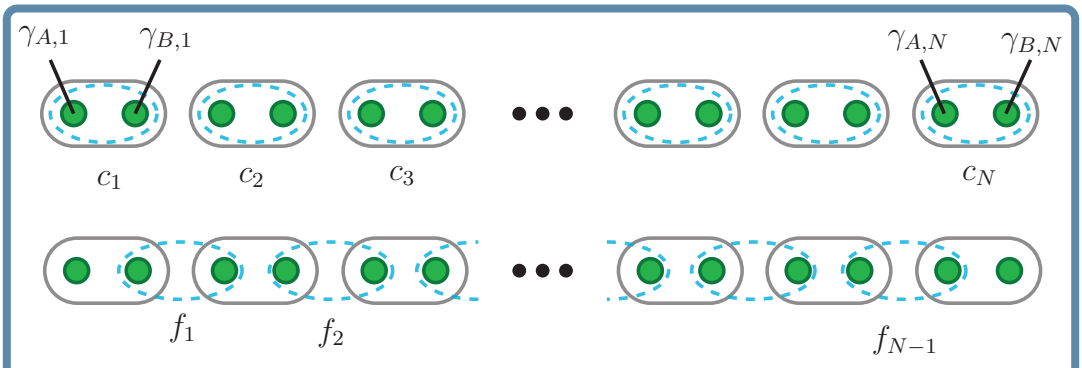

Figure 2: Sketch of the two different couplings for the Majorana operators $c_n = \frac{1}{2}\left(\gamma_{A,n} + i\gamma_{B,n}\right)$ where Majoranas on the same site are combined and $f_n = \frac{1}{2}\left(\gamma_{B,n} + i\gamma_{A,n+1}\right)$ where adjacent Majoranas are combined. In the last case, two uncoupled Majoranas $\gamma_{A,1}$ and $\gamma_{B,N}$ live at each edge.

Before in eq. (2.2), fermions were split into Majorana operators on the same site. If one now combines fermions on adjacent sites by writing new electron annihilation

operators as $f_n = \frac{1}{2}\left(\gamma_{B,n} + i\gamma_{A,n+1}\right) = \frac{i}{2}\left(c_n^\dagger - c_n + c_{n+1}^\dagger + c_{n+1}\right)$ the Hamiltonian then becomes

$$\begin{aligned} H &= \frac{it}{2}\sum_{n=1}^{N-1}(f_n^\dagger + f_n)i(f_n^\dagger - f_n) \\ &= t\sum_{n=1}^{N-1}\left(f_n^\dagger f_n - \frac{1}{2}\right) \end{aligned} \tag{2.5}$$

Which is diagonal in this basis, and shows the bulk gap of the system. The GS of the system $|\psi\rangle$ is the vacuum determined by the f_n operators, i.e. the state obeying $f_n|\psi\rangle = 0$. Two wavefunctions obey this criteria, and they can be written as [14]

$$|\psi_\pm\rangle = \frac{1}{\sqrt{2^N}}\prod_n^N\left(1 \pm c_n^\dagger\right)|0\rangle = \frac{1}{\sqrt{2^N}}\left(1 \pm c_1^\dagger\right)\left(1 \pm c_2^\dagger\right)\cdots\left(1 \pm c_N^\dagger\right)|0\rangle \tag{2.6}$$

Where $|0\rangle$ defines the vacuum of the original fermion operators, $c_n|0\rangle = 0$. These states are degenerate $E_+ = \langle\psi_+|H|\psi_+\rangle = E_- = \langle\psi_-|H|\psi_-\rangle$ for open boundary conditions. Exited states are then obtained by applying the creation operator repeatedly $f_n^\dagger|\psi_\pm\rangle$. We can combine $|\psi_+\rangle$ and $|\psi_-\rangle$ to new GSs of even and odd parity, i.e. even and odd number of fermionic operators

$$\begin{aligned} |\psi_{even}\rangle &= \frac{1}{\sqrt{2}}\left(|\psi_+\rangle + |\psi_-\rangle\right) \\ |\psi_{odd}\rangle &= \frac{1}{\sqrt{2}}\left(|\psi_+\rangle - |\psi_-\rangle\right) \end{aligned} \tag{2.7}$$

These states describe the degenerate ground-state, with two states of opposite parity, which is unique to the topological phase. What is interesting about the Hamiltonian (2.5) is that the last link $f_N^\dagger f_N$ does not appear due to the boundary conditions (had they been periodic, for example by considering a Kitaev ring, this term would enter the Hamiltonian). Looking at eq. 2.4 one finds that $\gamma_{A,1}$ and $\gamma_{B,N}$ are nowhere to be seen, so these describe zero energy Majorana modes situated at the end of the chain. These highly non-local MFs combine to give the fermionic operator $f_N = \frac{1}{2}\left(\gamma_{A,1} + i\gamma_{B,N}\right) = \frac{1}{2}\left(c_1^\dagger + c_1 + c_N - c_N^\dagger\right)$, which can be occupied at zero energy cost, resulting in a double degeneracy of all states. The f_N and $f_N^\dagger$ transform between the states in the degenerate subspace spanned by the GSs

$$f_N|\psi_{even}\rangle = 0 \qquad\qquad f_N^\dagger|\psi_{even}\rangle = |\psi_{odd}\rangle \tag{2.8}$$

And the occupancy of the fermion defined by the edge Majoranas has eigenvalues

$$\begin{aligned} &f_N^\dagger f_N|\psi_{even}\rangle = 0 \\ &f_N^\dagger f_N|\psi_{odd}\rangle = f_N^\dagger f_N f_N^\dagger|\psi_{even}\rangle = f_N^\dagger\left(1 - f_N^\dagger f_N\right)|\psi_{even}\rangle = f_N^\dagger|\psi_{even}\rangle = |\psi_{odd}\rangle \end{aligned} \tag{2.9}$$

So $0 \vee 1$ if the state is unoccupied or occupied respectively. The Majorana modes commute with the Hamiltonian $[H, \gamma_{A,1}] = [H, \gamma_{B,N}] = 0$, which ensures they have trivial dynamics, since $\dot{\gamma} = i\,[H, \gamma]$. Having a system of many MFs further increases

the degeneracy of the ground-state, and as previously mentioned, these Majoranas obey non-Abelian exchange statistics. A multitude of these Majorana pairs can ideally be used as topologically protected qubits. In a more realistic model with $\mu \neq 0$ and $t \neq \Delta$ the MFs still exist, but have an exponential overlap into the bulk, so if two MFs come into close proximity they will combine and form an ordinary fermion. The real space wavefunction of the zero energy edge modes is found in section 2.1.4.

2.1.2 *The Kitaev model in momentum space*

We can examine some further properties of the 1D chain by transforming the Hamiltonian in eq. (2.1) to a momentum space representation. Here, a translational invariant system without edges is examined (and therefore no localized zero modes), but one can still investigate the bulk behaviour of the system, and discuss the concept of bulk TIs. The transformation to k-space is performed by using

$$c_n = \frac{1}{\sqrt{N}} \sum_k e^{ikn} c_k \qquad c_n^\dagger = \frac{1}{\sqrt{N}} \sum_k e^{-ikn} c_k^\dagger \qquad \frac{1}{N} \sum_{n=1}^{N} e^{i(k'-k)n} = \delta_{k'k} \tag{2.10}$$

Where the interatomic distance $a = 1$ is used throughout this thesis, for notational convenience. Performing the transformation gives the Kitaev Hamiltonian on following form

$$H = -\mu \sum_k c_k^\dagger c_k - \sum_k t \cos k \; c_k^\dagger c_k + \frac{\Delta}{2} \sum_k \left(c_{-k} c_k e^{ik} + c_k^\dagger c_{-k}^\dagger e^{-ik} \right) \tag{2.11}$$

Which can be written in the usual Bogoliubov-de Gennes (BDG) form

$$H = \frac{1}{2} \sum_k (C^\dagger)_k^\alpha \mathcal{H}^{\alpha\beta}(k) \; C_k^\beta \;, \qquad \mathcal{H}^{\alpha\beta}(k) = \xi_k \tau_z^{\alpha\beta} + \Delta \sin k \; \tau_y^{\alpha\beta} \doteq \begin{pmatrix} \xi_k & \Delta_k \\ \Delta_k^* & -\xi_k \end{pmatrix} \tag{2.12}$$

Where α, β are Nambu space indices, which throughout this thesis will be summed when repeated. The symbol $\doteq$ will be used for when an expression is represented by a matrix. We have the energy $\xi_k = -t \cos k - \mu$, the pairing function $\Delta_k = -i\Delta \sin k$, the annihilation Nambu spinor $C_k^\alpha \doteq \begin{pmatrix} c_k & c_{-k}^\dagger \end{pmatrix}^T$, and the τ operators are Pauli matrices that act on particle-hole space. The factor $\frac{1}{2}$ is due to double counting. The sine functions in the off-diagonal terms come from the fact that $c_{-k} c_k$ is anti-symmetric under $k \to -k$, so only the anti-symmetric part of e^{ik} remains when summing over all momenta k. This Hamiltonian is in a quadratic form and can be diagonalized by a Bogoliubov transformation. This is essentially a change of basis of the creation and annihilation operators, which preserves anti-commutation relations, $\lambda_k = u_k c_k + v_k c_{-k}^\dagger$, and can be constructed so as to diagonalize the Hamiltonian. The physical meaning is that this new basis describes creation (annihilation) of so-called

quasi-particle *Bogoliubons*. A choice can now be made that $u_k = u_{-k}$ together with $v_{-k} = -v_k$. We introduce the unitary transformation matrix U, with property

$$\begin{aligned}(U^\dagger)^{\alpha\beta} &\doteq \begin{pmatrix} u_k & v_k \\ v_{-k}^* & u_{-k}^* \end{pmatrix} = \begin{pmatrix} u_k & v_k \\ -v_k^* & u_k^* \end{pmatrix} \\ U^{\alpha\beta}\,(U^\dagger)^{\beta\lambda} &\doteq \begin{pmatrix} u_k^* & -v_k \\ v_k^* & u_k \end{pmatrix} \begin{pmatrix} u_k & v_k \\ -v_k^* & u_k^* \end{pmatrix} = \begin{pmatrix} |u_k|^2 + |v_k|^2 & 0 \\ 0 & |u_k|^2 + |v_k|^2 \end{pmatrix}\end{aligned} \tag{2.13}$$

So the unitarity condition $U^{\alpha\beta}\,(U^\dagger)^{\beta\lambda} = \delta^{\alpha\lambda}$, translates to the condition $|u_k|^2 + |v_k|^2 = 1$. The u_k and v_k obey the BDG equation

$$\begin{pmatrix} \xi_k & \Delta_k \\ \Delta_k^* & -\xi_k \end{pmatrix} \begin{pmatrix} u_k^* \\ v_k^* \end{pmatrix} = E_k \begin{pmatrix} u_k^* \\ v_k^* \end{pmatrix} \tag{2.14}$$

Allowing us to determine relations for the *coherence functions* u_k and v_k. The bulk-momentum space Hamiltonian $\mathcal{H}(k)$ obeys a Particle-Hole symmetry expressed as

$$\Xi\mathcal{H}(k)\Xi^{-1} = -\mathcal{H}(-k) \qquad\qquad \Xi = \tau_x K \tag{2.15}$$

With K being the operation of complex conjugation. This essentially means that for every state $|\psi(k)\rangle$ with energy E_k there exists another state $\Xi|\psi(-k)\rangle$ with $-E_k$ since

$$\mathcal{H}(k)\Xi|\psi(-k)\rangle = -\Xi\mathcal{H}(-k)|\psi(-k)\rangle = -E_{-k}\Xi|\psi(-k)\rangle = -E_k\Xi|\psi(-k)\rangle \tag{2.16}$$

Where the symmetry of the quasi-particle spectrum $E_k = E_{-k}$ is used. Inserting the eigenstate from (2.14), the BDG equation for the PH transformed state is

$$\mathcal{H}(k)\tau_x K \begin{pmatrix} u_{-k}^* \\ v_{-k}^* \end{pmatrix} = \begin{pmatrix} \xi_k & \Delta_k \\ \Delta_k^* & -\xi_k \end{pmatrix} \begin{pmatrix} -v_k \\ u_k \end{pmatrix} = -E_k \begin{pmatrix} -v_k \\ u_k \end{pmatrix} \tag{2.17}$$

Which shows the relation

$$v_k = -\left(\frac{E_k - \xi_k}{\Delta_k}\right) u_k \tag{2.18}$$

With the properties $u_k^* = u_k$ and $v_k^* = -v_k$. Inserting a unit matrix in the Hamiltonian written in terms of U and $U^\dagger$ allows us then to bring $\mathcal{H}^{\alpha\beta}(k)$ into diagonal form

$$H = \frac{1}{2}\sum_k \underbrace{(C^\dagger)_k^\alpha U^{\alpha\beta}}_{(\Lambda^\dagger)_k^\beta} \underbrace{(U^\dagger)^{\beta\lambda}\,\mathcal{H}^{\lambda\rho}(k)\,U^{\rho\sigma}}_{\tilde{\mathcal{H}}^{\beta\sigma}(k)} \underbrace{(U^\dagger)^{\sigma\nu} C_k^\nu}_{\Lambda_k^\sigma}, \qquad \tilde{\mathcal{H}}^{\alpha\beta}(k) \doteq \begin{pmatrix} E_k & 0 \\ 0 & -E_k \end{pmatrix} \tag{2.19}$$

Where the new particle-hole spinors are

$$\Lambda_k^\sigma \doteq \begin{pmatrix} \lambda_k \\ \lambda_{-k}^\dagger \end{pmatrix} = \begin{pmatrix} u_k & v_k \\ v_k & u_k \end{pmatrix} \begin{pmatrix} c_k \\ c_{-k}^\dagger \end{pmatrix} = \begin{pmatrix} u_k c_k + v_k c_{-k}^\dagger \\ v_k c_k + u_k c_{-k}^\dagger \end{pmatrix} \tag{2.20}$$

And E_k is the energy spectrum of $\mathcal{H}(k)$, found to be

$$E_k = \pm\sqrt{\xi_k^2 + |\Delta_k|^2} \tag{2.21}$$

This spectrum is plotted in figure 3 for various values of μ with fixed t, Δ. At $|t| = \mu$ the spectrum becomes gapless at $|k| = \pi$, and in section 2.1.3 we will see that this topological phase transition point separates two phases with different topological indices. Parameters will be measured in units of the hopping parameter t throughout this thesis.

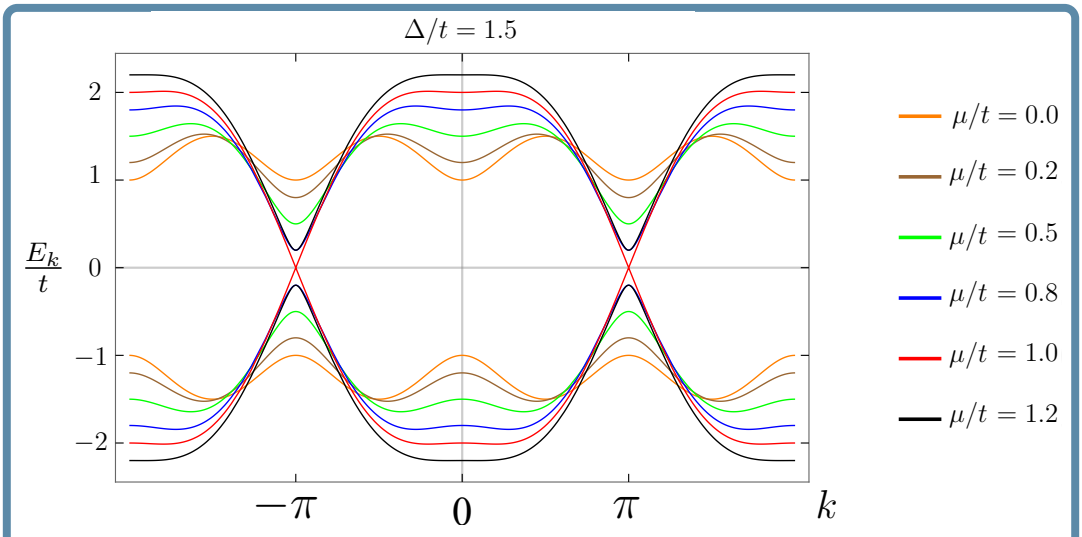

Figure 3: Plot of the quasi-particle energy spectrum E_k found in (2.21), in units of t, for fixed t, Δ and varying μ. As μ increases one observes a gap closing at $k = \pm\pi$, and $\mu = t$ marks the existence of a topological phase transition at this point in parameter space.

We can rewrite the equation for the transformed bulk momentum space Hamiltonian, to get expressions relating the Bogoliubon energies E_k, the energies ξ_k, and the functions u_k and v_k. This is done by using the unitarity of $U^{\alpha\beta}$

$$U^{\alpha\beta}\,\tilde{\mathcal{H}}^{\beta\lambda}(k)\,(U^\dagger)^{\lambda\rho} = \mathcal{H}^{\alpha\rho}(k) \tag{2.22}$$

Calculating the left side of the equation yields

$$\begin{pmatrix} E_k\left(u_k^2 - |v_k|^2\right) & 2E_k u_k v_k \\ -2E_k u_k v_k & -E_k\left(u_k^2 - |v_k|^2\right) \end{pmatrix} = \begin{pmatrix} \xi_k & \Delta_k \\ \Delta_k^* & -\xi_k \end{pmatrix} \tag{2.23}$$

Giving us the equations

$$\begin{aligned} \xi_k &= E_k\left(u_k^2 - |v_k|^2\right) \\ \Delta_k &= 2E_k u_k v_k \end{aligned} \tag{2.24}$$

Which together with the unitarity condition $u_k^2 + |v_k|^2 = 1$, allows us to calculate u_k from the first equation

$$\xi_k = E_k \left(2u_k^2 - 1\right) \leftrightarrow u_k = \sqrt{\frac{E_k + \xi_k}{2E_k}} \tag{2.25}$$

Combining this with (2.18) one can check that the 2nd equation in (2.24) is also solved

$$\begin{aligned} 2E_k u_k v_k &= -2E_k u_k^2 \left(\frac{E_k - \xi_k}{\Delta_k}\right) = -2E_k \left(\frac{E_k - \xi_k}{2E_k}\right)\left(\frac{E_k + \xi_k}{\Delta_k}\right) \\ &= -\frac{E_k^2 - \xi_k^2}{\Delta_k} = -\frac{|\Delta_k|^2}{\Delta_k} = -\frac{\Delta^2 \sin^2 k}{-i\Delta \sin k} = \Delta_k \checkmark \end{aligned} \tag{2.26}$$

v_k can now be calculated

$$\begin{aligned} v_k &= -\left(\frac{E_k - \xi_k}{\Delta_k}\right) u_k = -\frac{|\Delta_k|}{\Delta_k}\left(\frac{E_k - \xi_k}{|\Delta_k|}\right)\sqrt{\frac{E_k + \xi_k}{2E_k}} = -\frac{|\Delta_k|}{\Delta_k}\sqrt{\left(\frac{E_k - \xi_k}{|\Delta_k|}\right)^2 \frac{E_k + \xi_k}{2E_k}} \\ &= -\frac{\Delta \sin k}{-i\Delta \sin k}\sqrt{\frac{E_k^2 - \xi_k^2}{|\Delta_k|^2} \cdot \frac{E_k - \xi_k}{2E_k}} = \frac{\Delta_k}{|\Delta_k|}\sqrt{\frac{E_k - \xi_k}{2E_k}} \end{aligned} \tag{2.27}$$

Where the prefactor on v_k ensures that $v_{-k} = -v_k$ since $\Delta_k = -\Delta_{-k}$. In conclusion

$$u_k = \sqrt{\frac{E_k + \xi_k}{2E_k}}\,, \qquad v_k = \frac{\Delta_k}{|\Delta_k|}\sqrt{\frac{E_k - \xi_k}{2E_k}} \tag{2.28}$$

These two functions are plotted in figure 26 in Appendix A.1 for various values of μ. In this form the Hamiltonian becomes

$$\begin{aligned} H &= \frac{1}{2}\sum_k (\Lambda^\dagger)_k^\alpha \, \tilde{\mathcal{H}}^{\alpha\beta}(k) \, \Lambda_k^\beta = \frac{1}{2}\sum_k \begin{pmatrix} \lambda_k^\dagger & \lambda_{-k} \end{pmatrix} \begin{pmatrix} E_k & 0 \\ 0 & -E_k \end{pmatrix} \begin{pmatrix} \lambda_k \\ \lambda_{-k}^\dagger \end{pmatrix} \\ &= \sum_k E_k \lambda_k^\dagger \lambda_k + \text{const.} \end{aligned} \tag{2.29}$$

Completing the diagonalization. In Appendix A.2 the normalised many-body GS wavefunction is found, corresponding to the vacuum of Bogoliubons

$$\lambda_k |\Psi\rangle = 0\,, \qquad |\Psi\rangle = \prod_{k>0} \left(u_k + v_k c_{-k}^\dagger c_k^\dagger\right)|0\rangle \tag{2.30}$$

2.1.3 *Topological invariant*

The Kitaev Hamiltonian in eq. (2.12) possesses symmetries that enable us to find the *Altland-Zirnbauer* or *Cartan* symmetry class. The three symmetries of interest are time-reversal (TR) Θ, particle-hole (PH) Ξ and the combination of the two, known as chiral symmetry (C) $\Pi = \Xi\Theta$. The squares of these operators determine the symmetry

class of the system. This information, together with the dimensionality of the system, allows one to find the topological classification [28]. The three symmetries act on the bulk-momentum-space Hamiltonian as

$$\begin{aligned}\Theta\mathcal{H}(k)\Theta^{-1} &= \quad \mathcal{H}(-k)\\ \Xi\mathcal{H}(k)\Xi^{-1} &= -\mathcal{H}(-k)\\ \Pi\mathcal{H}(k)\Pi^{-1} &= -\mathcal{H}(k)\end{aligned} \tag{2.31}$$

In this case, the Hamiltonian (2.12), has generalised TR symmetry $\Theta = K$, PH symmetry $\Xi = \tau_x K$ and C symmetry $\Pi = \Xi\Theta = \tau_x$, where again K is the complex conjugation operation. We can check if the Kitaev Hamiltonian obeys (2.31)

$$\begin{aligned}\Theta\mathcal{H}(k)\Theta^{-1} &= K\left(\xi_k\tau_z + \Delta\sin k\ \tau_y\right)K = \left(\xi_k\tau_z - \Delta\sin k\ \tau_y\right) = \mathcal{H}(-k)\\ \Xi\mathcal{H}(k)\Xi^{-1} &= \tau_x K\left(\xi_k\tau_z + \Delta\sin k\ \tau_y\right)\tau_x K\\ &= \tau_x\left(\xi_k\tau_z - \Delta\sin k\ \tau_y\right)\tau_x = \left(-\xi_k\tau_z + \Delta\sin k\ \tau_y\right) = -\mathcal{H}(-k)\\ \Pi\mathcal{H}(k)\Pi^{-1} &= \tau_x\left(\xi_k\tau_z + \Delta\sin k\ \tau_y\right)\tau_x = \left(-\xi_k\tau_z - \Delta\sin k\ \tau_y\right) = -\mathcal{H}(k)\end{aligned} \tag{2.32}$$

Where the properties $\xi_{-k} = \xi_k$, and $\tau_i\tau_j\tau_i = -\tau_j$ if $i \neq j$ has been used. Since $\Theta^2 = 1$, $\Xi^2 = 1$, $\Pi^2 = 1$, this model belongs to symmetry class BDI, which in $1D$ has a topological classification described by a $\mathcal{Z}$ TI. The value of the TI determines the number of boundary excitations, and since a $\mathcal{Z}$ invariant can be any integer, there can exist any number of Majoranas on the boundaries between topological and trivial phases. If one allowed Δ to be complex, one would instead have

$$\begin{aligned}\mathcal{H}^{\alpha\beta}(k) &\doteq \begin{pmatrix}\xi_k & -i|\Delta|\sin k\ e^{-i\varphi}\\ i|\Delta|\sin k\ e^{i\varphi} & -\xi_k\end{pmatrix}\\ &= \xi_k\tau_z^{\alpha\beta} + |\Delta|\sin k\cos\varphi\ \tau_y^{\alpha\beta} - |\Delta|\sin k\sin\varphi\ \tau_x^{\alpha\beta}\end{aligned} \tag{2.33}$$

The addition of a τ_x term odd in k in the bulk-momentum-space Hamiltonian has the result of breaking generalised time-reversal Θ and chiral symmetry Π, but not PH symmetry Ξ

$$\begin{aligned}\Xi\mathcal{H}(k)\Xi^{-1} &= \tau_x K\left(\xi_k\tau_z + |\Delta|\sin k\cos\varphi\ \tau_y - |\Delta|\sin k\sin\varphi\ \tau_x\right)\tau_x K\\ &= \tau_x\left(\xi_k\tau_z - |\Delta|\sin k\cos\varphi\ \tau_y - |\Delta|\sin k\sin\varphi\ \tau_x\right)\tau_x\\ &= \left(-\xi_k\tau_z + |\Delta|\sin k\cos\varphi\ \tau_y - |\Delta|\sin k\sin\varphi\ \tau_x\right) = -\mathcal{H}(-k)\end{aligned} \tag{2.34}$$

Which corresponds to symmetry class D with a $\mathcal{Z}_2$ index for $1D$ systems. A $\mathcal{Z}_2$ index is binary, resulting in only one Majorana on each boundary, which is what happens in realistic systems.

We now want to define a TI for our system from the bulk Hamiltonian, which for a non-trivial case will exhibit Zero modes on the boundary to other phases. To define this invariant number, the Hamiltonian $\mathcal{H}(k)$ can be transformed into the

Majorana basis. In real space, the Majorana condition is $\gamma_x = \gamma_x^\dagger$, and one can find the momentum space version of this by evaluating

$$\begin{aligned} \gamma_x &= \frac{1}{\sqrt{N}} \sum_k \gamma_k e^{ikx} \\ \gamma_x^\dagger = \frac{1}{\sqrt{N}} \sum_k \gamma_k^\dagger e^{-ikx} &\underset{k\to -k}{=} \frac{1}{\sqrt{N}} \sum_k \gamma_{-k}^\dagger e^{ikx} \end{aligned} \tag{2.35}$$

by comparison one sees that the Majorana condition in k-space is $\gamma_k = \gamma_{-k}^\dagger$. The following k-space Majorana operators are now introduced

$$\begin{aligned} \gamma_{A,k} &= \quad c_{-k}^\dagger + c_k & c_k &= \frac{1}{2}\left(\gamma_{A,k} + i\gamma_{B,k}\right) \\ \gamma_{B,k} &= i\left(c_{-k}^\dagger - c_k\right) & c_{-k}^\dagger &= \frac{1}{2}\left(\gamma_{A,k} - i\gamma_{B,k}\right) \end{aligned} \tag{2.36}$$

From which we see that the particle-hole spinors C_k^α and $(C^\dagger)_k^\alpha$ transform as

$$\begin{aligned} C_k^\alpha \doteq \begin{pmatrix} c_k \\ c_{-k}^\dagger \end{pmatrix} &= \underbrace{\frac{1}{2}\begin{pmatrix} 1 & i \\ 1 & -i \end{pmatrix}}_{\tilde{U}^{\alpha\beta}} \underbrace{\begin{pmatrix} \gamma_{A,k} \\ \gamma_{B,k} \end{pmatrix}}_{\Gamma_k^\beta} \\ (C^\dagger)_k^\alpha \doteq \begin{pmatrix} c_k^\dagger & c_{-k} \end{pmatrix} &= \underbrace{\begin{pmatrix} \gamma_{A,-k} & \gamma_{B,-k} \end{pmatrix}}_{\Gamma_{-k}^\beta} \underbrace{\frac{1}{2}\begin{pmatrix} 1 & 1 \\ -i & i \end{pmatrix}}_{(\tilde{U}^\dagger)^{\beta\alpha}} \end{aligned} \tag{2.37}$$

Where $\Gamma_{-k}^T = \Gamma_k^\dagger$ is seen from the Majorana condition for γ. In this basis, the Hamiltonian becomes

$$H = \frac{1}{2}\sum_k (C^\dagger)_k^\alpha \, \mathcal{H}^{\alpha\beta}(k) \, C_k^\beta = \frac{i}{2}\sum_k \Gamma_{-k}^\sigma \, \chi^{\sigma\rho}(k) \, \Gamma_k^\rho \,, \quad i\chi^{\sigma\rho}(k) = (\tilde{U}^\dagger)^{\sigma\alpha} \, \mathcal{H}^{\alpha\beta}(k) \, \tilde{U}^{\beta\rho} \tag{2.38}$$

So the Majorana basis Hamiltonian is described by the skew-symmetric matrix $\chi(k)$

$$\chi^{\sigma\rho}(k) \doteq (-i)\frac{1}{2}\begin{pmatrix} 1 & 1 \\ -i & i \end{pmatrix}\begin{pmatrix} \xi_k & \Delta_k \\ \Delta_k^* & -\xi_k \end{pmatrix}\frac{1}{2}\begin{pmatrix} 1 & i \\ 1 & -i \end{pmatrix} = \frac{1}{2}\begin{pmatrix} 0 & \xi_k - \Delta_k \\ -(\xi_k + \Delta_k) & 0 \end{pmatrix} \tag{2.39}$$

Kitaev showed that one can assign a TI to this model, described by the Pfaffian of $\chi(k)$ at the time-reversal invariant momenta points $k = 0, \pi$, given by [7]

$$W = \operatorname{sgn}\left(\operatorname{Pf}\left[\chi(0)\right]\operatorname{Pf}\left[\chi(\pi)\right]\right) \tag{2.40}$$

If one uses the fact that

$$A = \begin{pmatrix} 0 & a \\ -a & 0 \end{pmatrix}, \qquad \operatorname{Pf}\left[A\right] = a \tag{2.41}$$

And

$$\chi(0) = \frac{1}{2}\begin{pmatrix} 0 & -(t+\mu) \\ t+\mu & 0 \end{pmatrix} \qquad \chi(\pi) = \frac{1}{2}\begin{pmatrix} 0 & t-\mu \\ -(t-\mu) & 0 \end{pmatrix} \tag{2.42}$$

One obtains

$$W = \operatorname{sgn}\left(-\frac{1}{4}(t+\mu)(t-\mu)\right) = \begin{cases} -1 & |t| > |\mu| \\ 1 & |t| < |\mu| \end{cases} \tag{2.43}$$

Where $W = -1$ marks the topological phase [7]. An example of this phase was the symmetric point discussed in section 2.1.1, where $\mu = 0$ and $t = \Delta$. Here we saw that isolated Majorana zero modes existed on the edges of the wire. The edges separate the topologically trivial phase of the vacuum with the topological phase of the wire. Another example of being in the topological phase is calculated in Appendix B, for a slightly more general case with parameters $\mu = 0, t \neq \Delta$. The next section contains a calculation of the exact zero modes wave function in the limit of an infinite sized wire, the form of which was mentioned in Kitaev's original paper [19]. The similarity between this analytically determined wavefunction and the one found numerically for a finite wire, is striking and will be shown in section 2.1.5.

2.1.4 *Exact edge state wavefunctions in continuous real space*

We can find the exact zero mode WF for an infinite chain by starting with the bulk-momentum space Hamiltonian

$$\mathcal{H}(k) = (-\mu - t\cos k)\tau_z + \Delta \sin k\ \tau_y \tag{2.44}$$

We assume that the zero energy edge state WF will be of the form of a constant PH spinor multiplied by a decaying exponential function

$$\psi_0(x) \propto \begin{pmatrix} u \\ v \end{pmatrix} e^{-qx} \tag{2.45}$$

corresponding to a plane wave $\psi(x) = e^{-ikx}$ with imaginary momentum $k = -iq$. We can now replace $k \to -iq$ in the Hamiltonian and solve for the q-value that leads to zero energy

$$\mathcal{H}(q) = (-\mu - t\cosh q)\tau_z - i\Delta \sinh q\ \tau_y \tag{2.46}$$

This amounts to solving the equation for the quasi-particle spectrum 2.21 for q at zero energy, i.e. $E_q = 0$

$$\begin{aligned} E_q &= \pm\sqrt{(-\mu - t\cosh q)^2 + (-i\Delta\sinh q)^2} = 0 \\ &\updownarrow \\ &(-\mu - t\cosh q)^2 + (-i\Delta\sinh q)^2 = 0 \\ &\updownarrow \\ &(t\cosh q + \mu)^2 = (\Delta\sinh q)^2 \\ &\updownarrow \\ &t\cosh q + \mu = \pm\Delta\sinh q \end{aligned} \tag{2.47}$$

So there are two different solutions, one for q and one for $-q$. Starting with the positive solution, one gets

$$\begin{aligned} &\frac{t}{2}\left(e^q + e^{-q}\right) + \mu = \frac{\Delta}{2}\left(e^q - e^{-q}\right) \\ &\updownarrow \\ &t\left(1 + e^{-2q}\right) + 2\mu e^{-q} = \Delta\left(1 - e^{-2q}\right) \\ &\updownarrow \\ &(t+\Delta)\,e^{-2q} + 2\mu e^{-q} + t - \Delta = 0 \\ &\updownarrow \\ &e^{-q} = \frac{-\mu \pm \sqrt{\mu^2 - t^2 + \Delta^2}}{t+\Delta} = \rho_\pm \end{aligned} \tag{2.48}$$

So the exponential function becomes $e^{-qx} = \rho_\pm^x$. Now the spinor corresponding to this solution makes $\tau_z - i\tau_y$ vanish

$$\begin{pmatrix} 1 & -1 \\ 1 & -1 \end{pmatrix}\begin{pmatrix} u \\ v \end{pmatrix} = \underline{0} \rightarrow \begin{pmatrix} u \\ v \end{pmatrix} = \begin{pmatrix} 1 \\ 1 \end{pmatrix} \tag{2.49}$$

So one solution for the edgestate WF is

$$\psi_0'(x) = \mathcal{N}'\begin{pmatrix} 1 \\ 1 \end{pmatrix}\left(\alpha_+'\rho_+^x + \alpha_-'\rho_-^x\right) \tag{2.50}$$

with boundary condition $\psi_0'(0) = 0 \rightarrow \alpha_+' + \alpha_-' = 0$, and normalisation $\mathcal{N}'$. The normalisation using $\alpha_+' = 1, \alpha_-' = -1$ is found[1] to be

$$\begin{aligned} \sum_{x=0}^{\infty}\psi_0'^{\dagger}(x)\psi_0'(x) = \sum_{x=0}^{\infty} 2\mathcal{N}'^2\left(\rho_+^x - \rho_-^x\right)^2 = 1 \\ \updownarrow \\ \mathcal{N}' = \sqrt{\frac{\Delta\left(t^2 - \mu^2\right)}{2t\left(\mu^2 - t^2 + \Delta^2\right)}} \end{aligned} \tag{2.51}$$

So the complete WF becomes

[1] using *Mathematica*^{TM}

$$\psi_0'(x) = \sqrt{\frac{\Delta\left(t^2-\mu^2\right)}{2t\left(\mu^2-t^2+\Delta^2\right)}}\begin{pmatrix}1\\1\end{pmatrix}\left(\rho_+^x-\rho_-^x\right) \tag{2.52}$$

And the norm squared of this WF is plotted in figure 4.

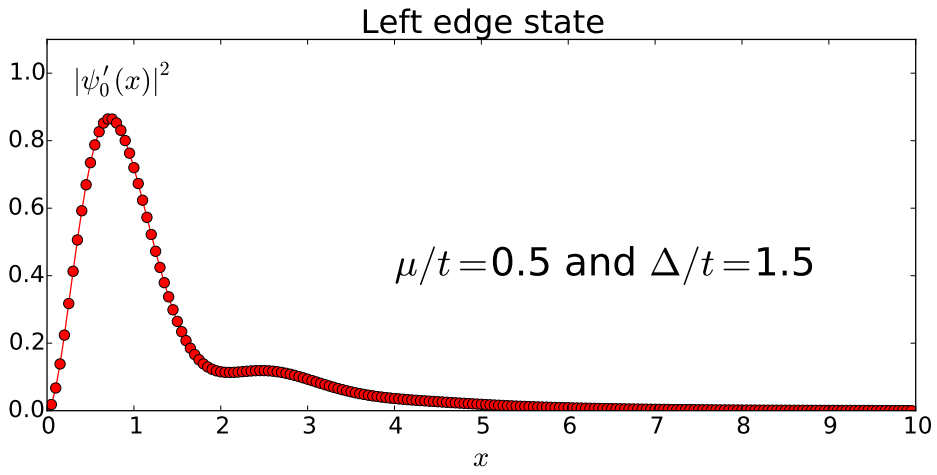

Figure 4: Plot of norm squared for the continuous zero energy mode in (2.52), for parameters inside of the topological phase. We see, as expected, that the state is exponentially localised on the edge.

The second solution (for $-q$) has instead a spinor which makes $\tau_z + i\tau_y$ vanish (the sign difference on τ_y comes from the Hamiltonian, setting $q \to -q$). This solution becomes

$$\psi_0''(x) = \mathcal{N}''\begin{pmatrix}-i\\i\end{pmatrix}\left(\alpha_+''\rho_+^{-x}+\alpha_-''\rho_-^{-x}\right) \tag{2.53}$$

With boundary condition $\psi_0''(N+1) = 0 \to \alpha_+''\rho_+^{-(N+1)} + \alpha_-''\rho_-^{-(N+1)} = 0$. I have multiplied with a factor i for later convenience. It should be mentioned that the exactness of these results imply taking the $N \to \infty$ limit for which $\mathcal{N}'' = \mathcal{N}'$ [2]. These two wavefunctions can be used to create the zero mode Majorana operators (which are the same found in [19])

$$\begin{aligned}\gamma' &= \sum_x (\psi_0'^{\dagger})^{\alpha}(x)C_x^{\alpha} = \sqrt{\frac{\Delta\left(t^2-\mu^2\right)}{2t\left(\mu^2-t^2+\Delta^2\right)}}\sum_x\left(\rho_+^x-\rho_-^x\right)\begin{pmatrix}1 & 1\end{pmatrix}\begin{pmatrix}c_x\\c_x^{\dagger}\end{pmatrix}\\ &= \sqrt{\frac{\Delta\left(t^2-\mu^2\right)}{2t\left(\mu^2-t^2+\Delta^2\right)}}\sum_x\left(\rho_+^x-\rho_-^x\right)\underbrace{\left(c_x^{\dagger}+c_x\right)}_{\gamma_{A,x}}\end{aligned} \tag{2.54}$$

[2] This limit was performed in Mathematica

Imposing the boundary conditions, the second solution becomes

$$\gamma'' = \sum_x (\psi_0''^{\dagger})^{\alpha}(x) C_x^{\alpha} = \sqrt{\frac{\Delta\left(t^2-\mu^2\right)}{2t\left(\mu^2-t^2+\Delta^2\right)}} \sum_x \left(\rho_+^{N+1}\rho_+^{-x} - \rho_-^{N+1}\rho_-^{-x}\right) \begin{pmatrix} -i & i \end{pmatrix} \begin{pmatrix} c_x \\ c_x^{\dagger} \end{pmatrix}$$
$$= \sqrt{\frac{\Delta\left(t^2-\mu^2\right)}{2t\left(\mu^2-t^2+\Delta^2\right)}} \sum_x \left(\rho_+^{N+1}\rho_+^{-x} - \rho_-^{N+1}\rho_-^{-x}\right) \underbrace{i\left(c_x^{\dagger} - c_x\right)}_{\gamma_{B,x}} \tag{2.55}$$

Which can be combined into the fermionic operator for the zero energy state $f_0 = \frac{1}{2}\left(\gamma' + i\gamma''\right)$. The topological criteria $|t| > |\mu|$ is also encoded in these states, which can be seen by analysing the coefficients ρ_+ and ρ_- and see where in parameter space the boundary conditions can be satisfied. Figure 5 contains a region plot of where one obtains $|\rho_\pm| < 1$ which is necessary for the edge states to exist (to ensure they do not diverge at large x). In the last sub-figure it is shown that the only region where both $|\rho_+|, |\rho_-| < 1$ is when $|t| > |\mu|$ which is the topological phase $W = -1$, found in 2.1.3. The first Majorana γ' resides on the left side, i.e has a WF with maximum at $x = 1$, while γ'' lives on the right hand side with a maximum value at $x = N$.

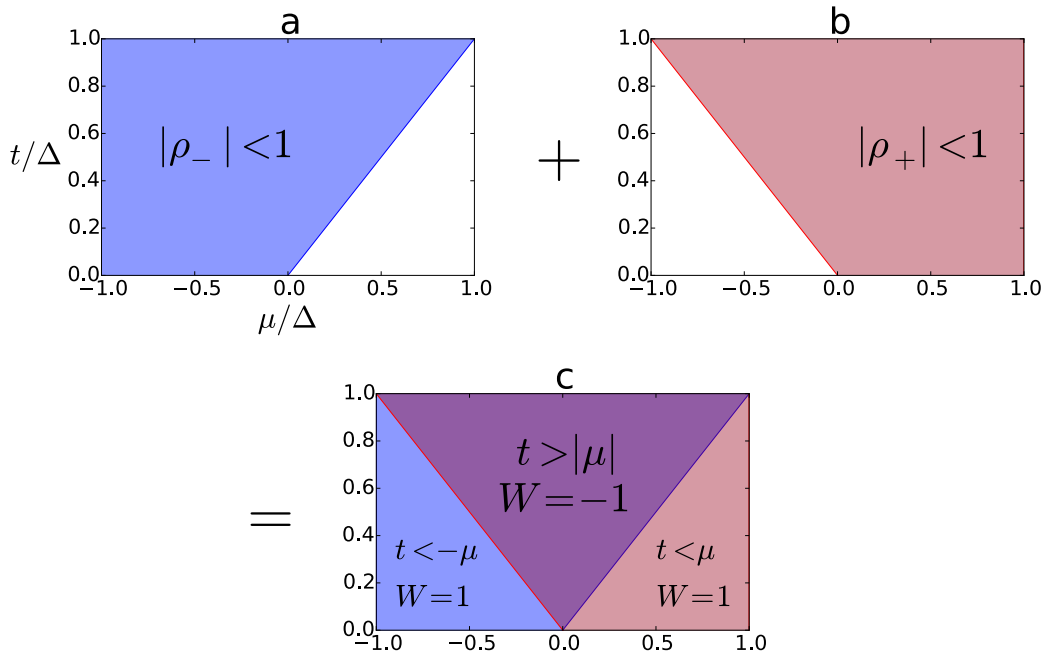

Figure 5: Subfigure *a* and *b* are region plots of parameter space where $|\rho_\pm| < 1$, with μ/Δ on the x-axis and t/Δ on the y-axis. These regions are therefore independent of Δ as long as $\Delta \neq 0$. The combined regions are plotted in *c*, and to be able to satisfy the boundary conditions, both $|\rho_+|, |\rho_-| < 1$ are needed, so it is only in this overlapped region (purple) that the edge state exists. This region has $|t| > |\mu|$ which was shown to be the topological phase, with a TI of value $W = -1$.

The characteristic length scale for these states ξ is defined as the distance at which the wavefunction decreases by a factor e, i.e. where $\psi_0(x+\xi) = e^{-1}\psi_0(x)$, so one chooses the largest of $|\rho_+|$ or $|\rho_-|$ (and denote it ρ), since this is the factor that extends the most into the bulk. One can then define

$$|\rho|^{x+\xi} = e^{-1}|\rho|^x \leftrightarrow |\rho|^\xi = e^{-1} \leftrightarrow \xi = \frac{1}{\ln\frac{1}{|\rho|}} = \frac{1}{|\ln|\rho||} \tag{2.56}$$

Which diverges right at the topological transition point $|\mu| = |t| \Rightarrow |\rho| = 1 \Rightarrow \xi \to \infty$. For the symmetric case discussed earlier with $\mu = 0, \Delta = t \neq 0$, one finds $\rho \to 0$ and then $\xi \to 0$ which fits with the previous results of having two un-paired Majoranas at each end of the chain, which do not decay into the bulk. In the general case considered in this section, the two zero modes at each end of the wire will have a small exponential overlap, so there will be a small energy splitting described by the Hamiltonian [19]

$$H_{eff} = \frac{i}{2}\Gamma\gamma'\gamma'' \qquad\qquad \Gamma \propto e^{-N/\xi} \tag{2.57}$$

In order for the preferred degeneracy of the GSs to be realized, one needs to ensure $\frac{N}{\xi} >> 1$ so that $\Gamma \to 0$. If this is not achievable, then there will be finite size effects, which is the topic of the next section. Later in this thesis we will examine the real space characteristics of the edge states, in the presence of interactions.

2.1.5 *Numerical solution to the finite Kitaev Chain*

In section 2.1.1 we discovered that the Hamiltonian takes a very simple form in the majorana basis at the symmetric point $\mu = 0, \Delta = t$. In section 2.1.4 the zero energy states were found for an infinite wire, for general parameters. In this section we want to find all the eigenstates and the energy spectrum for this discrete model away from the symmetric point, which will be done numerically. It is then possible to detect a change in the zero modes localized behaviour, and see how a finite sized system can affect the energy splitting of the degenerate ground-state. It is convenient to again recast the real space Kitaev Hamiltonian in eq. (2.1) in particle-hole form, such that it becomes

$$H = \frac{1}{2}\sum_{ij}\begin{pmatrix} c_i^\dagger & c_i \end{pmatrix}\begin{pmatrix} -\mathbf{t}_{ij} - \mu\delta_{ij} & \mathbf{\Delta}_{ij} \\ \mathbf{\Delta}_{ij}^\dagger & \mathbf{t}_{ij}^T + \mu\delta_{ij} \end{pmatrix}\begin{pmatrix} c_j \\ c_j^\dagger \end{pmatrix} = \frac{1}{2}\sum_{ij}(C^\dagger)_i^\alpha \mathcal{H}_{ij}^{\alpha\beta} C_j^\beta \tag{2.58}$$

Where $\mathcal{H}_{ij}^{\alpha\beta}$ is the first-quantization Nambu space Hamiltonian matrix (sandwiched between creation and annihilation operators to give the second quantization version). The "hopping matrix" is Hermitian $\mathbf{t} = \mathbf{t}^\dagger$, and the "pairing matrix" anti-hermitian $\mathbf{\Delta}^\dagger = -\mathbf{\Delta}$. For nearest neighbour coupling they are

$$\mathbf{t}_{ij} = \frac{t}{2}\left(\delta_{i,j+1} + \delta_{i+1,j}\right) \doteq \frac{t}{2}\begin{pmatrix} 0 & 1 & 0 & 0 \\ 1 & 0 & 1 & 0 \\ 0 & 1 & 0 & \ddots \\ 0 & 0 & \ddots & 0 \end{pmatrix}$$
$$\mathbf{\Delta}_{ij} = \frac{\Delta}{2}\left(\delta_{i,j+1} - \delta_{i+1,j}\right) \doteq \frac{\Delta}{2}\begin{pmatrix} 0 & -1 & 0 & 0 \\ 1 & 0 & -1 & 0 \\ 0 & 1 & 0 & \ddots \\ 0 & 0 & \ddots & 0 \end{pmatrix} \tag{2.59}$$

For a translational invariant system, one can define the momentum space functions

$$\begin{aligned} t(k) &= \sum_{ij} \mathbf{t}_{ij} e^{-ik(i-j)} = \sum_{ij} \frac{t}{2}\left(\delta_{i,j+1} + \delta_{i+1,j}\right) e^{-ik(i-j)} = t\cos k \\ \Delta(k) &= \sum_{ij} \mathbf{\Delta}_{ij} e^{-ik(i-j)} = \sum_{ij} \frac{\Delta}{2}\left(\delta_{i,j+1} - \delta_{i+1,j}\right) e^{-ik(i-j)} = -i\Delta\sin k \\ \mu(k) &= \mu \end{aligned} \tag{2.60}$$

Such that we end up with the bulk-momentum space Hamiltonian from (2.12). The Hamiltonian can be diagonalized by introducing new operators

$$\begin{pmatrix} f_n \\ f_n^\dagger \end{pmatrix} = \sum_i \begin{pmatrix} u_{in}^* & v_{in}^* \\ v_{in} & u_{in} \end{pmatrix} \begin{pmatrix} c_i \\ c_i^\dagger \end{pmatrix} \tag{2.61}$$

with the inverse transformation

$$\begin{pmatrix} c_i \\ c_i^\dagger \end{pmatrix} = \sum_n \begin{pmatrix} u_{in} & v_{in}^* \\ v_{in} & u_{in}^* \end{pmatrix} \begin{pmatrix} f_n \\ f_n^\dagger \end{pmatrix} \tag{2.62}$$

So, the f-operators will be a complicated superposition of the electron creation and annihilation operators. This means that eigenstates for the Hamiltonian will in general be superpositions of occupied and unoccupied states. As previously mentioned, a state where the occupied (electron) and unoccupied (hole) coefficient are equal is a Majorana mode. The transformation defined by (2.61) and (2.62) should be thought of as a huge matrix multiplication

$$\begin{pmatrix} f_1 \\ \vdots \\ f_N \\ f_1^\dagger \\ \vdots \\ f_N^\dagger \end{pmatrix} = \underbrace{\begin{pmatrix} \underline{\underline{u}}^\dagger & \underline{\underline{v}}^\dagger \\ \underline{\underline{v}}^T & \underline{\underline{u}}^T \end{pmatrix}}_{\underline{\underline{U}}^\dagger} \begin{pmatrix} c_1 \\ \vdots \\ c_N \\ c_1^\dagger \\ \vdots \\ c_N^\dagger \end{pmatrix} \qquad \begin{pmatrix} c_1 \\ \vdots \\ c_N \\ c_1^\dagger \\ \vdots \\ c_N^\dagger \end{pmatrix} = \underbrace{\begin{pmatrix} \underline{\underline{u}} & \underline{\underline{v}}^* \\ \underline{\underline{v}} & \underline{\underline{u}}^* \end{pmatrix}}_{\underline{\underline{U}}} \begin{pmatrix} f_1 \\ \vdots \\ f_N \\ f_1^\dagger \\ \vdots \\ f_N^\dagger \end{pmatrix} \tag{2.63}$$

Where $\underline{\underline{u}}$ and $\underline{\underline{v}}$ is $N \times N$ matrices, and $\underline{\underline{U}}$ is $2N \times 2N$. This transformation is unitary if $\underline{\underline{U}}^\dagger\ \underline{\underline{U}} = \mathbb{I}_{2N\times 2N}$ which requires that $\underline{\underline{u}}^\dagger\underline{\underline{u}} + \underline{\underline{v}}^\dagger\underline{\underline{v}} = \mathbb{I}_{N\times N}$ and $\underline{\underline{u}}^\dagger\underline{\underline{v}}^* + \underline{\underline{v}}^\dagger\underline{\underline{u}}^* = \underline{\underline{0}}$. Now, as usual it is desirable to construct $\underline{\underline{U}}$ such that the Hamiltonian is diagonalized,

which means that this transformation matrix must consist of the eigenvectors of the Hamiltonian, in other words, $\underline{\underline{u}}$ and $\underline{\underline{v}}$ must solve the BDG equations

$$\sum_j \mathcal{H}_{ij}^{\alpha\beta} \begin{pmatrix} u_{jn} \\ v_{jn} \end{pmatrix}^{\beta} = \sum_j \begin{pmatrix} -\mathbf{t}_{ij} - \mu\delta_{ij} & \mathbf{\Delta}_{ij} \\ -\mathbf{\Delta}_{ij} & \mathbf{t}_{ij} + \mu\delta_{ij} \end{pmatrix} \begin{pmatrix} u_{jn} \\ v_{jn} \end{pmatrix} = \epsilon_n \begin{pmatrix} u_{in} \\ v_{in} \end{pmatrix} \tag{2.64}$$

and by complex conjugation and switching u and v (PH transformation) one also has the negative energy solution

$$\sum_j \mathcal{H}_{ij}^{\alpha\beta} \begin{pmatrix} v_{jn}^* \\ u_{jn}^* \end{pmatrix}^{\beta} = \sum_j \begin{pmatrix} -\mathbf{t}_{ij} - \mu\delta_{ij} & \mathbf{\Delta}_{ij} \\ -\mathbf{\Delta}_{ij} & \mathbf{t}_{ij} + \mu\delta_{ij} \end{pmatrix} \begin{pmatrix} v_{jn}^* \\ u_{jn}^* \end{pmatrix} = -\epsilon_n \begin{pmatrix} v_{in}^* \\ u_{in}^* \end{pmatrix} \tag{2.65}$$

We can show that the Hamiltonian is diagonal by explicit calculation

$$\begin{aligned} H =& \frac{1}{2}\sum_{ij} (C^\dagger)_i^\alpha \mathcal{H}_{ij}^{\alpha\beta} C_j^\beta = \frac{1}{2}\sum_{ijnm} \begin{pmatrix} f_m^\dagger & f_m \end{pmatrix} \begin{pmatrix} u_{im}^* & v_{im}^* \\ v_{im} & u_{im} \end{pmatrix} \mathcal{H}_{ij}^{\alpha\beta} \begin{pmatrix} u_{jn} & v_{jn}^* \\ v_{jn} & u_{jn}^* \end{pmatrix} \begin{pmatrix} f_n \\ f_n^\dagger \end{pmatrix} \\ =& \frac{1}{2}\sum_{inm} \begin{pmatrix} f_m^\dagger & f_m \end{pmatrix} \begin{pmatrix} u_{im}^* & v_{im}^* \\ v_{im} & u_{im} \end{pmatrix} \begin{pmatrix} \epsilon_n u_{in} & -\epsilon_n v_{in}^* \\ \epsilon_n v_{in} & -\epsilon_n u_{in}^* \end{pmatrix} \begin{pmatrix} f_n \\ f_n^\dagger \end{pmatrix} \\ =& \frac{1}{2}\sum_{nm} \begin{pmatrix} f_m^\dagger & f_m \end{pmatrix} \begin{pmatrix} \epsilon_n\delta_{nm} & 0 \\ 0 & -\epsilon_n\delta_{nm} \end{pmatrix} \begin{pmatrix} f_n \\ f_n^\dagger \end{pmatrix} = \frac{1}{2}\sum_n \begin{pmatrix} f_n^\dagger & f_n \end{pmatrix} \underbrace{\begin{pmatrix} \epsilon_n & 0 \\ 0 & -\epsilon_n \end{pmatrix}}_{\tilde{\mathcal{H}}_{nn}^{\sigma\sigma}} \begin{pmatrix} f_n \\ f_n^\dagger \end{pmatrix} \\ =& \sum_n \epsilon_n \left(f_n^\dagger f_n - \frac{1}{2} \right) \end{aligned} \tag{2.66}$$

Where $\tilde{\mathcal{H}}_{nn}^{\sigma\sigma}$ is $\mathcal{H}_{ij}^{\alpha\beta}$ in the diagonal basis. The wave functions are given by $\Psi_{jn}^\beta \doteq \begin{pmatrix} u_{jn} \\ v_{jn} \end{pmatrix}$ and the norm squared of these are plotted in figure 6. One can observe that for $|t| > |\mu|$ zero energy modes Ψ_{jL}^β and Ψ_{jR}^β exist (L =left side, R =right side), and these have wavefunctions that decay into the chain. The electron and hole part of the edge states (Ψ_{jL}^1 and Ψ_{jL}^2) are equal, which is necessary for the Majorana condition. One can also notice the similarity between the numerically found edge state for this finite system, and the analytically found state in section 2.1.4, which is not surprising since the system size is fairly large $N = 200$. It should be noted that the continuous WF is found by making the discrete Kitaev model continuous, so the comparison of the two is valid at integer points in real space.

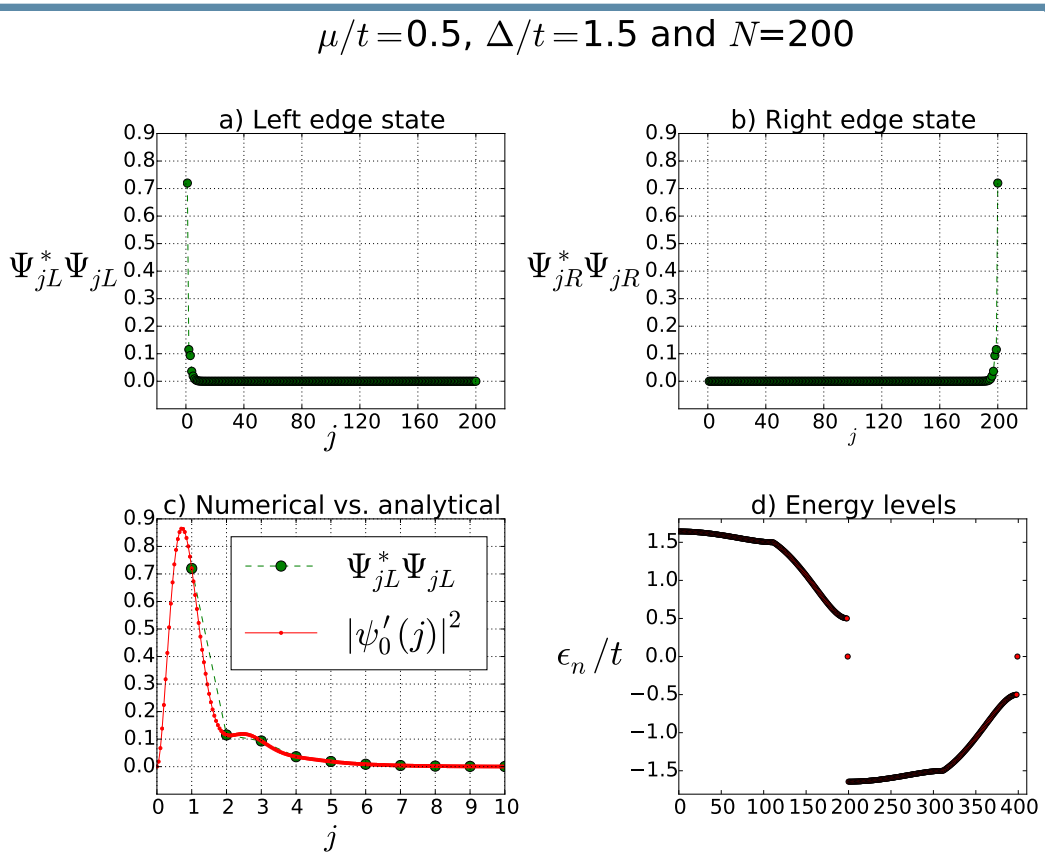

Figure 6: *a-b)* Plot of the norm squared of the zero modes for specific values of the parameters in the model (green). *c)* Zoom in of the edge state, where one notices the exponential decay into the bulk, and the similarity to the analytical result for the edge state (red) from (2.52). *d)* The two edge states are clearly visible in the energy spectrum, being two states with zero energy. The energy spectrum is sorted to have ϵ_n followed by $-\epsilon_n$.

In figure 7 it is shown what happens if the system is in the topologically trivial state $|\mu| > |t|$. Here the zero energy edge states vanish into the bulk, as seen in the spectrum. In the first sub-plot, the eigenstate of the lowest eigenvalue is plotted, which now is just a bulk WF. The continuous WF is also plotted, and for parameters corresponding to the trivial phase, the edge state WF grows indefinitely and is therefore not valid, since it cannot satisfy boundary conditions or be normalised.

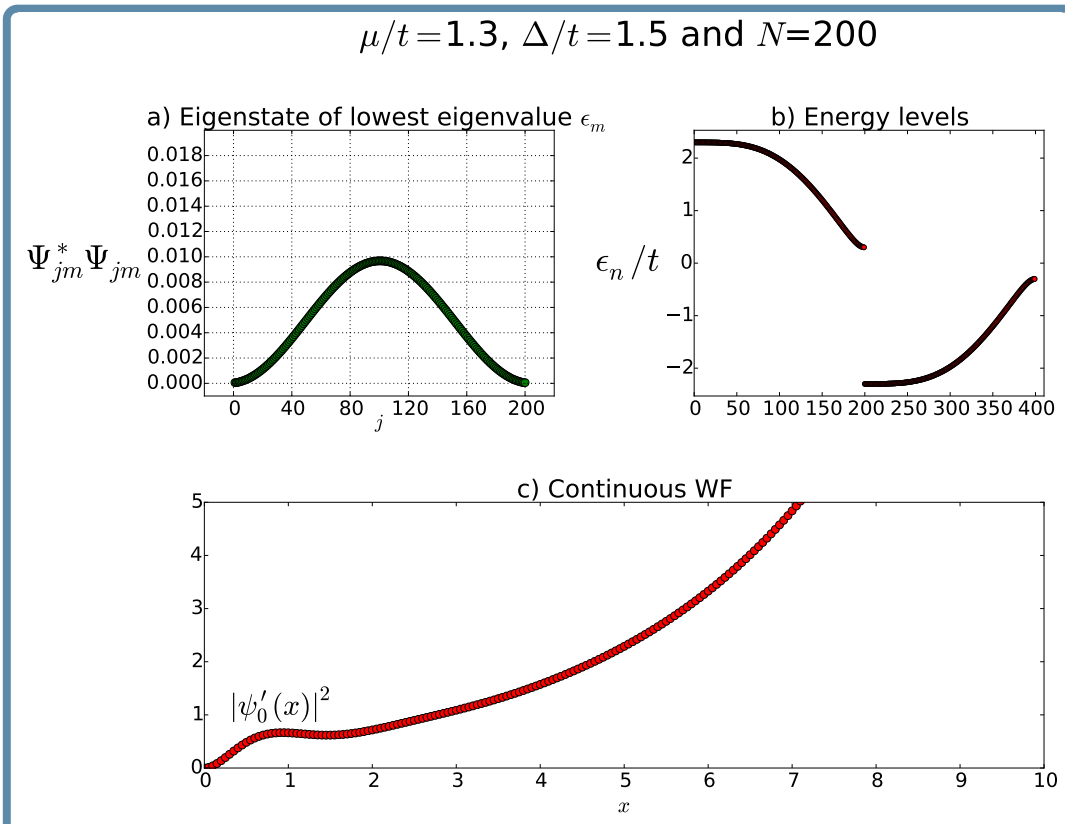

Figure 7: Plots for the trivial case, where no zero energy states exist in the spectrum. *a)* We see that the state with lowest eigenvalue ϵ_m is now a bulk state. *b)* No zero modes exist in the energy epctrum. *c)* For these parameter values, the exact edge state found for the continuous model diverges.

The energy spectrum as a function of the chemical potential μ is plotted in figure 8. For $\mu < t$ there are clear zero energy states, but for $\mu > t$ the two states enter the gapped bulk spectrum. The transition is not exactly at $\mu = t$ due to the finite size of the system, but for a large system this marks the topological phase transition.

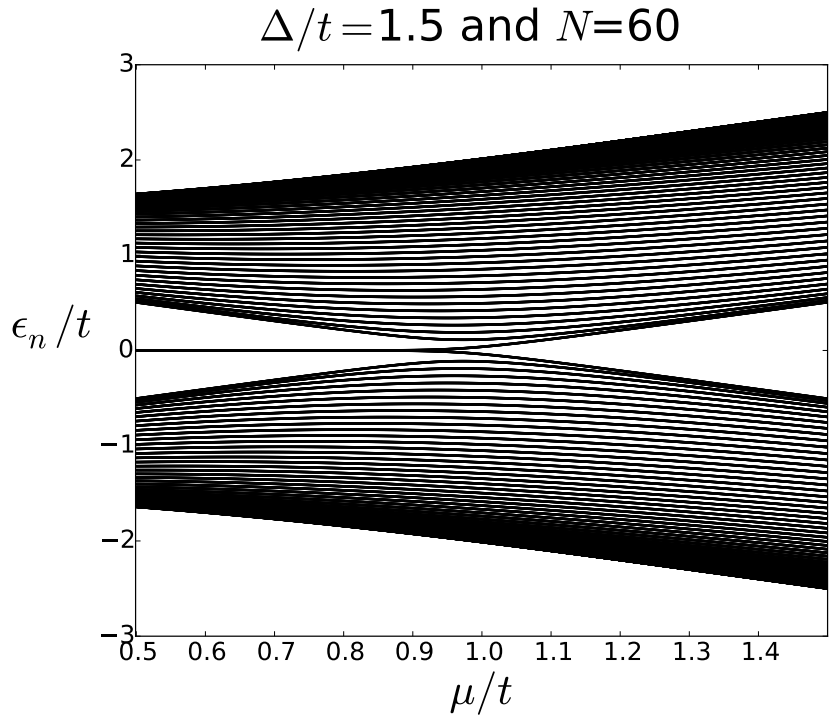

Figure 8: Energy spectrum ϵ_n for the general Kitaev Hamiltonian in (2.58) as a function of μ . The zero energy states split from each other at the topological phase transition at the critical value $\mu = t$. This point is not exact since the states have an exponential overlap in a finite system.

This concludes the analysis of the Hamiltonian formulation of the non-interacting Kitaev chain. The next sections will instead be using the GFs of the system. The goal is in the end to make sense of the classification of topological phases when interactions are added, and for this we seek a formulation of symmetry classes, topology and boundary states using many-body GFs instead of non-interacting eigenfunctions found in single-particle Quantum Mechanics.

2.2 GREEN'S FUNCTION DESCRIPTION

We can analyse the Kitaev model further by finding the GFs for the Hamiltonian, and from this, extract information about the density of states, and real space coherence of the zero modes. A GF description is preferred, since we later in this thesis add interactions to the model, and want to formalise a perturbation theory using Feynman diagrams. In addition, as mentioned, research has found that the effects of interactions in topological states of matter can be captured by generalizing TIs to

using GFs rather than the Bloch eigenstates [15]. The essential object is the Matsubara imaginary time Gorkov-Nambu GF which is a matrix in Nambu space

$$\begin{aligned}\mathcal{G}_0^{\alpha\beta}(\nu,\tau\,;\,\nu',\tau') &= -\langle T_\tau\left(C_\nu^\alpha(\tau)(C^\dagger)_{\nu'}^\beta(\tau')\right)\rangle_0 \doteq \begin{pmatrix}\mathcal{G}_0^{ee}(\nu,\tau;\nu',\tau') & \mathcal{G}_0^{eh}(\nu,\tau;\nu',\tau')\\ \mathcal{G}_0^{he}(\nu,\tau;\nu',\tau') & \mathcal{G}_0^{hh}(\nu,\tau;\nu',\tau')\end{pmatrix}\\ &= \begin{pmatrix}-\langle T_\tau\left(c_\nu(\tau)c_{\nu'}^\dagger(\tau')\right)\rangle_0 & -\langle T_\tau\left(c_\nu(\tau)c_{\nu'}(\tau')\right)\rangle_0\\ -\langle T_\tau\left(c_\nu^\dagger(\tau)c_{\nu'}^\dagger(\tau')\right)\rangle_0 & -\langle T_\tau\left(c_\nu^\dagger(\tau)c_{\nu'}(\tau')\right)\rangle_0\end{pmatrix}\end{aligned} \tag{2.67}$$

Here, the subscript zero refers to an average taken wrt. the non-interacting Kitaev Hamiltonian denoted by H_0. Imaginary times are denoted by τ and generic quantum numbers by ν. The τ dependence of the operators is determined in the Heisenberg picture for imaginary times, $c(\tau) = e^{H\tau}c\,e^{-H\tau}$. T_τ is the time-ordering operator, which orders operators with largest τ to the left, giving a sign for every odd permutation of fermionic operators. The Greek superscripts are Nambu indices, and help discern between the various kinds of GFs, with e for electrons and h for holes. The off-diagonal terms are usually called the Anomalous GFs. If the system is at equilibrium, the Matsubara GF depends only on the difference $\tau - \tau'$, as the Hamiltonian will then commute with itself at different times, and the trace is invariant to cyclic permutations [4]

$$\begin{aligned}\mathcal{G}(\tau,\tau') &= -\frac{1}{Z}\mathrm{Tr}\left(e^{-\beta H}e^{H\tau}c\;e^{-H\tau}e^{H\tau'}c^\dagger\;e^{-H\tau'}\right)\\ &= -\frac{1}{Z}\mathrm{Tr}\left(e^{-\beta H}e^{H(\tau-\tau')}c\;e^{-H(\tau-\tau')}c^\dagger\right)\\ &= \mathcal{G}(\tau-\tau')\end{aligned} \tag{2.68}$$

Where $Z = \mathrm{Tr}\left[e^{-\beta H}\right]$ is the partition function, with $\beta = \frac{1}{k_B T}$. Thus, the GF can be described using only one time variable $\tau - \tau' \to \tau$. We now want to explore this in discrete real space, so we can analyse the behaviour of the zero modes, and compare with what was observed in section 2.1.5. Equation (2.67) then becomes

$$\begin{aligned}\mathcal{G}_0^{\alpha\beta}(i,\tau\,;\,j,0) &= -\langle T_\tau\left(C_i^\alpha(\tau)(C^\dagger)_j^\beta(0)\right)\rangle_0 \doteq \begin{pmatrix}\mathcal{G}_0^{ee}(i,\tau\,;\,j,0) & \mathcal{G}_0^{eh}(i,\tau\,;\,j,0)\\ \mathcal{G}_0^{he}(i,\tau\,;\,j,0) & \mathcal{G}_0^{hh}(i,\tau\,;\,j,0)\end{pmatrix}\\ &= \begin{pmatrix}-\langle T_\tau\left(c_i(\tau)c_j^\dagger(0)\right)\rangle_0 & -\langle T_\tau\left(c_i(\tau)c_j(0)\right)\rangle_0\\ -\langle T_\tau\left(c_i^\dagger(\tau)c_j^\dagger(0)\right)\rangle_0 & -\langle T_\tau\left(c_i^\dagger(\tau)c_j(0)\right)\rangle_0\end{pmatrix}\end{aligned} \tag{2.69}$$

2.2.1 *GF from the Euclidean path integral*

The GF in (2.69) can be found using various methods, one is shown in Appendix C.1 called the *Equation of motion* method. The procedure is to take a τ-derivative of the GF, and then use Heisenbergs EOM $\partial_\tau A(\tau) = [H, A](\tau)$ to create a system of coupled equations for the different Nambu GFs. Here it will be found in a neat way using the fermionic euclidean path integral, with basics described in Appendix C.2. The idea is to construct a generating functional from the quantum partition function, which has been made into a path integral by the usual insertion of identities, in this case written in terms of fermionic coherent states. We start with the Kitaev Hamiltonian

(2.58), which has both Nambu and site structure, so there is one fermionic field for each value of Nambu and site index. The free action can in this case be written as

$$S_0\left[\overline{\Psi},\Psi\right] = \int_0^\beta d\tau \sum_{ij}\sum_{\sigma\rho} \overline{\Psi}_i^\sigma \left(\delta^{\sigma\rho}\delta_{ij}\,\partial_\tau + \mathcal{H}_{ij}^{\sigma\rho}\right)\Psi_j^\rho, \qquad \Psi_j^\rho = \begin{pmatrix}\psi_j\\ \overline{\psi}_j\end{pmatrix} \tag{2.70}$$

With $\mathcal{H}_{ij}^{\sigma\rho}$ from (2.58). To calculate the GF, one introduces the generating functional, which is the partition function with added source fields $\overline{\eta}$ and η

$$\mathcal{Z}_0[\overline{\eta},\eta] = \int \mathcal{D}\overline{\Psi}\mathcal{D}\Psi\; e^{-S_0\left[\overline{\Psi},\Psi\right]+\overline{\eta}_i^\sigma\;\Psi_i^\sigma+\overline{\Psi}_i^\sigma\;\eta_i^\sigma} \tag{2.71}$$

And by performing the Gaussian integration of the fermionic fields using (C.27), this becomes

$$\mathcal{Z}_0[\overline{\eta},\eta] = \det\left(\partial_\tau - \mathcal{H}\right) e^{\int d\tau_n d\tau_m \sum_{nm}\sum_{\sigma\rho}\overline{\eta}_n^\sigma(\tau_n)\left[(\partial_\tau+\mathcal{H})^{-1}\right]^{\sigma\rho}_{(n,\tau_n;m,\tau_m)}\eta_m^\rho(\tau_m)} \tag{2.72}$$

The GF can now be calculated (where creation/annihilation operators C and $C^\dagger$ are now replaced with the coherent state eigenvalues Ψ and $\overline{\Psi}$ respectively)

$$\mathcal{G}_0^{\alpha\beta}(i,\tau_i;j,\tau_j) = -\langle\Psi_i^\alpha(\tau_i)\overline{\Psi}_j^\beta(\tau_j)\rangle_0 = \frac{\int \mathcal{D}\overline{\Psi}\mathcal{D}\Psi\;\left(\Psi_i^\alpha(\tau_i)\overline{\Psi}_j^\beta(\tau_j)\right)\;e^{-S_0\left[\overline{\Psi},\Psi\right]}}{\int \mathcal{D}\overline{\Psi}\mathcal{D}\Psi\; e^{-S_0\left[\overline{\Psi},\Psi\right]}} \tag{2.73}$$

This can be done by using the generating functional

$$\mathcal{G}_0^{\alpha\beta}(i,\tau_i;j,\tau_j) = \frac{1}{\mathcal{Z}_0\left[0,0\right]}\frac{\delta}{\delta\overline{\eta}_i^\alpha(\tau_i)}\frac{\delta}{\delta\eta_j^\beta(\tau_j)}\mathcal{Z}_0\left[\overline{\eta},\eta\right]|_{\overline{\eta}=\eta=0} \tag{2.74}$$

Where the functional derivative is defined as

$$\frac{\delta}{\delta\eta_j^\beta(\tau_j)}\,\eta_m^\rho(\tau_m) = \delta(\tau_j-\tau_m)\delta_{jm}\delta^{\beta\rho} \tag{2.75}$$

Using this yields

$$\begin{aligned}
&\mathcal{G}_0^{\alpha\beta}(i,\tau_i;j,\tau_j)\\
&= \frac{1}{\mathcal{Z}_0\left[0,0\right]}\frac{\delta}{\delta\overline{\eta}_i^\alpha(\tau_i)}\left(-\int d\tau_n\sum_n\sum_\sigma\overline{\eta}_n^\sigma(\tau_n)\left[\left(\partial_\tau+\mathcal{H}\right)^{-1}\right]^{\sigma\beta}_{(n,\tau_n;j,\tau_j)}\right)\mathcal{Z}_0\left[\overline{\eta},\eta\right]|_{\overline{\eta}=\eta=0}\\
&= \frac{1}{\mathcal{Z}_0\left[0,0\right]}\left[\left(-\partial_\tau-\mathcal{H}\right)^{-1}\right]^{\alpha\beta}_{(i,\tau_i;j,\tau_j)}\mathcal{Z}_0\left[\overline{\eta},\eta\right]|_{\overline{\eta}=\eta=0}\\
&= \left[\left(-\partial_\tau-\mathcal{H}\right)^{-1}\right]^{\alpha\beta}_{(i,\tau_i;j,\tau_j)}
\end{aligned} \tag{2.76}$$

Using the product rule in the first line, only the term with the functional derivative of the parentheses is kept, since the other term vanishes when setting $\overline{\eta}=\eta=0$ in the end. Transforming this GF to Matsubara frequencies can be written as

$$\mathcal{G}_0^{\alpha\beta}(i,\tau_i;j,\tau_j) = \langle\tau_i|\mathcal{G}_0^{\alpha\beta}(i,j)|\tau_j\rangle = \sum_{ik_n,ip_n}\langle\tau_i|ik_n\rangle\langle ik_n|\mathcal{G}_0^{\alpha\beta}(i,j)|ip_n\rangle\langle ip_n|\tau_j\rangle \tag{2.77}$$

Where one can now use

$$\langle \tau | ik_n \rangle = \frac{1}{\sqrt{\beta}} e^{-ik_n \tau} \tag{2.78}$$

But since the system is in equilibrium, the GF only depends on the difference $\tau_i - \tau_j$, and the Matsubara frequency basis is diagonal

$$\begin{aligned} \mathcal{G}_0^{\alpha\beta}(i, \tau_i; j, \tau_j) &= \sum_{ik_n, ip_n} \langle \tau_i | ik_n \rangle \mathcal{G}_0^{\alpha\beta}(i, j; ik_n) \delta_{ik_n, ip_n} \langle ip_n | \tau_j \rangle \\ &= \frac{1}{\beta} \sum_{ik_n} \mathcal{G}_0^{\alpha\beta}(i, j; ik_n) e^{-ik_n(\tau_i - \tau_j)} \end{aligned} \tag{2.79}$$

With

$$\mathcal{G}_0^{\alpha\beta}(i, j; ik_n) = \left[(ik_n - \mathcal{H})^{-1} \right]_{ij}^{\alpha\beta} \tag{2.80}$$

Which is the same result as from the EOM method. Here we have transformed to Matsubara frequency, but kept the real space dependency intact. If the system is translational invariant, in addition to being in equilibrium, then

$$\mathcal{G}_0^{\alpha\beta}(x, \tau; x', \tau') = \langle x, \tau_x | \mathcal{G}_0^{\alpha\beta} | x', \tau' \rangle = \frac{1}{\beta \mathcal{V}} \sum_{k, ik_n} \mathcal{G}_0^{\alpha\beta}(k; ik_n) e^{ik(x - x') - ik_n(\tau - \tau')} \tag{2.81}$$

With

$$\mathcal{G}_0^{\alpha\beta}(k; ik_n) = \left[(ik_n - \mathcal{H}(k))^{-1} \right]^{\alpha\beta} \tag{2.82}$$

Where it was applied that

$$\langle x, \tau | k, ik_n \rangle = \frac{1}{\sqrt{\beta \mathcal{V}}} e^{ikx - ik_n \tau} \tag{2.83}$$

One can introduce an immaculate notation where a 4D space-imaginary time is introduced $\tilde{x} = (\tau, x, y, z)$ together with a four momentum $\tilde{k} = (ik_n, k_x, k_y, k_z)$. Letting the indices run from $\alpha = 0, 1, 2, 3$ one can then write

$$\langle \tilde{x} | \tilde{k} \rangle = \frac{1}{\sqrt{\beta \mathcal{V}}} e^{i\tilde{k} \cdot \tilde{x}}, \qquad \tilde{k} \cdot \tilde{x} = \eta^{\alpha\beta} k_\alpha x_\beta, \qquad \eta^{\alpha\beta} = \mathrm{diag}(-1, 1, 1, 1) \tag{2.84}$$

Where $\eta^{\alpha\beta}$ is the Minkowski metric. Using the Path integral formalism, one can then add interactions to the free action, expand the exponential in the generating functional, and then take functional derivatives to get the correlation functions. Wick's theorem and the Feynman rules then emerge from the calculations. In the following sections this will be done in the operator formalism following [4]. In Appendix C.4 the analysis of this section has been performed for the bare GF in the Majorana basis. Depending on what calculation one wants to perform, it can be advantageous to use this form instead. Similarly, in Appendix C.5 the specific forms of the electron and Majorana GFs are found in momentum space, and can be used in a translational invariant system, where k is a good quantum number.

2.2.2 *Diagonalizing the Green's function*

One can diagonalize the GF in a similar fashion as with the Hamiltonian in section 2.1.5. Inserting the transformed Nambu spinors into the definition of the free Matsubara GF

$$\begin{aligned}
\mathcal{G}_0^{\alpha\beta}(i,\tau\,;\,j,0) &= -\langle T_\tau \left(C_i^\alpha(\tau)(C^\dagger)_j^\beta(0) \right) \rangle_0 \\
&\doteq -\sum_{nm} \begin{pmatrix} u_{in} & v_{in}^* \\ v_{in} & u_{in}^* \end{pmatrix} \langle T_\tau \left(\begin{pmatrix} f_n(\tau) \\ f_n^\dagger(\tau) \end{pmatrix} \begin{pmatrix} f_m^\dagger & f_m \end{pmatrix} \right) \rangle_0 \begin{pmatrix} u_{jm}^* & v_{jm}^* \\ v_{jm} & u_{jm} \end{pmatrix} \\
&= \sum_{nm} \begin{pmatrix} u_{in} & v_{in}^* \\ v_{in} & u_{in}^* \end{pmatrix} \begin{pmatrix} -\langle T_\tau \left(f_n(\tau) f_m^\dagger \right) \rangle_0 & -\langle T_\tau \left(f_n(\tau) f_m \right) \rangle_0 \\ -\langle T_\tau \left(f_n^\dagger(\tau) f_m^\dagger \right) \rangle_0 & -\langle T_\tau \left(f_n^\dagger(\tau) f_m \right) \rangle_0 \end{pmatrix} \begin{pmatrix} u_{jm}^* & v_{jm}^* \\ v_{jm} & u_{jm} \end{pmatrix}
\end{aligned} \tag{2.85}$$

Calculating one of the terms in the matrix

$$-\langle T_\tau \left(f_n(\tau) f_m^\dagger \right) \rangle_0 = -\theta(\tau) \langle f_n(\tau) f_m^\dagger \rangle_0 + \theta(-\tau) \langle f_m^\dagger f_n(\tau) \rangle_0 \tag{2.86}$$

Now, the τ-dependence of the operators is found using Heisenberg's EOM for imaginary time

$$\begin{aligned}
\partial_\tau f_n^\dagger(\tau) &= \left[H_0, f_n^\dagger \right](\tau) \\
\partial_\tau f_n(\tau) &= \left[H_0, f_n \right](\tau)
\end{aligned} \tag{2.87}$$

Using the relation

$$[AB, C] = A\{B, C\} - \{A, C\}B \tag{2.88}$$

An by inserting this, one obtains

$$\begin{aligned}
\partial_\tau f_n^\dagger(\tau) &= \quad \epsilon_n f_n^\dagger(\tau) \qquad \leftrightarrow \qquad f_n^\dagger(\tau) = f_n^\dagger \, e^{\epsilon_n \tau} \\
\partial_\tau f_n(\tau) &= -\epsilon_n f_n(\tau) \qquad \leftrightarrow \qquad f_n(\tau) = f_n \, e^{-\epsilon_n \tau}
\end{aligned} \tag{2.89}$$

So the matrix element in question becomes

$$\begin{aligned}
-\langle T_\tau \left(f_n(\tau) f_m^\dagger \right) \rangle_0 &= -\theta(\tau) \langle f_n f_m^\dagger \rangle_0 \, e^{-\epsilon_n \tau} + \theta(-\tau) \langle f_m^\dagger f_n \rangle_0 \, e^{-\epsilon_n \tau} \\
&= -\theta(\tau) \left[1 - n_F(\epsilon_n) \right] \delta_{nm} \, e^{-\epsilon_n \tau} + \theta(-\tau) n_F(\epsilon_n) \delta_{nm} \, e^{-\epsilon_n \tau}
\end{aligned} \tag{2.90}$$

Where $n_F(\epsilon_n) = \frac{1}{e^{\beta\epsilon_n}+1}$. The off-diagonal terms vanish

$$-\langle T_\tau \left(f_n(\tau) f_m \right) \rangle_0 = -\theta(\tau) \langle f_n f_m \rangle_0 \, e^{-\epsilon_n \tau} + \theta(-\tau) \langle f_m f_n \rangle_0 \, e^{-\epsilon_n \tau} = 0 \tag{2.91}$$

If one transforms to Matsubara frequencies

$$\mathcal{G}_0^{\alpha\beta}(i,j;ik_n) = \int_0^\beta d\tau \, \mathcal{G}_0^{\alpha\beta}(i,\tau\,;\,j,0) \, e^{ik_n\tau}, \qquad k_n = \frac{2n+1}{\beta}\pi \tag{2.92}$$

One gets

$$\mathcal{G}_0^{\alpha\beta}(i,j;ik_n) \doteq \sum_n \begin{pmatrix} u_{in} & v_{in}^* \\ v_{in} & u_{in}^* \end{pmatrix} \begin{pmatrix} \int_0^\beta d\tau \left[n_F(\epsilon_n)-1\right] e^{(ik_n-\epsilon_n)\tau} & 0 \\ 0 & -\int_0^\beta d\tau\, n_F(\epsilon_n) e^{(ik_n+\epsilon_n)\tau} \end{pmatrix} \begin{pmatrix} u_{jn}^* & v_{jn}^* \\ v_{jn} & u_{jn} \end{pmatrix} \tag{2.93}$$

The first matrix element is

$$\begin{aligned} &\int_0^\beta d\tau \left[n_F(\epsilon_n)-1\right] e^{(ik_n-\epsilon_n)\tau} = \frac{\left[n_F(\epsilon_n)-1\right]}{ik_n-\epsilon_n}\left[e^{(ik_n-\epsilon_n)\tau}\right]_0^\beta \\ &= \frac{\left[n_F(\epsilon_n)-1\right]}{ik_n-\epsilon_n}\left[e^{ik_n\beta}e^{-\beta\epsilon}-1\right] = \frac{\left[1-n_F(\epsilon_n)\right]}{ik_n-\epsilon_n}\left[e^{-\beta\epsilon}+1\right] \\ &= \frac{\left[\frac{e^{\beta\epsilon_n}+1}{e^{\beta\epsilon_n}+1}-\frac{1}{e^{\beta\epsilon_n}+1}\right]}{ik_n-\epsilon_n}\left[\frac{e^{\beta\epsilon}+1}{e^{\beta\epsilon_n}}\right] = \frac{1}{ik_n-\epsilon_n} \end{aligned} \tag{2.94}$$

Where $e^{ik_n\beta} = e^{i\frac{2n+1}{\beta}\pi\beta} = -1$ has been used. Similarly for the other entry

$$-\int_0^\beta d\tau n_F(\epsilon_n) e^{(ik_n+\epsilon_n)\tau} = \frac{-n_F(\epsilon_n)}{ik_n+\epsilon_n}\left[e^{(ik_n+\epsilon_n)\tau}\right]_0^\beta = \frac{-n_F(\epsilon_n)}{ik_n+\epsilon_n}\left[e^{ik_n\beta}e^{\beta\epsilon}-1\right]$$

$$= \frac{n_F(\epsilon_n)}{ik_n+\epsilon_n}\left[e^{\beta\epsilon}+1\right] = \frac{1}{ik_n+\epsilon_n} \tag{2.95}$$

$$\tag{2.96}$$

So the GF becomes

$$\begin{aligned} \mathcal{G}_0^{\alpha\beta}(i,j;ik_n) &\doteq \sum_n \begin{pmatrix} u_{in} & v_{in}^* \\ v_{in} & u_{in}^* \end{pmatrix} \underbrace{\begin{pmatrix} \frac{1}{ik_n-\epsilon_n} & 0 \\ 0 & \frac{1}{ik_n+\epsilon_n} \end{pmatrix}}_{\tilde{\mathcal{G}}_0^{\sigma\sigma}(n;ik_n)} \begin{pmatrix} u_{jn}^* & v_{jn}^* \\ v_{jn} & u_{jn} \end{pmatrix} \\ &= \sum_n U_{in}^{\alpha\sigma}\tilde{\mathcal{G}}_0^{\sigma\sigma}(n;ik_n)(U^\dagger)_{nj}^{\sigma\beta} \end{aligned} \tag{2.97}$$

Alternatively, this can be written as a matrix equation in Nambu and site space

$$\underline{\underline{\mathcal{G}_0}}(ik_n) = \underline{\underline{U}}\;\underline{\underline{\tilde{\mathcal{G}}_0}}(ik_n)\;\underline{\underline{U}}^\dagger \tag{2.98}$$

Where $\underline{\underline{\tilde{\mathcal{G}}_0}}(ik_n)$ is now a diagonal matrix in both site and Nambu space. This can also be seen from

$$\underline{\underline{\mathcal{G}_0}}^{-1}\;\underline{\underline{\mathcal{G}_0}} = \mathbb{I} \;\leftrightarrow\; \underline{\underline{U}}^\dagger\;\underline{\underline{\mathcal{G}_0}}^{-1}\;\underline{\underline{U}}\;\underline{\underline{U}}^\dagger\;\underline{\underline{\mathcal{G}_0}}\;\underline{\underline{U}} = \underline{\underline{U}}^\dagger\;\underline{\underline{U}} = \mathbb{I} \tag{2.99}$$

showing that the GF transforms as the Hamiltonian. This can be rewritten as

$$\begin{aligned} \underline{\underline{U}}^\dagger\;\underline{\underline{\mathcal{G}_0}}\;\underline{\underline{U}} &= \left(\underline{\underline{U}}^\dagger\;\left(ik_n\mathbb{I}-\underline{\underline{\mathcal{H}}}\right)\;\underline{\underline{U}}\right)^{-1} = \left(ik_n\mathbb{I}-\underline{\underline{\tilde{\mathcal{H}}}}\right)^{-1} = \\ &= \left(\begin{pmatrix} ik_n & 0 \\ 0 & ik_n \end{pmatrix} - \begin{pmatrix} \epsilon_n & 0 \\ 0 & -\epsilon_n \end{pmatrix}\right)^{-1} = \begin{pmatrix} \frac{1}{ik_n-\epsilon_n} & 0 \\ 0 & \frac{1}{ik_n+\epsilon_n} \end{pmatrix} = \underline{\underline{\tilde{\mathcal{G}}_0}} \end{aligned} \tag{2.100}$$

This allows us to write the non-diagonal GF in terms of the coherence matrices u_{in} and v_{in}, which were introduced in the context of diagonalising the Hamiltonian

$$\begin{aligned}\mathcal{G}_0^{\alpha\beta}(i,j;ik_n) &\doteq \sum_n \begin{pmatrix} u_{in} & v_{in}^* \\ v_{in} & u_{in}^* \end{pmatrix} \begin{pmatrix} \frac{1}{ik_n-\epsilon_n} & 0 \\ 0 & \frac{1}{ik_n+\epsilon_n} \end{pmatrix} \begin{pmatrix} u_{jn}^* & v_{jn}^* \\ v_{jn} & u_{jn} \end{pmatrix} \\ &= \sum_n \begin{pmatrix} u_{in} & v_{in}^* \\ v_{in} & u_{in}^* \end{pmatrix} \begin{pmatrix} \frac{1}{ik_n-\epsilon_n} u_{jn}^* & \frac{1}{ik_n-\epsilon_n} v_{jn}^* \\ \frac{1}{ik_n+\epsilon_n} v_{jn} & \frac{1}{ik_n+\epsilon_n} u_{jn} \end{pmatrix} \\ &= \sum_n \begin{pmatrix} u_{in}\,\frac{1}{ik_n-\epsilon_n}\,u_{jn}^* + v_{in}^*\,\frac{1}{ik_n+\epsilon_n}\,v_{jn} & u_{in}\,\frac{1}{ik_n-\epsilon_n}\,v_{jn}^* + v_{in}^*\,\frac{1}{ik_n+\epsilon_n}\,u_{jn} \\ v_{in}\,\frac{1}{ik_n-\epsilon_n}\,u_{jn}^* + u_{in}^*\,\frac{1}{ik_n+\epsilon_n}\,v_{jn} & v_{in}\,\frac{1}{ik_n-\epsilon_n}\,v_{jn}^* + u_{in}^*\,\frac{1}{ik_n+\epsilon_n}\,u_{jn} \end{pmatrix}\end{aligned} \tag{2.101}$$

In our case, $\underline{\underline{u}}$ and $\underline{\underline{v}}$ are real matrices, and we can perform analytical continuation $(ik_n \to \omega + i\eta)$ with $\eta = 0^+$, to find the frequency dependent retarded GF

$$\begin{aligned}&(G_0^R)^{\alpha\beta}(i,j;\omega) \doteq \\ &\sum_n \begin{pmatrix} u_{in}\,\frac{1}{\omega+i\eta-\epsilon_n}\,u_{jn} + v_{in}\,\frac{1}{\omega+i\eta+\epsilon_n}\,v_{jn} & u_{in}\,\frac{1}{\omega+i\eta-\epsilon_n}\,v_{jn} + v_{in}\,\frac{1}{\omega+i\eta+\epsilon_n}\,u_{jn} \\ v_{in}\,\frac{1}{\omega+i\eta-\epsilon_n}\,u_{jn} + u_{in}\,\frac{1}{\omega+i\eta+\epsilon_n}\,v_{jn} & v_{in}\,\frac{1}{\omega+i\eta-\epsilon_n}\,v_{jn} + u_{in}\,\frac{1}{\omega+i\eta+\epsilon_n}\,u_{jn} \end{pmatrix}\end{aligned} \tag{2.102}$$

Which can then be used for further calculations when setting up a perturbation series for the interacting GF.

2.2.3 *Spectral function and local density of states*

To see explicitly how states are distributed, one defines the spectral function

$$(\mathcal{A}_0)^{\alpha\beta}(i,j;\omega) = -2\mathrm{Im}\left[(G_0^R)^{\alpha\beta}(i,j;\omega)\right] \tag{2.103}$$

And uses the Sokhotski–Plemelj theorem

$$\lim_{\eta\to 0^+} \frac{1}{x \pm i\eta} = \mathcal{P}\frac{1}{x} \mp i\pi\delta(x) \tag{2.104}$$

Where $\mathcal{P}$ refers to the Cauchy principal value. The spectral function becomes

$$\begin{aligned}&(\mathcal{A}_0)^{\alpha\beta}(i,j;\omega) \doteq \\ &2\pi\sum_n \begin{pmatrix} u_{in}\delta(\omega-\epsilon_n)u_{jn} + v_{in}\delta(\omega+\epsilon_n)v_{jn} & u_{in}\delta(\omega-\epsilon_n)v_{jn} + v_{in}\delta(\omega+\epsilon_n)u_{jn} \\ v_{in}\delta(\omega-\epsilon_n)u_{jn} + u_{in}\delta(\omega+\epsilon_n)v_{jn} & v_{in}\delta(\omega-\epsilon_n)v_{jn} + u_{in}\delta(\omega+\epsilon_n)u_{jn} \end{pmatrix}\end{aligned} \tag{2.105}$$

Looking at the local spectral function $(i = j)$,

$$\begin{aligned}&(\mathcal{A}_0)^{\alpha\beta}(i,i;\omega) \doteq \\ &2\pi\sum_n \begin{pmatrix} u_{in}^2\delta(\omega-\epsilon_n) + v_{in}^2\delta(\omega+\epsilon_n) & u_{in}v_{in}\left[\delta(\omega-\epsilon_n) + \delta(\omega+\epsilon_n)\right] \\ u_{in}v_{in}\left[\delta(\omega-\epsilon_n) + \delta(\omega+\epsilon_n)\right] & v_{in}^2\delta(\omega-\epsilon_n) + u_{in}^2\delta(\omega+\epsilon_n) \end{pmatrix}\end{aligned} \tag{2.106}$$

one observes that it has Dirac peaks at each ϵ_n and $-\epsilon_n$. If the energy of a specific eigenstate $\omega = \epsilon_m \in \epsilon_n$ is inserted, then the diagonal of this local spectral function contains the square of the wavefunction corresponding to the state ϵ_m. This means that the wavefunctions are encoded in this local spectral function, which is a more convenient measure when interactions are added. There is a subtlety in that these Dirac peaks are infinite in magnitude, so they only make sense inside an integral. If this analysis is to be performed on a computer, one must insert a small value for η, since delta functions are not handled in a proper way numerically. This has the effect that the delta functions instead become broadened Lorentzian functions of the form

$$-2\mathrm{Im}\left(\frac{1}{\omega + i\eta - \epsilon_m}\right) = \frac{2\eta}{(\omega - \epsilon_n)^2 + \eta^2} \tag{2.107}$$

With a width determined by η. This is an $N \times N$ diagonal matrix, and when inserting $\omega = \epsilon_m$ this function "picks out" ϵ_m from the diagonal matrix, and multiplies it by $\frac{2\eta}{\eta^2} = \frac{2}{\eta}$, which is a very large number since η is small. In principle, η should be as small as possible, to make sure we only get contributions from ϵ_m which is the wavefunction we want to analyse. If this is done, the wavefunction will be scaled by $\frac{2}{\eta}$, so we need to take this into account when comparing (if we divide by this factor we find the weight of the delta function). In figure 9 we see the electronic part of the local spectral function as it decays into the chain. This is compared with $|u|^2$ from the wave-function corresponding to the zero mode.

The local spectral function is a probability distribution which obeys the sum rule

$$\int_{-\infty}^{\infty} \frac{d\omega}{2\pi} (\mathcal{A}_0)^{\alpha\beta}(i, i; \omega) = \delta^{\alpha\beta} \tag{2.108}$$

Which is also true for the full spectral function when interactions are added [4]. We saw that the bare spectral function is given by delta functions in the excitation spectrum for the non-interacting Hamiltonian (ϵ_n). When adding interactions, these will differ from delta function peaks, but will in general still be highly peaked, and one can then discuss when the single quasi-particle description is still valid.

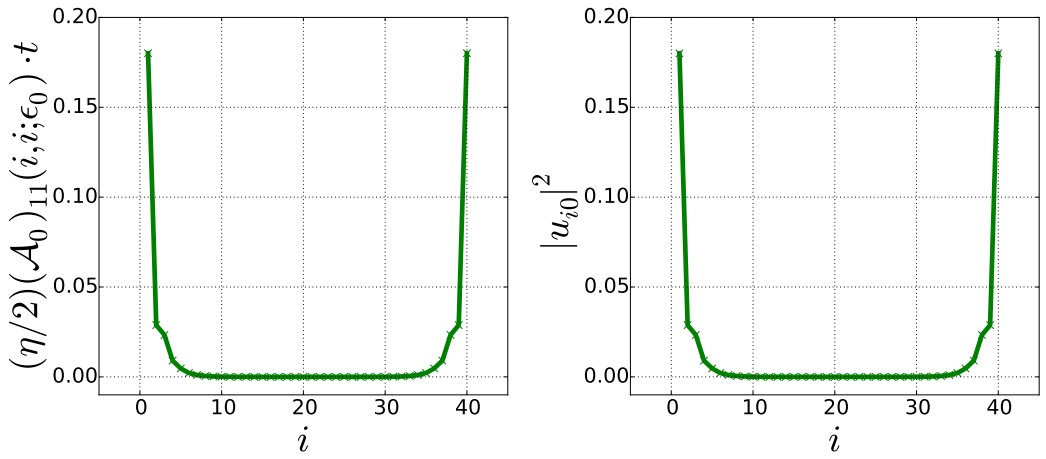

Figure 9: Comparison of the electronic (ee or 11 Nambu space index) of the bare local spectral function at the edge state energy $\omega = \epsilon_0$, with the WF of the edge state. The relation between these is given by eq. (2.106). The spectral function has units of inverse energy, and can be made dimensionless by multiplication of t.

2.2.4 *Numerical calculation of the real space Green's function*

In this section we cover the results of a numerical calculation of eq. (2.103), which is plotted in figure 10 and 11. Here we see the local spectral function at the edge of the wire, as a function of energy ω, and the zero energy mode peaks are clearly visible. The local spectral function is also the local density of states, i.e. the occupation n_ν of some quantum state ν is [4]

$$n_\nu = \langle c_\nu^\dagger c_\nu \rangle = \int_{-\infty}^{\infty} \frac{d\omega}{2\pi} \mathcal{A}(\nu, \omega) n_F(\omega) \tag{2.109}$$

So we can investigate how the spectral function depends on energy at the edge of the wire, which is relevant if one wishes to find the current in a tunnelling experiment. In the bottom of the plots we see the energy spectrum ϵ_n at which the spectral function is highly peaked. The apparent asymmetry in the strength of the peaks is due to the fact that the values of $|v|^2$ are a lot larger than $|u|^2$ for the bulk states, and this value is visible when including the artificial broadening η. Looking at (2.106) one should then expect for the $(\mathcal{A}_0)_{11}$ component that the negative energies are more visible in the plot, which is the case. Conversely, for the $(\mathcal{A}_0)_{22}$ component it should be the opposite case, which is observed to be correct.

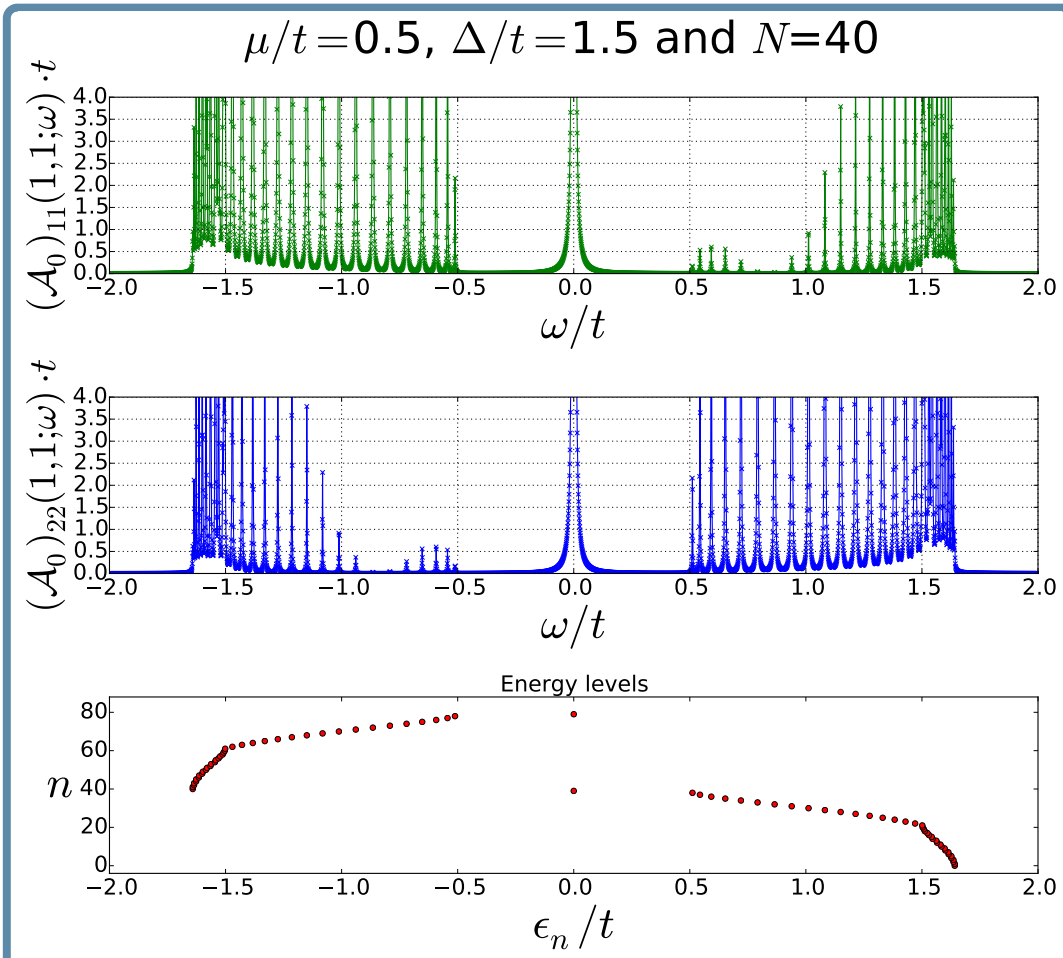

Figure 10: Plot of the components of the non-interacting spectral function for the Kitaev chain and energy spectrum for comparison, with parameters in the topological phase. Here, zero energy states are seen as peaks at $\omega = 0$. The width is controlled by the inserted imaginary part $i\eta = i0^+$. The asymmetry between positive and negative energy is due to the fact that $|v|^2 > |u|^2$ in the bulk, which is seen from the fact that the asymmetry in $(\mathcal{A}_0)_{22}$ is the reverse of $(\mathcal{A}_0)_{11}$.

In figure 11 with parameters corresponding to the trivial phase of the system, no zero energy states exists, both in the spectrum and in the spectral function.

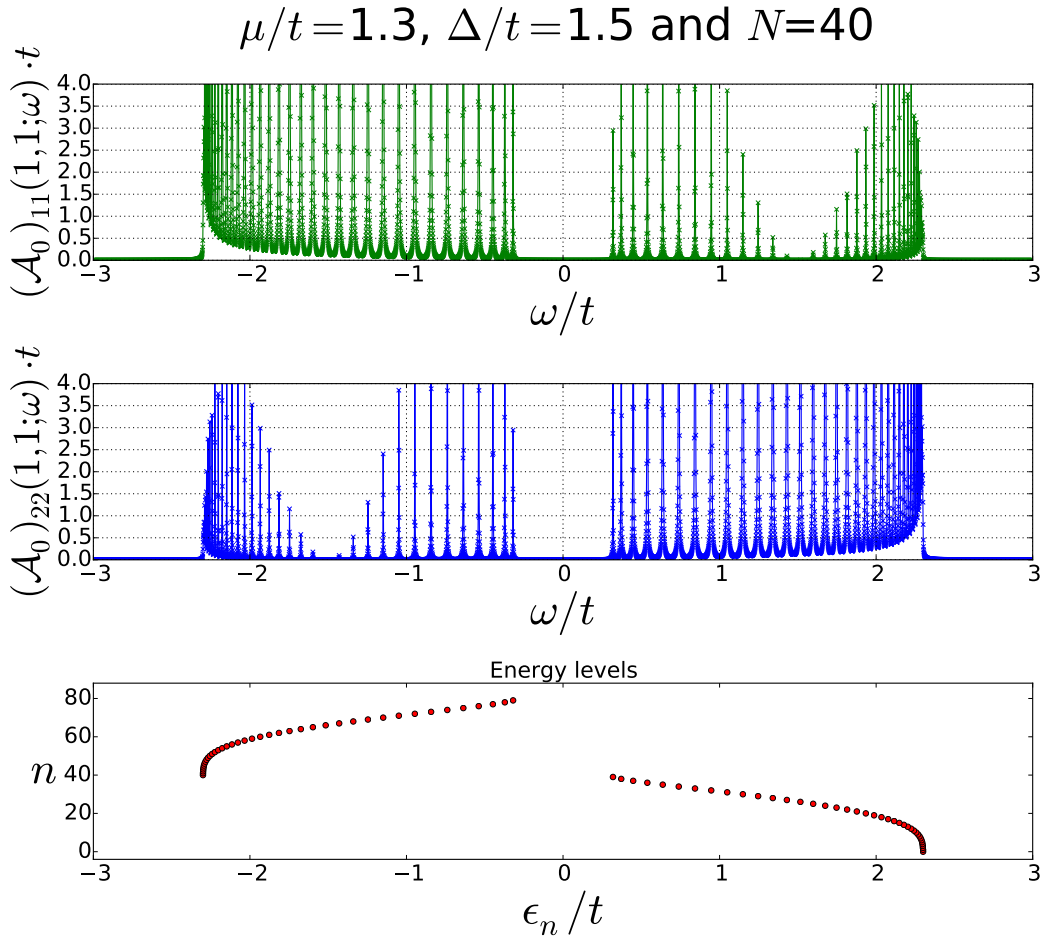

Figure 11: Components of the spectral function and energy spectrum in the trivial phase, where no edge states are observed.

We have now described the Kitaev chain in terms of GFs, and looked at the characteristics of the zero modes, giving us the necessary tools to investigate what happens when interactions are present. The same can be done for the topological aspects of the theory, where we look at symmetry classes and TIs. The next section will explore how to generalise the topological classification of free electrons, to one that includes interactions.

2.3 TOPOLOGICAL CLASSIFICATION OF INTERACTING SYSTEMS

2.3.1 *Generalization of symmetries to Green's functions*

As mentioned during the introduction, the recent decades of research in Topological quantum systems have, among other things, resulted in a description of topological phases by their symmetry classes (Altland-Zirnbauer), determined by Time-reversal, Particle-hole and Chiral symmetry. This was briefly discussed in section 2.1.3. These systems are characterized by TIs, which in non-interacting systems, are given by winding numbers or integrals of Berry-curvature, calculated from the Bloch-eigenfunctions to the non-interacting Hamiltonian. In an interacting system however,

these single-particle states cannot be obtained. These two concepts, the concept of symmetry classes and the corresponding TI for the system, need to be generalised to interacting systems. A way to do this, is to use the GF for the system, translate the symmetry properties to GFs, and cast the TIs in a form in which the GF enters. This section follows the work done in [15].
Now, we want to see how the symmetries of TR $\to \Theta$, PH $\to \Xi$ and C$\to \Pi$, translate from the Hamiltonian to the GF. To summarize, the symmetry conditions for the bulk-momentum space Hamiltonian is

$$\begin{aligned} \Theta\mathcal{H}(k)\Theta^{-1} &= \quad \mathcal{H}(-k) \\ \Xi\mathcal{H}(k)\Xi^{-1} &= -\mathcal{H}(-k) \\ \Pi\mathcal{H}(k)\Pi^{-1} &= -\mathcal{H}(k) \end{aligned} \tag{2.110}$$

With a non-interacting GF defined by

$$G_0(k,\omega) = \left[\omega - \mathcal{H}(k)\right]^{-1} \tag{2.111}$$

Where ω is a complex frequency. In principle one could just replace $\mathcal{H}(k)$ with $-G_0(k,0)^{-1}$ in the equations for the TIs, then everything would be written in terms of the GF. This is, however, not the correct procedure, since one cannot be sure that the symmetries are preserved once interactions are turned on $G_0(k,\omega) \to G(k,\omega)$. We need to translate the symmetry properties of the GFs to ones that include interactions, which will be done in the following. To do this, we find out how the symmetry transformations affect the second quantized operators, since these enter the full GF. The second quantized Hamiltonian (2nd quant. objects now carry a hat) can be written in terms of the real space Hamiltonian

$$\hat{H} = \hat{c}_i^\dagger \mathcal{H}_{ij} \hat{c}_j \tag{2.112}$$

Where i,j are summed. The three symmetries require $\mathcal{H}_{ij}$ to obey the following equations

$$\begin{aligned} T^\dagger \mathcal{H}^* T &= \quad \mathcal{H} \\ P^\dagger \mathcal{H}^* P &= -\mathcal{H} \\ Q^\dagger \mathcal{H} Q &= -\mathcal{H} \end{aligned} \tag{2.113}$$

With T, P and $Q = P^*T$ are the unitary matrix part of Θ, Ξ, Π. As before, time-reversal and particle-hole symmetry can square to 1 or -1, i.e. $P^*P = \pm 1, T^*T = \pm 1$ giving us the 10 symmetry classes needed to describe all non-interacting topological systems. Using these properties, and that $\mathcal{H}$ is Hermitian, the three symmetry conditions can be written on a form similar to before

$$\begin{aligned} T\mathcal{H}T^{-1} &= \quad \mathcal{H}^T \\ P\mathcal{H}P^{-1} &= -\mathcal{H}^T \\ Q\mathcal{H}Q^{-1} &= -\mathcal{H} \end{aligned} \tag{2.114}$$

Let us now see how a non-interacting GF $G_0(\omega) = [\omega - \mathcal{H}]^{-1}$, which contains a Hamiltonian with these symmetries, will transform under these operations.

$$\begin{aligned} TG_0(\omega)T^{-1} &= \left[T\left(\omega - \mathcal{H}\right)T^{-1}\right]^{-1} = \left[\omega - \mathcal{H}^T\right]^{-1} = \quad G_0(\omega)^T \\ PG_0(\omega)P^{-1} &= \left[P\left(\omega - \mathcal{H}\right)P^{-1}\right]^{-1} = \left[\omega + \mathcal{H}^T\right]^{-1} = -G_0(-\omega)^T \\ QG_0(\omega)Q^{-1} &= \left[Q\left(\omega - \mathcal{H}\right)Q^{-1}\right]^{-1} = \left[\omega + \mathcal{H}\right]^{-1} = \quad -G_0(-\omega) \end{aligned} \tag{2.115}$$

Where $(A^{-1})^T = (A^T)^{-1}$ for any matrix A has been used. The goal is now to generalize the symmetries in (2.114) so that the interacting GF $G(\omega)$ obeys (2.115). To do this, we utilize how the unitary symmetry transformations affect the second quantized Hamiltonian, consisting of creation and annihilation operators (now denoted as $\hat{T}, \hat{P}, \hat{Q}$ to show that they work on the second quantized operators, instead of T, P, Q which are matrices). From analysing how $\mathcal{H}$ transforms in (2.114), the symmetry transformation of an interacting many-body Hamiltonian is defined to be [15][3]

$$\begin{aligned} \hat{T}\hat{H}\hat{T}^\dagger &= \hat{H}^* \\ \hat{P}\hat{H}\hat{P}^\dagger &= \hat{H} \\ \hat{Q}\hat{H}\hat{Q}^\dagger &= \hat{H}^* \end{aligned} \tag{2.116}$$

Where the complex conjugation operation does not affect creation/annihilation operators. Let us check these for the non-interacting case where one has $\hat{H} = c_i^\dagger \mathcal{H}_{ij} c_j$. In this case $\hat{H}^* = c_i^\dagger \mathcal{H}_{ij}^* c_j = c_i^\dagger \mathcal{H}_{ij}^T c_j$. Writing these symmetries out will show how $\hat{c}$ and $\hat{c}^\dagger$ transform, e.g. for TR

$$\begin{aligned} \hat{T}\hat{H}\hat{T}^\dagger &= \hat{T}\hat{c}_i^\dagger \mathcal{H}_{ij}\hat{c}_j\hat{T}^\dagger = \left(\hat{T}\hat{c}_i^\dagger\hat{T}^\dagger\right)\mathcal{H}_{ij}\left(\hat{T}\hat{c}_j\hat{T}^\dagger\right) = \left(\hat{c}_n^\dagger T_{ni}\right)\mathcal{H}_{ij}\left(T_{jm}^\dagger \hat{c}_m\right) \\ &= \hat{c}_n^\dagger \mathcal{H}_{nm}^T \hat{c}_m = \hat{H}^* \end{aligned} \tag{2.117}$$

For PH

$$\begin{aligned} \hat{P}\hat{H}\hat{P}^\dagger &= \hat{P}\hat{c}_i^\dagger \mathcal{H}_{ij}\hat{c}_j\hat{P}^\dagger = \left(\hat{P}\hat{c}_i^\dagger\hat{P}^\dagger\right)\mathcal{H}_{ij}\left(\hat{P}\hat{c}_j\hat{P}^\dagger\right) = \left(P_{in}\hat{c}_n\right)\mathcal{H}_{ij}\left(\hat{c}_m^\dagger P_{mj}^\dagger\right) \\ &= \hat{c}_m^\dagger\left(-P_{in}\mathcal{H}_{ij}P_{mj}^\dagger\right)\hat{c}_n = \hat{c}_m^\dagger\left(-P_{mj}^\dagger \mathcal{H}_{ji}^T P_{in}\right)\hat{c}_n = \hat{c}_m^\dagger \mathcal{H}_{mn}\hat{c}_n = \hat{H} \end{aligned} \tag{2.118}$$

Where a general assumption of $\mathrm{Tr}\mathcal{H}$ has been made. For Q symmetry

$$\begin{aligned} \hat{Q}\hat{H}\hat{Q}^\dagger &= \hat{Q}\,\hat{c}_i^\dagger \mathcal{H}_{ij}\hat{c}_j\,\hat{Q}^\dagger = \left(\hat{Q}\hat{c}_i^\dagger\hat{Q}^\dagger\right)\mathcal{H}_{ij}\left(\hat{Q}\hat{c}_j\hat{Q}^\dagger\right) = \left(\hat{c}_n Q_{ni}\right)\mathcal{H}_{ij}\left(Q_{jm}^\dagger \hat{c}_m^\dagger\right) \\ &= \hat{c}_m^\dagger\left(-Q_{ni}\mathcal{H}_{ij}Q_{jm}^\dagger\right)\hat{c}_n = \hat{c}_m^\dagger \mathcal{H}_{mn}^T \hat{c}_n = \hat{H}^* \end{aligned} \tag{2.119}$$

[3] According to [15] this definition is not unique, since there is an alternative way to define the chiral symmetry. They mention that the one shown here is the most natural definition for application, so therefore we will proceed using (2.116).

So to sum up, the transformations that entail (2.116) are for the 2nd quantized operators

$$\begin{aligned}
\hat{T}\hat{c}_i^\dagger\hat{T}^\dagger &= \sum_n \hat{c}_n^\dagger T_{ni} & \hat{T}\hat{c}_i\hat{T}^\dagger &= \sum_n T_{in}^\dagger \hat{c}_n \\
\hat{P}\hat{c}_i^\dagger\hat{P}^\dagger &= \sum_n P_{in}\hat{c}_n & \hat{P}\hat{c}_i\hat{P}^\dagger &= \sum_n \hat{c}_n^\dagger P_{ni}^\dagger \\
\hat{Q}\hat{c}_i^\dagger\hat{Q}^\dagger &= \sum_n \hat{c}_n Q_{ni} & \hat{Q}\hat{c}_i\hat{Q}^\dagger &= \sum_n Q_{in}^\dagger \hat{c}_n^\dagger
\end{aligned} \tag{2.120}$$

Where $\hat{Q} = \hat{P}^\dagger\hat{T}$ can be derived from the properties of the matrices $Q = P^*T$. Now we have the necessities to check if the interacting GF obeys the symmetries in (2.115), when the many-body Hamiltonian has the symmetries in (2.116). First we define the so-called *Greater* and *Lesser* GFs as

$$\begin{aligned}
G_{ij}^{>}(t) &= -i\langle \hat{c}_i(t)\hat{c}_j^\dagger(0)\rangle \\
G_{ij}^{<}(t) &= \quad i\langle \hat{c}_j^\dagger(0)\hat{c}_i(t)\rangle
\end{aligned} \tag{2.121}$$

From these one can determine the Retarded and Advanced GFs

$$\begin{aligned}
G_{ij}^{R}(t) &= \quad \theta(t)\left(G_{ij}^{>}(t) - G_{ij}^{<}(t)\right) \\
G_{ij}^{A}(t) &= -\theta(-t)\left(G_{ij}^{>}(t) - G_{ij}^{<}(t)\right)
\end{aligned} \tag{2.122}$$

The Fourier transforms of these define the GF $G_{ij}(\omega)$ in the full complex plane (G^R on the upper half-plane and G^A on the lower). It is thus enough to show that $G_{ij}^{>}(t)$ and $G_{ij}^{<}(t)$ transform under the symmetry operations (2.115) for us to conclude that $G_{ij}(\omega)$ does as well. Some of the symmetries in (2.115) send $\omega \to -\omega$ for complex ω. To get the retarded GF we analytically continue $G_{ij}^R(\omega) = G_{ij}(\omega + i\eta)$, so the symmetries transform the retarded GF to the advanced GF $G_{ij}(-\omega - i\eta) = G_{ij}^A(-\omega)$. All results will be shown for $t > 0$ for $G_{ij}^{>}(t)$, but are also valid for $t < 0$, and $G_{ij}^{<}(t)$. First, let us examine Time Reversal symmetry, which implies that for every many-body state $|n\rangle$ there exist a time-reversed state $\hat{T}^\dagger|n^*\rangle$ with the same energy, since $\hat{H}\hat{T}^\dagger|n^*\rangle = \hat{T}^\dagger\hat{T}\hat{H}\hat{T}^\dagger|n^*\rangle = \hat{T}^\dagger\hat{H}^*|n^*\rangle = E_n\hat{T}^\dagger|n^*\rangle$. Specifically, one can assume the GS to be TR invariant

$$\hat{T}^\dagger|0^*\rangle = |0\rangle \qquad \hat{T}|0\rangle = |0^*\rangle \tag{2.123}$$

And also, we will need the identity

$$\langle n|\hat{A}|m\rangle = \langle m^*|\hat{A}^T|n^*\rangle \tag{2.124}$$

The zero temperature GF is determined from the GS, and under TR this is then given as

$$\begin{aligned} T\ iG^{>}(t)\ T^{\dagger} &= T_{ij}\ iG^{>}_{jk}(t)\ T^{\dagger}_{kl} = T_{ij}\ T^{\dagger}_{kl}\langle 0|e^{i\hat{H}t}\hat{c}_j e^{-i\hat{H}t}\hat{c}^{\dagger}_k|0\rangle \\ &= T_{ij}\ T^{\dagger}_{kl}\langle 0|\hat{T}^{\dagger}e^{i\hat{H}^*t}\hat{T}\hat{c}_j\hat{T}^{\dagger}e^{-i\hat{H}^*t}\hat{T}\hat{c}^{\dagger}_k\hat{T}^{\dagger}\hat{T}|0\rangle \\ &= T_{ij}\ T^{\dagger}_{kl}\ T^{\dagger}_{js}\ T_{pk}\langle 0^*|e^{i\hat{H}^*t}\hat{c}_s e^{-i\hat{H}^*t}\hat{c}^{\dagger}_p|0^*\rangle \\ &= T_{ij}\ T^{\dagger}_{js}\ T_{pk}\ T^{\dagger}_{kl}\langle 0|\hat{c}_p e^{-i\hat{H}t}\hat{c}^{\dagger}_s e^{i\hat{H}t}|0\rangle \\ &= \delta_{is}\ \delta_{pl}\ iG^{>}_{ps}(t) = iG^{>}_{li}(t) = iG^{>}_{il}(t)^T = iG^{>}(t)^T \end{aligned} \tag{2.125}$$

Which is exactly the symmetry transformation property from (2.115). For particle-hole symmetry the GS satisfies

$$\hat{P}|0\rangle = \hat{P}^{\dagger}|0\rangle = |0\rangle \tag{2.126}$$

Transforming the GF yields

$$\begin{aligned} P\ iG^{>}(t)\ P^{\dagger} &= P_{ij}\ iG^{>}_{jk}(t)\ P^{\dagger}_{kl} = P_{ij}\ P^{\dagger}_{kl}\langle 0|e^{i\hat{H}t}\hat{c}_j e^{-i\hat{H}t}\hat{c}^{\dagger}_k|0\rangle \\ &= P_{ij}\ P^{\dagger}_{kl}\langle 0|\hat{P}^{\dagger}e^{i\hat{H}t}\hat{P}\hat{c}_j\hat{P}^{\dagger}e^{-i\hat{H}t}\hat{P}\hat{c}^{\dagger}_k\hat{P}^{\dagger}\hat{P}|0\rangle \end{aligned} \tag{2.127}$$

Now, this expression will become simpler later if $\hat{P}^{\dagger}$ and $\hat{P}$ are commuted such that

$$\begin{aligned} &= P_{ij}\ P^{\dagger}_{kl}\langle 0|\hat{P}e^{i\hat{H}t}\hat{P}^{\dagger}\hat{c}_j\hat{P}^{\dagger}e^{-i\hat{H}t}\hat{P}\hat{c}^{\dagger}_k\hat{P}\hat{P}^{\dagger}|0\rangle \\ &= P_{ij}\ P^{\dagger}_{kl}\langle 0|e^{i\hat{H}t}\hat{P}^{\dagger}\hat{c}_j\hat{P}^{\dagger}e^{-i\hat{H}t}\hat{P}\hat{c}^{\dagger}_k\hat{P}|0\rangle \end{aligned} \tag{2.128}$$

The $\hat{P}^{\dagger}\hat{c}_j\hat{P}^{\dagger}$ and $\hat{P}\hat{c}^{\dagger}_k\hat{P}$ transformation rule is found by

$$\begin{aligned} \hat{P}\hat{H}\hat{P}^{\dagger} &= \left(\hat{P}\hat{c}^{\dagger}_i\hat{P}\right)\ \mathcal{H}_{ij}\ \left(\hat{P}^{\dagger}\hat{c}_j\hat{P}^{\dagger}\right) = \hat{c}_s P_{si}\ \mathcal{H}_{ij}\ P^{\dagger}_{jm}\hat{c}^{\dagger}_m \\ &= \hat{c}^{\dagger}_m\left(-P_{si}\ \mathcal{H}_{ij}\ P^{\dagger}_{jm}\right)\hat{c}_s = \hat{c}^{\dagger}_m\mathcal{H}_{ms}\hat{c}_s = \hat{H} \end{aligned} \tag{2.129}$$

So the transformation is

$$\hat{P}\hat{c}^{\dagger}_i\hat{P} = \sum_n \hat{c}_n P_{ni} \qquad \hat{P}^{\dagger}\hat{c}_i\hat{P}^{\dagger} = \sum_n P^{\dagger}_{in}\hat{c}^{\dagger}_n \tag{2.130}$$

Inserting this gives us

$$\begin{aligned} P\ iG^{>}(t)\ P^{\dagger} &= P_{ij}\ P^{\dagger}_{kl}\ P^{\dagger}_{jm}\ P_{nk}\langle 0|e^{i\hat{H}t}\hat{c}^{\dagger}_m e^{-i\hat{H}t}\hat{c}_n|0\rangle \\ &= -P_{ij}\ P^{\dagger}_{jm}\ P_{nk}\ P^{\dagger}_{kl}\langle 0|T_t\hat{c}_n e^{i\hat{H}t}\hat{c}^{\dagger}_m e^{-i\hat{H}t}|0\rangle \\ &= -\delta_{im}\ \delta_{nl}\ iG^{>}_{nm}(-t) = -iG^{>}_{il}(-t)^T = -iG^{>}(-t)^T \end{aligned} \tag{2.131}$$

With T_t being the time-ordering operator, and again, t is assumed positive, but results hold for negative times as well. This confirms the expected PH symmetry transformation rule. For chiral symmetry the GS can be taken to be invariant, i.e.

$$\hat{Q}^{\dagger}|0^*\rangle = |0\rangle \qquad \hat{Q}|0\rangle = |0^*\rangle \tag{2.132}$$

Using this, the chiral symmetry transforms the GF as

$$\begin{aligned} Q\, iG^{>}(t)\, Q^{\dagger} &= Q_{ij}\, iG^{>}_{jk}(t)\, Q^{\dagger}_{kl} = Q_{ij}\, Q^{\dagger}_{kl} \langle 0| e^{i\hat{H}t} \hat{c}_j e^{-i\hat{H}t} \hat{c}^{\dagger}_k |0\rangle \\ &= Q_{ij}\, Q^{\dagger}_{kl} \langle 0| \hat{Q}^{\dagger} e^{i\hat{H}^* t} \hat{Q} \hat{c}_j \hat{Q}^{\dagger} e^{-i\hat{H}t} \hat{Q} \hat{c}^{\dagger}_k \hat{Q}^{\dagger} \hat{Q} |0\rangle \\ &= Q_{ij}\, Q^{\dagger}_{kl}\, Q^{\dagger}_{js}\, Q_{pk} \langle 0^*| e^{i\hat{H}^* t} \hat{c}^{\dagger}_s e^{-i\hat{H}^* t} \hat{c}_p |0^*\rangle \\ &= Q_{ij}\, Q^{\dagger}_{js}\, Q_{pk}\, Q^{\dagger}_{kl} \langle 0| \hat{c}^{\dagger}_p e^{-i\hat{H}t} \hat{c}_s e^{i\hat{H}t} |0\rangle \\ &= -Q_{ij}\, Q^{\dagger}_{js}\, Q_{pk}\, Q^{\dagger}_{kl} \langle 0| T_t e^{-i\hat{H}t} \hat{c}_s e^{i\hat{H}t} \hat{c}^{\dagger}_p |0\rangle \\ &= -\delta_{is}\, \delta_{pl}\, iG^{>}_{sp}(-t) = -iG^{>}_{il}(-t) = -iG^{>}(-t) \end{aligned} \tag{2.133}$$

Showing the final symmetry operation of (2.115). We can then conclude that the interacting GF transforms under the symmetry transformations like the non-interacting case. For the Kitaev chain, the Hamiltonian is (2.58), where $\mathcal{H}^{\alpha\beta}_{ij}$ is a Nambu and site space matrix. We can determine the symmetry matrices $\mathcal{T}, \mathcal{P}$ and $\mathcal{Q}$ (instead of T, P and Q since the matrices now has Nambu structure)

$$\begin{aligned} \mathcal{T}^{\dagger} \mathcal{H}^* \mathcal{T} &= \mathcal{T}^{\dagger} \left[\left(-t_{ij} - \mu \delta_{ij} \right) \tau_z + i \tau_y \Delta_{ij} \right] \mathcal{T} = \quad \mathcal{H} \\ \mathcal{P}^{\dagger} \mathcal{H}^* \mathcal{P} &= \mathcal{P}^{\dagger} \left[\left(-t_{ij} - \mu \delta_{ij} \right) \tau_z + i \tau_y \Delta_{ij} \right] \mathcal{P} = -\mathcal{H} \\ \mathcal{Q}^{\dagger} \mathcal{H} \mathcal{Q} &= \mathcal{Q}^{\dagger} \left[\left(-t_{ij} - \mu \delta_{ij} \right) \tau_z + i \tau_y \Delta_{ij} \right] \mathcal{Q} = -\mathcal{H} \end{aligned} \tag{2.134}$$

From which one can conclude the simple form of the matrices

$$\mathcal{T}^{\alpha\beta}_{ij} = \delta_{ij} \delta^{\alpha\beta} \qquad \mathcal{P}^{\alpha\beta}_{ij} = \tau^{\alpha\beta}_x \delta_{ij} \qquad \mathcal{Q}^{\alpha\beta}_{ij} = \tau^{\alpha\beta}_x \delta_{ij} \tag{2.135}$$

With α, β as Nambu indices. We can cast the transformation of the 2nd quantized creation and annihilation operators from (2.120) in Nambu space as well

$$\begin{aligned} \hat{\mathcal{T}} \left(\hat{C}^{\dagger} \right)^{\alpha}_{i} \hat{\mathcal{T}}^{\dagger} &= \sum_n \left(\hat{C}^{\dagger} \right)^{\beta}_{n} \mathcal{T}^{\beta\alpha}_{ni} & \hat{\mathcal{T}} \hat{C}^{\alpha}_{i} \hat{\mathcal{T}}^{\dagger} &= \sum_n \left(\mathcal{T}^{\dagger} \right)^{\alpha\beta}_{in} \hat{C}^{\beta}_{n} \\ \hat{\mathcal{P}} \left(\hat{C}^{\dagger} \right)^{\alpha}_{i} \hat{\mathcal{P}}^{\dagger} &= \sum_n \mathcal{P}^{\alpha\beta}_{in} \hat{C}^{\beta}_{n} & \hat{\mathcal{P}} \hat{C}^{\alpha}_{i} \hat{\mathcal{P}}^{\dagger} &= \sum_n \left(\hat{C}^{\dagger} \right)^{\beta}_{n} \left(\mathcal{P}^{\dagger} \right)^{\beta\alpha}_{ni} \\ \hat{\mathcal{Q}} \left(\hat{C}^{\dagger} \right)^{\alpha}_{i} \hat{\mathcal{Q}}^{\dagger} &= \sum_n \hat{C}^{\beta}_{n} \mathcal{Q}^{\beta\alpha}_{ni} & \hat{\mathcal{Q}} \hat{C}^{\alpha}_{i} \hat{\mathcal{Q}}^{\dagger} &= \sum_n \left(\mathcal{Q}^{\dagger} \right)^{\alpha\beta}_{in} \left(\hat{C}^{\dagger} \right)^{\beta}_{n} \end{aligned} \tag{2.136}$$

Which means

$$\begin{aligned} \hat{\mathcal{T}} \hat{H} \hat{\mathcal{T}}^{\dagger} &= \hat{H}^* \\ \hat{\mathcal{P}} \hat{H} \hat{\mathcal{P}}^{\dagger} &= \hat{H} \\ \hat{\mathcal{Q}} \hat{H} \hat{\mathcal{Q}}^{\dagger} &= \hat{H}^* \end{aligned} \tag{2.137}$$

For this specific model the symmetries are (2.135), so one can conclude

$$\begin{aligned} \hat{\mathcal{T}}\hat{c}_i^\dagger\hat{\mathcal{T}}^\dagger &= \hat{c}_i^\dagger & \hat{\mathcal{T}}\hat{c}_i\hat{\mathcal{T}}^\dagger &= \hat{c}_i \\ \hat{\mathcal{P}}\hat{c}_i^\dagger\hat{\mathcal{P}}^\dagger &= \hat{c}_i^\dagger & \hat{\mathcal{P}}\hat{c}_i\hat{\mathcal{P}}^\dagger &= \hat{c}_i \\ \hat{\mathcal{Q}}\hat{c}_i^\dagger\hat{\mathcal{Q}}^\dagger &= \hat{c}_i^\dagger & \hat{\mathcal{Q}}\hat{c}_i\hat{\mathcal{Q}}^\dagger &= \hat{c}_i \end{aligned} \tag{2.138}$$

So the non-Nambu operators do not change under the symmetries. The Nambu operators change in a way that obeys the rules for the 2nd quantized Hamiltonian (2.137), with (2.135) as well. Thus the Nambu-Gorkov GF will also obey the GF symmetries (2.115), a fact we have shown also holds when including interactions. As a sanity check, let us see if the non-interacting Hamiltonian, written as

$$\hat{H}_0 = \sum_{ij}\left(-t_{ij} - \mu\delta_{ij}\right)\hat{c}_i^\dagger\hat{c}_j + \frac{\Delta_{ij}}{2}\left(\hat{c}_i^\dagger\hat{c}_j^\dagger - \hat{c}_i\hat{c}_j\right) \tag{2.139}$$

obeys the symmetries in (2.116) using the transformations (2.138). These are satisfied if $\hat{H} = \hat{H}^*$ which is true if $t_{ij} = t_{ij}^*$ and $\Delta_{ij} = \Delta_{ij}^*$. This is true for our case (remember that complex conjugation does not affect creation/annihilation operators), so everything is consistent.

2.3.2 *TI for interacting systems*

As mentioned in the beginning of the section, we want to describe the momentum space topology of these systems, and this is mainly done by determining TIs. For non-interacting systems these can only change when closing the bulk gap, and on boundaries there will be zero energy excitations. For interacting systems, this correspondence between bulk and boundary might change. As a simple example, to illustrate how the GF contains information about the momentum space topology, let us look at a TI for interacting $0D$ systems is given by [15]

$$N_0 = \mathrm{Tr}\int_{-\infty}^{\infty}\frac{d\Omega}{2\pi i}\mathcal{G}^{-1}\partial_\Omega\mathcal{G} \tag{2.140}$$

Where $\mathcal{G}(i\Omega) = G(\omega \to i\Omega)$ for $\Omega \in \mathbb{R}$ is the Matsubara GF and $i\Omega$ is the Matsubara frequency, which is a continuous variable at zero temperature. An important thing to notice is that both the Matsubara GF and its inverse enter the expression, so they both contribute to the value of the TI. Rewriting this one can conclude

$$N_0 = \mathrm{Tr}\int_{-\infty}^{\infty}\frac{d\Omega}{2\pi i}\partial_\Omega \ln\mathcal{G} = \int_{-\infty}^{\infty}\frac{d\Omega}{2\pi i}\partial_\Omega \ln\det\mathcal{G} \tag{2.141}$$

Where the identity $\mathrm{Tr}\ln = \ln\det$ is used. For the non-interacting case with $\mathcal{G}_0(i\Omega) = [i\Omega - \mathcal{H}]^{-1}$, one can use that the determinant is invariant under a unitary transformation, $\det\mathcal{G}_0 = \det U\tilde{\mathcal{G}}_0U^\dagger = \det U\det\tilde{\mathcal{G}}_0\det U^\dagger = \det UU^\dagger\det\tilde{\mathcal{G}}_0 = \det\tilde{\mathcal{G}}_0$ where $\tilde{\mathcal{G}}_0$ is diagonal, concluding

$$\det\mathcal{G}_0 = \prod_n\frac{1}{i\Omega - \epsilon_n} \tag{2.142}$$

By inserting this in the TI and using the property for the logarithm function $\ln \prod_n f(n) = \sum_n \ln f(n)$

$$N_0 = \sum_n \int_{-\infty}^{\infty} \frac{d\Omega}{2\pi i} \partial_\Omega \ln \frac{1}{i\Omega - \epsilon_n} = \sum_n \frac{1}{2\pi} \arg \left[\frac{1}{i\Omega - \epsilon_n} \right] \Bigg|_{-\infty}^{\infty} = \sum_n \frac{1}{2\pi} \arg \left[\frac{-i\Omega - \epsilon_n}{\Omega^2 + \epsilon_n^2} \right] \Bigg|_{-\infty}^{\infty}$$
$$= \sum_n \frac{1}{2\pi} \text{ArcTan} \left[\frac{\Omega}{\epsilon_n} \right] \Bigg|_{-\infty}^{\infty} = \frac{1}{2} \sum_n \text{sign } \epsilon_n \tag{2.143}$$

This contains the characteristics one expects, since the only way for N_0 to change by an integer, is by one state moving from positive to negative or vice versa, thus closing the gap. The integer changes when the system undergoes a topological phase transition. In the non-interacting case, the TI is a sum of all positive energy states minus all the negative, and these are signalled by poles in the single-particle GF. In [15] they show that the interacting GF not only contains poles, but also zeroes, which are also picked up by (2.141). The form of the determinant of the interacting GF is shown to be

$$\det G = \frac{\prod_s^{D_h - D_f} (\omega - r_s)}{\prod_n^{D_h} (\omega - \epsilon_n)} \tag{2.144}$$

Where r_s marks the position of a zero, while ϵ_n are the energies leading to poles in the determinant. D_h is the size of the combined Hilbert space of one extra electron or hole above the GS, and D_f is the number of degrees of freedom, which is just the number of creation and annihilation operators. Generally there are more states than operators $D_f \leq D_h$ but for a non-interacting system this inequality is saturated $D_f = D_h$, and all zeroes disappear. Zeroes disappear by merging with poles, and conversely, poles and zeroes emerge in pairs. The TI for the interacting case becomes

$$N_0 = \frac{1}{2} \sum_n \text{sign } \epsilon_n - \frac{1}{2} \sum_s \text{sign } r_s \tag{2.145}$$

So zeroes crossing from positive to negative or the other way around is a way for the interacting system to change TI, without closing the bulk gap, so the simple picture of the classification of Topological systems becomes more complicated when adding interactions, which is perhaps not a surprise. The fact that zeroes also can change the TI means that there is no generally valid bulk-boundary correspondence in interacting systems. The consequence of this analysis is that a boundary between two different topological phases need not have zero energy excitations, but instead have a zero energy zero of the GF, giving rise to the differing TI [10]. In [23] they have shown that this mechanism is behind the conclusion in Kitaev-Fidkowski [11], where it was shown that the system of interacting Majoranas in 8 chains could be adiabatically changed to the topologically trivial case, i.e. a reduction of the classification $\mathcal{Z} \to \mathcal{Z}_8$. The zeroes appearing in the interacting case signals a vanishing single-particle coherence, and is thus inherently a result of many-body interactions. A zero in the GF can be attributed to a pole in the self-energy, so it is an interesting quest to analyse the pole structure of $\Sigma(\omega)$ and see how a dynamical part of a self-energy can change the TI. We will se later that the TI for 1D chiral systems can be cast using the zero energy GF, so the dynamical contribution of $\Sigma(\omega)$ can in principle be inferred from $\Sigma(0)$. Up to now, the TI has only been calculated using

DMRG and other methods, which was done in [22] for electron-electron interactions in the Kitaev chain (discussed in chapter 4) and in [23] for the Peierls-Hubbard model. The hope was to analyse the TI including interactions, but it ended up being beyond the scope of this thesis for reasons of numerical complexity. In [23] they have a model similar to Fidkowski and Kitaev, and show that when they have 4 chains (4 and not 8 since they consider fermions instead of Majoranas), the zero energy poles are replaced by zeroes, showing that the zeroes in the GF are of great importance and call for further analysis.

2.3.3 *1D topological invariant with chiral symmetry*

In this section we want to investigate how to define a TI for the Kitaev chain that still works in the presence of interactions. It turns out to be possible for a 1D system with Chiral symmetry. This TI can be defined in the following way (due to [15] [23] [32]). The Kitaev Hamiltonian obeys

$$\sum_{jk}(\Pi^\dagger)^{\alpha\sigma}_{il}\mathcal{H}^{\sigma\rho}_{lk}\Pi^{\rho\beta}_{kj} = -\mathcal{H}^{\alpha\beta}_{ij} \qquad \Pi^{\alpha\beta}_{ij} = \delta_{ij}\tau_x^{\alpha\beta} \tag{2.146}$$

Written in the basis of the chiral operator τ_x such that $\Pi = U^\dagger \Pi U$ and $\mathcal{H} = U^\dagger \mathcal{H} U$ with $U = \frac{1}{\sqrt{2}}\begin{pmatrix}1 & 1\\ 1 & -1\end{pmatrix} = \frac{1}{\sqrt{2}}(\tau_z + \tau_x)$ one gets

$$\Pi^{\alpha\beta}_{ij} = \delta_{ij}\tau_z^{\alpha\beta} \qquad \mathcal{H}^{\alpha\beta}_{ij} \doteq \begin{pmatrix}0 & V_{ij}\\ V^\dagger_{ij} & 0\end{pmatrix} \qquad V_{ij} = -t_{ij} - \mu\delta_{ij} - \Delta_{ij} \tag{2.147}$$

Or in momentum space

$$\mathcal{H}^{\alpha\beta}(k) \doteq \begin{pmatrix}0 & V(k)\\ V^\dagger(k) & 0\end{pmatrix} \qquad V(k) = -t\cos k - \mu + i\Delta\sin k \tag{2.148}$$

The energy spectrum (the same found in (2.21)) and Bloch eigenfunctions are easily found to be

$$E_k = \pm|V(k)| = \pm\sqrt{(-t\cos k - \mu)^2 + (\Delta\sin k)^2}\,, \qquad |u_{k,\pm}\rangle = \frac{1}{\sqrt{2}}\begin{pmatrix}e^{i\varphi(k)}\\ \pm 1\end{pmatrix} \tag{2.149}$$

With $\varphi(k) = \arg[V(k)]$. The Bloch WF in the old basis is just $|\tilde{u}_{k,\pm}\rangle = U|u_{k,\pm}\rangle$. Now, a TI has been found by the procedure described in [8][26]. The TI is found as a coefficient in a low energy effective field theory of the system, describing a Topological Quantum Field Theory (TQFT). This is topological in the sense that the action is independent of the metric describing the space-time geometry [20]. The effective theory is found by coupling free fermions to an external gauge field A, then integrating out the fermions, resulting in an effective action for the gauge field $S_{eff}[A]$. The TI will be a coefficient to this effective action, which has the form of a Chern-Simons theory, a term that is only defined in $2d+1$ dimensions. By dimensional reduction, a TI can be defined for odd dimensions with a chiral

symmetry [6] (our case), which for the GFs mean (For now, the matrix notation will be suppressed , i.e. $\Pi^{\alpha\beta} \to \Pi$)

$$G(k,\omega) = -\Pi G(k,-\omega)\Pi \tag{2.150}$$

This TI uses the GFs at zero energy [23] [10] .

$$N_d = \frac{C_{d-1}}{2}\epsilon_{k_1\dots k_d}\mathrm{Tr}\int_{BZ} d^dk\ \Pi\ g^{-1}\partial_{k_1}g\dots g^{-1}\partial_{k_d}g\ , \qquad g(k) = \mathcal{G}(k,0) \tag{2.151}$$

Where d is an odd dimension, and

$$C_d = (2\pi i)^{-\frac{d}{2}-1}(\frac{d}{2})!/(d+1)! \tag{2.152}$$

So for the 1D case, the TI is

$$N_1 = \mathrm{Tr}\int_{BZ}\frac{dk}{4\pi i}\ \Pi\ g^{-1}\partial_k g\ , \qquad g(k) = \mathcal{G}(k,0) \tag{2.153}$$

Which is again exactly what we are interested in, since having a TI expressed in terms of the GFs allows us describe interacting systems. The fact that N_1 is TI can be seen by taking the derivative wrt. some parameter α of the Hamiltonian (α could be hopping, chemical potential, pairing strength, interactions strength etc.)

$$\begin{aligned}\frac{dN_1}{d\alpha} &= \mathrm{Tr}\int_{BZ}\frac{dk}{4\pi i}\ \partial_\alpha\left(\Pi\ g^{-1}\partial_k g\right) = \mathrm{Tr}\int_{BZ}\frac{dk}{4\pi i}\ \left(\Pi\ \partial_\alpha g^{-1}\partial_k g + \Pi\ g^{-1}\partial_\alpha\partial_k g\right)\\ &= \mathrm{Tr}\int_{BZ}\frac{dk}{4\pi i}\ \left(-\Pi\ g^{-1}\partial_\alpha g\ g^{-1}\partial_k g + \Pi\ g^{-1}\partial_k\partial_\alpha g\right)\end{aligned} \tag{2.154}$$

Where the derivative of an inverse matrix $\frac{d}{dk}\underline{\underline{A}}^{-1} = -\underline{\underline{A}}^{-1}\ \left[\frac{d}{dk}\underline{\underline{A}}\right]\ \underline{\underline{A}}^{-1}$ is used. Using that g and Π anti-commute ($g\Pi = -\Pi g$), and the cyclic properties of the trace

$$\begin{aligned}\frac{dN_1}{d\alpha} &= \mathrm{Tr}\int_{BZ}\frac{dk}{4\pi i}\ \left(-\Pi\ g^{-1}\partial_k g\ g^{-1}\partial_\alpha g + \Pi\ g^{-1}\partial_k\partial_\alpha g\right)\\ &= \mathrm{Tr}\int_{BZ}\frac{dk}{4\pi i}\ \left(\Pi\ \partial_k g^{-1}\partial_\alpha g + \Pi\ g^{-1}\partial_k\partial_\alpha g\right)\\ &= \mathrm{Tr}\int_{BZ}\frac{dk}{4\pi i}\ \Pi\partial_k\left(g^{-1}\partial_\alpha g\right) = 0\end{aligned} \tag{2.155}$$

Since the integral of a total derivative over the entire BZ is zero. N_1 does not change by varying the parameter α continuously, and is thus a TI. For now, we consider the non-interacting GF $\mathcal{G}_0$. One can determine the TI by utilizing the property that the trace is basis independent, so that it is possible to write the GF in the basis of the chiral operator Π such that

$$\Pi = \tau_z\ , \qquad g(k) = (-\mathcal{H}(k))^{-1} = \begin{pmatrix} 0 & -V^\dagger(k)^{-1} \\ -V(k)^{-1} & 0\end{pmatrix} \tag{2.156}$$

We could also just have written the zero energy GF (C.52) in the chiral basis directly, giving the same result. The TI then becomes

$$\begin{aligned} N_1 &= \mathrm{Tr}\int_{BZ}\frac{dk}{4\pi i}\,\tau_z\begin{pmatrix}0 & -V(k)\\ -V^\dagger(k) & 0\end{pmatrix}\begin{pmatrix}0 & -\partial_k V^\dagger(k)^{-1}\\ -\partial_k V(k)^{-1} & 0\end{pmatrix}\\ &= \mathrm{Tr}\int_{BZ}\frac{dk}{4\pi i}\,\tau_z\begin{pmatrix}V(k)\partial_k V(k)^{-1} & 0\\ 0 & V^\dagger(k)\partial_k V^\dagger(k)^{-1}\end{pmatrix}\\ &= \int_{BZ}\frac{dk}{4\pi i}\left(V(k)\partial_k V(k)^{-1} - V^\dagger(k)\partial_k V^\dagger(k)^{-1}\right)\\ &= -\int_{BZ}\frac{dk}{2\pi i}\,V(k)^{-1}\partial_k V(k) \end{aligned} \tag{2.157}$$

Where both $V^\dagger(k) = V(-k)$ and partial integration was used. This TI describes the *winding* of the function $V(k)$ around the origin as k sweeps the Brillouin zone, a process we will examine in detail in the following. In figure 12 the real and imaginary parts of the function $V(k)$ are plotted in the top row, as k covers the interval $[-\pi,\pi]$ for fixed t,Δ and different μ. The TI in (2.157) is the form of a contour integral, and the integrand $\frac{\partial_k V(k)}{V(k)}$ has a simple pole at $V(z_0)=0$ located at the origin of the Argand diagram. If the contour integral does not include this pole, then Cauchy's theorem tells us that the integral is zero. If the pole is included, then the *Residue Theorem* dictates the result of the integral [27], and for simple poles with integrands of the form $f(z)=\frac{g(z)}{h(z)}$ with $h(z_0)=0$ we then have $\mathrm{Res}(f,z_0)=\frac{g(z_0)}{h'(z_0)}$. For this case the TI thus becomes

$$N_1 = -\oint\frac{dk}{2\pi i}\,\frac{\partial_k V(k)}{V(k)} = 2\pi i\sum Residues = -\frac{2\pi i}{2\pi i}\frac{\partial_k V(k)|_{k=z_0}}{\partial_k V(k)|_{k=z_0}} = -1 \tag{2.158}$$

And from the function $V(k) = -t\cos k - \mu + i\Delta\sin k$, one sees that the pole is included when $|t|>|\mu|$, giving

$$N_1 = \begin{cases} 0 & |t|<|\mu| \;\; trivial\\ -1 & |t|>|\mu| \;\; topological\end{cases} \tag{2.159}$$

In figure 12 the energy spectrum 2.21 is also plotted. The gap is present for both the trivial and the topological phase, but exactly where they cross defines a topological phase transition, signified by the gap closing.

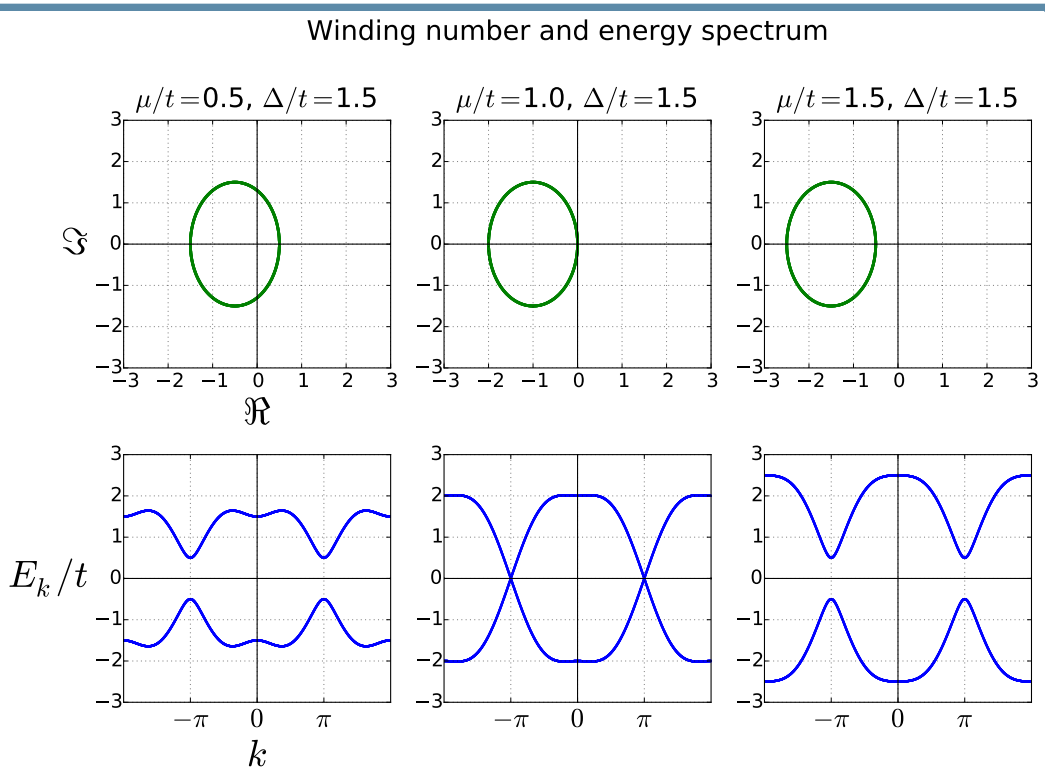

Figure 12: In the first column of plots $|t| > |\mu|$ so $N_1 = -1$ corresponding to a system in the topological phase (the contour winds around the origin). In the middle column $|t| = |\mu|$ which is exactly at the transition point, where the gap in the spectrum at $\{-\pi, \pi\}$ closes. In the last column, the origin is not included in the contour, so $N_1 = 0$ and no edge states exists at the boundary. For the symmetric case $t = \Delta$, the contour of $V(k)$ is a circle instead of an ellipse.

In this non-interacting case, one was able to determine the Bloch functions, so let us calculate the Zak phase [9], which is the Berry phase accumulated for the Bloch eigenfunctions when k varies over the entire Brillouin zone

$$\mathcal{Z} = i \oint dk \, \langle u_k | \partial_k | u_k \rangle = i \oint \frac{dk}{2} \begin{pmatrix} e^{-i\varphi(k)} & \pm 1 \end{pmatrix} \partial_k \begin{pmatrix} e^{i\varphi(k)} \\ \pm 1 \end{pmatrix} =$$
$$i \oint \frac{dk}{2} \begin{pmatrix} e^{-i\varphi(k)} & \pm 1 \end{pmatrix} \begin{pmatrix} i e^{i\varphi(k)} \partial_k \varphi(k) \\ 0 \end{pmatrix} = -\frac{1}{2} \oint dk \, \frac{d\varphi(k)}{dk} = -\frac{\Delta\varphi}{2} \tag{2.160}$$

Where $\Delta\varphi$ is the total accumulated phase. In figure 12 it is shown how the phase $\varphi(k)$, which here is the angle that $V(k)$ makes in the Argand diagram, changes with varying k. If the origin is not contained in the circle, then there is no difference in phase, i.e. $\Delta\varphi = 0$. If, however, the origin is included, the phase will have changed $\Delta\varphi = 2\pi$ (the vector $V(k)$ has wound an entire circle around the origin). We can thus conclude that the Zak phase is related to the TI by πN_1. A similar analysis of the topological criteria for the SSH model is performed in Appendix D.1. Also, the relation between this Berry phase TI and the Pfaffian TI from before was shown in [5].

3 THE INTERACTING KITAEV CHAIN - ELECTRON-BOSON

3.1 ELECTRON-BOSON INTERACTIONS

In this section we will investigate how the characteristics of the Majorana zero modes change, when the system contains bosonic modes that the electrons can interact with. The Hamiltonian we want to investigate is

$$H = H_K + H_b + H_{el-b} \tag{3.1}$$

Where H_K is the normal Kitaev Hamiltonian, H_b is the Hamiltonian for the free bosons and H_{el-b} describes the coupling between electrons and bosons. The latter two Hamiltonians are chosen to be

$$H_b = \sum_\lambda \omega_\lambda \left(a_\lambda^\dagger a_\lambda + \frac{1}{2} \right) \tag{3.2}$$

$$H_{el-b} = \sum_{\nu\nu'\lambda} g_{\nu\nu'\lambda}\, c_\nu^\dagger c_{\nu'} \underbrace{\left(a_\lambda + a_\lambda^\dagger \right)}_{\varphi_\lambda} \tag{3.3}$$

Where ω_λ is the energy spectrum for the free phonons, and $g_{\nu\nu'\lambda}$ is the interaction strength. These are written using arbitrary quantum numbers (ν, ν', λ), since we want to derive the Feynman rules for the general case, and then afterwards inspect the real space version where the quantum numbers becomes lattice sites $(\nu, \nu', \lambda) \to (i, j, l)$.

3.1.1 *Nambu-Gorkov GF*

We want to find the propagator that describes a particle going from state ν_a at τ_a to state ν_b at τ_b, interacting along the way. This is described by the full Nambu-Gorkov GF

$$\begin{aligned}
\mathcal{G}^{\beta\alpha}(\nu_b, \tau_b\ ;\ \nu_a, \tau_a) &= -\langle T_\tau \left(C^\beta_{\nu_b}(\tau_b)(C^\dagger)^\alpha_{\nu_a}(\tau_a) \right) \rangle \\
&\doteq \begin{pmatrix} \mathcal{G}^{ee}(\nu_b, \tau_b\ ;\ \nu_a, \tau_a) & \mathcal{G}^{eh}(\nu_b, \tau_b\ ;\ \nu_a, \tau_a) \\ \mathcal{G}^{he}(\nu_b, \tau_b\ ;\ \nu_a, \tau_a) & \mathcal{G}^{hh}(\nu_b, \tau_b\ ;\ \nu_a, \tau_a) \end{pmatrix} \\
&\doteq \begin{pmatrix} -\langle T_\tau \left(c_{\nu_b}(\tau_b) c^\dagger_{\nu_a}(\tau_a) \right) \rangle & -\langle T_\tau \left(c_{\nu_b}(\tau_b) c_{\nu_a}(\tau_a) \right) \rangle \\ -\langle T_\tau \left(c^\dagger_{\nu_b}(\tau_b) c^\dagger_{\nu_a}(\tau_a) \right) \rangle & -\langle T_\tau \left(c^\dagger_{\nu_b}(\tau_b) c_{\nu_a}(\tau_a) \right) \rangle \end{pmatrix}
\end{aligned} \tag{3.4}$$

Where again α and β are Nambu indices, and the C operators are Nambu spinors $C^\beta_{\nu_b} = \begin{pmatrix} c_{\nu_b} \\ c^\dagger_{\nu_b} \end{pmatrix}$. The average is now wrt. the full Hamiltonian, which includes electron-boson interactions. Calculating this GF will be done by creating a perturbation series in the interaction coefficient $g_{\nu\nu'\lambda}$, and then use Feynman diagrams to represent terms of a given order. The GF in equation (3.4) will be viewed diagrammatically as

$$\mathcal{G}^{\beta\alpha}(\nu_b,\tau_b\,;\,\nu_a,\tau_a) = \underset{\nu_b\tau_b\beta \qquad \nu_a\tau_a\alpha}{\text{= = = = = = = =}} \doteq \begin{pmatrix} \nu_b\tau_b \;\; \mathcal{G}^{ee} \;\; \nu_a\tau_a & \nu_b\tau_b \;\; \mathcal{G}^{eh} \;\; \nu_a\tau_a \\ \nu_b\tau_b \;\; \mathcal{G}^{he} \;\; \nu_a\tau_a & \nu_b\tau_b \;\; \mathcal{G}^{hh} \;\; \nu_a\tau_a \end{pmatrix}$$

Where the dashed line denotes the Nambu matrix GF structure (the matrix indices are denoted by β, α being e or h), and the plain arrows are specific entrances in this matrix, referring to the various kinds of GFs (ee, eh, he, hh). To differentiate between them, look from right to left, and if the arrow points along this direction it is an electronic component otherwise it is a hole component. The bare version is

$$\mathcal{G}_0^{\beta\alpha}(\nu_b,\tau_b\,;\,\nu_a,\tau_a) = \underset{\nu_b\tau_b\beta \qquad \nu_a\tau_a\alpha}{\text{- - - - - - - -}} \doteq \begin{pmatrix} \nu_b\tau_b \;\; \mathcal{G}_0^{ee} \;\; \nu_a\tau_a & \nu_b\tau_b \;\; \mathcal{G}_0^{eh} \;\; \nu_a\tau_a \\ \nu_b\tau_b \;\; \mathcal{G}_0^{he} \;\; \nu_a\tau_a & \nu_b\tau_b \;\; \mathcal{G}_0^{hh} \;\; \nu_a\tau_a \end{pmatrix}$$

We have already calculated the free GF for the electrons using the Kitaev model Hamiltonian, both in real space in section 2.2.4, which was done numerically, and for momentum space in Appendix C.5. We will also need the bosonic Matsubara GF for the free phonons

$$\mathcal{D}_0(\lambda_b,\tau_b;\lambda_a,\tau_a) \equiv -\langle T_\tau \left(\hat{\varphi}_{\lambda_b}(\tau_b)\hat{\varphi}^\dagger_{\lambda_a}(\tau_a)\right)\rangle_0 \tag{3.5}$$

Where the subscript zero refers to the non-interacting part of the Hamiltonian, which in this case is H_b. The hat over the operators $\hat{\varphi}_\lambda(\tau)$ declares the usage of the imaginary time interaction picture $\hat{\varphi}_\lambda(\tau) = e^{H_b\tau}\varphi_\lambda e^{-H_b\tau}$. Usually the τ evolution is in the Heisenberg picture, but these two pictures coincide since H_b does not depend on time. This GF is calculated in Appendix C.3 and is given by

$$\mathcal{D}_0(\lambda_b,\lambda_a;iq_n) = \underset{\lambda_b \qquad\qquad \lambda_a}{\sim\sim\sim\sim\sim} = \delta_{\lambda_b\lambda_a}\frac{2\,\omega_{\lambda_a}}{(iq_n)^2-\omega^2_{\lambda_a}} \tag{3.6}$$

3.2 PERTURBATION THEORY FOR ELECTRON-PHONON INTERACTIONS

In this section we set up a perturbation theory for calculating the full GFs in equation (3.4). The small parameter is the interaction strength $g_{\nu\nu'\lambda}$. The basic interaction vertex is

$H_{el-b} =$ 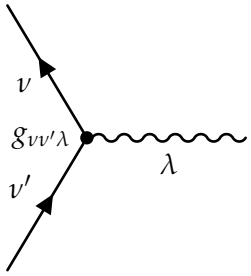

Which, together with the bare GFs for both the bosons and the electrons, constitute our basic ingredients in the diagrams. First, let us write the basic interaction in Nambu space (using that $g_{\nu\nu'\lambda} = g^*_{\nu'\nu\lambda}$ since the Hamiltonian is Hermitian)

$$\begin{aligned} H_{el-b} &= \sum_{\nu\nu'\lambda} g_{\nu\nu'\lambda}\, c^\dagger_\nu c_{\nu'} \varphi_\lambda = \frac{1}{2}\sum_{\nu\nu'\lambda}\left(g_{\nu\nu'\lambda}\, c^\dagger_\nu c_{\nu'} + g^*_{\nu'\nu\lambda} c^\dagger_\nu c_{\nu'}\right)\varphi_\lambda \\ &= \frac{1}{2}\sum_{\nu\nu'\lambda}\left(g_{\nu\nu'\lambda}\, c^\dagger_\nu c_{\nu'} + g^*_{\nu'\nu\lambda}\left[\delta_{\nu\nu'} - c_{\nu'} c^\dagger_\nu\right]\right)\varphi_\lambda \\ &= \frac{1}{2}\sum_{\nu\nu'\lambda}\left(g_{\nu\nu'\lambda}\, c^\dagger_\nu c_{\nu'} - g^*_{\nu\nu'\lambda} c_\nu c^\dagger_{\nu'}\right)\varphi_\lambda \\ &= \frac{1}{2}\sum_{\nu\nu'\lambda}\begin{pmatrix} c^\dagger_\nu & c_\nu\end{pmatrix}\begin{pmatrix} g_{\nu\nu'\lambda} & 0 \\ 0 & -g^*_{\nu\nu'\lambda}\end{pmatrix}\begin{pmatrix} c_{\nu'} \\ c^\dagger_{\nu'}\end{pmatrix}\varphi_\lambda = \frac{1}{2}\sum_{\nu\nu'\lambda} g_{\nu\nu'\lambda}\,(C^\dagger)^\sigma_\nu\,\tau_z^{\sigma\sigma'}\,C^{\sigma'}_{\nu'}\varphi_\lambda \end{aligned} \tag{3.7}$$

Assuming $g_{\nu\nu'\lambda}$ is real matrix (which it will be for our purpose). If this is not the case, then one should use the matrix $\begin{pmatrix} g_{\nu\nu'\lambda} & 0 \\ 0 & -g^*_{\nu\nu'\lambda}\end{pmatrix}$ at each vertex. Summation over repeated Nambu indices σ and σ' is implied. The constant term $\delta_{\nu\nu'}$ is discarded, and the factor $\frac{1}{2}$ is due to the usual double counting of particle-hole contributions, which is included only when writing out the full occupation number Hamiltonian with creation and annihilation operators, but ignored when calculating everything in Nambu matrices. Now let us look at $\mathcal{G}^{\beta\alpha}(\nu_b,\tau_b\,;\,\nu_a,\tau_a)$ describing the dressed Nambu space propagator for going from imaginary time and quantum number a to b.

$$\begin{aligned} \mathcal{G}^{\beta\alpha}(\nu_b,\tau_b\,;\,\nu_a,\tau_a) &= -\langle T_\tau\left(C^\beta_{\nu_b}(\tau_b)(C^\dagger)^\alpha_{\nu_a}(\tau_a)\right)\rangle \\ &= \frac{-\mathrm{Tr}\left[e^{-\beta H}\,T_\tau\left(C^\beta_{\nu_b}(\tau_b)(C^\dagger)^\alpha_{\nu_a}(\tau_a)\right)\right]}{\mathrm{Tr}\left[e^{-\beta H}\right]} \end{aligned} \tag{3.8}$$

This GF is written in the Heisenberg picture, but a systematic way of expanding the average in powers of the interaction is best done in the interaction picture, which is shown in detail in Appendix E.1. The definition of the interaction picture is that operators are chosen to follow τ evolution wrt. the bare Hamiltonian $H_0 = H_K + H_b$

and states wrt. to the perturbation $V = H_{el-b}$ [4]. Doing this one can exchange the Boltzmann weight with a unitary operator $\hat{U}$ via $e^{-\beta H} = e^{-\beta H_0}\hat{U}(\beta, 0)$ where

$$\hat{U}(\tau, \tau_0) = \sum_{n=0}^{\infty} \frac{(-1)^n}{n!} \int_{\tau_0}^{\tau} d\tau_1 \cdots \int_{\tau_0}^{\tau} d\tau_n T_\tau \left(\hat{V}(\tau_1) \dots \hat{V}(\tau_n)\right) = T_\tau e^{-\int_{\tau_0}^{\tau} d\tau_1 \hat{V}(\tau_1)} \tag{3.9}$$

Allowing us to write the full GF as

$$\mathcal{G}^{\beta\alpha}(\nu_b, \tau_b\ ;\ \nu_a, \tau_a) = \frac{-\langle T_\tau \left(\hat{U}(\beta, 0)\hat{C}^{\beta}_{\nu_b}(\tau_b)(\hat{C}^{\dagger})^{\alpha}_{\nu_a}(\tau_a)\right)\rangle_0}{\langle \hat{U}(\beta, 0)\rangle_0} \tag{3.10}$$

This form of the GF is easier to work with, compared to (3.8), since the averaging is done wrt. to the bare Hamiltonian. One expands $\hat{U}(\beta, 0)$ to the desired order in the interaction, write multi-particle averages as products of single-electron averages, which then yields an approximate value for the full GF. Using the interaction Hamiltonian from equation (3.3) gives

$$\begin{aligned}
&\mathcal{G}^{\beta\alpha}(\nu_b, \tau_b\ ;\ \nu_a, \tau_a) = \\
&\frac{-\sum_{n=1}^{\infty} \frac{(-1)^n}{n!} \int_0^{\beta} d\tau_1 \cdots \int_0^{\beta} d\tau_n \langle T_\tau \left(\hat{V}(\tau_1) \dots \hat{V}(\tau_n)\hat{C}^{\beta}_{\nu_b}(\tau_b)(\hat{C}^{\dagger})^{\alpha}_{\nu_a}(\tau_a)\right)\rangle_0}{\sum_{n=1}^{\infty} \frac{(-1)^n}{n!} \int_0^{\beta} d\tau_1 \cdots \int_0^{\beta} d\tau_n \langle T_\tau \left(\hat{V}(\tau_1) \dots \hat{V}(\tau_n)\right)\rangle_0}
\end{aligned} \tag{3.11}$$

With

$$\hat{V}(\tau) = \sum_{\nu\nu'\lambda} g_{\nu\nu'\lambda} (\hat{C}^{\dagger})^{\sigma}_{\nu}(\tau) \tau_z^{\sigma\sigma'} \hat{C}^{\sigma'}_{\nu'}(\tau) \hat{\varphi}_\lambda(\tau) \tag{3.12}$$

Since the average is wrt. the bare Hamiltonian, the electronic and bosonic degrees of freedom decouple, and one gets a product between an average containing only electron spinor operators and one with only boson operators. Inserting the interaction terms, one encounters terms like

$$\begin{aligned}
&\langle T_\tau \Big(\hat{\varphi}_{\lambda_1}(\tau_1) \dots \hat{\varphi}_{\lambda_n}(\tau_n)\ (\hat{C}^{\dagger})^{\sigma_1}_{\nu_1}(\tau_1) \tau_z^{\sigma_1\sigma_1'} \hat{C}^{\sigma_1'}_{\nu_1'}(\tau_1) \\
&\dots (\hat{C}^{\dagger})^{\sigma_n}_{\nu_n}(\tau_n) \tau_z^{\sigma_n\sigma_n'} \hat{C}^{\sigma_n'}_{\nu_n'}(\tau_n)\ \hat{C}^{\beta}_{\nu_b}(\tau_b)(\hat{C}^{\dagger})^{\alpha}_{\nu_a}(\tau_a)\Big)\rangle_0 \\
=&\langle T_\tau \left(\hat{\varphi}_{\lambda_1}(\tau_1) \dots \hat{\varphi}_{\lambda_n}(\tau_n)\right)\rangle_0\ \langle T_\tau \Big((\hat{C}^{\dagger})^{\sigma_1}_{\nu_1}(\tau_1) \tau_z^{\sigma_1\sigma_1'} \hat{C}^{\sigma_1'}_{\nu_1'}(\tau_1) \\
&\dots (\hat{C}^{\dagger})^{\sigma_n}_{\nu_n}(\tau_n) \tau_z^{\sigma_n\sigma_n'} \hat{C}^{\sigma_n'}_{\nu_n'}(\tau_n)\ \hat{C}^{\beta}_{\nu_b}(\tau_b)(\hat{C}^{\dagger})^{\alpha}_{\nu_a}(\tau_a)\Big)\rangle_0
\end{aligned} \tag{3.13}$$

The thermal average for the bosons is non-zero only for an even number of φ_λ operators. Using Wick's theorem allows us to write the many-particle GF as a product of single particle functions of the form

$$\langle T_\tau \left(\hat{\varphi}_{\lambda_i}(\tau_i)\hat{\varphi}_{\lambda_j}(\tau_j)\right)\rangle_0 = -\mathcal{D}_0(\lambda_i, \lambda_j; \tau_i - \tau_j) \tag{3.14}$$

The averages containing multiple electron spinor operators can also be expanded in products of singe-particle Nambu-Gorkov GFs by Wick's theorem. The calculation is detailed in Appendix E, where the full GF is calculated to 2nd order, and by looking at the diagrams and the terms they represent, one can conclude the following *Feynman Rules*

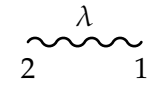

$$= -\mathcal{D}_0(\lambda; \tau_2 - \tau_1)$$

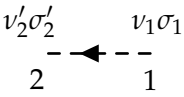

$$= \mathcal{G}_0^{\sigma_2'\sigma_1}(\nu_2', \nu_1; \tau_2 - \tau_1)$$

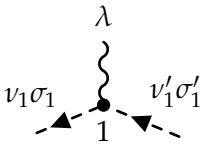

$$= \int_0^\beta d\tau_1 \sum_{\substack{\nu_1\nu_1'\lambda \\ \sigma_1\sigma_1'}} g_{\nu_1\nu_1'\lambda} \tau_z^{\sigma_1\sigma_1'}$$

For F fermion loops, multiply by $(-1)^F$

$\sum$ *topologically different* diagrams (3.15)

As an example, lets write out the following diagram

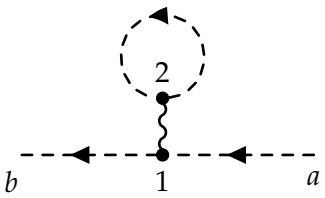

$$= \int d\tau_1 \int d\tau_2 \sum_{\substack{\sigma_1\sigma_1' \\ \sigma_2\sigma_2'}} \sum_{\substack{\nu_1\nu_1'\lambda \\ \nu_2\nu_2'}} g_{\nu_1\nu_1'\lambda} g_{\nu_2\nu_2'\lambda} \mathcal{D}_0(\lambda; \tau_2 - \tau_1)$$

$$\times \mathcal{G}_0^{\beta\sigma_1}(\nu_b, \nu_1; \tau_b - \tau_1) \tau_z^{\sigma_1\sigma_1'} \mathcal{G}_0^{\sigma_1'\alpha}(\nu_1', \nu_a; \tau_1 - \tau_a) \tau_z^{\sigma_2\sigma_2'} \mathcal{G}_0^{\sigma_2'\sigma_2}(\nu_2', \nu_2; 0)$$

$$= \int d\tau_1 \int d\tau_2 \sum_{\substack{\nu_1\nu_1'\lambda \\ \nu_2\nu_2'}} g_{\nu_1\nu_1'\lambda} g_{\nu_2\nu_2'\lambda} \mathcal{D}_0(\lambda; \tau_2 - \tau_1)$$

$$\times \underline{\underline{\mathcal{G}_0}}(\nu_b, \nu_1; \tau_b - \tau_1) \tau_z \underline{\underline{\mathcal{G}_0}}(\nu_1', \nu_a; \tau_1 - \tau_a) \mathrm{Tr}\left[\tau_z \underline{\underline{\mathcal{G}_0}}(\nu_2', \nu_2; 0)\right] \tag{3.16}$$

Where the minus sign for the fermion loop has cancelled with the one attached to the bosonic propagator, and the Nambu structure is written as matrix multiplication. Notice the tadpole part of the diagram becomes a trace in Nambu space. This notation compactifies a lot of the information, since it contains all the diagrams (ee, eh, he, hh) for a given process. This perturbation expansion has been performed using general quantum numbers, but in the following, we will assume a specific form of the interaction Hamiltonian. The goal is to compare the GF including interactions with the non-interacting case, and see how these change the behaviour of the GF.

3.3 EFFECTS OF CHARGE FLUCTUATIONS BY COUPLING TO A VOLTAGE GATE

A specific example if this bosonic interaction in question, is the system depicted in figure 13, which describes a topological nanowire coupled to a capacitative gate,

which has fluctuations in the potential due to some impedance in the system, which can be modelled by bosonic modes φ. The interaction we consider is now [1]

$$H_{el-b} = \sum_{im} g_i c_i^\dagger c_i (V_m a_m + V_m^* a_m^\dagger) = \frac{1}{2}\sum_i g_i (C^\dagger)_i^\sigma \ \tau_z^{\sigma\sigma'} \ C_i^{\sigma'} \ \varphi + \text{const.}$$
$$\varphi = \sum_m (V_m a_m + V_m^* a_m^\dagger) \tag{3.17}$$

Where in the Nambu description, we again ignore the constant term and the double counting factor. It is assumed g_i only depends on the position of the electron density, and that this couples to all the bosonic modes (φ is a sum over all m). In addition, one has the condition $g_i = g_i^*$ and $V_m = V_m^*$, in order for this interaction term to still obey the symmetries in (2.137).

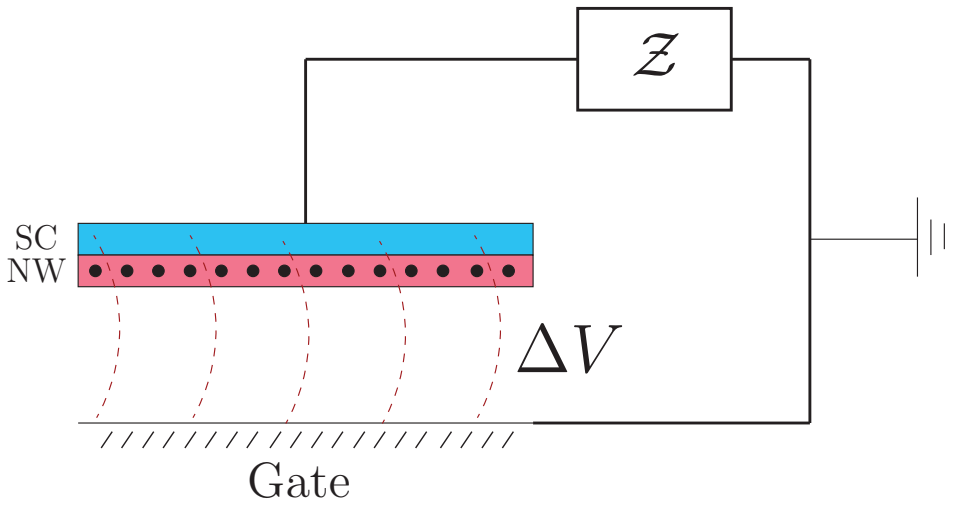

Figure 13: Sketch of the system, where a Kitaev chain is coupled to a gate. The potential difference from the superconductor to the gate leads to an effective potential in the NW which fluctuates. The power sources should be placed so as to ensure the capacitor with the NW is coupled in parallel with the impedance $\mathcal{Z}$. We have here considered a constant g_i coupling all sites, but this could in principle be made so that the gate only couples to part of the wire (as considered in [29]).

The new Matsubara GF for the boson is related to the old, by

$$\tilde{\mathcal{D}}_0(iq_n) = \sum_m |V_m|^2 \mathcal{D}_0(m, iq_n) \tag{3.18}$$

In Appendix E.3 some examples of calculations of diagrams are shown, and these are transformed into Matsubara frequency space, from which we can now write the Feynman rules in Real space - Matsubara frequency

[1] Similar to the one considered in [29]

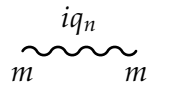

$$= -\sum_m |V_m|^2 \mathcal{D}_0(m; iq_n)$$

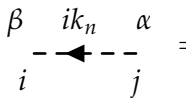

$$= \mathcal{G}_0^{\beta\alpha}(i, j; ik_n)$$

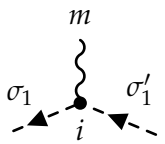

$$= \sum_i g_i \tau_z^{\sigma_1 \sigma_1'}$$

For F fermion loops, multiply by $(-1)^F$
$\sum$ *topologically different* diagrams
Conserve the Matsubara frequency at each vertex
Sum over repeated Nambu indices
Multiply by $\frac{1}{\beta}$ for each internal frequency ip_n and perform the sum $\sum_{ip_n}$

(3.19)

3.4 FOCK SELF-ENERGY TERM

If one wants to compute the full GF, one needs to sum all the diagrams

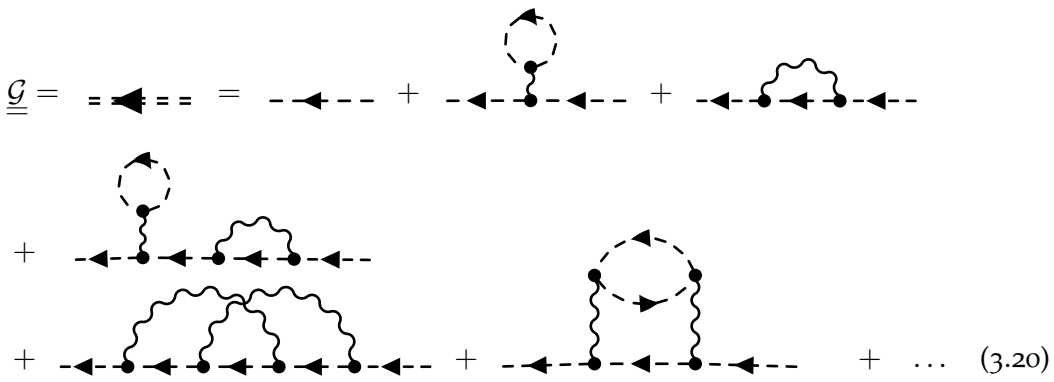

(3.20)

Which can be simplified by introducing the self energy, defined as the sum of all irreducible diagrams, without external lines

$\underline{\underline{\Sigma}} =$

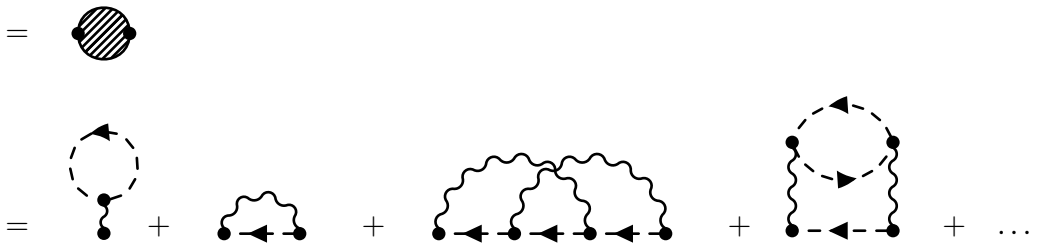

(3.21)

The full GF can then be written as [4].

$\underline{\underline{\mathcal{G}}}(i,j;ik_n) =$

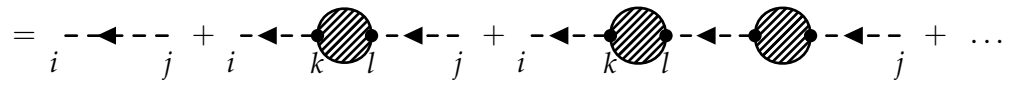

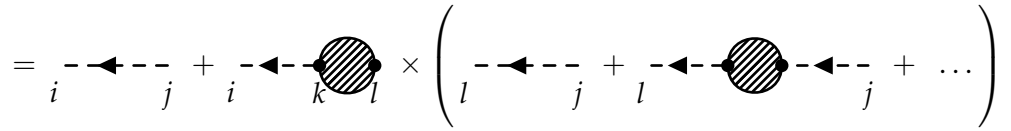

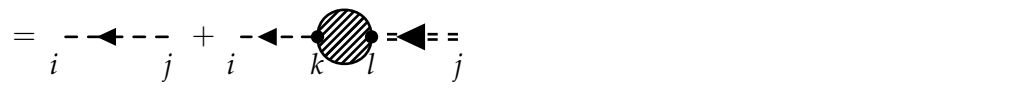

$$= \underline{\underline{\mathcal{G}_0}}(i,j;ik_n) + \sum_{kl} \underline{\underline{\mathcal{G}_0}}(i,k;ik_n)\underline{\underline{\Sigma}}(k,l;ik_n)\underline{\underline{\mathcal{G}}}(l,j;ik_n) \tag{3.22}$$

Which is the Dyson's equation for $\underline{\underline{\mathcal{G}}}(i,j;ik_n)$. In finite discrete real space, which is relevant for the numerical calculations, this will be $2N \times 2N$ matrices with the solution

$$\begin{aligned} \underline{\underline{\mathcal{G}}}(ik_n) &= \underline{\underline{\mathcal{G}_0}}(ik_n) + \underline{\underline{\mathcal{G}_0}}(ik_n)\underline{\underline{\Sigma}}(ik_n)\underline{\underline{\mathcal{G}}}(ik_n) = \left(1 - \underline{\underline{\mathcal{G}_0}}(ik_n)\underline{\underline{\Sigma}}(ik_n)\right)^{-1} \underline{\underline{\mathcal{G}_0}}(ik_n) \\ &= \left(\underline{\underline{\mathcal{G}_0}}(ik_n)^{-1}\left[1 - \underline{\underline{\mathcal{G}_0}}(ik_n)\underline{\underline{\Sigma}}(ik_n)\right]\right)^{-1} = \left(\underline{\underline{\mathcal{G}_0}}(ik_n)^{-1} - \underline{\underline{\Sigma}}(ik_n)\right)^{-1} \end{aligned} \tag{3.23}$$

Where I have used the fact that $(\underline{\underline{A}}\ \underline{\underline{B}})^{-1} = \underline{\underline{B}}^{-1}\ \underline{\underline{A}}^{-1}$. This expression for the full GF will be used extensively throughout the rest of this thesis. We now want to calculate the full GF using the Fock self-energy from eq. (E.25) [2], and then rewrite the GF in

[2] Since this is the lowest order diagram that could be interesting. The tadpole diagram is of the form of a trace, so it will just be a constant shift in energy

diagonal form which was seen in eq. (2.101), in order for us to perform the sum over Matsubara frequencies. The self-energy diagram we want to use is

$$\underline{\underline{\Sigma_F}}(i,j;ik_n) = \quad \underset{i}{\bullet}\!\!\leftarrow\!\!\bullet\!\!\rightarrow\!\!\bullet\!\!\leftarrow\!\!\bullet\ \underset{j}{} \quad = -\sum_{m,iq_n} \frac{g_i g_j}{\beta} |V_m|^2 \mathcal{D}_0(m;iq_n)\tau_z \underline{\underline{\mathcal{G}_0}}(i,j;ik_n - iq_n)\tau_z$$

$$= -\sum_{m,n,iq_n} \frac{g_i g_j}{\beta} |V_m|^2 \mathcal{D}_0(m;iq_n)\tau_z \begin{pmatrix} u_{in} & v_{in}^* \\ v_{in} & u_{in}^* \end{pmatrix} \begin{pmatrix} \frac{1}{ik_n - iq_n - \epsilon_n} & 0 \\ 0 & \frac{1}{ik_n - iq_n + \epsilon_n} \end{pmatrix} \begin{pmatrix} u_{jn}^* & v_{jn}^* \\ v_{jn} & u_{jn} \end{pmatrix} \tau_z$$

$$= \sum_n \begin{pmatrix} u_{in} & v_{in}^* \\ -v_{in} & -u_{in}^* \end{pmatrix} \begin{pmatrix} \Sigma^+(ik_n) & 0 \\ 0 & \Sigma^-(ik_n) \end{pmatrix} \begin{pmatrix} u_{jn}^* & -v_{jn}^* \\ v_{jn} & -u_{jn} \end{pmatrix} \tag{3.24}$$

Where

$$\begin{aligned} \Sigma^{\pm} &= -\sum_{m,iq_n} \frac{g_i g_j}{\beta} |V_m|^2 \mathcal{D}_0(m;iq_n) \frac{1}{ik_n - iq_n \mp \epsilon_n} \\ &= -\sum_{m,iq_n} \frac{g_i g_j}{\beta} |V_m|^2 \frac{2\omega_m}{(iq_n)^2 - \omega_m^2} \frac{1}{ik_n - iq_n \mp \epsilon_n} \end{aligned} \tag{3.25}$$

Where the bosonic GF from equation (3.6) has been inserted.

3.4.1 *Matsubara summation*

One can now perform the sum of the bosonic Matsubara frequencies iq_n, by the method of contour integration (as described in [4]). We write $\Sigma^+(ik_n)$ as

$$\Sigma^+(ik_n) = \frac{1}{\beta}\sum_{iq_n} g_0(iq_n)\,, \qquad g_0(iq_n) = -\sum_m g_i g_j |V_m|^2 \frac{2\omega_m}{(iq_n)^2 - \omega_m^2} \frac{1}{ik_n - iq_n - \epsilon_n}$$

The method is now to use complex analysis to write the sum as a contour integral over a complex variable z, and then use a function with poles at the bosonic Matsubara frequencies to pick out these from $g_0(z)$. The required function is the Bose-Einstein distribution function

$$n_B(z) = \frac{1}{e^{\beta z} - 1} \qquad \text{poles for } \; z = iq_n = i\frac{2n}{\beta}\pi \tag{3.26}$$

With residues

$$\begin{aligned} \operatorname*{Res}_{z \to iq_n} [n_B(z)] &= \lim_{z \to iq_n} \frac{z - iq_n}{e^{\beta z} - 1} \\ &= \lim_{\delta \to 0} \frac{\delta}{e^{\beta(\delta + iq_n)} - 1} = \lim_{\delta \to 0} \frac{\delta}{e^{\beta\delta} - 1} \overset{\text{L'Hôpital's rule}}{\to} \lim_{\delta \to 0} \frac{1}{\beta e^{\beta\delta}} = \frac{1}{\beta} \end{aligned} \tag{3.27}$$

Where L'Hôpital's rule is used, $\lim_{x\to 0}\frac{f(x)}{h(x)} = \lim_{x\to 0}\frac{f'(x)}{h'(x)}$ if $f(0) = h(0) = 0$. If one now creates a closed contour which encloses one of these Matsubara frequencies, then the Cauchy residue theorem gives

$$\oint \frac{dz}{2\pi i}\, n_B(z)g_0(z) = \operatorname*{Res}_{z\to iq_n}\left[n_B(z)g_0(z)\right] = \frac{1}{\beta}g_0(iq_n) \tag{3.28}$$

Comparing with the expression for $\Sigma^+(ik_n)$ confirms that if a contour C is chosen to enclose all frequencies iq_n, i.e. all poles of $n_B(z)$ and where $g_0(z)$ is analytic, then one can conclude

$$\Sigma^+(ik_n) = \int_C \frac{dz}{2\pi i}\, n_B(z)g_0(z) \tag{3.29}$$

Up until now, this derivation would also hold for a Matsubara summation of expressions containing the full GF. In that case one denotes it as $g(z)$, and for this function the poles are not known, but will have the form of branch cuts along the real axis (case treated in [4]). Continuing, one can use the fact that $g_0(z)$ only contains simple poles z_l, so it is analytic everywhere else. By choosing the contour C_∞ to include the entire complex plane, then one includes all poles from $n_B(z)$ and those from $g_0(z)$. The contour shown in blue in figure 14 is defined by $z = Re^{i\theta}$ with $R \to \infty$. The contour integral gives zero since the integrand goes to zero for $z \in C_\infty$

$$n_B(z)g_0(z) \propto \frac{1}{e^{\beta z}-1}\frac{1}{z^2-\omega_m^2}\frac{1}{ik_n - z - \epsilon_n} \overset{z\to C_\infty}{\propto} \begin{cases} e^{-\beta \mathrm{Re}(z)}\mathrm{Re}(z)^{-3} & \mathrm{Re}(z) > 0 \\ \mathrm{Re}(z)^{-3} & \mathrm{Re}(z) < 0 \end{cases} \tag{3.30}$$

So the contour integral gives zero, which is then equal to the contribution from $n_B(z)$ and $g_0(z)$

$$0 = \int_{C_\infty} \frac{dz}{2\pi i}\, n_B(z)g_0(z) = \frac{1}{\beta}\sum_{iq_n} g_0(iq_n) + \sum_l \operatorname*{Res}_{z=z_l}\left[g_0(z)\right]\; n_B(z_l) \tag{3.31}$$

Where the different contributions are denoted with their corresponding graphical notation from figure 14. One can thus conclude that

$$\begin{aligned}
\Sigma^+(ik_n) &= -\sum_l \operatorname*{Res}_{z=z_l}\left[g_0(z)\right]\; n_B(z_l) \\
&= \sum_l \operatorname*{Res}_{z=z_l}\left[\sum_m g_i g_j |V_m|^2 \frac{2\omega_m}{z^2-\omega_m^2}\frac{1}{ik_n - z - \epsilon_n}\right]\; n_B(z_l) \\
&= \sum_m g_i g_j |V_m|^2 \sum_l \operatorname*{Res}_{z=z_l}\left[\frac{2\omega_m}{(z-\omega_m)(z+\omega_m)}\frac{1}{ik_n - z - \epsilon_n}\right]\; n_B(z_l) \\
&= \sum_m g_i g_j |V_m|^2 \left[\frac{n_B(\omega_m)}{ik_n - \omega_m - \epsilon_n} - \frac{n_B(-\omega_m)}{ik_n + \omega_m - \epsilon_n} - \frac{2\omega_m\, n_B(ik_n - \epsilon_n)}{(ik_n - \epsilon_n - \omega_m)(ik_n - \epsilon_n + \omega_m)}\right]
\end{aligned} \tag{3.32}$$

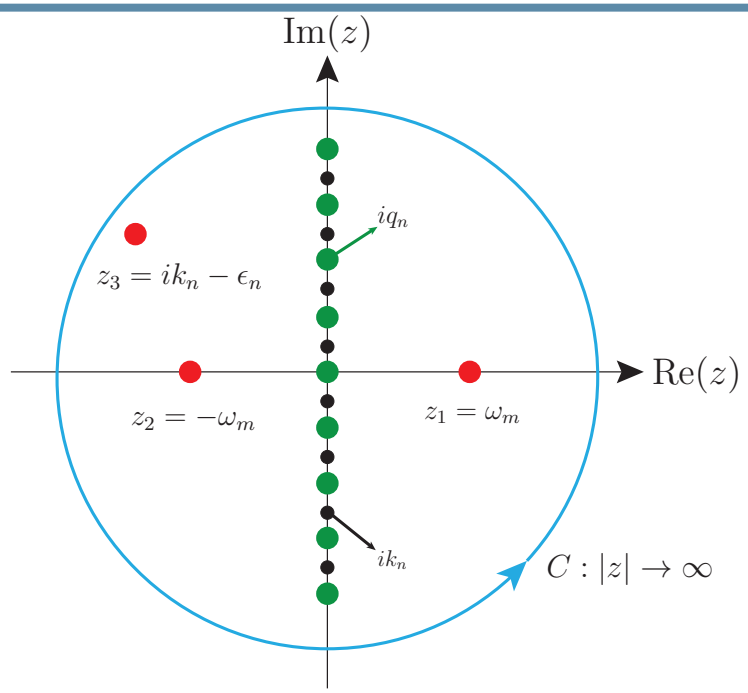

Figure 14: Figure illustrating the use of contour integration to determine the Matsubara sum $\Sigma^+(ik_n)$. The blue curve shows the contour C_∞, the green dots show the bosonic Matsubara frequencies $iq_n = i\frac{2n}{\beta}\pi$, the small black dots show the fermionic frequencies ik_n, and the red dots show the poles of $g_0(z)$ which occur at $z = z_l$.

Using $-n_B(-\omega) = n_B(\omega) + 1$ and $n_B(ik_n - \epsilon_n) = -n_F(-\epsilon_n)$ this yields

$$
\begin{aligned}
&\Sigma^+(ik_n) \\
&= \sum_m g_i g_j |V_m|^2 \left[\frac{n_B(\omega_m)}{ik_n - \omega_m - \epsilon_n} + \frac{n_B(\omega_m) + 1}{ik_n + \omega_m - \epsilon_n} + \frac{2\omega_m \, n_F(-\epsilon_n)}{(ik_n - \epsilon_n - \omega_m)\,(ik_n - \epsilon_n + \omega_m)} \right] \\
&= \sum_m g_i g_j |V_m|^2 \left[\frac{n_B(\omega_m)}{ik_n - \omega_m - \epsilon_n} + \frac{n_B(\omega_m) + 1}{ik_n + \omega_m - \epsilon_n} + \frac{n_F(-\epsilon_n)}{ik_n - \epsilon_n - \omega_m} - \frac{n_F(-\epsilon_n)}{ik_n - \epsilon_n + \omega_m} \right] \\
&= \sum_m g_i g_j |V_m|^2 \left[\frac{n_B(\omega_m) + n_F(-\epsilon_n)}{ik_n - \omega_m - \epsilon_n} + \frac{n_B(\omega_m) + 1 - n_F(-\epsilon_n)}{ik_n + \omega_m - \epsilon_n} \right]
\end{aligned} \tag{3.33}
$$

With a similar calculation for $\Sigma^-(ik_n)$ showing that

$$
\Sigma^\pm(ik_n) = \sum_m g_i g_j |V_m|^2 \left[\frac{n_B(\omega_m) + n_F(\mp\epsilon_n)}{ik_n - \omega_m \mp \epsilon_n} + \frac{n_B(\omega_m) + 1 - n_F(\mp\epsilon_n)}{ik_n + \omega_m \mp \epsilon_n} \right] \tag{3.34}
$$

As an interlude to this calculation, and before proceeding to perform the sum over bosonic energies, one can check if this self-energy still preserves the symmetries from (2.115) after the Matsubara frequency sum has been performed. The unitary

symmetry matrices were found in (2.135), and written out explicitly they affect the diagonal self-energy according to

$$\begin{aligned}\Sigma(\omega)^{\alpha\beta}_{nn} &= \Sigma(\omega)^{\beta\alpha}_{nn} \\ \tau_x^{\sigma\alpha}\Sigma(\omega)^{\alpha\beta}_{nn}\tau_x^{\beta\rho} &= -\Sigma(-\omega)^{\sigma\rho}_{nn}\end{aligned} \tag{3.35}$$

With ω complex, so we set $\omega = ik_n$. One now can write the following symmetry for specific Nambu entries, extracted from the second equation

$$\begin{aligned}\Sigma(ik_n)^{11}_{nn} &= -\Sigma(-ik_n)^{22}_{nn} \\ &\updownarrow \\ \Sigma^+(ik_n) &= -\Sigma^-(-ik_n)\end{aligned} \tag{3.36}$$

Where the consequence this symmetry has on (3.34) has also been noted. Checking if this is the case

$$\begin{aligned}-\Sigma^-(-ik_n) &= -\sum_m g_i g_j |V_m|^2 \left[\frac{n_B(\omega_m)+n_F(\epsilon_n)}{-ik_n-\omega_m+\epsilon_n} + \frac{n_B(\omega_m)+1-n_F(\epsilon_n)}{-ik_n+\omega_m+\epsilon_n}\right] \\ &= \sum_m g_i g_j |V_m|^2 \left[\frac{n_B(\omega_m)+n_F(\epsilon_n)}{ik_n+\omega_m-\epsilon_n} + \frac{n_B(\omega_m)+1-n_F(\epsilon_n)}{ik_n-\omega_m-\epsilon_n}\right] \\ &= \sum_m g_i g_j |V_m|^2 \left[\frac{n_B(\omega_m)+1-n_F(-\epsilon_n)}{ik_n+\omega_m-\epsilon_n} + \frac{n_B(\omega_m)+n_F(-\epsilon_n)}{ik_n-\omega_m-\epsilon_n}\right] = \Sigma^+(ik_n)\end{aligned} \tag{3.37}$$

Where $n_F(\epsilon_n) = 1 - n_F(-\epsilon_n)$ was used. It is now sufficient to calculate $\Sigma^+(ik_n)$ and infer $\Sigma^-(ik_n)$ from the relation above. Now we are ready to continue with the equation (3.34), which left us with a sum over bosonic energies ω_m. This can be performed by converting the sum to an integral by introducing the spectral density

$$\mathcal{J}(\omega_b) = \pi \sum_m |V_m|^2 \delta(\omega_b - \omega_m) \tag{3.38}$$

This function tells us how the bosonic levels are distributed, and is determined by the specifics of the system [3]. By insertion

$$\Sigma^\pm(ik_n) = \frac{1}{\pi}\int d\omega_b \mathcal{J}(\omega_b) g_i g_j \left[\frac{n_B(\omega_b)+n_F(\mp\epsilon_n)}{ik_n-\omega_b\mp\epsilon_n} + \frac{n_B(\omega_b)+1-n_F(\mp\epsilon_n)}{ik_n+\omega_b\mp\epsilon_n}\right] \tag{3.39}$$

Now, the actual form of $\mathcal{J}(\omega_b)$ can be determined from physical principles. The system is effectively an RC-circuit, and assuming the fluctuations are small, one can use results from Linear Response theory. First, one can relate $\mathcal{J}(\omega_b)$ to the retarded

[3] This idea is credited to Morten Munk-Nielsen, as it was used in his Thesis https://cmt.nbi.ku.dk/student_projects/master_theses/Master_Thesis_Morten_Munk-Nielsen.pdf

bosonic GF $\tilde{\mathcal{D}}_0(iq_n) \Rightarrow \tilde{\mathcal{D}}_0^R(\omega_b + i\eta)$ where analytical continuation is performed on (3.18). We can write this correlation function in terms of $\mathcal{J}(\omega_b)$

$$\begin{aligned}\tilde{\mathcal{D}}_0^R(\omega_b) &= \sum_m \left(\frac{|V_m|^2}{\omega_b + i\eta - \omega_m} - \frac{|V_m|^2}{\omega_b + i\eta + \omega_m} \right) \\ &= \sum_m |V_m|^2 \left(\mathcal{P}\frac{1}{\omega_b - \omega_m} - \mathcal{P}\frac{1}{\omega_b + \omega_m} - i\pi\delta(\omega_b - \omega_m) + i\pi\delta(\omega_b + \omega_m) \right)\end{aligned} \tag{3.40}$$

So one can conclude

$$\begin{aligned}\mathrm{Im}\left[\tilde{\mathcal{D}}_0^R(\omega_b)\right] &= \pi \sum_m |V_m|^2 \left(\delta(\omega_b + \omega_m) - \delta(\omega_b - \omega_m)\right) \\ &= \mathcal{J}(-\omega_b) - \mathcal{J}(\omega_b) = -\mathcal{J}(\omega_b)\end{aligned} \tag{3.41}$$

Where it is used that $\mathcal{J}(\omega_b) = 0$ for $\omega_b < 0$ since ω_m is positive. From Linear Response theory, one has the relation [4]

$$\begin{aligned}\mathrm{Re}\left[\frac{1}{Z_{tot}(\omega_b)}\right] = \mathrm{Re}\left[\frac{ie^2}{\omega_b} C_{II}^R(\omega_b)\right] &= -\mathrm{Im}\left[\frac{e^2}{\omega_b} C_{II}^R(\omega_b)\right] \\ &\updownarrow \\ \mathrm{Im}\left[C_{II}^R(\omega_b)\right] &= -\frac{\omega_b}{e^2}\mathrm{Re}\left[\frac{1}{Z_{tot}(\omega_b)}\right]\end{aligned} \tag{3.42}$$

where $Z_{tot}(\omega_b)$ is the frequency dependant total impedance, and $C_{II}^R(\omega_b)$ is the retarded current-current correlation function. Since the system is a frequency independent impedance Z_0 coupled in parallel to a capacitor, the total impedance is

$$Z_{tot}(\omega_b) = \left(i\omega_b C + \frac{1}{Z_0}\right)^{-1} \tag{3.43}$$

In the classical limit, the current-current correlation function $C_{II}^R(\omega_b)$ is related to the $\langle\varphi\varphi\rangle$ correlation function $\tilde{\mathcal{D}}_0^R(\omega_b)$ by Ohm's law, and with this assumption one can write

$$C_{II}^R(\omega_b) = |Z_{tot}(\omega_b)|^{-2} \tilde{\mathcal{D}}_0^R(\omega_b) \tag{3.44}$$

So by collecting (3.42) and (3.44) one gets

$$\begin{aligned}\mathrm{Im}\left[\tilde{\mathcal{D}}_0^R(\omega_b)\right] &= -\frac{\omega_b}{e^2}|Z_{tot}(\omega_b)|^2 \mathrm{Re}\left[\frac{1}{Z_{tot}(\omega_b)}\right] = -\frac{\omega_b}{e^2}\frac{1}{\omega_b^2 C^2 + Z_0^{-2}}\frac{1}{Z_0} \\ &= -\frac{\omega_b}{e^2}\frac{1}{\omega_b^2 C^2 Z_0 + Z_0^{-1}} = -\frac{\omega_b}{e^2 C}\frac{1}{\omega_b^2 C Z_0 + (CZ_0)^{-1}} = -\frac{1}{e^2 C}\frac{\omega_b \omega_0}{\omega_b^2 + \omega_0^2}\end{aligned} \tag{3.45}$$

Where $\omega_0 = \frac{1}{CZ_0}$ is the characteristic frequency of the RC-circuit. By using (3.41) one can then conclude

$$\mathcal{J}(\omega_b) = \frac{\theta(\omega_b)}{e^2 C} \frac{\omega_b \omega_0}{\omega_b^2 + \omega_0^2} \tag{3.46}$$

Using this spectral function for the bosonic modes, $\Sigma^{\pm}(ik_n)$ can now be calculated

$$\Sigma^{\pm}(ik_n) = \\ \frac{\omega_0}{\pi e^2 C} g_i g_j \int_{-\infty}^{\infty} d\omega_b \, \frac{\theta(\omega_b)\omega_b}{\omega_b^2 + \omega_0^2} \left[\frac{n_B(\omega_b) + n_F(\mp\epsilon_n)}{ik_n - \omega_b \mp \epsilon_n} + \frac{n_B(\omega_b) + 1 - n_F(\mp\epsilon_n)}{ik_n + \omega_b \mp \epsilon_n} \right] \tag{3.47}$$

After analytical continuation the retarded Fock self-energy then becomes

$$\underline{\underline{\Sigma}}_F^R(i,j;\omega_e + i\eta) = \sum_n \begin{pmatrix} u_{in} & v_{in}^* \\ -v_{in} & -u_{in}^* \end{pmatrix} \begin{pmatrix} \Sigma^+(\omega_e + i\eta) & 0 \\ 0 & \Sigma^-(\omega_e + i\eta) \end{pmatrix} \begin{pmatrix} u_{jn}^* & -v_{jn}^* \\ v_{jn} & -u_{jn} \end{pmatrix} \tag{3.48}$$

To perform the integral over bosonic energies ω_b in $\Sigma^{\pm}$ it is advantageous to use the identity in (2.104) to split the integral into a real and an imaginary part. The strategy is now to calculate as much of the integral as possible analytically, before letting a computer do the rest.

3.4.2 *Energy integration of self-energy - Treating divergences*

We want to calculate

$$\begin{aligned} &\Sigma^+(\omega_e + i\eta) \\ &= \frac{\omega_0}{\pi e^2 C} g_i g_j \int_0^{\infty} d\omega_b \, \frac{\omega_b}{\omega_b^2 + \omega_0^2} \left[\frac{n_B(\omega_b) + n_F(-\epsilon_n)}{\omega_e + i\eta - \omega_b - \epsilon_n} + \frac{n_B(\omega_b) + 1 - n_F(-\epsilon_n)}{\omega_e + i\eta + \omega_b - \epsilon_n} \right] \\ &= \alpha \int_0^{\infty} d\omega_b \, \frac{1}{\omega_b^2 + \omega_0^2} \left[\frac{F_1(\omega_b) + F_2(\omega_b)}{\omega_e + i\eta - \omega_b - \epsilon_n} + \frac{F_1(\omega_b) + \omega_b - F_2(\omega_b)}{\omega_e + i\eta + \omega_b - \epsilon_n} \right] \end{aligned} \tag{3.49}$$

Where

$$\begin{aligned} \alpha &= \frac{\omega_0}{\pi e^2 C} g_i g_j \\ F_1(\omega_b) &= \omega_b n_B(\omega_b) \\ F_2(\omega_b, \epsilon_n) &= \omega_b n_F(-\epsilon_n) \end{aligned} \tag{3.50}$$

For the sake of simplicity, let us look exclusively at the first term I_1, and define $\epsilon \equiv \omega_e - \epsilon_n$

$$I_1 = \alpha \int_0^{\infty} d\omega_b \, F_1(\omega_b) \, \frac{1}{\omega_b^2 + \omega_0^2} \left[\frac{1}{\epsilon + i\eta - \omega_b} \right] \tag{3.51}$$

We use once more that

$$\lim_{\eta \to 0} \frac{1}{\epsilon + i\eta - \omega_b} = \mathcal{P} \frac{1}{\epsilon - \omega_b} - i\pi \, \delta(\epsilon - \omega_b) \tag{3.52}$$

So I_1 becomes

$$I_1 = -i\pi\alpha \int_0^\infty d\omega_b \, F_1(\omega_b) \, \frac{\delta(\epsilon - \omega_b)}{\omega_b^2 + \omega_0^2} + \alpha \, \mathcal{P} \int_0^\infty d\omega_b \, F_1(\omega_b) \, \frac{1}{\omega_b^2 + \omega_0^2} \, \frac{1}{\epsilon - \omega_b}$$
$$= -i\pi\alpha \, \frac{F_1(\epsilon)}{\epsilon^2 + \omega_0^2} + \alpha \, \mathcal{P} \int_0^\infty d\omega_b \, F_1(\omega_b) \, \frac{1}{\omega_b^2 + \omega_0^2} \, \frac{1}{\epsilon - \omega_b} \quad (3.53)$$

Where $\epsilon > 0$ is now assumed temporarily. Here the principal value of an integral with a pole on the real axis $x = z_0$ is defined as [27]

$$\mathcal{P} \int_a^b f(x)dx = \lim_{\delta \to 0} \int_a^{z_0 - \delta} f(x)dx + \int_{z_0 + \delta}^b f(x)dx \quad (3.54)$$

The imaginary part was simple to calculate analytically, so now one can determine the real part which contains the principal value integral

$$\mathcal{P} \int_0^\infty d\omega_b \, F_1(\omega_b) \, \frac{1}{\omega_b^2 + \omega_0^2} \, \frac{1}{\epsilon - \omega_b} \quad (3.55)$$

The integrand of which is seen in the first plot in figure 15, for positive ϵ. This complicated integral can be split into two parts by adding and subtracting a term

$$\mathcal{P} \int_0^\infty d\omega_b \, \frac{F_1(\omega_b)}{(\omega_b^2 + \omega_0^2)(\epsilon - \omega_b)}$$
$$= \underbrace{\int_0^\infty d\omega_b \, \frac{F_1(\omega_b) - F_1(\epsilon)}{(\omega_b^2 + \omega_0^2)(\epsilon - \omega_b)}}_{\text{Numerical integration} \equiv \sigma_1} + \underbrace{\mathcal{P} \int_0^\infty d\omega_b \, \frac{F_1(\epsilon)}{(\omega_b^2 + \omega_0^2)(\epsilon - \omega_b)}}_{\text{Analytical integration}} \quad (3.56)$$

And as seen in figure 15, the first part is complicated, but has no divergences, so this can be handled by numerical integration (and denoted by σ_1). The second part has a divergence, but it is possible to determine this principal part of the integral analytically.

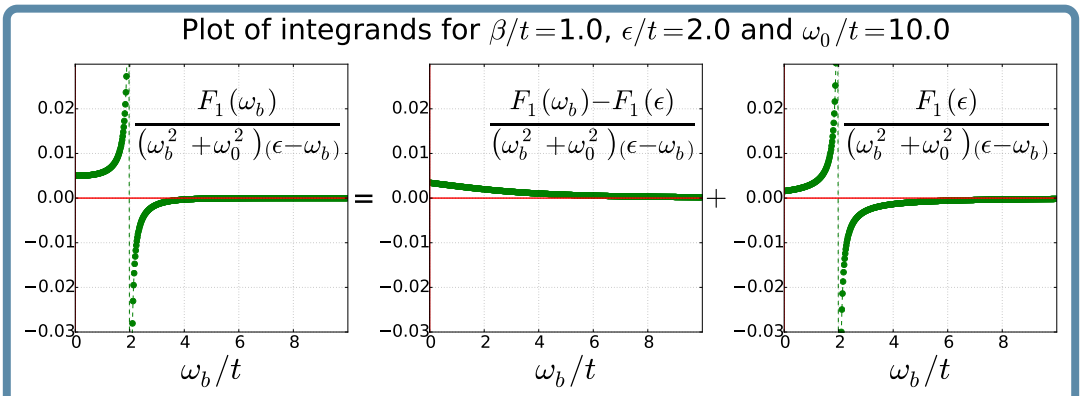

Figure 15: Plot of the integrands in (3.56), to show that the complicated and uncontrolled integral can be split up into two parts. One of them, denoted by σ_1, is convergent but too complicated to calculate analytically, so will be solved on a computer. The other can be solved analytically which is done in detail in F. This is not based on realistic parameters, but used to illustrate the idea behind the calculation.

This is done in detail in Appendix F, leaving us with the final result

$$I_1 = \underbrace{-i\pi\alpha \ \frac{F_1(\epsilon)}{\epsilon^2+\omega_0^2}}_{\text{Imaginary part}} + \underbrace{\alpha\left[\frac{F_1(\epsilon)}{2\omega_0\epsilon^2+2\omega_0^3}\right]\left(\pi\epsilon+\omega_0\ln\left(\frac{\epsilon^2}{\omega_0^2}\right)\right)}_{\text{Analytical}} + \underbrace{\alpha\sigma_1}_{\text{Numerical}} \tag{3.57}$$

So, we succesfully calculated the imaginary part (the first term), and analytically calculated the problematic part of the real component. The last part $\alpha\sigma_1$ is a well-behaving numerical integration. The procedure is now to determine all the other terms in (3.49). Since the integral is over positive ω_b, and ϵ is assumed positive, only the $\frac{1}{\epsilon-\omega_b}$ terms have divergences, while the $\frac{1}{\epsilon+\omega_b}$ terms have no problem (other than being very complicated), so these can be determined numerically. If ϵ is negative this picture would reverse, and the $\frac{1}{\epsilon+\omega_b}$ integrals would now have divergences. From the symmetry of the expression (3.49), one can conclude that some terms will depend on the sign of ϵ. By carefully tracking these signs, one finds

$$\begin{aligned}\Sigma^+(\epsilon) =& \alpha\,\frac{F_1(|\epsilon|)+\text{sign}(\epsilon)F_2(|\epsilon|,\epsilon_n)-\epsilon\theta(-\epsilon)}{\epsilon^2+\omega_0^2}\left(-i\pi+\frac{1}{2\omega_0}\left[\pi\epsilon+\text{sign}(\epsilon)\omega_0\ln\frac{\epsilon^2}{\omega_0^2}\right]\right)\\ &+\alpha\left[\text{sign}(\epsilon)\left(\sigma_1+\sigma_2+\sigma_3\right)+\theta(\epsilon)\sigma_4+\sigma_5+\theta(-\epsilon)\frac{\pi}{2\omega_0}\right]\end{aligned} \tag{3.58}$$

Where

$$\sigma_1 = \int_0^\infty d\omega_b \frac{F_1(\omega_b) - F_1(|\epsilon|)}{(\omega_b^2 + \omega_0^2)(|\epsilon| - \omega_b)}, \qquad \sigma_2 = \int_0^\infty d\omega_b \frac{F_2(\omega_b, \epsilon_n) - F_2(|\epsilon|, \epsilon_n)}{(\omega_b^2 + \omega_0^2)(|\epsilon| - \omega_b)}$$
$$\sigma_3 = \int_0^\infty d\omega_b \frac{F_1(\omega_b)}{(\omega_b^2 + \omega_0^2)(|\epsilon| + \omega_b)}, \qquad \sigma_4 = \int_0^\infty d\omega_b \frac{\omega_b}{(\omega_b^2 + \omega_0^2)(|\epsilon| + \omega_b)}$$
$$\sigma_5 = \int_0^\infty d\omega_b \frac{-F_2(\omega_b, \epsilon_n)}{(\omega_b^2 + \omega_0^2)(|\epsilon| + \omega_b)} \tag{3.59}$$

Are all determined numerically. The expression for the hole contribution Σ^- is found by using (3.36) to write it in terms of the electronic part.

3.5 THE FULL SPECTRAL FUNCTION - ELECTRON-BOSON INTERACTION

We can now determine the full retarded GF

$$\underline{\underline{\mathcal{G}}}^R(\omega_e) = \left(\underline{\underline{\mathcal{G}}}_0^R(\omega_e)^{-1} - \underline{\underline{\Sigma}}_F^R(\omega_e)\right)^{-1} \tag{3.60}$$

Which is a giant matrix in Nambu- and site space. We look at its properties by analysing the spectral function $\underline{\underline{\mathcal{A}}}(\omega_e) = -2\mathrm{Im}(\underline{\underline{\mathcal{G}}}^R(\omega_e))$ on the edge of the wire as a function of energy. This would be relevant for calculating the current in a tunnelling experiment, where the edge is coupled to a lead. We can also, for a fixed energy, see how the spectral function decays into the wire, to see if the broadening from the interactions result in a change of the exponential decay of the edge states (described in section 2.2). Broadening in the general sense can happen when interactions are present, where the spectral weight is changed due to the electrons exchanging energy with the bosons (here this is due to charge fluctuations). This could also be due to phonons or electrons if we consider these kind of interactions.

We can imagine performing af tunnelling experiment on the wire, by coupling one end to a lead, and have the other side grounded, so that a current can flow through the nanowire. The lead is weakly coupled to the wire (controlled by $\Gamma \propto 2\pi|T|^2 d_N(\epsilon_F)$, where T is the tunnel coupling strength and $d_N(\epsilon_F)$ is the density of states of the lead consisting of a normal metal). In this weak coupling limit ($\Gamma << k_B T$) the differential conductance becomes

$$\frac{dI}{dV} = \Gamma \int d\omega \left(-\frac{\partial n_F(\omega - eV)}{\partial \omega}\right) \mathcal{A}_{11}(1,1;\omega) \tag{3.61}$$

Where $\mathcal{A}_{11}(1,1;\omega)$ is the electronic part of the spectral function for the first site, and V is the voltage bias. For low temperatures ($k_B T << \mathrm{Im}(\Sigma^R)$), this becomes

$$\frac{dI}{dV} \approx \Gamma \mathcal{A}_{11}(1,1;eV) \tag{3.62}$$

So, measuring the differential conductance as a function of bias voltage, will give you the form of the spectral function. The results of calculating the full spectral function numerically is shown in figure 16, comparing it with the non-interacting case. The non-interacting GF has a small imaginary part $i\eta$ added for visibility. As one can see in the plots, the height of the zero energy peak has been diminished by

broadening, due to the imaginary part of the self-energy $\mathrm{Im}(\Sigma^R)$. To compare with an experiment as described, one would have to insert realistic parameters.

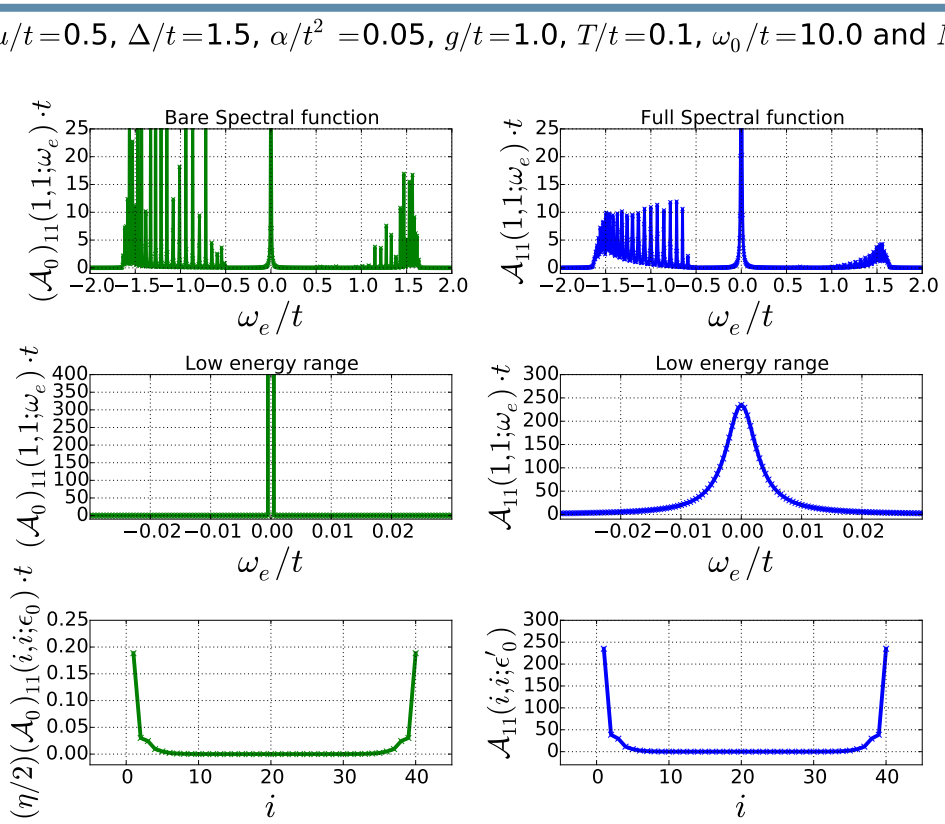

Figure 16: Comparison between spectral function of the non-interacting and the interacting system. On the left, the peaks are true Dirac peaks broadened by a small artificial imaginary part $i\eta$, for the purpose of visualization. On the right, the broadening is due to $\mathrm{Im}(\Sigma^R)$. The bottom two plots shows that the local coherence decays into the bulk with the same rate for both cases. Here ϵ_0' is the renormalised zero mode energy, which is the energy where the full spectral function is peaked (middle right picture), which is still located at zero energy.

The full spectral function still obeys the symmetries of the system, which is derived from (3.36)

$$\begin{aligned} &\Sigma(ik_n)^{11}_{11} = -\Sigma(-ik_n)^{22}_{11} \;\Rightarrow\; G(\omega+i\eta)^{11}_{11} = -G(-\omega-i\eta)^{22}_{11} \\ &\Rightarrow\; G^R(\omega)^{11}_{11} = -\left[G(-\omega)^{22}_{11}\right]^* \;\Rightarrow\; \mathcal{A}(\omega)^{11}_{11} = \mathcal{A}(-\omega)^{22}_{11} \end{aligned} \tag{3.63}$$

Which is confirmed by figure 17.

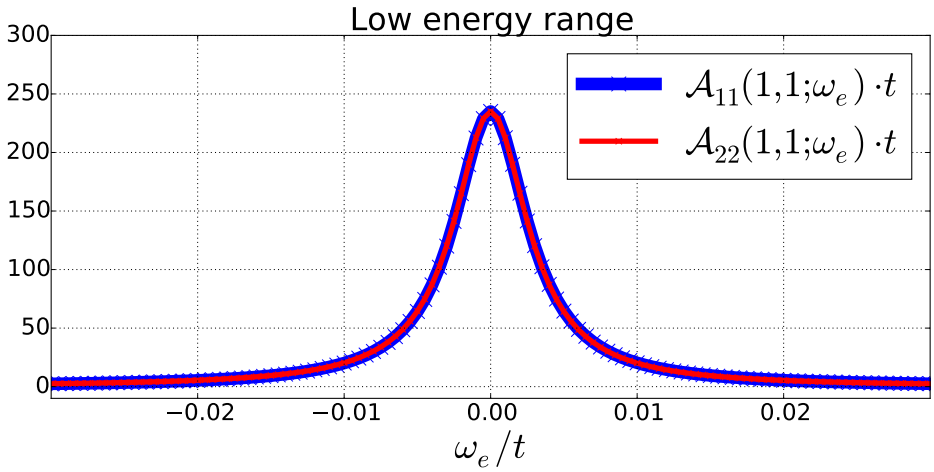

Figure 17: Plot of the electron and hole part of the local spectral function on the edge, as a function of energy. The symmetry $\mathcal{A}(\omega)^{11}_{11} = \mathcal{A}(-\omega)^{22}_{11}$ is shown to be intact for the interacting system.

In the bottom two sub-figures of figure 16 the local bare spectral function is on the left, with two clear peaks on the edge, compared with the interacting case on the right. The form of the functions are identical, and the decay rates into the bulk likewise.

It is possible that the inclusion of the bosonic interactions has changed the phase diagram of the Kitaev model. The interaction term has a τ_z Nambu structure similar to the chemical potential term, so it may have led to a change in chemical potential $\mu \to \tilde{\mu}$, thereby changing the range of the topological regime. To analyse the modified phase diagram, it was at this point desirable to try and calculate the TI for 1D interacting chiral systems using (2.153). The calculation would still involve a high amount of numerical calculations, so it was concluded that a clear analytical expression was unobtainable. To be able to compare the framework discussed up until now with recent relevant literature, we move on to include nearest neighbour electron-electron interactions, where a variety of methods will be considered. For this type of interaction, various authors have calculated phase diagrams using numerical methods called Density Matrix Renormalisation Group (DMRG) and Exact Diagonalisation. Also, for specific values of the parameters in the theory, it is possible to calculate the many-body GS exactly. The aim is now to describe these results, and also see if the zero modes are stable, when interactions between the electrons are considered, by again calculating the full GF using perturbation theory.

4

THE INTERACTING KITAEV CHAIN - ELECTRON-ELECTRON

4.1 ELECTRON-ELECTRON INTERACTIONS

4.1.1 *Nearest neighbour interaction*

We want to use the methods developed in previous chapters to investigate how electron-electron interactions affect the zero-modes in our system. A general interaction of this kind can be written as $\sum_{ijkl} W_{ijkl} c_i^\dagger c_j^\dagger c_k c_l$, but we will consider an interaction that couples to the density of electrons at different points. The interaction thus becomes

$$H_{e-e} = \sum_{ii'} W_{ii'}\ c_i^\dagger c_{i'}^\dagger c_{i'} c_i \tag{4.1}$$

Which obeys the symmetry (2.137) if $W_{ii'} = W_{ii'}^*$. This condition can be checked by commuting operators and renaming dummy variables, from which one gets

$$\sum_{ii'} W_{ii'}\ c_i^\dagger c_{i'}^\dagger c_{i'} c_i = \sum_{ii'} W_{ii'}\ c_{i'}^\dagger c_i^\dagger c_i c_{i'} = \sum_{ii'} W_{i'i}\ c_i^\dagger c_{i'}^\dagger c_{i'} c_i \tag{4.2}$$

So $W_{ii'} = W_{i'i}$ is symmetric, and together with the condition of being Hermitian $W_{ii'} = W_{i'i}^*$, the reality condition is true $W_{ii'} = W_{ii'}^*$, so the interaction term H_{e-e} will still preserve the symmetries of the BDI class. In a translationally invariant system, $W_{ii'}$ depends only on the difference $|i - i'|$, but can in general be location specific (an electron might feel more interaction depending on where in the wire it is located). In this chapter we want to consider a nearest neighbour electron-electron interaction, as this type has been considered frequently in recent years of research [18][22][24][25]. Thus, we begin analysing the Kitaev model subject to a short range $e-e$ interaction term, where $W_{ii'} = \frac{W}{2}\left(\delta_{i+1,i'} + \delta_{i,i'+1}\right)$. This short-range model is described by the following Hamiltonian

$$\begin{aligned} H &= H_K + H_{int} \\ H_K &= -\mu \sum_{n=1}^{N} c_n^\dagger c_n - \sum_{n=1}^{N-1} \left[\frac{t}{2}\left(c_n^\dagger c_{n+1} + c_{n+1}^\dagger c_n\right) - \frac{\Delta}{2}\left(c_n c_{n+1} + c_{n+1}^\dagger c_n^\dagger\right)\right] \\ H_{int} &= W \sum_{n=1}^{N-1} c_n^\dagger c_{n+1}^\dagger c_{n+1} c_n \end{aligned} \tag{4.3}$$

Where H_K is the normal Kitaev Hamiltonian, and H_{int} is a short range interaction controlled by the interaction strength W. The two-particle term H_{int} prohibits us from writing the Hamiltonian in the single-particle BDG form (2.58).

4.2 INTERACTION HAMILTONIAN IN MAJORANA BASIS

In the following sections we will use a modified version of the Hamiltonian (4.3), where the occupation is shifted $n_j = c_j^\dagger c_j$ with an average value $\langle n_j \rangle = \frac{1}{2}$. By this shift in reference point of the chemical potential, the Hamiltonian in the Majorana basis becomes significantly more simple, which also happens with the Nambu space structure. The Hamiltonian is thus

$$\begin{aligned} H_K &= -\mu \sum_{n=1}^{N} \left(c_n^\dagger c_n - \frac{1}{2} \right) - \sum_{n=1}^{N-1} \left[\frac{t}{2} \left(c_n^\dagger c_{n+1} + c_{n+1}^\dagger c_n \right) - \frac{\Delta}{2} \left(c_n c_{n+1} + c_{n+1}^\dagger c_n^\dagger \right) \right] \\ H_{int} &= W \sum_{n=1}^{N-1} \left(c_n^\dagger c_n - \frac{1}{2} \right) \left(c_{n+1}^\dagger c_{n+1} - \frac{1}{2} \right) \end{aligned} \tag{4.4}$$

In the Majorana basis (2.2) the Kitaev Hamiltonian H_K becomes

$$H_K \Rightarrow -\frac{\mu}{2} \sum_{n=1}^{N} i\gamma_{A,n}\gamma_{B,n} - \frac{i}{4} \sum_{n=1}^{N-1} \left[(t+\Delta)\, \gamma_{A,n+1}\gamma_{B,n} + (t-\Delta)\, \gamma_{A,n}\gamma_{B,n+1} \right] \tag{4.5}$$

And H_{int} becomes

$$H_{int} \Rightarrow -\frac{W}{4} \sum_{n=1}^{N-1} \gamma_{A,n}\gamma_{B,n}\gamma_{A,n+1}\gamma_{B,n+1} = \frac{W}{4} \sum_{n=1}^{N-1} \gamma_{A,n}\gamma_{A,n+1}\gamma_{B,n}\gamma_{B,n+1} \tag{4.6}$$

Which is a quartic Majorana interaction term, including all four Majoranas between two fermions.

4.3 JORDAN-WIGNER TRANSFORMATION

4.3.1 *Non-interacting*

One way to solve the interacting problem is to perform a Jordan-Wigner transformation [18][25]. This transformation maps a 1D fermionic system to a chain of spin-$\frac{1}{2}$ particles, by viewing an occupied state as spin up $|\uparrow\rangle = |1\rangle$, and an unoccupied state as spin down $|\downarrow\rangle = |0\rangle$. Creating a particle corresponds to flipping a spin from down to up, $f^\dagger \to \sigma^+$, annihilating a particle is the reverse process $f \to \sigma^-$, and the occupation is equivalent to the z-component of the spin, $f^\dagger f \to \sigma^z$. Naively, one might write the following relations

$$f_n^\dagger = \sigma_n^+ = \frac{1}{2} \left(\sigma_n^x + i\sigma_n^y \right) \qquad f_n = \sigma_n^- = \frac{1}{2} \left(\sigma_n^x - i\sigma_n^y \right) \tag{4.7}$$

With which one can conclude

$$\begin{aligned} 2f_n^\dagger f_n - 1 = 2\sigma_n^+\sigma_n^- - 1 &= \frac{1}{2} \left(\sigma_n^x + i\sigma_n^y \right) \left(\sigma_n^x - i\sigma_n^y \right) - 1 \\ &= \frac{i}{2} \left[\sigma_n^y, \sigma_n^x \right] = \sigma_n^z \end{aligned} \tag{4.8}$$

Where $\left[\sigma_n^\alpha, \sigma_{n'}^\beta \right] = 2i\delta_{nn'}\epsilon^{\alpha\beta\lambda}\sigma_n^\lambda$ was used. This mapping preserves the same-site anti-commutation relation $\{f_n, f_n^\dagger\} = 1$ but since spins at different sites commute, we

have $\left[f_n, f_{n'}^\dagger\right] = 0$ which is an incorrect result for the exchange statistics of fermions; different fermions anti-commute. To solve this problem one attaches a *Jordan-Wigner string* to the operators f and $f^\dagger$, which is a phase factor determined by the number of occupied states behind the site in question. Mathematically, one constructs new operators c and $c^\dagger$ as

$$\begin{aligned} c_n^\dagger &= f_n^\dagger \cdot e^{+i\pi \sum_j^{n-1} f_j^\dagger f_j} \\ c_n &= e^{-i\pi \sum_j^{n-1} f_j^\dagger f_j} \cdot f_n \\ c_n^\dagger c_n &= f_n^\dagger f_n \end{aligned} \tag{4.9}$$

The hope is that these operators will now obey the legitimate fermion anti-commutation relations. The phase factor can be written in terms of spin-operators as

$$\begin{aligned} e^{\pm i\pi \sum_j^{n-1} f_j^\dagger f_j} &= \prod_j^{n-1} e^{\pm i\pi f_j^\dagger f_j} = \prod_j^{n-1} e^{\pm i\frac{\pi}{2}\left(\sigma_j^z+1\right)} = \prod_j^{n-1} \pm i e^{\pm i\frac{\pi}{2}\sigma_j^z} \\ &= \prod_j^{n-1} \pm i \left[\cos\left(\pm\frac{\pi}{2}\right) + i\,\sigma_j^z\ \sin\left(\pm\frac{\pi}{2}\right)\right] = \prod_j^{n-1}\left(-\sigma_j^z\right) \end{aligned} \tag{4.10}$$

Employing these results, one can write the JW transform and its inverse transform as

$$\begin{aligned} c_n^\dagger &= \sigma_n^+ \prod_j^{n-1}\left(-\sigma_j^z\right) & \sigma_n^+ &= c_n^\dagger \cdot e^{-i\pi \sum_j^{n-1} c_j^\dagger c_j} \\ c_n &= \prod_j^{n-1}\left(-\sigma_j^z\right)\sigma_n^- & \sigma_n^- &= e^{+i\pi \sum_j^{n-1} c_j^\dagger c_j} \cdot c_n \\ c_n^\dagger c_n &= \frac{1}{2}\left(\sigma_n^z + 1\right) & \sigma_n^z &= 2c_n^\dagger c_n - 1 \end{aligned} \tag{4.11}$$

We can check the anti-commutation relations (shown here for the case $n \leq n'$)

$$\begin{aligned} \{c_n, c_{n'}^\dagger\} &= \prod_j^{n-1}\left(-\sigma_j^z\right)\sigma_n^-\sigma_{n'}^+ \prod_j^{n'-1}\left(-\sigma_j^z\right) + \sigma_{n'}^+ \prod_j^{n'-1}\left(-\sigma_j^z\right)\prod_j^{n-1}\left(-\sigma_j^z\right)\sigma_n^- \\ &= \sigma_n^-\sigma_{n'}^+ \prod_{j=n}^{n'-1}\left(-\sigma_j^z\right) + \prod_{j=n}^{n'-1}\left(-\sigma_j^z\right)\sigma_{n'}^+\sigma_n^- \end{aligned} \tag{4.12}$$

If $n \neq n'$

$$\begin{aligned} \{c_n, c_{n'}^\dagger\} &= \sigma_n^-\left(-\sigma_n^z\right) \prod_{j=n+1}^{n'-1}\left(-\sigma_j^z\right)\sigma_{n'}^+ + \left(-\sigma_n^z\right)\sigma_n^- \prod_{j=n+1}^{n'-1}\left(-\sigma_j^z\right)\sigma_{n'}^+ \\ &= -\{\sigma_n^-, \sigma_n^z\} \prod_{j=n+1}^{n'-1}\left(-\sigma_j^z\right)\sigma_{n'}^+ = 0 \end{aligned} \tag{4.13}$$

Where $\{\sigma_n^\alpha, \sigma_n^\beta\} = 2\delta_{\alpha\beta}$ was used. If $n = n'$ then the strings cancel each other

$$\begin{aligned}\{c_n, c_n^\dagger\} &= \sigma_n^- \sigma_n^+ + \sigma_n^+ \sigma_n^- = \{\sigma_n^-, \sigma_n^+\} \\ &= \frac{1}{4}\left(\{\sigma_n^x, \sigma_n^x\} - i\{\sigma_n^y, \sigma_n^x\} + i\{\sigma_n^x, \sigma_n^y\} + \{\sigma_n^y, \sigma_n^y\}\right) = 1 \end{aligned} \tag{4.14}$$

So, in conclusion, $\{c_n, c_{n'}^\dagger\} = \delta_{nn'}$ which is the correct fermionic statistics. We can also write the JW transform for the Majorana operators

$$\begin{aligned} \gamma_{A,n} &= \prod_j^{n-1}\left(-\sigma_j^z\right)\sigma_n^x & \sigma_n^x &= \gamma_{A,n}\prod_j^{n-1}\left(-i\gamma_{A,j}\gamma_{B,j}\right) \\ \gamma_{B,n} &= \prod_j^{n-1}\left(-\sigma_j^z\right)\left(-\sigma_n^y\right) & \sigma_n^y &= -\gamma_{B,n}\prod_j^{n-1}\left(-i\gamma_{A,j}\gamma_{B,j}\right) \\ & & \sigma_n^z &= i\gamma_{A,n}\gamma_{B,n} \end{aligned} \tag{4.15}$$

Inserting these into (4.5) gives us the JW transformed Hamiltonian

$$H_K = -\frac{\mu}{2}\sum_{n=1}^{N}\sigma_n^z + \frac{i}{4}\sum_{n=1}^{N-1}\left[(t+\Delta)\,\sigma_{n+1}^x\sigma_n^z\sigma_n^y + (t-\Delta)\,\sigma_n^x\sigma_n^z\sigma_{n+1}^y\right] \tag{4.16}$$

Using now that

$$\sigma_n^\alpha\sigma_n^\beta = \frac{1}{2}\left(\{\sigma_n^\alpha, \sigma_n^\beta\} + \left[\sigma_n^\alpha, \sigma_n^\beta\right]\right) = \delta_{\alpha\beta} + i\epsilon^{\alpha\beta\lambda}\sigma^\lambda \tag{4.17}$$

We get

$$H_K = -B\sum_{n=1}^{N}\sigma_n^z - \sum_{n=1}^{N-1}\left[J_x\,\sigma_n^x\sigma_{n+1}^x + J_y\,\sigma_n^y\sigma_{n+1}^y\right] \tag{4.18}$$

Where $B = \frac{\mu}{2}$, $J_x = \frac{t+\Delta}{4}$ and $J_y = \frac{t-\Delta}{4}$. This is the form of a XY-model with a constant magnetic field determined by μ, while J_x and J_y are transverse spin coupling terms. The topological phase for the Kitaev chain is now equivalent to magnetic order in the spin chain, so they share the same phase diagram [13]. The total number of fermions is measured by the operator

$$F = \sum_j^N c_j^\dagger c_j = \frac{1}{2}\sum_j^N\left(\sigma_j^z + 1\right) \tag{4.19}$$

Which does not commute with the Hamiltonian $[H_K, F] \neq 0$, so F is not a conserved quantity (this is due to the anomalous terms cc and $c^\dagger c^\dagger$ in the Hamiltonian, seen by the fact that $[H_K, F] = 0$ if $\Delta = 0 \Rightarrow J_x = J_y$). A conserved quantity is the fermion parity $P = (-1)^F$. This is measured by the operator

$$P = (-1)^F = e^{i\pi F} = e^{i\pi\sum_j^N c_j^\dagger c_j} = \prod_j^N\left(-\sigma_j^z\right) = \prod_j^N\left(-i\gamma_{A,j}\gamma_{B,j}\right) \tag{4.20}$$

Which commutes with the Hamiltonian $[H, P] = 0$. We can check if the Hamiltonian (4.18) reduces to (2.4) for the symmetric point $\mu = 0, t = \Delta$. For these parameters H_K becomes

$$\begin{aligned} H_K &= -\frac{t}{2}\sum_{n=1}^{N-1}\sigma_n^x\sigma_{n+1}^x = -\frac{t}{2}\sum_{n=1}^{N-1}\prod_{j}^{n-1}\left(-\sigma_j^z\right)\gamma_{A,n}\prod_{j}^{n}\left(-\sigma_j^z\right)\gamma_{A,n+1} \\ &= -\frac{t}{2}\sum_{n=1}^{N-1}\gamma_{A,n}\left(-\sigma_n^z\right)\gamma_{A,n+1} = \frac{it}{2}\sum_{n=1}^{N-1}\gamma_{A,n}\gamma_{A,n}\gamma_{B,n}\gamma_{A,n+1} = \frac{it}{2}\sum_{n=1}^{N-1}\gamma_{B,n}\gamma_{A,n+1} \end{aligned} \tag{4.21}$$

Which is what we expected. Again, the two end Majoranas commute with the Hamiltonian $[H, \gamma_{A,1}] = [H, \gamma_{B,N}] = 0$. The two degenerate GSs of this Hamiltonian is the tensor product of either all spin up or all spin down in the x-basis

$$|\psi_\uparrow\rangle = \prod_n^N |\uparrow_n\rangle^x \qquad\qquad |\psi_\downarrow\rangle = \prod_n^N |\downarrow_n\rangle^x \tag{4.22}$$

If we want to compare these GSs with the ones in (2.6), we need to rotate all the spins to align with the z-axis, since it is along this axis an empty $|\downarrow_n\rangle^z$ or occupied $|\uparrow_n\rangle^z$ state was defined. This is done by applying the rotation $R(\varphi, \mathbf{n}) = e^{-\frac{i\varphi}{2}\sigma\cdot\mathbf{n}}$ to each spin. For example one can examine $|\psi_\uparrow\rangle$, and see that $|\uparrow_n\rangle^x$ is just $|\downarrow_n\rangle^z$ rotated around the y-axis by $\varphi = -\frac{\pi}{2}$. This fact allows us to write

$$\begin{aligned} |\psi_\uparrow\rangle &= \prod_n^N e^{i\frac{\pi}{4}\sigma_n^y}|\downarrow_n\rangle^z = \prod_n^N\left(\cos\frac{\pi}{4} + i\,\sigma_n^y\sin\frac{\pi}{4}\right)|\downarrow_n\rangle^z = \frac{1}{\sqrt{2^N}}\prod_n^N\left(1 + i\,\sigma_n^y\right)|\downarrow_n\rangle^z \\ &= \frac{1}{\sqrt{2^N}}\prod_n^N\left(1 + \sigma_n^+ - \sigma_n^-\right)|\downarrow_n\rangle^z = \frac{1}{\sqrt{2^N}}\prod_n^N\left(1 + \sigma_n^+\right)|\downarrow_n\rangle^z \end{aligned} \tag{4.23}$$

If one now performs the inverse JW transform, $\prod_n^N |\downarrow_n\rangle^z = |0\rangle$ is the vacuum of fermions and using (4.11) one gets

$$\begin{aligned} |\psi_\uparrow\rangle &= \frac{1}{\sqrt{2^N}}\prod_n^N\left(1 + c_n^\dagger\cdot e^{-i\pi\sum_j^{n-1}c_j^\dagger c_j}\right)|0\rangle \\ &= \frac{1}{\sqrt{2^N}}\left(1 + c_1^\dagger\right)\left(1 + c_2^\dagger\right)\cdots\left(1 + c_N^\dagger\right)|0\rangle = |\psi_+\rangle \end{aligned} \tag{4.24}$$

Where the phase factor from the JW string results in us having to write the product in ascending order. This WF is identical to the one in (2.6). If instead calculating $|\psi_\downarrow\rangle$ one has to instead rotate the spins with $\varphi = \frac{\pi}{2}$

$$\begin{aligned} |\psi_\downarrow\rangle &= \prod_n^N -e^{-i\frac{\pi}{4}\sigma_n^y}|\downarrow_n\rangle^z = \frac{(-1)^N}{\sqrt{2^N}}\prod_n^N\left(1 - i\,\sigma_n^y\right)|\downarrow_n\rangle^z \\ &= \frac{(-1)^N}{\sqrt{2^N}}\prod_n^N\left(1 - \sigma_n^+\right)|\downarrow_n\rangle^z = \frac{1}{\sqrt{2^N}}\prod_n^N\left(1 - c_n^\dagger\cdot e^{-i\pi\sum_j^{n-1}c_j^\dagger c_j}\right)|0\rangle \\ &= \frac{(-1)^N}{\sqrt{2^N}}\left(1 - c_1^\dagger\right)\left(1 - c_2^\dagger\right)\cdots\left(1 - c_N^\dagger\right)|0\rangle = (-1)^N|\psi_-\rangle \end{aligned} \tag{4.25}$$

The $(-1)^N$ comes from the fact that when $|\downarrow_n\rangle^z$ is rotated by $R(\frac{\pi}{2}, \hat{\mathbf{y}})$ one gets $-|\downarrow_n\rangle^x$. We can identify the two degenerate GSs from (2.7) as

$$\begin{aligned} |\psi_{even}\rangle &= \frac{1}{\sqrt{2}}\left(|\psi_\uparrow\rangle + (-1)^N|\psi_\downarrow\rangle\right) \\ |\psi_{odd}\rangle &= \frac{1}{\sqrt{2}}\left(|\psi_\uparrow\rangle - (-1)^N|\psi_\downarrow\rangle\right) \end{aligned} \tag{4.26}$$

Let us check these states for a chain of length $N = 3$. Here the GSs become

$$\begin{aligned} |\psi^3_{even}\rangle &= \frac{1}{\sqrt{2}}\left(|\psi_\uparrow\rangle - |\psi_\downarrow\rangle\right) \\ |\psi^3_{odd}\rangle &= \frac{1}{\sqrt{2}}\left(|\psi_\uparrow\rangle + |\psi_\downarrow\rangle\right) \end{aligned} \tag{4.27}$$

We can annihilate $|\psi^3_{even}\rangle$ with $f_3 = \frac{1}{2}\left(\gamma_{A,1} + i\gamma_{B,3}\right)$ by using the JW transformation rules

$$\begin{aligned} f_3|\psi^3_{even}\rangle &= \frac{1}{2}\left(\gamma_{A,1} + i\gamma_{B,3}\right)\frac{1}{\sqrt{2}}\left(|\uparrow_1\rangle^x|\uparrow_2\rangle^x|\uparrow_3\rangle^x - |\downarrow_1\rangle^x|\downarrow_2\rangle^x|\downarrow_3\rangle^x\right) \\ &= \frac{1}{2\sqrt{2}}\left(\sigma^x_1 - i\sigma^z_1\sigma^z_2\sigma^y_3\right)\left(|\uparrow_1\rangle^x|\uparrow_2\rangle^x|\uparrow_3\rangle^x - |\downarrow_1\rangle^x|\downarrow_2\rangle^x|\downarrow_3\rangle^x\right) \end{aligned} \tag{4.28}$$

Writing the Pauli matrices in the x-basis

$$\begin{aligned} \sigma^x_j &= |\uparrow_j\rangle^x\langle\uparrow_j|^x - |\downarrow_j\rangle^x\langle\downarrow_j|^x \\ \sigma^y_j &= i|\uparrow_j\rangle^x\langle\downarrow_j|^x - i|\downarrow_j\rangle^x\langle\uparrow_j|^x \\ \sigma^z_j &= |\uparrow_j\rangle^x\langle\downarrow_j|^x + |\downarrow_j\rangle^x\langle\uparrow_j|^x \end{aligned} \tag{4.29}$$

Allows us to calculate further

$$\begin{aligned} f_3|\psi^3_{even}\rangle = \frac{1}{2\sqrt{2}}(&|\uparrow_1\rangle^x|\uparrow_2\rangle^x|\uparrow_3\rangle^x + |\downarrow_1\rangle^x|\downarrow_2\rangle^x|\downarrow_3\rangle^x \\ &- |\downarrow_1\rangle^x|\downarrow_2\rangle^x|\downarrow_3\rangle^x - |\uparrow_1\rangle^x|\uparrow_2\rangle^x|\uparrow_3\rangle^x) = 0 \end{aligned} \tag{4.30}$$

And

$$\begin{aligned} f_3^\dagger|\psi^3_{even}\rangle &= \frac{1}{2}\left(\gamma_{A,1} - i\gamma_{B,3}\right)\frac{1}{\sqrt{2}}\left(|\uparrow_1\rangle^x|\uparrow_2\rangle^x|\uparrow_3\rangle^x - |\downarrow_1\rangle^x|\downarrow_2\rangle^x|\downarrow_3\rangle^x\right) \\ &= \frac{1}{2\sqrt{2}}\left(\sigma^x_1 + i\sigma^z_1\sigma^z_2\sigma^y_3\right)\left(|\uparrow_1\rangle^x|\uparrow_2\rangle^x|\uparrow_3\rangle^x - |\downarrow_1\rangle^x|\downarrow_2\rangle^x|\downarrow_3\rangle^x\right) \\ &= \frac{1}{\sqrt{2}}(|\uparrow_1\rangle^x|\uparrow_2\rangle^x|\uparrow_3\rangle^x + |\downarrow_1\rangle^x|\downarrow_2\rangle^x|\downarrow_3\rangle^x) = |\psi^3_{odd}\rangle \end{aligned} \tag{4.31}$$

So everything fits nicely with section 2.1.1.

4.3.2 *Interacting*

The interacting part of the Hamiltonian in (4.6) can also be JW transformed

$$\begin{aligned} H_{int} &= \frac{W}{4}\sum_{n=1}^{N-1}\prod_{j}^{n-1}\left(-\sigma_j^z\right)\sigma_n^x\prod_{j}^{n}\left(-\sigma_j^z\right)\sigma_{n+1}^x\prod_{j}^{n-1}\left(-\sigma_j^z\right)\left(-\sigma_n^y\right)\prod_{j}^{n}\left(-\sigma_j^z\right)\left(-\sigma_{n+1}^y\right) \\ &= \frac{W}{4}\sum_{n=1}^{N-1}\sigma_n^x\sigma_n^z\sigma_{n+1}^x\sigma_n^y\sigma_n^z\sigma_{n+1}^y = -\frac{W}{4}\sum_{n=1}^{N-1}\sigma_n^x\sigma_n^y\sigma_{n+1}^x\sigma_{n+1}^y = \frac{W}{4}\sum_{n=1}^{N-1}\sigma_n^z\sigma_{n+1}^z \end{aligned} \tag{4.32}$$

Which is an added coupling between z-components of spin, controlled by $J_z = -\frac{W}{4}$. The total Hamiltonian is then an XYZ model with constant magnetic field.

4.4 PHASE DIAGRAM AND EXACT GROUND STATES AT FINE-TUNED POINT

The phase diagram of the Kitaev chain with nearest neighbour interactions is known from the mapping to a XYZ spin chain in an external magnetic field, which was discussed in the previous section. The phase diagram is plotted in figure 18, which is from [24], where they calculated it using DMRG and ED. Here they set $\Delta = t$, so $J_y = 0$. Interestingly, and in direct relation to this thesis, in [22] they investigate parts of the phase diagram by calculating the interacting TI from (2.153) using DMRG and ED and show that the TI changes due to poles in the zero energy GF as predicted by the considerations in section 2.3.3.

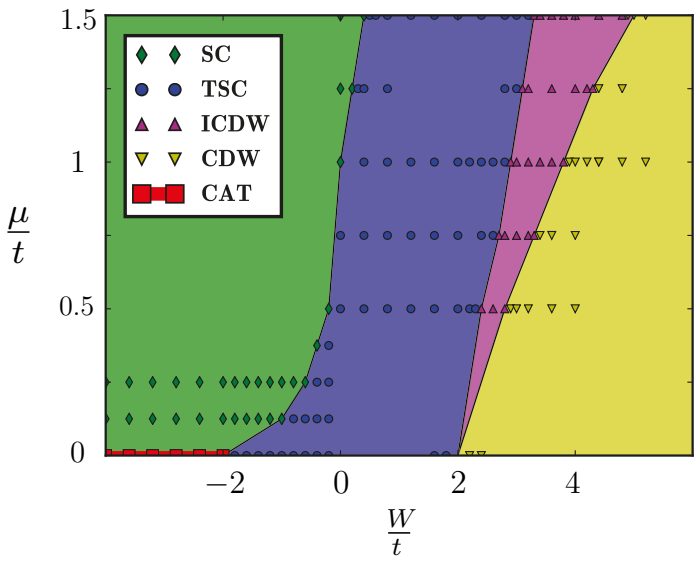

Figure 18: Phase diagram for $\Delta = t$. SC - Superconductor, TSC - Topological Superconductor, ICDW - Incommensurate Charge Density Wave, CDW - Charge Density Wave, CAT - Schrödinger's cat phase. We observe that the range of chemical potential μ in which the system is in the topological phase is extended by adding a repulsive interaction $W/t > 0$, which is quite surprising. This picture is from [18], and in their model t and Δ does not have a factor $\frac{1}{2}$ and $U = \frac{W}{4}$. The bottom line defined by $\mu = 0$ is also found and described in [22].

We know the line in the phase diagram corresponding to the non-interacting case $W = 0$, which has a criterion for being topology non-trivial at $\frac{\mu}{t} < 1$. We can check the line in the phase diagram defined by $\mu = 0$, for which the JW transformed interacting Hamiltonian in (4.18) with (4.32) becomes

$$H = \sum_{n=1}^{N-1} \left[-\frac{t}{2}\, \sigma_n^x \sigma_{n+1}^x + \frac{W}{4} \sigma_n^z \sigma_{n+1}^z \right] \tag{4.33}$$

Now, the interaction term was troublesome since each σ_n^z contains two Majorana operators. To handle this quartic term one can perform a rotation of all the spins around the x-axis, such that the interaction term becomes two σ_n^y operators (each consisting of one Majorana operator), thereby reducing a quartic term to a quadratic one [31]. This is done by rotating all spins by $R(-\frac{\pi}{2}, \hat{\mathbf{x}}) = e^{\frac{i\pi}{4}\sigma^x}$ such that

$$\tilde{H} = RHR^{-1} \qquad\qquad R = \prod_n^N e^{\frac{i\pi}{4}\sigma_n^x} \tag{4.34}$$

By inserting this one obtains

$$\begin{aligned}
\tilde{H} &= \sum_{n=1}^{N-1} \left[-\frac{t}{2}\, R\sigma_n^x \sigma_{n+1}^x R^{-1} + \frac{W}{4} R\sigma_n^z \sigma_{n+1}^z R^{-1} \right] \\
&= \sum_{n=1}^{N-1} \left[-\frac{t}{2}\, R\sigma_n^x R^{-1} R\sigma_{n+1}^x R^{-1} + \frac{W}{4} R\sigma_n^z R^{-1} R\sigma_{n+1}^z R^{-1} \right] \\
&= \sum_{n=1}^{N-1} \left[-\frac{t}{2}\, \tilde{\sigma}_n^x \tilde{\sigma}_{n+1}^x + \frac{W}{4} \tilde{\sigma}_n^y \tilde{\sigma}_{n+1}^y \right]
\end{aligned} \tag{4.35}$$

We can now introduce new Majorana operators $\tilde{\gamma}_{A,n}$ and $\tilde{\gamma}_{B,n}$ using the inverse JW transformation 4.15, and write the Hamiltonian as

$$\begin{aligned}
\tilde{H} = \sum_{n=1}^{N-1} &- \frac{t}{2}\, \tilde{\gamma}_{A,n} \prod_j^{n-1} \left(-i\tilde{\gamma}_{A,j}\tilde{\gamma}_{B,j} \right) \tilde{\gamma}_{A,n+1} \prod_j^{n} \left(-i\tilde{\gamma}_{A,j}\tilde{\gamma}_{B,j} \right) \\
&+ \frac{W}{4} \tilde{\gamma}_{B,n} \prod_j^{n-1} \left(-i\tilde{\gamma}_{A,j}\tilde{\gamma}_{B,j} \right) \tilde{\gamma}_{B,n+1} \prod_j^{n} \left(-i\tilde{\gamma}_{A,j}\tilde{\gamma}_{B,j} \right) \\
= \sum_{n=1}^{N-1} &- \frac{t}{2}\, \tilde{\gamma}_{A,n} \left(-i\tilde{\gamma}_{A,n}\tilde{\gamma}_{B,n} \right) \tilde{\gamma}_{A,n+1} + \frac{W}{4} \tilde{\gamma}_{B,n} \left(-i\tilde{\gamma}_{A,n}\tilde{\gamma}_{B,n} \right) \tilde{\gamma}_{B,n+1} \\
= \sum_{n=1}^{N-1} &\frac{it}{2}\, \tilde{\gamma}_{B,n}\tilde{\gamma}_{A,n+1} + \frac{iW}{4} \tilde{\gamma}_{A,n}\tilde{\gamma}_{B,n+1}
\end{aligned} \tag{4.36}$$

And finally, transforming back to fermionic operators

$$\begin{aligned}\tilde{H} &= \sum_{n=1}^{N-1} \frac{it}{2} \left[i\left(\tilde{c}_n^\dagger - \tilde{c}_n\right)\left(\tilde{c}_{n+1}^\dagger + \tilde{c}_{n+1}\right)\right] + \frac{iW}{4}\left[\left(\tilde{c}_n^\dagger + \tilde{c}_n\right) i\left(\tilde{c}_{n+1}^\dagger - \tilde{c}_{n+1}\right)\right] \\ &= \sum_{n=1}^{N-1} \left(-\frac{t}{2} + \frac{W}{4}\right) \left[\tilde{c}_n^\dagger \tilde{c}_{n+1} + \tilde{c}_{n+1}^\dagger \tilde{c}_n\right] + \left(\frac{t}{2} + \frac{W}{4}\right)\left[\tilde{c}_{n+1}^\dagger \tilde{c}_n^\dagger + \tilde{c}_n \tilde{c}_{n+1}\right] \\ &= \sum_{n=1}^{N-1} -\frac{\tilde{t}}{2} \left[\tilde{c}_n^\dagger \tilde{c}_{n+1} + \tilde{c}_{n+1}^\dagger \tilde{c}_n\right] + \frac{\tilde{\Delta}}{2}\left[\tilde{c}_{n+1}^\dagger \tilde{c}_n^\dagger + \tilde{c}_n \tilde{c}_{n+1}\right] \end{aligned} \tag{4.37}$$

Which is just a non-interacting Kitaev chain without zero chemical potential, with $\tilde{t} = t - \frac{W}{2}$ and $\tilde{\Delta} = t + \frac{W}{2}$. The spectrum in k-space is

$$\tilde{E}_k = \pm\sqrt{\tilde{t}^2 \cos^2 k + \tilde{\Delta}^2 \sin^2 k} \tag{4.38}$$

Which becomes gapless at either $\tilde{t} = 0$ or $\tilde{\Delta} = 0$, which translates to $\frac{W}{t} = 2$ and $\frac{W}{t} = -2$ respectively. This signals two topological phase transitions separating three different phases. The nature of the phases $\frac{W}{t} > 2$ (Charge-density wave) and $\frac{W}{t} < -2$ (CAT - Shrödinger's cat phase) are discussed in [18], [22] and [25]. When in between these two boundaries, the ground-state is degenerate and the system is in the topological phase. Here there will exist a many-body generalization of the Majorana modes Γ, which commutes with the Hamiltonian $[H, \Gamma]$.

It can been shown that the degenerate GSs can still be found exactly, if the chemical potential is fine-tuned to a specific value of the other parameters (W, Δ and t) defining a line in the phase diagram inside the topological phase. It should be noted that a ground-state degeneracy is not enough to conclude the existence of Majorana modes, but it has been shown in [18] that the exact solution in question can be adiabatically connected to the non-interacting, non-trivial Kitaev chain. In this paper they also find operators that transform between the degenerate GSs, are Hermitian, and are localized near the edges, which is an interacting generalisation of the Majorana mode. It also reduces to the usual Majoranas in the non-interacting limit.

One can consider a case where the chemical potential is $\mu/2$ on the first and last site, but μ on all others, the Hamiltonian can be written as the sum

$$H = \sum_n^{N-1} h_n \tag{4.39}$$

where

$$\begin{aligned} h_n = &-\frac{\mu}{2}\left(c_n^\dagger c_n + c_{n+1}^\dagger c_{n+1} - 1\right) - \frac{t}{2}\left(c_n^\dagger c_{n+1} + c_{n+1}^\dagger c_n\right) + \frac{\Delta}{2}\left(c_n c_{n+1} + c_{n+1}^\dagger c_n^\dagger\right) \\ &+ W\left(c_n^\dagger c_n - \frac{1}{2}\right)\left(c_{n+1}^\dagger c_{n+1} - \frac{1}{2}\right) \end{aligned} \tag{4.40}$$

Since the h_n does not commute with neighbouring sites, they cannot be diagonalized simultaneously. However, for some value of μ the GSs of H minimizes all h_n separately, and this is called the *frustration free* condition (frustration as referring to

the corresponding spin system) [18]. Defining the vacuum state $c_n|vac\rangle = 0$ for any n, one can then define a basis for h_n , $|\circ\,\circ\rangle = |vac\rangle$, $|\bullet\,\circ\rangle = c_n^\dagger|vac\rangle$, $|\circ\,\bullet\rangle = c_{n+1}^\dagger|vac\rangle$, $|\bullet\,\bullet\rangle = c_n^\dagger c_{n+1}^\dagger|vac\rangle$. Written in this basis h_n can be represented by the matrix

$$h_n \doteq \begin{array}{c} \begin{matrix} |\circ\,\circ\rangle & |\bullet\,\bullet\rangle & |\bullet\,\circ\rangle & |\circ\,\bullet\rangle \end{matrix} \\ \begin{pmatrix} \frac{W}{4}+\frac{\mu}{2} & -\frac{\Delta}{2} & 0 & 0 \\ -\frac{\Delta}{2} & \frac{W}{4}-\frac{\mu}{2} & 0 & 0 \\ 0 & 0 & -\frac{W}{4} & -\frac{t}{2} \\ 0 & 0 & -\frac{t}{2} & -\frac{W}{4} \end{pmatrix} \end{array} = \begin{pmatrix} h_n^{even} & 0 \\ 0 & h_n^{odd} \end{pmatrix} \tag{4.41}$$

Where it is apparent that h_n is block diagonal due to the parity symmetry $[H, P] = 0$, i.e. it splits into an even- and odd parity space. The GS of h_n^{even} is the lowest eigenvalue found by the determinant equation

$$\begin{vmatrix} \frac{W}{4}+\frac{\mu}{2}-\lambda & -\frac{\Delta}{2} \\ -\frac{\Delta}{2} & \frac{W}{4}-\frac{\mu}{2}-\lambda \end{vmatrix} = 0$$

$$\lambda^2 - \frac{W}{2}\lambda + \frac{W^2}{16} - \frac{\mu^2}{4} - \frac{\Delta^2}{4} = 0 \Rightarrow \lambda = \frac{W}{4} \pm \sqrt{\left(\frac{\mu}{2}\right)^2 + \left(\frac{\Delta}{2}\right)^2} \tag{4.42}$$

So the ground-state energy is

$$\epsilon_0^{even} = \frac{W}{4} - \sqrt{\left(\frac{\mu}{2}\right)^2 + \left(\frac{\Delta}{2}\right)^2} \tag{4.43}$$

The corresponding wavefunction is found by solving the matrix equation

$$\begin{pmatrix} \frac{W}{4}+\frac{\mu}{2}-\epsilon_0^{even} & -\frac{\Delta}{2} \\ -\frac{\Delta}{2} & \frac{W}{4}-\frac{\mu}{2}-\epsilon_0^{even} \end{pmatrix} \begin{pmatrix} 1 \\ \beta \end{pmatrix} = \begin{pmatrix} 0 \\ 0 \end{pmatrix} \tag{4.44}$$

Leading to the equation for β

$$-\frac{\Delta}{2} + \left(\sqrt{\left(\frac{\mu}{2}\right)^2 + \left(\frac{\Delta}{2}\right)^2} - \frac{\mu}{2}\right)\beta = 0$$

$$\Rightarrow \beta = \frac{\frac{\Delta}{2}}{\sqrt{\left(\frac{\mu}{2}\right)^2 + \left(\frac{\Delta}{2}\right)^2} - \frac{\mu}{2}} = \frac{\Delta}{\sqrt{\mu^2+\Delta^2} - \mu} = \frac{\frac{\Delta}{\mu}}{\sqrt{1+\left(\frac{\Delta}{\mu}\right)^2} - 1} \tag{4.45}$$

using the trick

$$\cot\frac{\theta}{2} = \frac{\tan\theta}{\sqrt{1+\tan^2\theta} - 1} \tag{4.46}$$

We can then conclude that the un-normalized wavefunction is

$$|\psi_0^{even}\rangle = |\circ\,\circ\rangle + \cot\frac{\theta}{2}|\bullet\,\bullet\rangle \qquad\qquad \theta = \arctan\frac{\Delta}{\mu} \tag{4.47}$$

For the odd parity sector one has instead the equation

$$\begin{vmatrix} -\frac{W}{4}-\lambda & -\frac{t}{2} \\ -\frac{t}{2} & -\frac{W}{4}-\lambda \end{vmatrix} = 0$$
$$\lambda^2 + \frac{W}{2}\lambda + \frac{W^2}{16} - \frac{t^2}{4} = 0 \Rightarrow \lambda = -\frac{W}{4} \pm \frac{t}{2} \tag{4.48}$$

So the ground-state energy is now

$$\epsilon_0^{odd} = -\left(\frac{W}{4} + \frac{t}{2}\right) \tag{4.49}$$

The un-normalized wavefunction is read off as

$$|\psi_0^{odd}\rangle = |\bullet\,\circ\rangle + |\circ\,\bullet\rangle \tag{4.50}$$

The necessary condition for topological order is a degenerate ground-state which happens if

$$\frac{W}{4} - \sqrt{\left(\frac{\mu}{2}\right)^2 + \left(\frac{\Delta}{2}\right)^2} = -\left(\frac{W}{4} + \frac{t}{2}\right) \tag{4.51}$$

Or by simplifying, this becomes a condition for the chemical potential

$$\mu = \mu^* = \sqrt{(W+t)^2 - \Delta^2} \tag{4.52}$$

Which is the *frustration free* condition mentioned in [18] (this is the point where the XYZ-model is exactly solvable). We can construct similar states as the ones in section 2.1.1 as a superposition of the two degenerate GSs (now $\theta = \theta^* = \arctan\frac{\Delta}{\mu^*}$)

$$\begin{aligned} |\psi_0^{\pm}\rangle &= |\psi_0^{even}\rangle \pm \alpha|\psi_0^{odd}\rangle \\ &= \left(1 + \cot\frac{\theta^*}{2} c_n^\dagger c_{n+1}^\dagger \pm \alpha c_n^\dagger \pm \alpha c_{n+1}^\dagger\right)|vac\rangle \end{aligned} \tag{4.53}$$

If one chooses $\alpha = \sqrt{\cot\frac{\theta^*}{2}}$ then this gets a nice factorized form

$$|\psi_0^{\pm}\rangle = \left(1 \pm \alpha c_n^\dagger\right)\left(1 \pm \alpha c_{n+1}^\dagger\right)|vac\rangle \tag{4.54}$$

These are the GSs for h_n, so the GS for the entire H is the product of all these WF's that minimize each h_n independently. The exact GSs WF and energy then become

$$\begin{aligned} |\Psi_0^{\pm}\rangle &= \frac{1}{(1+\alpha^2)^{N/2}}\left(1 \pm \alpha c_1^\dagger\right)\left(1 \pm \alpha c_2^\dagger\right)\cdots\left(1 \pm \alpha c_N^\dagger\right)|vac\rangle \\ E_0 &= -(N-1)\left(\frac{W}{4} + \frac{t}{2}\right) \end{aligned} \tag{4.55}$$

These energies are plotted in 19 as a function of W, for the first small chains of size $N = 2, 3, 4$, together with the value of the GS energy, found by exact diagonalization

of the many-body Hamiltonian, as described in appendix G. This is shown for $\Delta = t$ and $\mu = \mu^* = \sqrt{W^2 + 2Wt}$. As one can see they are in perfect agreement.

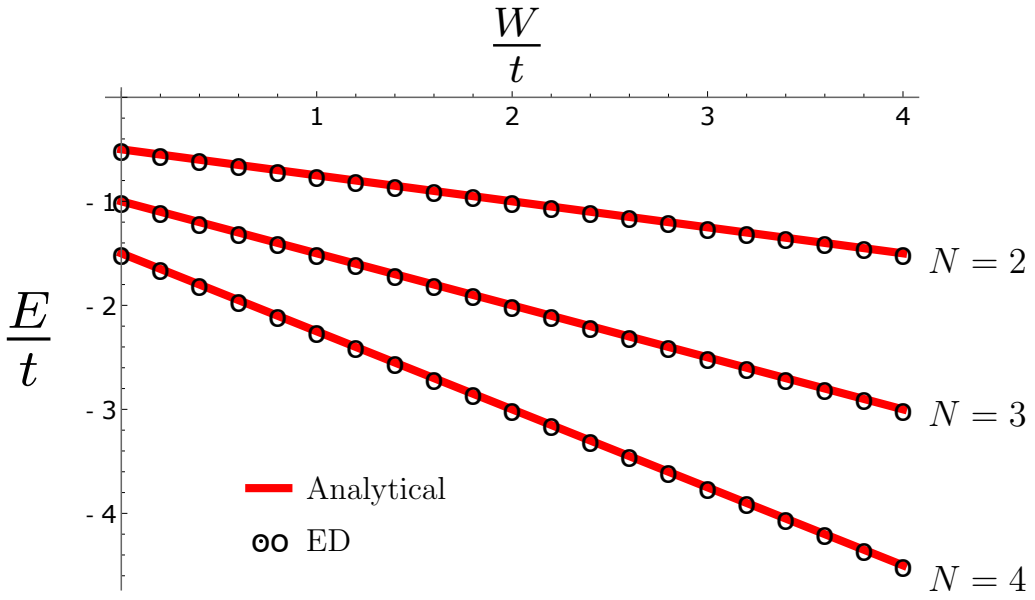

Figure 19: Plot of the analytically found energies (4.55) (red) of the interacting Kitaev chain at the frustration free point defined in (4.52). This function is compared with the lowest eigenvalue of an exact diagonalisation (black rings), and it can be concluded that they are commensurate.

4.5 PERTURBATION THEORY FOR E-E INTERACTION

In this section we want to look at the boundary zero modes, and how these are affected by the interactions. For this we will develop a perturbation series like in section 3.2, but now with the density coupled electron-electron interaction in (4.1). The derivation is nearly identical, so explanations will be brief. We consider the interaction where the quantum numbers i, j refer to real space sites, and that the functional dependence of these (the distance of the interaction) is encoded in W_{ij}. We now employ the same trick as for bosons, and rewrite the interaction in Nambu space, but again it is beneficial to write the Hamiltonian with reference to the half-filled system, if one wants a simple expression for H_{int}. This is demonstrated by calculating

$$\begin{aligned} H_{e-e} &= \frac{1}{2}\sum_{ii'} \frac{W_{ii'}}{2} \left((C^\dagger)_i^\sigma \, \tau_z^{\sigma\rho} \, C_i^\rho\right) \left((C^\dagger)_{i'}^{\sigma'} \, \tau_z^{\sigma'\rho'} \, C_{i'}^{\rho'}\right) \\ &= \frac{1}{2}\sum_{ii'} \frac{W_{ii'}}{2} \left(c_i^\dagger c_i - c_i c_i^\dagger\right) \left(c_{i'}^\dagger c_{i'} - c_{i'} c_{i'}^\dagger\right) = \sum_{ii'} W_{ii'} \left(c_i^\dagger c_i - \frac{1}{2}\right) \left(c_{i'}^\dagger c_{i'} - \frac{1}{2}\right) \end{aligned} \tag{4.56}$$

Where repeated Nambu indices are summed. This shows that the Nambu space interaction Hamiltonian in the first line is particularly simple. We just have to

include a factor $\frac{1}{2}$ on the interaction strength. We want to calculate the full GF $\mathcal{G}^{\beta\alpha}(b,\tau_b\,;\,a,\tau_a)$, which is the propagator going from site a at imaginary time τ_a to b at τ_b. As before, this is a matrix in Nambu space, with indices α and β. This GF given by a thermal average wrt. the full Hamiltonian, and by writing all operators in the interaction picture, one can then expand the imaginary time propagator $\hat{U}(\beta,0)$ in powers of the interaction. We want to calculate

$$\begin{aligned}\mathcal{G}^{\beta\alpha}(b,\tau_b\,;\,a,\tau_a) &= \frac{-\langle T_\tau\left(\hat{U}(\beta,0)\hat{C}_b^\beta(\tau_b)(\hat{C}^\dagger)_a^\alpha(\tau_a)\right)\rangle_0}{\langle\hat{U}(\beta,0)\rangle_0} \\ &= \frac{-\sum_{n=1}^\infty \frac{(-1)^n}{n!}\int_0^\beta d\tau_1\cdots\int_0^\beta d\tau_n\langle T_\tau\left(\hat{P}(\tau_1)\ldots\hat{P}(\tau_n)\hat{C}_b^\beta(\tau_b)(\hat{C}^\dagger)_a^\alpha(\tau_a)\right)\rangle_0}{\sum_{n=1}^\infty \frac{(-1)^n}{n!}\int_0^\beta d\tau_1\cdots\int_0^\beta d\tau_n\langle T_\tau\left(\hat{P}(\tau_1)\ldots\hat{P}(\tau_n)\right)\rangle_0}\end{aligned} \tag{4.57}$$

As described in [4] one needs to be careful with τ-ordering, since creation operators precede annihilation operators in the interaction, which is written as

$$\begin{aligned}&\hat{P}(\tau_1) = \\ &\int_0^\beta d\tau_{1'}\sum_{i_1 i_{1'}}\left((\hat{C}^\dagger)_{i_1}^{\sigma_1}(\tau_1+\eta)\tau_z^{\sigma_1\rho_1}\hat{C}_{i_1}^{\rho_1}(\tau_1)\right)W(i_1,i_{1'})\left((\hat{C}^\dagger)_{i_{1'}}^{\sigma_{1'}}(\tau_{1'}+\eta)\tau_z^{\sigma_{1'}\rho_{1'}}\hat{C}_{i_{1'}}^{\rho_{1'}}(\tau_{1'})\right)\end{aligned} \tag{4.58}$$

Where the interaction function is $W(i_1,i_1') = \frac{W_{i_1 i_{1'}}}{2}\,\delta(\tau_1-\tau_{1'})$, and $\eta = 0^+$ is added to ensure that creation operators are to the left in the time ordering. From now on this will be suppressed in the notation, but will be included in the Feynman rules. The rest of the derivation follows the one in [4] but now with an added Nambu structure. Everything is similar to the method in section 3.2, we now expand to a desired order, and use Wick's theorem to change from multiple operator averages to products of single particle averages. For example, expanding the numerator up to first order gives

$$\begin{aligned}&-\langle T_\tau\left(\hat{U}(\beta,0)\hat{C}_b^\beta(\tau_b)(\hat{C}^\dagger)_a^\alpha(\tau_a)\right)\rangle_0 \approx \mathcal{G}_0^{\beta\alpha}(b,\tau_b\,;\,a,\tau_a) + \iint_0^\beta d\tau_1 d\tau_{1'}\sum_{i_1 i_{1'}}W(i_1,i_{1'}) \\ &\times\tau_z^{\sigma_1\rho_1}\tau_z^{\sigma_{1'}\rho_{1'}}\langle T_\tau\left((\hat{C}^\dagger)_{i_1}^{\sigma_1}(\tau_1)\hat{C}_{i_1}^{\rho_1}(\tau_1)(\hat{C}^\dagger)_{i_{1'}}^{\sigma_{1'}}(\tau_{1'})\hat{C}_{i_{1'}}^{\rho_{1'}}(\tau_{1'})\hat{C}_b^\beta(\tau_b)(\hat{C}^\dagger)_a^\alpha(\tau_a)\right)\rangle_0\end{aligned} \tag{4.59}$$

Where using Wicks theorem on the last 6-operator average result in the same type of diagrams as seen in the second line of (E.16). The terms arising from the expansion can again be represented by Feynman diagrams, and the Feynman rules for this interaction in discrete real space and imaginary time are, after a careful tracking of signs and indices, shown to be

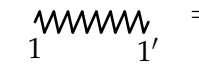

$$= -W(i_1, i_{1'})$$

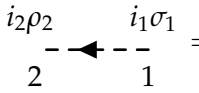

$$= \mathcal{G}_0^{\rho_2\sigma_1}(i_2, i_1; \tau_2 - \tau_1), \qquad \tau_1 \to \tau_1 + \eta$$

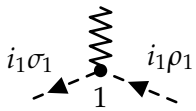

$$= \int_0^\beta d\tau_1 \sum_{i_1} \tau_z^{\sigma_1\rho_1}$$

$\sum$ *topologically different* diagrams
Repeated Nambu indices are summed
For F fermion loops, multiply $(-1)^F$ (4.60)

Let us look at the first relevant diagram $\mathcal{G}^P$ (assuming that a Hartree-Fock analysis has already been performed) which is second order in W

$$\mathcal{G}_P^{\beta\alpha}(b, a; \tau_b - \tau_a) =$$

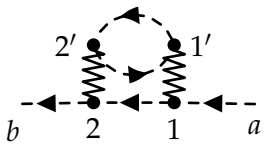

$$= -\sum_{\substack{i_1 i_{1'} \\ i_2 i_{2'}}} \iiint d\tau_1 d\tau_{1'} d\tau_2 d\tau_{2'}$$

$$\times W(i_1, i_{1'}) W(i_2, i_{2'}) \tau_z^{\sigma_1\rho_1} \tau_z^{\sigma_{1'}\rho_{1'}} \tau_z^{\sigma_2\rho_2} \tau_z^{\sigma_{2'}\rho_{2'}} \mathcal{G}_0^{\beta\sigma_2}(b, i_2; \tau_b - \tau_2) \mathcal{G}_0^{\rho_2\sigma_1}(i_2, i_1; \tau_2 - \tau_1)$$
$$\times \mathcal{G}_0^{\rho_1\alpha}(i_1, \alpha; \tau_1 - \tau_a) \mathcal{G}_0^{\rho_{2'}\sigma_{1'}}(i_{2'}, i_{1'}; \tau_{2'} - \tau_{1'}) \mathcal{G}_0^{\rho_{1'}\sigma_{2'}}(i_{1'}, i_{2'}; \tau_{1'} - \tau_{2'}) \tag{4.61}$$

And by inserting the Matsubara frequency transformed functions one gets

$$\mathcal{G}_P^{\beta\alpha}(b, a; \tau_b - \tau_a) = \frac{1}{\beta} \sum_{ikn} \Big(-\frac{1}{\beta^2} \sum_{iq_n ip_n} \sum_{\substack{i_1 i_{1'} \\ i_2 i_{2'}}} \frac{W_{i_1 i_{1'}}}{2} \frac{W_{i_2 i_{2'}}}{2}$$
$$\times \tau_z^{\sigma_1\rho_1} \tau_z^{\sigma_{1'}\rho_{1'}} \tau_z^{\sigma_2\rho_2} \tau_z^{\sigma_{2'}\rho_{2'}} \mathcal{G}_0^{\beta\sigma_2}(b, i_2; ik_n) \mathcal{G}_0^{\rho_2\sigma_1}(i_2, i_1; ik_n - iq_n) \mathcal{G}_0^{\rho_1\alpha}(i_1, \alpha; ik_n)$$
$$\times \mathcal{G}_0^{\rho_{2'}\sigma_{1'}}(i_{2'}, i_{1'}; ip_n + iq_n) \mathcal{G}_0^{\rho_{1'}\sigma_{2'}}(i_{1'}, i_{2'}; ip_n)) e^{-ik_n(\tau_b - \tau_a)} \tag{4.62}$$

Where $\mathcal{G}_P^{\beta\alpha}(b, a; ik_n)$ is isolated in the parentheses. Here, ip_n is a fermionic Matsubara frequency and iq_n is bosonic. To see the Matsubara frequency conservation, this function is diagrammatically

$$\mathcal{G}_P^{\beta\alpha}(b, a; ik_n) =$$

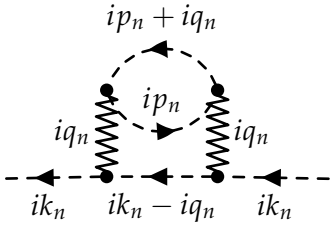

(4.63)

And the Feynman rules in real space, Matsubara frequency is then

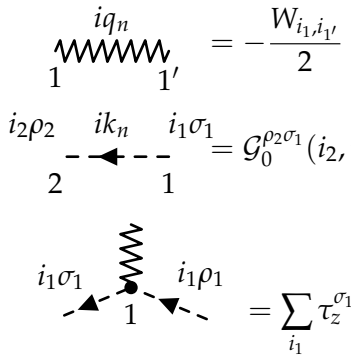

$\sum$ *topologically different* diagrams
Repeated Nambu indices are summed
Conserve Matsubara frequency in all vertices
Multiply $\frac{1}{\beta}$ for each internal frequency ik_n , and sum $\sum_{ik_n}$
Multiply $e^{ik_n\eta}$ for each "same time" diagram, where $\eta = 0^+$
For F fermion loops, multiply $(-1)^F$ (4.64)

The rule with $e^{ik_n\eta}$ is because of the small imaginary time parameter that was added in (4.58). The pair-bubble diagram will be calculated in the next section, and then added as a self-energy to the full GF, to see if this changes the zero modes.

4.6 SELF-ENERGY DIAGRAM CALCULATION

We write $\mathcal{G}_P^{\beta\alpha}(b, a; ik_n)$ as

$$\mathcal{G}_P^{\beta\alpha}(b, a; ik_n) = \quad = \sum_{i_1 i_2} \mathcal{G}_0^{\beta\sigma_2}(b, i; ik_n)\Sigma_P^{\sigma_2\rho_1}(i, j; ik_n)\mathcal{G}_0^{\rho_1\alpha}(j, b; ik_n) \tag{4.65}$$

With the self-energy, written as a matrix in Nambu space

$$\underline{\underline{\Sigma_P}}(i, j; ik_n) = \quad = -\frac{1}{4\beta^2} \sum_{iq_n ip_n} \sum_{lk} W_{jl} W_{ik}\ \tau_z \underline{\underline{\mathcal{G}_0}}(i, j; ik_n - iq_n)\tau_z$$
$$\cdot \mathrm{Tr}\left[\underline{\underline{\mathcal{G}_0}}(k, l; ip_n + iq_n)\tau_z \underline{\underline{\mathcal{G}_0}}(l, k; ip_n)\tau_z\right] \tag{4.66}$$

This self-energy is what we want to insert in the Dyson equation (3.23). This self energy preserves all the symmetries of the original GF, since for example $\Pi G(\omega)\Pi = -G(-\omega)$ translates directly to the self energy $\Pi\Sigma(\omega)\Pi = -\Sigma(-\omega)$,

and by inserting $\Pi = \tau_x \delta_{ij}$, this holds. We want to perform the Matsubara frequency summation over iq_n and ip_n. To perform the Matsubara summation (and since we eventually want to plug this into a numerical calculation), one can write out the self-energy with all the messy indices (here upper indices are Nambu and lower are site number $\mathcal{G}_0^{\beta\alpha}(i,j;ik_n) \equiv \mathcal{G}_0(ik_n)_{ij}^{\beta\alpha}$). Also, we want to write the diagonal GF as in (2.97), so we add transformation matrices U and $U^\dagger$ at all GFs and use that τ_z is diagonal in site-space. This gives

$$\begin{aligned}\Sigma_P(ik_n)_{ij}^{\beta\alpha} = -\frac{1}{\beta^2}\sum_{iq_n ip_n}\sum_{\substack{lk\\mbd}} W_{jl}W_{ik}\,(\tau_z)_{ii}^{\beta\sigma_1}U_{im}^{\sigma_1\sigma_m}\tilde{\mathcal{G}}_0(ik_n - iq_n)_{mm}^{\sigma_m\sigma_m}(U^\dagger)_{mj}^{\sigma_m\sigma_2}(\tau_z)_{jj}^{\sigma_2\alpha}\\ \cdot U_{kb}^{\sigma_3\sigma_b}\tilde{\mathcal{G}}_0(ip_n + iq_n)_{bb}^{\sigma_b\sigma_b}(U^\dagger)_{bl}^{\sigma_b\sigma_4}(\tau_z)_{ll}^{\sigma_4\sigma_5}U_{ld}^{\sigma_5\sigma_d}\tilde{\mathcal{G}}_0(ip_n)_{dd}^{\sigma_d\sigma_d}(U^\dagger)_{dk}^{\sigma_d\sigma_6}(\tau_z)_{kk}^{\sigma_6\sigma_3}\end{aligned} \tag{4.67}$$

Now one can write

$$\mathcal{P}(\epsilon_b,\epsilon_d;iq_n) = -\frac{1}{\beta}\sum_{ip_n}\tilde{\mathcal{G}}_0(ip_n+iq_n)_{bb}^{\sigma_b\sigma_b}\tilde{\mathcal{G}}_0(ip_n)_{dd}^{\sigma_d\sigma_d} = -\frac{1}{\beta}\sum_{ip_n}\frac{1}{ip_n+iq_n-\epsilon_b}\cdot\frac{1}{ip_n-\epsilon_d} \tag{4.68}$$

Where one can now perform the Matsubara sum over ip_n.
After performing all the Matsubara sums, one can insert the vector of eigenvalues $\epsilon_m = (\epsilon_1,\epsilon_2,\dots,\epsilon_N,-\epsilon_1,-\epsilon_2,\dots,-\epsilon_N)$ and similarly with ϵ_b and ϵ_d, and then perform the summation over site and Nambu indices in (4.67). $\mathcal{P}(\epsilon_b,\epsilon_d;iq_n)$ has only simple poles, and can therefore be calculated by the same method described in section 3.4, noting that this time the sum is over fermionic Matsubara frequencies. One can now write

$$\mathcal{P}(\epsilon_b,\epsilon_d;iq_n) = \frac{1}{\beta}\sum_{ip_n} g_0(ip_n) \qquad g_0(ip_n) = -\frac{1}{ip_n+iq_n-\epsilon_b}\cdot\frac{1}{ip_n-\epsilon_d} \tag{4.69}$$

Again, one wants to write the sum as a contour integral over a complex variable $ip_n = z$, and use a function with poles at the fermionic Matsubara frequencies to pick out the frequencies from $g_0(z)$ (in figure 14, these are the black dots on the imaginary axis). This is now the Fermi-Dirac distribution function

$$n_F(z) = \frac{1}{e^{\beta z}+1} \qquad \text{poles for } z = ip_n = i\frac{2n+1}{\beta}\pi \tag{4.70}$$

With residues

$$\begin{aligned}\operatorname*{Res}_{z\to ip_n}[n_F(z)] &= \lim_{z\to ip_n}\frac{z-ip_n}{e^{\beta z}+1} = \lim_{\delta\to 0}\frac{\delta}{e^{\beta(\delta+ip_n)}+1}\\ &= \lim_{\delta\to 0}\frac{\delta}{-e^{\beta\delta}+1} \overset{\text{L'Hôpital's rule}}{\to} \lim_{\delta\to 0}\frac{1}{-\beta e^{\beta\delta}} = -\frac{1}{\beta}\end{aligned} \tag{4.71}$$

Which is negative of what was achieved for bosonic frequencies. This means that there is a sign difference in (3.31), such that

$$\mathcal{P}(\epsilon_b,\epsilon_d;iq_n) = \sum_l \operatorname*{Res}_{z=z_l}[g_0(z)]\;n_F(z_l) \tag{4.72}$$

Where z_l are the poles of $g_0(z)$, which can be evaluated from (4.69) to be $z_1 = \epsilon_b - iq_n$ and $z_2 = \epsilon_d$. Performing the calculation of residues yields

$$\mathcal{P}(\epsilon_b, \epsilon_d; iq_n) = -\frac{n_F(\epsilon_b - iq_n)}{\epsilon_b - iq_n - \epsilon_d} - \frac{n_F(\epsilon_d)}{\epsilon_d + iq_n - \epsilon_b} = \frac{n_F(\epsilon_b) - n_F(\epsilon_d)}{iq_n + \epsilon_d - \epsilon_b} \tag{4.73}$$

Where $n_F(\epsilon_b - iq_n) = n_F(\epsilon_b)$ was used since iq_n is a bosonic Matsubara frequency. The imaginary part of the retarded pair-bubble function will lead to a broadening of the GF, but for low energies, when summing over energies, it is suppressed exponentially in the gap size, seen from

$$\begin{aligned}\sum_{bd} \text{Im}\left[\mathcal{P}^R(\epsilon_b, \epsilon_d; \omega)\right] &= \sum_{bd} \text{Im}\left[\frac{n_F(\epsilon_b) - n_F(\epsilon_d)}{\omega + i\eta + \epsilon_d - \epsilon_b}\right] \\ &= -\pi \sum_{bd} \left[n_F(\epsilon_b) - n_F(\epsilon_d)\right] \delta(\omega + \epsilon_d - \epsilon_b) = -\pi \sum_{b} \left[n_F(\epsilon_b) - n_F(\epsilon_b - \omega)\right]\end{aligned} \tag{4.74}$$

And now using the fact that the states lie outside of the gap $\epsilon_b \approx \Delta >> T$, one gets

$$\begin{aligned}\sum_{bd} \text{Im}\left[\mathcal{P}^R(\epsilon_b, \epsilon_d; \omega)\right] &= -\pi \sum_{b} \left[\frac{1}{e^{\epsilon_b/T} + 1} - \frac{1}{e^{(\epsilon_b - \omega)/T} + 1}\right] \\ &\propto e^{-\frac{\Delta}{T}} \left[1 - e^{\frac{\omega}{T}}\right] \overset{\omega \approx 0}{=} \frac{\omega}{T} e^{-\frac{\Delta}{T}}\end{aligned} \tag{4.75}$$

Which shows that $\frac{\Delta}{T}$ controls how much the bubble diagram can affect the GF. Δ is here chosen to parametrize the gap, but in reality this should be the effective gap in the spectrum. A quick note here, if one takes a symmetric combination

$$\begin{aligned}\mathcal{P}(\epsilon_b, \epsilon_d; iq_n) + \mathcal{P}(\epsilon_d, \epsilon_b; iq_n) &= \frac{n_F(\epsilon_b) - n_F(\epsilon_d)}{iq_n + \epsilon_d - \epsilon_b} + \frac{n_F(\epsilon_d) - n_F(\epsilon_b)}{iq_n + \epsilon_b - \epsilon_d} \\ = \left(n_F(\epsilon_b) - n_F(\epsilon_d)\right) &\left[\frac{1}{iq_n - \tilde{\omega}} - \frac{1}{iq_n + \tilde{\omega}}\right] = \tilde{\mathcal{D}}_0(iq_n)\end{aligned} \tag{4.76}$$

Then it has a similar pole structure as the bosonic GF (C.38), except now $\omega_b = \tilde{\omega} = \epsilon_b - \epsilon_d$. So the pair bubble can be interpreted as a bosonic excitation, i.e.

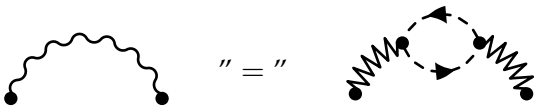

(4.77)

Now we define

$$\begin{aligned}\mathcal{Q}(\epsilon_m, \epsilon_b, \epsilon_d; ik_n) &= \frac{1}{\beta} \sum_{iq_n} \tilde{\mathcal{G}}_0(ik_n - iq_n)^{\sigma_m \sigma_m}_{mm} \mathcal{P}(\epsilon_b, \epsilon_d; iq_n) \\ &= \frac{1}{\beta} \sum_{iq_n} \frac{1}{ik_n - iq_n - \epsilon_m} \cdot \frac{n_F(\epsilon_b) - n_F(\epsilon_d)}{iq_n + \epsilon_d - \epsilon_b} = \frac{1}{\beta} \sum_{iq_n} h_0(iq_n)\end{aligned} \tag{4.78}$$

Where now

$$\mathcal{Q}(\epsilon_m, \epsilon_b, \epsilon_d; ik_n) = -\sum_l \underset{z=z_l}{\text{Res}} \left[h_0(z)\right] \; n_B(z_l) \tag{4.79}$$

Which has poles at $z_1 = ik_n - \epsilon_m$ and $z_2 = \epsilon_b - \epsilon_d$. Inserting the residues gives

$$\begin{aligned}\mathcal{Q}(\epsilon_m, \epsilon_b, \epsilon_d; ik_n) &= \frac{[n_F(\epsilon_b) - n_F(\epsilon_d)]\, n_B(ik_n - \epsilon_m)}{ik_n - \epsilon_m + \epsilon_d - \epsilon_b} + \frac{[n_F(\epsilon_b) - n_F(\epsilon_d)]\, n_B(\epsilon_b - \epsilon_d)}{\epsilon_b - \epsilon_d - ik_n + \epsilon_m} \\ &= \frac{[n_F(\epsilon_d) - n_F(\epsilon_b)]\, n_F(-\epsilon_m)}{ik_n - \epsilon_m + \epsilon_d - \epsilon_b} + \frac{[n_F(\epsilon_d) - n_F(\epsilon_b)]\, n_B(\epsilon_b - \epsilon_d)}{ik_n - \epsilon_m + \epsilon_d - \epsilon_b} \\ &= \frac{[n_F(\epsilon_d) - n_F(\epsilon_b)]\, [n_F(-\epsilon_m) + n_B(\epsilon_b - \epsilon_d)]}{ik_n - \epsilon_m + \epsilon_d - \epsilon_b} \end{aligned} \tag{4.80}$$

Which then enables us to write out the self-energy as

$$\begin{aligned}\Sigma_P(ik_n)_{ij}^{\beta\alpha} = \sum_{\substack{lk \\ mbd}} & W_{jl} W_{ik} \mathcal{Q}(\epsilon_m, \epsilon_b, \epsilon_d; ik_n)\ (\tau_z)_{ii}^{\beta\sigma_1} U_{im}^{\sigma_1\sigma_m} (U^\dagger)_{mj}^{\sigma_m\sigma_2} (\tau_z)_{jj}^{\sigma_2\alpha} \\ & \cdot U_{kb}^{\sigma_3\sigma_b} (U^\dagger)_{bl}^{\sigma_b\sigma_4} (\tau_z)_{ll}^{\sigma_4\sigma_5} U_{ld}^{\sigma_5\sigma_d} (U^\dagger)_{dk}^{\sigma_d\sigma_6} (\tau_z)_{kk}^{\sigma_6\sigma_3}\end{aligned} \tag{4.81}$$

First one needs to check for divergences since when summing over b and d there will be values where they are equal, but this means that the part in $\mathcal{Q}(\epsilon_m, \epsilon_b, \epsilon_d; ik_n)$ with the bose-einstein distribution approaches the limit

$$\lim_{\epsilon_b \to \epsilon_d} \frac{[n_F(\epsilon_d) - n_F(\epsilon_b)]\, n_B(\epsilon_b - \epsilon_d)}{ik_n - \epsilon_m + \epsilon_d - \epsilon_b} = \lim_{\epsilon_b \to \epsilon_d} \frac{[n_F(\epsilon_d) - n_F(\epsilon_b)]}{ik_n - \epsilon_m + \epsilon_d - \epsilon_b} \frac{1}{e^{\beta(\epsilon_b - \epsilon_d)} - 1} \to \frac{0}{0} \tag{4.82}$$

So one should calculate the limit of these problematic parts, and then separate these from the sum. Using L'Hôpital's rule one can analyse the limit

$$\begin{aligned}&\lim_{\epsilon_b \to \epsilon_d} \frac{1}{ik_n - \epsilon_m + \epsilon_d - \epsilon_b} \left[\frac{1}{e^{\beta\epsilon_d} + 1} - \frac{1}{e^{\beta\epsilon_b} + 1}\right] \frac{1}{e^{\beta(\epsilon_b - \epsilon_d)} - 1} \\ &= \lim_{\epsilon_b \to \epsilon_d} \frac{1}{ik_n - \epsilon_m + \epsilon_d - \epsilon_b} \left[\frac{e^{\beta\epsilon_d} - e^{\beta\epsilon_b}}{e^{\beta(\epsilon_d + \epsilon_b)} + e^{\beta\epsilon_d} + e^{\beta\epsilon_b} + 1}\right] \frac{1}{e^{\beta(\epsilon_b - \epsilon_d)} - 1} \\ &= \frac{1}{ik_n - \epsilon_m} \left[\frac{e^{\beta\epsilon_d}}{e^{2\beta\epsilon_d} + 2e^{\beta\epsilon_d} + 1}\right] \lim_{c \to 0} \frac{1 - e^{\beta c}}{e^{\beta c} - 1} \\ &= \frac{1}{ik_n - \epsilon_m} \left[\frac{-e^{\beta\epsilon_d}}{e^{2\beta\epsilon_d} + 2e^{\beta\epsilon_d} + 1}\right] \lim_{c \to 0} \frac{\beta e^{\beta c}}{\beta e^{\beta c}} = \frac{1}{ik_n - \epsilon_m} \left[\frac{-e^{\beta\epsilon_d}}{e^{2\beta\epsilon_d} + 2e^{\beta\epsilon_d} + 1}\right]\end{aligned} \tag{4.83}$$

So the limit is well defined. This ensures that the numerical calculations are controlled. One can now calculate (4.81) numerically, and analyse the resulting spectral function, which will be the subject in the following section.

4.7 THE FULL SPECTRAL FUNCTION - ELECTRON-ELECTRON INTERACTIONS

In this section we again look at the local spectral function for the full interacting GF. As previously mentioned, a relevant parameter for the magnitude of the self-energy is $\frac{\Delta}{T}$, which can be calculated from an estimate of the realistic parameters in such a system. These are chosen to be in the range of $T \approx 100mK$ and $\Delta \approx 200\mu eV$. Δ will vary from specific material values, since the gap in our model is an effective gap resulting from proximity to a type-s superconductor, and will therefore be lower. We cannot check the part of the phase diagram with an attractive interaction $W < 0$ since our self energy is of the order W^2, so an odd power diagram is needed to

examine this example. Also, the system size was only $N = 20$ due to the amount of heavy numerical calculations.

In figure 21 one observes that for fixed values of t, μ and Δ/T but increasing interaction strength W, the local spectral function decreases significantly, which is most visible on the edges. The usual sum rule for the spectral function (2.108) is for energy, and a similar rule does not exist for the site index i (summing up all i's just gives the total density of states at that energy). It is therefore not immediately clear what is the primary cause of the decrease in height of the coherence function. Broadening is due to the imaginary part of the self-energy $\mathrm{Im}(\Sigma^R)$, and the reduction of the peak is associated with a renormalisation constant $Z < 1$. The full spectral function has two parts, one is the quasi-particle contribution, which has a weight determined by Z, and one is the remaining complicated many-body interaction part $\mathcal{A}'(\omega)$ [4].

$$\mathcal{A}(\omega) = 2\pi Z\delta(\omega - \tilde{\epsilon}) + \mathcal{A}'(\omega) \tag{4.84}$$

Where $\tilde{\epsilon}$ is a renormalised energy due to the real part of the self-energy $\mathrm{Re}(\Sigma^R)$. The renormalisation constant Z is also related to the quasi-particle life-time by $\frac{1}{\tau(\omega)} = -2Z\mathrm{Im}(\Sigma^R(\omega))$, so a quasi-particle with long life-time is associated with a highly peaked spectral function.

It could be that the spectral function diminishes due to broadening, due to the weight of the peak decreasing from the renormalisation factor Z, or the location of the peaks changing due to $\mathrm{Re}\Sigma$. To try and discern which of these has the most influence, we can look at figure 20, where the spectral function on the edge $\mathcal{A}_{11}(1, 1, \omega)$ is plotted as a function of energy (only shown here for $W/t = 0.2$). The conclusion of which factor is decisive for the energy profile of the spectral function on the edge was not attainable due to low computing power. The comparison at different W is more precise if one locates the zero mode peak in $\mathcal{A}_{11}(1, 1; \omega)$, and uses this as the new energy ϵ_0' for checking the spacial decay of coherence into the bulk. We conclude that the energy still resides very close to ϵ_0 so this will be used as the reference energy when comparing different interaction strengths and temperatures.

To study the decay rate of the various functions (and thus the localisation of the zero modes), we can look at figure 22 where the functions are normalised to have the same value on the first site. We see that for larger interaction strengths the decay rate decreases, meaning that as interactions increase, the zero mode coherence decays further into the bulk. In this sense, we can thus conclude that the edge modes are more localized for low W.

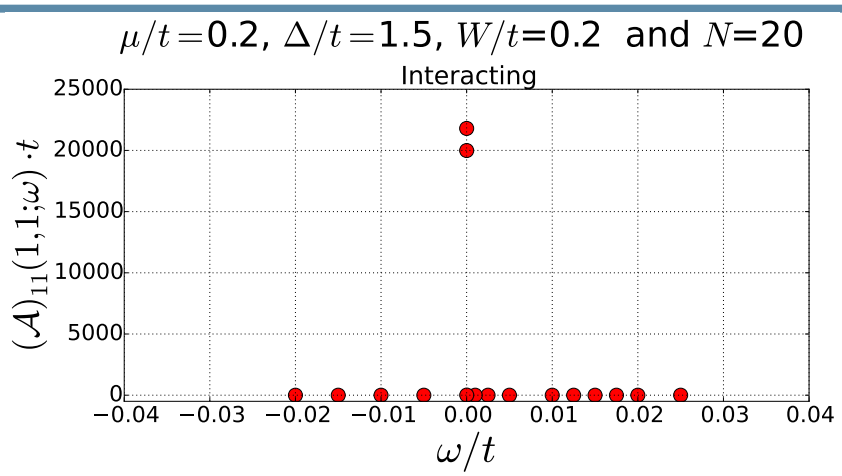

Figure 20: Plot of the local spectral function on the edge of the wire, as a function of energy. This allows us to locate the renormalised zero mode energy, which is found to be approximately equal to the non-interacting eigenvalue ϵ_0. Due to the large amount of numerical calculations, this is plotted for a couple of points and not as a smooth function.

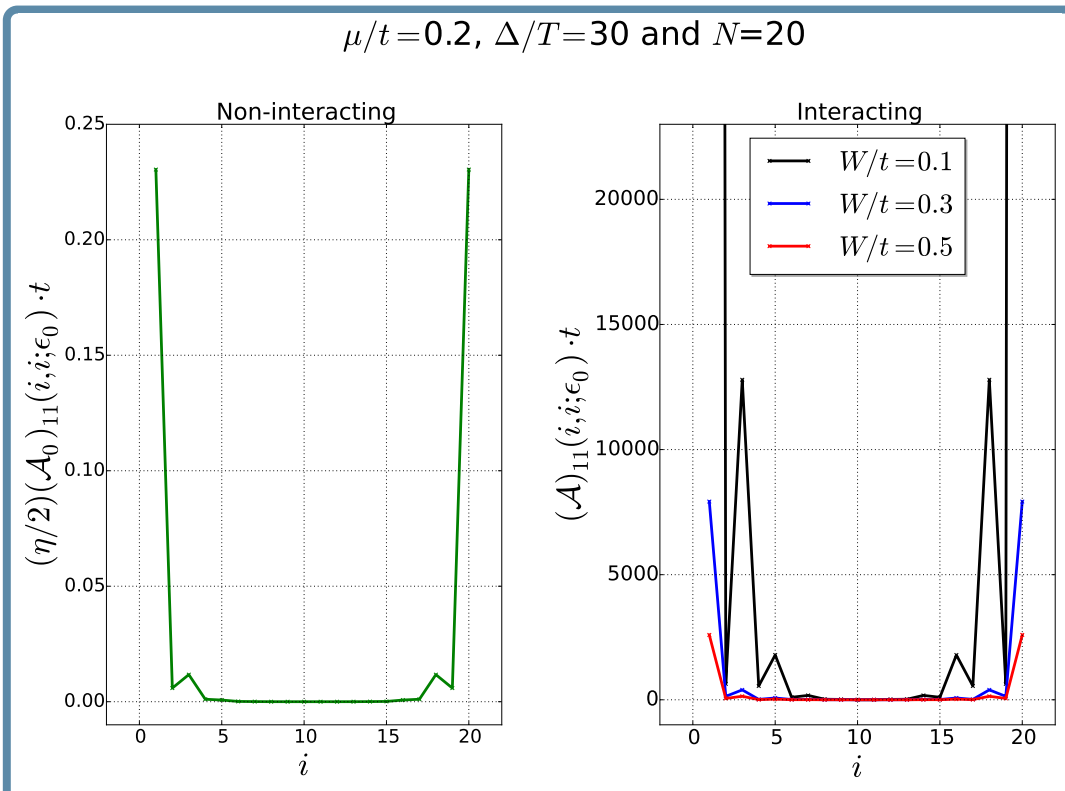

Figure 21: Plot of both the non-interacting and interacting spectral functions, as a function of site on the wire, at the zero mode energy ϵ_0. The function decreases greatly as W is increased, which will affect the differential conductance in an imagined tunnelling experiment.

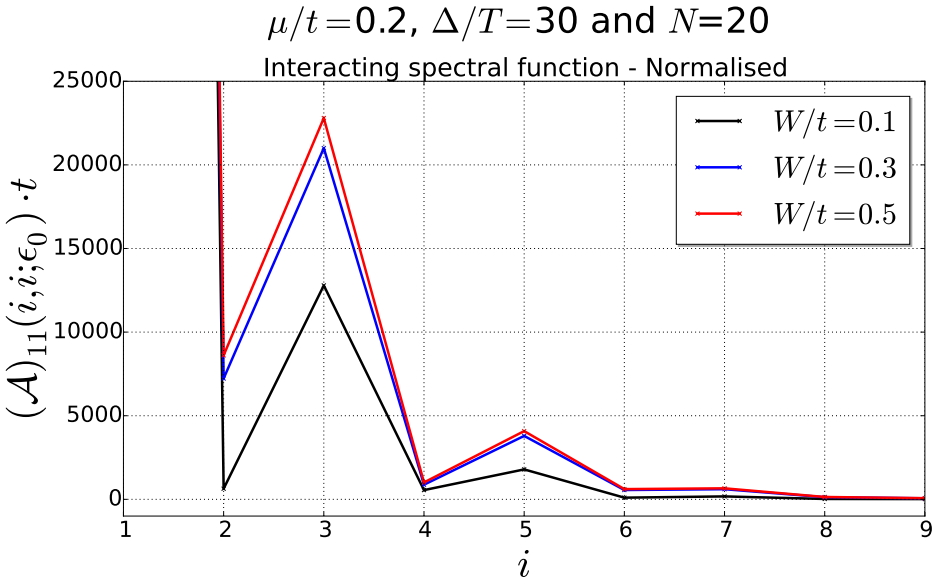

Figure 22: Plot of the full spectral function at $\omega = \epsilon_0$ as a function of site index, where each function has been normalised such that the have the same value on the edge. This is to see if rate of decay for the local coherence is affected by the interactions. We see that larger values of W makes the function decay further into the bulk.

In figure 23 the local spectral function is plotted, now for fixed W and increasing temperature.

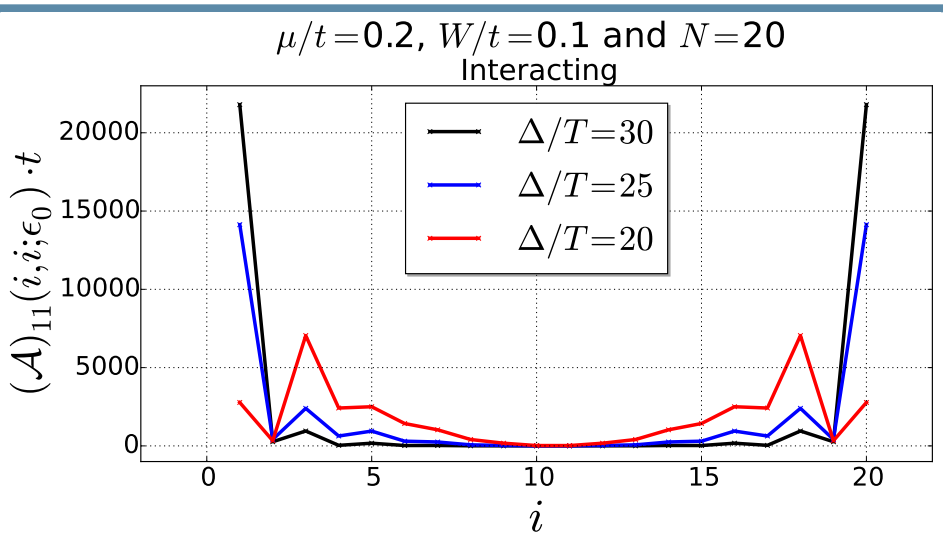

Figure 23: Plot of the local spectral function with fixed W, for various temperatures. We see that the local coherence on the first site diminishes with increasing temperature.

As before, we want to see how the rate of decay is affected by the increasing temperatures, so the normalised results are shown in 24. The function reaches further into the bulk of the chain for higher temperatures, so in an experiment where a high current signal is preferred, a low temperature will benefit the coherence peak of the zero mode.

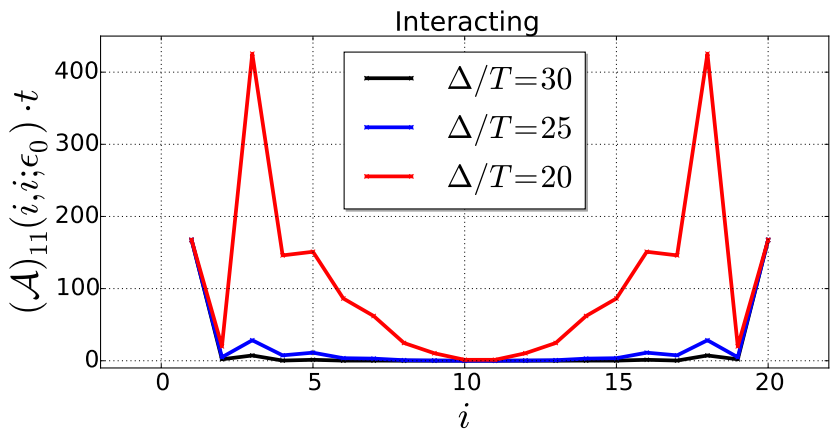

Figure 24: Local spectral function at different temperatures, but normalised to have the same value on the first site, so one can see the differing decay rates. Higher temperatures will lead to a broadening of the zero mode peak, and to the function spilling further into the bulk of the wire.

So, from the plots of the spectral function we can conclude that interaction strength and temperature leads to a broadening of the spectral peak located at the zero mode energy. In the next section we will check if the symmetries of the interacting GF presented in section 2.3 are preserved in this model.

4.8 SYMMETRIES OF THE FULL GREEN'S FUNCTION FOR ELECTRON-ELECTRON INTERACTIONS

We can check to see if the symmetries in (2.115) are still preserved for the full GF, which in section 2.3 is showed should be the case. These translate to

$$\begin{aligned} \mathcal{T}G(\omega)^{\alpha\beta}_{ij}\mathcal{T}^\dagger &= \quad G(\omega)^{\beta\alpha}_{ji} \\ \mathcal{P}G(\omega)^{\alpha\beta}_{ij}\mathcal{P}^\dagger &= -G(-\omega)^{\beta\alpha}_{ji} \\ \mathcal{Q}G(\omega)^{\alpha\beta}_{ij}\mathcal{Q}^\dagger &= -G(-\omega)^{\alpha\beta}_{ij} \end{aligned} \tag{4.85}$$

Using the symmetries for this model, found in (2.135), one can write out explicitly how symmetry operations transform the local spectral function. The spectral function is given as the imaginary value of the retarded GF, but under symmetry operations it will be relevant to flip the sign on $i\eta$ in the GF, which can be achieved by

complex conjugation of the GF. We use that $-2\mathrm{Im}\left[G^A(\omega)\right] = -2\mathrm{Im}\left[G^R(\omega)^*\right] = 2\mathrm{Im}\left[G^R(\omega)\right] = -\mathcal{A}(\omega)$. The spectral function then has the following symmetries

$$\begin{aligned} \mathcal{A}(\omega)_{ii}^{\alpha\beta} &= \mathcal{A}(\omega)_{ii}^{\beta\alpha} \\ \tau_x^{\sigma\alpha}\mathcal{A}(\omega)_{ii}^{\alpha\beta}\tau_x^{\beta\rho} &= \mathcal{A}(-\omega)_{ii}^{\sigma\rho} \end{aligned} \tag{4.86}$$

Writing out the Nambu space matrices, one then gets

$$\begin{aligned} \begin{pmatrix} \mathcal{A}(\omega)_{ii}^{11} & \mathcal{A}(\omega)_{ii}^{12} \\ \mathcal{A}(\omega)_{ii}^{21} & \mathcal{A}(\omega)_{ii}^{22} \end{pmatrix} &= \begin{pmatrix} \mathcal{A}(\omega)_{ii}^{11} & \mathcal{A}(\omega)_{ii}^{21} \\ \mathcal{A}(\omega)_{ii}^{12} & \mathcal{A}(\omega)_{ii}^{22} \end{pmatrix} \\ \begin{pmatrix} \mathcal{A}(\omega)_{ii}^{22} & \mathcal{A}(\omega)_{ii}^{21} \\ \mathcal{A}(\omega)_{ii}^{12} & \mathcal{A}(\omega)_{ii}^{11} \end{pmatrix} &= \begin{pmatrix} \mathcal{A}(-\omega)_{ii}^{11} & \mathcal{A}(-\omega)_{ii}^{21} \\ \mathcal{A}(-\omega)_{ii}^{12} & \mathcal{A}(-\omega)_{ii}^{22} \end{pmatrix} \end{aligned} \tag{4.87}$$

Which is checked for $\mathcal{A}(\omega)_{ii}^{11} = \mathcal{A}(-\omega)_{ii}^{22}$ and $\mathcal{A}(\omega)_{ii}^{22} = \mathcal{A}(-\omega)_{ii}^{11}$ with the energy at the zero-mode $\omega = \epsilon_0$, and plotted in figure 25

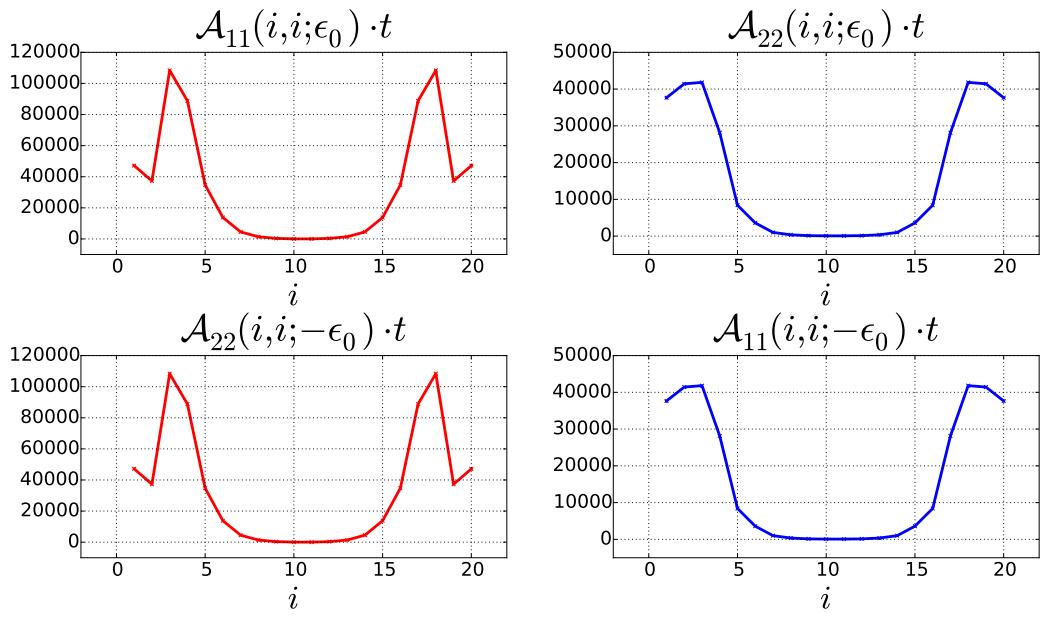

Figure 25: Plot of some of the components of the last line in (4.87), i.e. a survey of the PH symmetry for the interacting GF. The plot is arranged so that $\mathcal{A}(\omega)_{ii}^{11} = \mathcal{A}(-\omega)_{ii}^{22}$ is shown in the first column and $\mathcal{A}(\omega)_{ii}^{22} = \mathcal{A}(-\omega)_{ii}^{11}$ in the second. The asymmetry between electron and hole parts of the spectral function is from having a finite μ. The action of sending $\mu \to -\mu$ will exchange electrons and holes and these plots will swap left to right column. At $\mu = 0$ the left and right will be identical.

We see that the calculated symmetries are still preserved when interactions are include, fitting with the conclusions from previous sections.

5 OUTLOOK

There are a few topics that would have been a natural extension to this thesis work, and these will be covered in this section. It goes without saying that this list is not exhaustive, since the area of Interacting Topological Systems is still fairly unexplored territory, with many fascinating concepts yet to be discovered.

The framework developed for analysing the Kitaev model numerically (section 2.1.5) could be used to study effects of including next-nearest neighbour hopping or superconducting pairing. It would be interesting to investigate the effect of these on the zero modes and the phase diagram.

The exploration of the phase diagrams for different topological systems with interactions can be done by determining the generalised TI, which at the moment is only feasible using more advanced numerical procedures like Density Matrix Renormalisation Group and Exact Diagonalisation. The latter was performed for small chains in this thesis, due to the immense size of the Hilbert space ($2^N \times 2^N$). The modification of the phase diagrams due to interactions would be an especially fascinating thing to be able to probe.

There is some very intriguing mathematical physics in describing the TIs for interacting systems (discussed in 2.3.3). The TI is derived to be the coefficient of an induced Chern-Simons term, describing an effective topological quantum field theory (TQFT). Investigating TQFTs would be a very compelling direction to take after this analysis, particularly delving into the work of [26], where they showed that a classification of time-reversal invariant Topological Insulators in $(3+1)d$ and $(2+1)d$ is obtained from a fundamental $(4+1)d$ insulator from dimensional reduction. These exotic systems exhibit some novel electrodynamical effects that would be interesting to describe using the response functions attained from the effective action. In addition, this research area has mostly focused on Topological Insulators, so it would also be interesting to follow some of the work done in trying to discover an effective TQFT for p-wave superconductors [16], and to study its relation to the concepts described in this thesis.

Another fascinating inquiry for this subject, is how the momentum space topology changes, when adding interactions. An example of this is the work done by Kitaev and Fidkowski in [11], where they showed that the $\mathcal{Z}$ invariant of the Kitaev model reduced to $\mathcal{Z}_8$ in the presence of interactions. In [23] they showed that this change topological classification was triggered by the Green's function acquiring zeroes in the eigenvalue spectrum. It would have been very interesting to be able to study this concrete example, as a direct application of what was described in section 2.3.

6 CONCLUSION

In this thesis we have explored various facets of Interacting Topological Systems, by studying bosonic and fermionic interactions for the concrete example of a 1D p-wave superconductor, described by the Kitaev model. Chapter 2 introduced the non-interacting Kitaev chain and demonstrated the existence of boundary Majorana zero modes for various points in parameter space. The bulk-boundary correspondence was examined by connecting the presence of Majoranas to the non-trivial bulk momentum space topology. After this, the wavefunction of the exact zero modes were found for general parameters in an infinitely long wire. In order to describe how interactions affected the edge states in the finite wire system, a numerical framework was established, and the findings were used to corroborate the previously determined analytical results. The non-interacting Green's function for the Kitaev model was then determined, and analysed numerically. The relation between the zero mode wavefunction and the local spectral function was demonstrated.

Concepts from the study of topological systems, such as Altland-Zirnbauer/Cartan symmetry classes and Topological Invariants were then generalised to include interacting systems, by casting all equations in a form containing the many-body Green's function. It was shown that the symmetries of the Green's function are still present when interactions are introduced. The preservation of the symmetries were monitored throughout the thesis. The Topological Invariant for interacting 1D chiral system was shown to be correct in the non-interacting limit and possible consequences of adding interactions were discussed.

Electron-Boson interactions were incorporated by writing down a perturbation series in the interaction term. The bosons were modelling charge fluctuations in a system configuration where the nanowire is coupled to a capacitative gate, in parallel with a resistance. A low order self energy diagram was calculated and implemented numerically, to see how the bosonic modes change the spectral function. This lead to broadening of the spectral peaks, but had no apparent change to the exponential decay of the local spectral function into the bulk.

Next, we treated Electron-Electron interactions by adding a repulsive nearest neighbour two-body interaction between electrons. This model could be solved by performing a Jordan-Wigner transformation, changing electron operators to spin operators. Under this operation the Hamiltonian mapped to an XYZ spin model, with a phase diagram that was then explored for symmetric parameter values. For a specific line in parameter space the exact many-body ground state was found, and the ground state energy was compared to a result obtained by exact diagonalization for small wire lengths. These two results turned out to be identical.

Finally, a perturbation series calculation was performed for the case of Electron-Electron interactions. The real space dependence of the local spectral function was inspected for various temperatures and interaction strengths. It was seen that in-

creasing these latter two parameters led to a decrease of the spectral function on the edge of the wire, as well as making the zero mode coherence extend further into the bulk of the system. The symmetries of the bare Green's function was showed to still be obeyed for the full version, thus confirming the results from the previous chapters. Lastly, some prospects of future research were discussed.

A

DETAILS FOR THE CONTINUOUS MOMENTUM SPACE KITAEV CHAIN

A.1 COHERENCE FACTORS

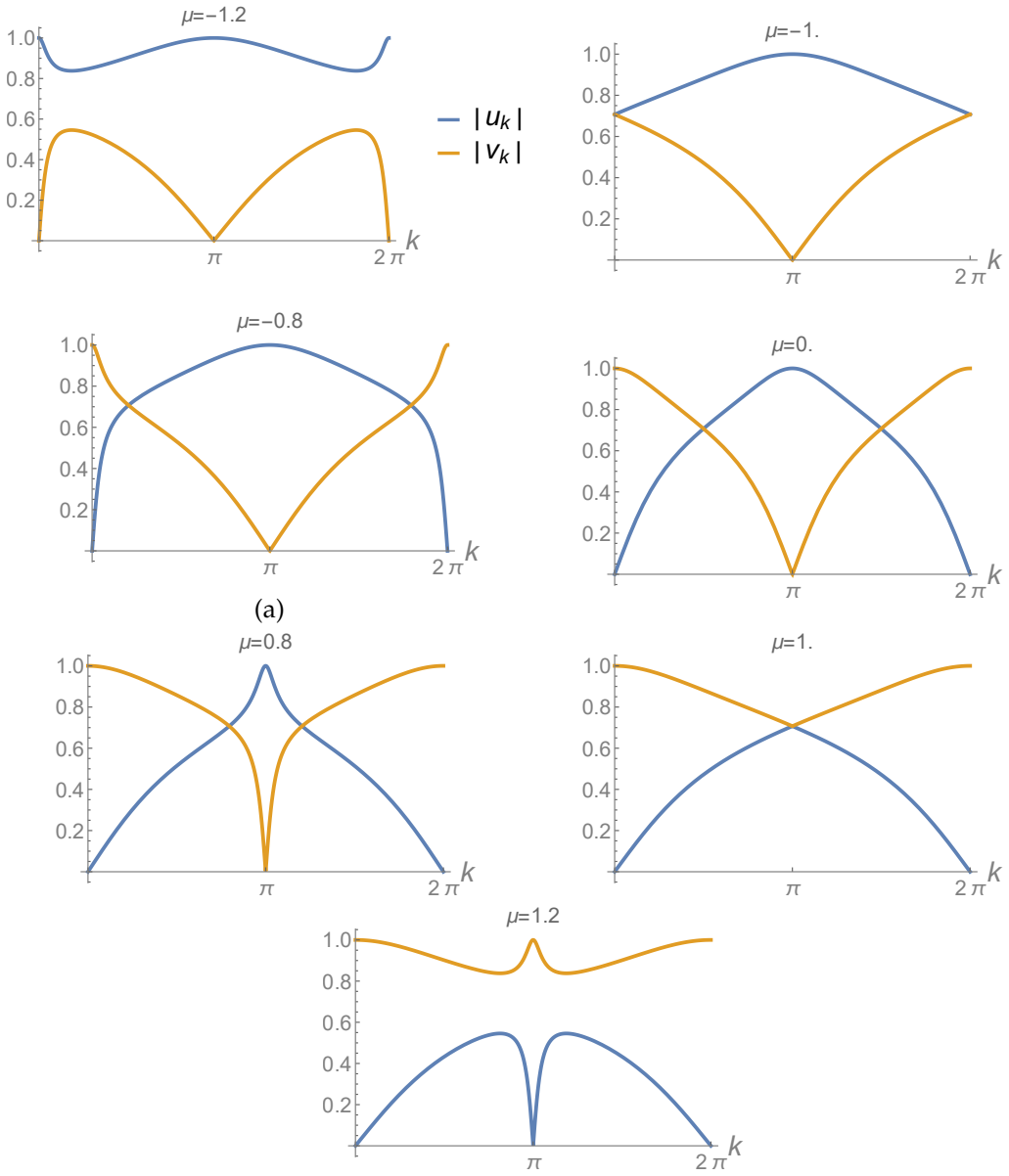

(a)

(b)

Figure 26: Plots of the coherence functions from 2.28 for various μ in units of t, and $\Delta/t = 1.5$. Only in the topological phase $|\mu| < |t|$ do the functions cross, which is necessary for Majorana type edge states.

A.2 MANY-BODY GROUND STATE

We can find the many-body ground state corresponding to the vacuum of Bogoliubons

$$\begin{aligned} \lambda_k|\Psi\rangle &= 0 \\ \left(u_k c_k + v_k c_{-k}^\dagger\right)|\Psi\rangle &= 0 \end{aligned} \tag{A.1}$$

The ground state can be assumed to be a superposition of all possible combinations of cooper pairs multiplied by some function α_k dependent on the coherence factors u_k and v_k

$$|\Psi\rangle = \mathcal{N}\exp\left(\frac{1}{2}\sum_{k'}\alpha_{k'}c_{-k'}^\dagger c_{k'}^\dagger\right)|0\rangle \tag{A.2}$$

Where $\mathcal{N}$ is a normalisation factor, and $\alpha_{k'}$ is an odd function, since $c_{-k'}^\dagger c_{k'}^\dagger$ is odd and we want the sum over k' to be non-zero. We can insert this function to find the coefficients $\alpha_{k'}$

$$\left(u_k c_k + v_k c_{-k}^\dagger\right)\exp\left(\frac{1}{2}\sum_{k'}\alpha_{k'}c_{-k'}^\dagger c_{k'}^\dagger\right)|0\rangle = 0 \tag{A.3}$$

We can pull the exponential function to the left by using that $\left[c_{-k'}^\dagger, c_{-k'}^\dagger c_{k'}^\dagger\right] = 0$ and that the following relation holds

$$c_k\ \exp\left(\frac{1}{2}\sum_{k'}\alpha_{k'}c_{k'}^\dagger c_{-k'}^\dagger\right) = \exp\left(\sum_{k'}\frac{1}{2}\alpha_{k'}c_{k'}^\dagger c_{-k'}^\dagger\right)\ \left(c_k - \alpha_k c_{-k}^\dagger\right) \tag{A.4}$$

This can be shown by using the Baker-Campbell-Hausdorff relation

$$e^{-G}Ae^{G} = A - [G,A] + \frac{(-1)^2}{2!}[G,[G,A]] + \ldots \tag{A.5}$$

Which in this case means

$$\begin{aligned} \exp\left(-\frac{1}{2}\sum_{k'}\alpha_{k'}c_{-k'}^\dagger c_{k'}^\dagger\right)\ c_k\ \exp\left(\frac{1}{2}\sum_{k'}\alpha_{k'}c_{-k'}^\dagger c_{k'}^\dagger\right) &= c_k - \frac{1}{2}\sum_{k'}\alpha_{k'}\left[c_{-k'}^\dagger c_{k'}^\dagger\ , c_k\right] \\ &= c_k - \frac{1}{2}\sum_{k'}\alpha_{k'}\left(c_{-k'}^\dagger\ \{c_{k'}^\dagger\ , c_k\} - \{c_{-k'}^\dagger\ , c_k\}c_{k'}^\dagger\right) \\ &= c_k - \frac{1}{2}\alpha_k c_{-k}^\dagger + \frac{1}{2}\alpha_{-k}c_{-k}^\dagger = \underline{\underline{c_k - \alpha_k c_{-k}^\dagger}} \end{aligned} \tag{A.6}$$

Where I have used that $\alpha_k = -\alpha_{-k}$. Equation (A.3) now becomes

$$\begin{aligned}
\exp\left(\sum_{k'}\alpha_{k'}c^\dagger_{-k'}c^\dagger_{k'}\right)\left(u_k\left(c_k-\alpha_k c^\dagger_{-k}\right)+v_k c^\dagger_{-k}\right)|0\rangle = 0 \\
\exp\left(\sum_{k'}\alpha_{k'}c^\dagger_{-k'}c^\dagger_{k'}\right)\left(-u_k\alpha_k c^\dagger_{-k}+v_k c^\dagger_{-k}\right)|0\rangle = 0 \\
\rightarrow \alpha_k = \frac{v_k}{u_k} = \left(\frac{\xi_k - E_k}{\Delta_k}\right)
\end{aligned} \tag{A.7}$$

Thus, if we use Pauli's exclusion principle $(c^\dagger_{-k}c^\dagger_k)^n = 0$ for $n > 1$, the ground state many-body wavefunction becomes

$$|\Psi\rangle = \mathcal{N}\prod_{k>0}\left(1+\frac{v_k}{u_k}c^\dagger_{-k}c^\dagger_k\right)|0\rangle \tag{A.8}$$

Notice the factor $\frac{1}{2}$ on α_k is gone since the product is changed to be only for positive k. The normalisation factor $\mathcal{N}$ can be found by imposing $\langle\Psi|\Psi\rangle = 1$

$$\begin{aligned}
|\mathcal{N}|^2\prod_{k>0}\prod_{k'>0}\langle 0|\left(1+\frac{v^*_k}{u^*_k}c_k c_{-k}\right)\left(1+\frac{v_{k'}}{u_{k'}}c^\dagger_{-k'}c^\dagger_{k'}\right)|0\rangle = 1 \\
|\mathcal{N}|^2\prod_{k>0}\langle 0|\left(1+\frac{|v_k|^2}{|u_k|^2}c_k c_{-k}c^\dagger_k c^\dagger_{-k}\right)|0\rangle = 1 \\
|\mathcal{N}|^2\prod_{k>0}\langle 0|\left(1+\frac{|v_k|^2}{|u_k|^2}\right)|0\rangle = 1
\end{aligned} \tag{A.9}$$

Where I have used the anti-commutation relations for the fermionic operators to re-arrange the products. For the total product to give unity, we can ensure that each factor obeys

$$\begin{aligned}
|\mathcal{N}|^2\left(1+\frac{|v_k|^2}{|u_k|^2}\right) = 1 \\
|\mathcal{N}|^2 = \frac{|u_k|^2}{|u_k|^2+|v_k|^2} = |u_k|^2
\end{aligned} \tag{A.10}$$

So the normalised many-body wavefunction becomes

$$|\Psi\rangle = \prod_{k>0}\left(u_k + v_k c^\dagger_{-k}c^\dagger_k\right)|0\rangle \tag{A.11}$$

B

ANALYTICAL SOLUTIONS FOR $\mu = 0, T \neq \Delta$ AND $N =$ ODD

The diagonal Hamiltonian for the Kitaev chain obtained in equation (2.5) is very interesting, but it assumes the fine-tuned parameters $\mu = 0, t = \Delta$. A slightly less symmetric point can be considered if the chemical potential is zero $\mu = 0$ and the chain has an odd number of sites. In this case, it is actually possible to calculate eigenstates analytically, which we will see in the following calculations. The Hamiltonian in the Majorana basis (2.3) with these parameters becomes

$$\begin{aligned} H &= -\frac{i}{4}\sum_{n=1}^{N-1}\left[(t+\Delta)\,\gamma_{A,n+1}\gamma_{B,n} + (t-\Delta)\,\gamma_{A,n}\gamma_{B,n+1}\right] \\ &= \sum_{n=1}^{N-1}\left[t_1\gamma_{A,n}\gamma_{B,n+1} + t_2\gamma_{A,n+1}\gamma_{B,n}\right] \end{aligned}$$

Where I have introduced the two coupling parameters $t_1 = -\frac{i}{4}(t-\Delta)$ and $t_2 = -\frac{i}{4}(t+\Delta)$. This Hamiltonian can be written in a matrix form as

$$H = \frac{1}{2}\sum_{nm}\begin{pmatrix}\gamma_{A,n} & \gamma_{B,n}\end{pmatrix}\begin{pmatrix}0 & \mathbf{T}_{nm} \\ \mathbf{T}^{\dagger}_{nm} & 0\end{pmatrix}\begin{pmatrix}\gamma_{A,m} \\ \gamma_{B,m}\end{pmatrix} = \frac{1}{2}\sum_{nm}\Gamma^{\alpha}_{n}\,\chi^{\alpha\beta}_{nm}\,\Gamma^{\beta}_{m} \tag{B.1}$$

Where we have

$$\mathbf{T} \doteq \begin{pmatrix} 0 & t_1 & 0 & 0 & 0 \\ t_2 & 0 & t_1 & 0 & 0 \\ 0 & t_2 & 0 & t_1 & 0 \\ 0 & 0 & t_2 & 0 & \ddots \\ 0 & 0 & 0 & \ddots & 0 \end{pmatrix} \qquad \Gamma^{\alpha}_{m} \doteq \begin{pmatrix} \gamma_{A,1} \\ \vdots \\ \gamma_{A,N} \\ \gamma_{B,1} \\ \vdots \\ \gamma_{B,N} \end{pmatrix} \tag{B.2}$$

This system can be visualized by figure 27, where one can notice the system decouples into two sub-chains, shown in different colours.

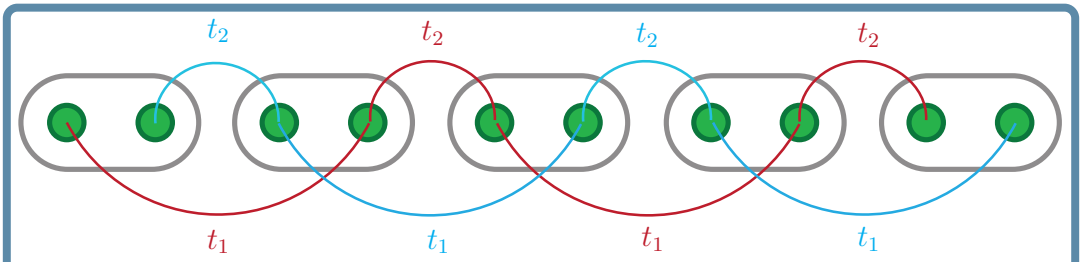

Figure 27: Visualisation of the various couplings included in (B.1) for a chain of $N = 5$ sites. We observe that the red and blue chains are decoupled, so we can try to write the Hamiltonian in this basis.

We will solve this system using the following procedure. As always, we would like to diagonalise the Hamiltonian by transforming it using a matrix consisting of eigenvectors of the Hamiltonian. The old operators are then linear combinations of the new ones with the wavefunctions as expansion coefficients. To find the complicated eigenstates in the electronic basis, we first find them in the Majorana basis and then transform back to electron operators using equation (2.2). It is not immediately clear what these Majorana eigenvectors are analytically, but if we transform the matrix χ into a new basis via $\Gamma^{\alpha}_{m} = \sum_l U^{\alpha\beta}_{ml} \tilde{\Gamma}^{\beta}_{l}$, i.e.

$$H = \frac{1}{2}\Gamma^T \chi \Gamma = \frac{1}{2} \underbrace{\Gamma^T U}_{\tilde{\Gamma}^T} \underbrace{U^T \chi U}_{\tilde{\chi}} \underbrace{U^T \Gamma}_{\tilde{\Gamma}} \tag{B.3}$$

and $U\,U^T = \mathbb{1}$, then the Hamiltonian decouples into two seperate blocks, each being the Hamiltonian for the famous Su-Schrieffer-Heeger (SSH) model (or sometimes called Shockley edge state model), describing chains with alternating hopping. The matrix $\tilde{\chi}$ is

$$\tilde{\chi} = \begin{pmatrix} C_1 & 0 \\ 0 & C_2 \end{pmatrix} \qquad \tilde{\Gamma} = \begin{pmatrix} \gamma_{A,1} & \gamma_{B,2} & \cdots & \gamma_{A,N} & \gamma_{B,1} & \gamma_{A,2} & \cdots & \gamma_{B,N} \end{pmatrix}^T$$

$$C_1 = \begin{pmatrix} 0 & t_1 & 0 & 0 & 0 \\ t_1^* & 0 & t_2^* & 0 & 0 \\ 0 & t_2 & 0 & t_1 & 0 \\ 0 & 0 & t_1^* & 0 & \ddots \\ 0 & 0 & 0 & \ddots & 0 \end{pmatrix} \qquad C_2 = \begin{pmatrix} 0 & t_2^* & 0 & 0 & 0 \\ t_2 & 0 & t_1 & 0 & 0 \\ 0 & t_1^* & 0 & t_2^* & 0 \\ 0 & 0 & t_2 & 0 & \ddots \\ 0 & 0 & 0 & \ddots & 0 \end{pmatrix} \tag{B.4}$$

Where the colours are to to indicate which chain the Majorana operators belong to (from figure 27). Note here that the chain C_2 is just a reversed version of C_1. The eigenstates to this Hamiltonian are known, and it is diagonalised by the transformation

$$H = \frac{1}{2}\tilde{\Gamma}^T \tilde{\chi} \tilde{\Gamma} = \frac{1}{2} \underbrace{\tilde{\Gamma}^T \Psi}_{\tilde{\tilde{\Gamma}}^T} \underbrace{\Psi^T \tilde{\chi} \Psi}_{\tilde{\tilde{\chi}}} \underbrace{\Psi^T \tilde{\Gamma}}_{\tilde{\tilde{\Gamma}}} \tag{B.5}$$

Where the matrix Ψ contains all the eigenvectors as columns. The new states in the diagonal basis are

$$\tilde{\tilde{\Gamma}}_n^\alpha = \sum_l \Psi_{ln}^{\beta\alpha}\, \tilde{\Gamma}_l^\beta \tag{B.6}$$

Where the upper index α refers to the chain and n is an arbitrary eigenstate index. The transformation matrix obeys the following equation

$$\sum_l \tilde{\chi}_{ml}^{\alpha\beta}\, \Psi_{ln}^{\beta\lambda} = \tilde{E}_n^\lambda\, \Psi_{mn}^{\alpha\lambda} \tag{B.7}$$

$\tilde{\chi}$ and Ψ are diagonal in "chain" space, so these equations becomes one for each chain

$$\begin{aligned}
\tilde{\tilde{\Gamma}}_n^1 &= \sum_l \Psi_{ln}^{11}\, \tilde{\Gamma}_l^1 \\
\sum_l \tilde{\chi}_{ml}^{11}\, \Psi_{ln}^{11} &= \tilde{E}_n^1\, \Psi_{mn}^{11} \\
\tilde{\tilde{\Gamma}}_n^2 &= \sum_l \Psi_{ln}^{22}\, \tilde{\Gamma}_l^2 \\
\sum_l \tilde{\chi}_{ml}^{22}\, \Psi_{ln}^{22} &= \tilde{E}_n^2\, \Psi_{mn}^{22}
\end{aligned} \tag{B.8}$$

For simplicity we can start by only considering the first chain C_1, i.e. the first two equations, so that the upper index is 1 (and will be suppressed for the moment). For example, let us try to find the zero mode $\tilde{\tilde{\Gamma}}_0^1$ for which $\tilde{E}_0^1 = 0$.

$$\tilde{\tilde{\Gamma}}_0^1 = \sum_l \Psi_{l0}^{11}\, \tilde{\Gamma}_l^1 \qquad\qquad \sum_l \tilde{\chi}_{ml}^{11}\, \Psi_{l0}^{11} = 0 \tag{B.9}$$

By writing out the equations for each row (each m) in the second equation of (B.9) we find the recursive solution

$$\begin{aligned}
t_1 \Psi_{20} = 0 \quad &\leftrightarrow \quad \Psi_{20} = 0 \\
t_1^* \Psi_{10} + t_2^* \Psi_{30} = 0 \quad &\leftrightarrow \quad \Psi_{30} = \left(-\frac{t_1^*}{t_2^*}\right) \Psi_{10} \\
t_2 \Psi_{20} + t_1 \Psi_{40} = 0 \quad &\leftrightarrow \quad \Psi_{40} = \left(-\frac{t_1}{t_2}\right) \Psi_{20} = 0 \\
t_1^* \Psi_{30} + t_2^* \Psi_{50} = 0 \quad &\leftrightarrow \quad \Psi_{50} = \left(-\frac{t_1^*}{t_2^*}\right) \Psi_{30} = \left(-\frac{t_1^*}{t_2^*}\right)^2 \Psi_{10}
\end{aligned} \tag{B.10}$$

Setting $\Psi_{10} = 1$ and introducing a parameter z counting only the odd numbers ($l = 1 \to z = 1, l = 3 \to z = 2, l = 5 \to z = 3$ etc.), the zero mode is then

$$\Psi_0(z) = \mathcal{N}\left(-\frac{t_1^*}{t_2^*}\right)^{z-1} = \mathcal{N}\left(-\frac{\frac{i}{4}(t-\Delta)}{\frac{i}{4}(t+\Delta)}\right)^{z-1} = \mathcal{N}\delta^{z-1} \qquad \delta = \frac{\Delta - t}{\Delta + t} \tag{B.11}$$

For some normalisation constant $\mathcal{N}$. Notice that $\delta < 1$ is necessary for this function to converge for large z, which is satisfied since t and Δ are assumed to be positive

numbers (this encodes the topological criteria, since $\mu = 0$, so $|t| > 0$ is in the topological regime). The normalisation constant is found by

$$\sum_{z=1}^{\infty} \Psi_0(z)^* \Psi_0(z) = \sum_{z=1}^{\infty} |\mathcal{N}|^2 \delta^{2(z-1)} = 1 \leftrightarrow \mathcal{N} = \sqrt{1-\delta^2} \tag{B.12}$$

A similar solution is found for the C_2 chain, which is a reversed version of C_1. We get for the zero mode wavefunction

$$\begin{aligned} \Psi_{l0}^{11} &= \sqrt{1-\delta^2} \begin{pmatrix} 1 & 0 & \delta & \dots & \delta^{\frac{N-1}{2}} \end{pmatrix}^T \\ \Psi_{l0}^{22} &= \sqrt{1-\delta^2} \begin{pmatrix} \delta^{\frac{N-1}{2}} & \dots & \delta & 0 & 1 \end{pmatrix}^T \end{aligned} \tag{B.13}$$

Comparing with (B.4), we can see that the first chain is only non-zero on A sites, while the second is only non-zero on B sites. Using B.9, we get for the zero mode Bogoliubon

$$\begin{aligned} f_0^\dagger = \frac{1}{2}\left(\tilde{\Gamma}_0^1 - i\tilde{\Gamma}_0^2\right) &= \frac{1}{2}\sum_l \Psi_{l0}^{11}\, \tilde{\Gamma}_l^1 - i\left(\Psi_{l0}^{22}\, \tilde{\Gamma}_l^2\right) \\ &= \frac{\sqrt{1-\delta^2}}{2} \sum_{n=0}^{\frac{N-1}{2}} \delta^n \left(\gamma_{A,2n+1} - i\gamma_{B,N-2n}\right) \\ &= \frac{\sqrt{1-\delta^2}}{2} \sum_{n=0}^{\frac{N-1}{2}} \delta^n \left(c_{2n+1}^\dagger + c_{2n+1} + c_{N-2n}^\dagger - c_{N-2n}\right) \end{aligned} \tag{B.14}$$

Which is the exact zero mode[1]

[1] Daniel Loss et al. used these exact WFs in [29] to calculate the decoherence of Majoranas. To compare the functions, notice they have a sign error in the indices.

C

ANALYSIS OF THE NON-INTERACTING GREEN'S FUNCTION

C.1 EQUATIONS OF MOTION FOR THE BARE GF

Let us examine the electronic Green's function $\mathcal{G}_0^{ee}(i,\tau\ ;\ j,0)$, which can be found using the Equations of Motion method (EOM). The procedure is to look at the τ-derivative of the GF, and use that for operators dependent on imaginary time we have

$$\begin{aligned}\partial_\tau A(\tau) &= \partial_\tau \left(e^{H\tau} A\ e^{-H\tau}\right) = e^{H\tau} HA\ e^{-H\tau} - e^{H\tau} AH\ e^{-H\tau} \\ &= e^{H\tau}\left[H, A\right]\ e^{-H\tau} = \left[H, A\right](\tau)\end{aligned} \tag{C.1}$$

The Kitaev chain Hamiltonian can be written as

$$H_0 = -\sum_{ij} t_{ij} c_i^\dagger c_j - \mu \sum_i c_i^\dagger c_i + \frac{1}{2}\sum_{ij} \Delta_{ij}\left(c_i^\dagger c_j^\dagger - c_i c_j\right) \tag{C.2}$$

And taking the τ-derivative of the electronic GF then gives us one of the so-called Nambu-Gorkov equations

$$\begin{aligned}\partial_\tau \mathcal{G}_0^{ee}(i,\tau\ ;\ j,0) &= \partial_\tau\left(-\theta(\tau)\langle c_i(\tau) c_j^\dagger(0)\rangle_0 + \theta(-\tau)\langle c_j^\dagger(0) c_i(\tau)\rangle_0\right) \\ &= -\delta(\tau)\left(\langle c_i(\tau) c_j^\dagger(0) + c_j^\dagger(0) c_i(\tau)\rangle_0\right) - \langle T_\tau\left(\partial_\tau c_i(\tau) c_j^\dagger(0)\right)\rangle_0 \\ &= -\delta(\tau)\delta_{ij} - \langle T_\tau\left(\left[H_0, c_i\right](\tau)\ c_j^\dagger(0)\right)\rangle_0\end{aligned} \tag{C.3}$$

Let us first calculate the commutator using the Hamiltonian in equation (C.2)

$$\left[H_0, c_i\right] = -\sum_{mn} t_{mn}\left[c_m^\dagger c_n, c_i\right] - \mu\sum_n\left[c_n^\dagger c_n, c_i\right] + \frac{1}{2}\sum_{mn}\Delta_{mn}\left(\left[c_m^\dagger c_n^\dagger, c_i\right] - \left[c_m c_n, c_i\right]\right) \tag{C.4}$$

Where the commutators of multiple fermionic creation/annihilation operators obey

$$\left[AB, C\right] = A\{B, C\} - \{A, C\}B \tag{C.5}$$

giving us

$$\begin{aligned}\left[H_0, c_i\right] &= \sum_{mn} t_{mn}\delta_{mi} c_n + \mu\sum_n \delta_{in} c_n + \frac{1}{2}\sum_{mn}\Delta_{mn}\left(\delta_{in} c_m^\dagger - \delta_{im} c_n^\dagger\right) \\ &= \sum_m t_{im} c_m + \mu c_i + \frac{1}{2}\sum_m \Delta_{mi} c_m^\dagger - \frac{1}{2}\sum_n \Delta_{in} c_n^\dagger \\ &= \sum_m t_{im} c_m + \mu c_i - \sum_m \Delta_{im} c_m^\dagger\end{aligned} \tag{C.6}$$

where I have renamed dummy indices and used that the pairing matrix is antisymmetric $\Delta_{ij} = -\Delta_{ji}$. Inserting the commutator into the expression we get

$$\begin{aligned}&\partial_\tau \mathcal{G}_0^{ee}(i,\tau\ ;\ j,0) = \\ &-\delta(\tau)\delta_{ij} + \sum_m t_{im}\ \mathcal{G}_0^{ee}(m,\tau\ ;\ j,0) + \mu\ \mathcal{G}_0^{ee}(i,\tau\ ;\ j,0) - \sum_m \Delta_{im}\ \mathcal{G}_0^{he}(m,\tau\ ;\ j,0)\end{aligned} \tag{C.7}$$

So the differential equation for the electron-electron (*ee*) Green's function contains the *he* function, so we need to apply the same procedure to this GF, for the system of equations to close. We get then, the second Nambu-Gorkov equation

$$\begin{aligned}\partial_\tau \mathcal{G}_0^{he}(i,\tau\ ;\ j,0) &= \partial_\tau \left(-\theta(\tau)\langle c_i^\dagger(\tau)c_j^\dagger(0)\rangle_0 + \theta(-\tau)\langle c_j^\dagger(0)c_i^\dagger(\tau)\rangle_0\right) \\ &= -\delta(\tau)\left(\langle c_i^\dagger(\tau)c_j^\dagger(0) + c_j^\dagger(0)c_i^\dagger(\tau)\rangle_0\right) - \langle T_\tau\left(\partial_\tau c_i^\dagger(\tau)c_j^\dagger(0)\right)\rangle_0 \\ &= -\langle T_\tau\left(\left[H_0, c_i^\dagger\right](\tau)\ c_j^\dagger(0)\right)\rangle_0\end{aligned} \tag{C.8}$$

And the commutator is

$$\begin{aligned}\left[H_0, c_i^\dagger\right] &= -\sum_{mn} t_{mn}\left[c_m^\dagger c_n, c_i^\dagger\right] - \mu\sum_n\left[c_n^\dagger c_n, c_i^\dagger\right] + \frac{1}{2}\sum_{mn}\Delta_{mn}\left(\left[c_m^\dagger c_n^\dagger, c_i^\dagger\right] - \left[c_m c_n, c_i^\dagger\right]\right) \\ &= -\sum_{mn} t_{mn}\delta_{ni}c_m^\dagger - \mu\sum_n \delta_{in}c_n^\dagger - \frac{1}{2}\sum_{mn}\Delta_{mn}\left(\delta_{in}c_m - \delta_{im}c_n\right) \\ &= -\sum_m t_{im}c_m^\dagger - \mu c_i^\dagger - \frac{1}{2}\sum_m \Delta_{mi}c_m + \frac{1}{2}\sum_n \Delta_{in}c_n \\ &= -\sum_m t_{im}c_m^\dagger - \mu c_i^\dagger + \sum_m \Delta_{im}c_m\end{aligned} \tag{C.9}$$

Where I also used the symmetry for the Hopping matrix $t_{ij} = t_{ji}$. The EOM for this anomalous GF becomes

$$\begin{aligned}&\partial_\tau \mathcal{G}_0^{he}(i,\tau\ ;\ j,0) = \\ &-\sum_m t_{im}\ \mathcal{G}_0^{he}(m,\tau\ ;\ j,0) - \mu\ \mathcal{G}_0^{he}(i,\tau\ ;\ j,0) + \sum_m \Delta_{im}\ \mathcal{G}_0^{ee}(m,\tau\ ;\ j,0)\end{aligned} \tag{C.10}$$

Similar equations for the *eh* and *hh* GF's can be obtained, and then everything can be collected into one matrix equation in Nambu space.

$$\partial_\tau \underline{\underline{\mathcal{G}_0}}(i,\tau\ ;\ j,0) = -\delta(\tau)\delta_{ij}\mathbb{1} - \sum_m \begin{pmatrix} -t_{im} - \mu\delta_{im} & \Delta_{im} \\ -\Delta_{im} & t_{im} + \mu\delta_{im}\end{pmatrix}\underline{\underline{\mathcal{G}_0}}(m,\tau\ ;\ j,0) \tag{C.11}$$

Or by introducing the Nambu indices in greek letters α, β we can write this as

$$\partial_\tau \mathcal{G}_0^{\alpha\beta}(i,\tau\ ;\ j,0) = -\delta(\tau)\delta_{ij}\delta^{\alpha\beta} - \sum_{m,\rho}\mathcal{H}_{im}^{\alpha\rho}\mathcal{G}_0^{\rho\beta}(m,\tau\ ;\ j,0) \tag{C.12}$$

So this is a matrix equation in both Nambu and site space, where $\alpha\beta$ denotes the Nambu entry (ee, eh, he, hh) and ij is the site entry, so $\mathcal{H}$ and $\mathcal{G}_0$ are $2N \times 2N$ matrices. If we transform the GF's to Matsubara frequencies using

$$\mathcal{G}_0^{\alpha\beta}(i, \tau\ ;\ j, 0) = \frac{1}{\beta} \sum_{ik_n} \mathcal{G}_0^{\alpha\beta}(i, j; ik_n) e^{-ik_n \tau} \tag{C.13}$$

and rearrange the equation, it gives

$$\sum_{m,\rho} \left(ik_n \delta_{im} \delta^{\alpha\rho} - \mathcal{H}_{im}^{\alpha\rho} \right) \mathcal{G}_0^{\rho\beta}(m, j; ik_n) = \delta_{ij} \delta^{\alpha\beta} \tag{C.14}$$

Which means that the Green's function becomes

$$\mathcal{G}_0^{\alpha\beta}(i, j; ik_n) = \left[\left(ik_n \, \mathbb{1}_{2N\times 2N} - \underline{\underline{\mathcal{H}}} \right)^{-1} \right]_{ij}^{\alpha\beta} \tag{C.15}$$

with the Hamiltonian

$$\underline{\underline{\mathcal{H}}} = \left(-\underline{\underline{t}} - \mu \, \mathbb{1}_{N\times N} \right) \tau_z + i \underline{\underline{\Delta}} \tau_y \tag{C.16}$$

This is a $2N \times 2N$ matrix, for N being the length of the chain, which is hard to invert for humans. For a computer it is easier, which is why we analyse the real space Green's function numerically in section 2.2.4. In section C.5, however, the hopping and pairing matrices reduce to functions of k, and then the inverse is easier to find.

C.2 BASICS OF THE EUCLIDEAN FERMIONIC PATH INTEGRAL

Starting from the quantum partition function

$$\mathcal{Z} = \text{tr}\ e^{-\beta H} = \sum_n \langle n | e^{-\beta H} | n \rangle \tag{C.17}$$

Where n is the basis constituting your favourite complete set. The usual trick is now to insert resolutions of the identity, and for the fermionic path integral, these states will be fermionic coherent states, i.e. states that are eigenstates to the annihilation operator c

$$c|\psi\rangle = \psi|\psi\rangle \tag{C.18}$$

Acting once again with c gives us that $\psi^2 = 0$ since $c^2 = 0$. ψ is thus a peculiar object, called a *Grassmann* variable [30]. They anti-commute with each other $\{\psi_i, \psi_j\} = 0$ and with the fermionic operators $\{\psi_i, c_j\} = 0$. The coherent state is given by $|\psi\rangle = e^{-\psi c^\dagger}|0\rangle = \left(1 - \psi c^\dagger\right)|0\rangle = |0\rangle - \psi|1\rangle$, since

$$c|\psi\rangle = c|0\rangle - c\psi|1\rangle = \psi c|1\rangle = \psi|0\rangle = \psi\left(|0\rangle - \psi|1\rangle\right) = \psi|\psi\rangle \tag{C.19}$$

We also have the state

$$\langle\bar{\psi}|c^\dagger = \langle\bar{\psi}|\bar{\psi} \tag{C.20}$$

With $\langle\bar{\psi}| = \langle 0|e^{\bar{\psi}c} = \langle 0|\,(1+\bar{\psi}c) = \langle 0| - \langle 1|\bar{\psi}$. The inner product of these two coherent states is

$$\langle\bar{\psi}|\psi\rangle = (\langle 0| - \langle 1|\bar{\psi})\,(|0\rangle - \psi|1\rangle) = 1 + \bar{\psi}\psi = e^{\bar{\psi}\psi} \tag{C.21}$$

It should be noted that $\bar{\psi}$ is not the complex conjugate of ψ, and they should be treated as different objects. A few other identities for Grassmann variables are

$$\begin{aligned} \int d\psi = 0 \qquad & \int \psi_i d\psi_j = \delta_{ij} \\ \int d\bar{\psi}d\psi\ \psi\bar{\psi} = 1 \qquad & \int d\bar{\psi}d\psi\ \bar{\psi}\psi = -1 \\ \partial_{\psi_i}\psi_j = \delta_{ij} & \end{aligned} \tag{C.22}$$

And importantly, frequently used integrals are

$$\int \mathcal{D}\bar{\psi}\mathcal{D}\psi\ e^{-\sum_{ij}\bar{\psi}_i\ A_{ij}\ \psi_j} = \det A, \qquad \mathcal{D}\bar{\psi}\mathcal{D}\psi = \prod_i d\bar{\psi}_i d\psi_i \tag{C.23}$$

And

$$\int \mathcal{D}\bar{\psi}\mathcal{D}\psi\ e^{\sum_{ij}\left(-\bar{\psi}_i\ A_{ij}\ \psi_j + \bar{\eta}_i\psi_i + \bar{\psi}_i\eta_i\right)} \tag{C.24}$$

To calculate this last integral, we can shift the two fermionic fields by constants

$$\begin{aligned} \bar{\psi}_i &\to \bar{\psi}_i + \sum_k \bar{\eta}_k (A^{-1})_{ki} \\ \psi_i &\to \psi_i + \sum_k (A^{-1})_{ik}\eta_k \end{aligned} \tag{C.25}$$

The exponent then becomes (using that repeated indices are summed, and that dummy indices can be exchanged)

$$\begin{aligned} & -\left(\bar{\psi}_i + \bar{\eta}_k(A^{-1})_{ki}\right)\ A_{ij}\ \left(\psi_j + (A^{-1})_{jm}\eta_m\right) \\ & + \bar{\eta}_i\left(\psi_i + (A^{-1})_{im}\eta_m\right) + \left(\bar{\psi}_i + \bar{\eta}_k(A^{-1})_{ki}\right)\eta_i \\ = & -\bar{\psi}_i A_{ij}\psi_j - \bar{\eta}_j\psi_j - \bar{\psi}_i\eta_i - \bar{\eta}_k(A^{-1})_{ki}\eta_i \\ & + \bar{\eta}_i\psi_i + \bar{\eta}_i(A^{-1})_{im}\eta_m + \bar{\psi}_i\eta_i + \bar{\eta}_k(A^{-1})_{ki}\eta_i \\ = & \left(-\bar{\psi}_i A_{ij}\psi_j + \bar{\eta}_i(A^{-1})_{ij}\eta_j\right) \end{aligned} \tag{C.26}$$

Using (C.23) we can then conclude

$$\int \mathcal{D}\bar{\psi}\mathcal{D}\psi\ e^{\sum_{ij}\left(-\bar{\psi}_i\ A_{ij}\ \psi_j + \bar{\eta}_i\psi_i + \bar{\psi}_i\eta_i\right)} = \det A \cdot e^{\sum_{ij}\bar{\eta}_i\ (A^{-1})_{ij}\eta_j} \tag{C.27}$$

The resolution of the identity for the fermion coherent states is

$$\begin{aligned}\int d\bar{\psi}d\psi\ |\psi\rangle\langle\bar{\psi}|e^{-\bar{\psi}\psi} &= \int d\bar{\psi}d\psi\ \left(|0\rangle - \psi|1\rangle\right)\left(\langle 0| - \langle 1|\bar{\psi}\right)\left(1-\bar{\psi}\psi\right)\\ &= \int d\bar{\psi}d\psi\ \left(|0\rangle\langle 0| + \psi|1\rangle\langle 1|\bar{\psi}\right)\left(1-\bar{\psi}\psi\right)\\ &= |0\rangle\langle 0|\int d\bar{\psi}d\psi\,(-\bar{\psi}\psi) + |1\rangle\langle 1|\int d\bar{\psi}d\psi\,(\psi\bar{\psi})\\ &= |0\rangle\langle 0| + |1\rangle\langle 1| = \mathbb{1}\end{aligned} \tag{C.28}$$

Going back to the partition function, we split up the Boltzmann factor into N pieces

$$\mathcal{Z} = \operatorname{tr} e^{-\beta H} = \operatorname{tr} \lim_{N\to\infty}(e^{-\frac{\beta}{N}H})^N \tag{C.29}$$

And insert the identity between each separate piece. Taking the continuum limit results in the following path integral

$$\mathcal{Z} = \int \mathcal{D}\bar{\psi}\mathcal{D}\psi\ e^{-S[\bar{\psi},\psi]}, \qquad S\left[\bar{\psi},\psi\right] = \int_0^\beta d\tau\left[\bar{\psi}\partial_\tau\psi + H(\bar{\psi},\psi)\right] \tag{C.30}$$

Where $\bar{\psi}$ and ψ are functions of τ, $S\left[\bar{\psi},\psi\right]$ is called the Euclidean action, and

$$H(\bar{\psi},\psi) = \frac{\langle\bar{\psi}|H(c^\dagger,c)|\psi\rangle}{\langle\bar{\psi}\psi\rangle} \tag{C.31}$$

C.3 BOSONIC GF

The free Bosonic GF can be found by the following procedure (based on [4])

$$\begin{aligned}&\mathcal{D}_0(\lambda_b,\tau_b;\lambda_a,\tau_a) =\\ &= -\langle T_\tau\left(\left[\hat{a}_{\lambda_b}(\tau_b) + \hat{a}^\dagger_{\lambda_b}(\tau_b)\right]\left[\hat{a}^\dagger_{\lambda_a}(\tau_a) + \hat{a}_{\lambda_a}(\tau_a)\right]\right)\rangle_0\\ &= -\langle T_\tau\left(\hat{a}_{\lambda_b}(\tau_b)\hat{a}^\dagger_{\lambda_a}(\tau_a)\right)\rangle_0 - \langle T_\tau\left(\hat{a}^\dagger_{\lambda_b}(\tau_b)\hat{a}_{\lambda_a}(\tau_a)\right)\rangle_0\\ &= \begin{cases}-\delta_{\lambda_b\lambda_a}\left(\langle\hat{a}_{\lambda_a}(\tau)\hat{a}^\dagger_{\lambda_a}(0)\rangle_0 + \langle\hat{a}^\dagger_{\lambda_a}(\tau)\hat{a}_{\lambda_a}(0)\rangle_0\right) & \tau_b-\tau_a=\tau>0\\ -\delta_{\lambda_b\lambda_a}\left(\langle\hat{a}^\dagger_{\lambda_a}(0)\hat{a}_{\lambda_a}(\tau)\rangle_0 + \langle\hat{a}_{\lambda_a}(0)\hat{a}^\dagger_{\lambda_a}(\tau)\rangle_0\right) & \tau_b-\tau_a=\tau<0\end{cases}\end{aligned} \tag{C.32}$$

Now, the τ dependence on the operators can be found by using the Baker-Campbell-Hausdorff relation from eq. (A.5) on $\hat{a}_\lambda(\tau) = e^{H_b\tau}a_\lambda e^{-H_b\tau}$, or by evaluating the τ evolution equations

$$\begin{aligned}\partial_\tau\hat{a}^\dagger_\lambda(\tau) &= \left[H_b, a^\dagger_\lambda\right](\tau)\\ \partial_\tau\hat{a}_\lambda(\tau) &= \left[H_b, a_\lambda\right](\tau)\end{aligned} \tag{C.33}$$

Using the relation

$$\left[AB,C\right] = A\left[B,C\right] + \left[A,C\right]B \tag{C.34}$$

So we get

$$\begin{aligned} \partial_\tau \hat{a}^\dagger_\lambda(\tau) &= \quad \omega_\lambda \hat{a}^\dagger_\lambda(\tau) \qquad \leftrightarrow \qquad \hat{a}^\dagger_\lambda(\tau) = a^\dagger_\lambda \, e^{\omega_\lambda \tau} \\ \partial_\tau \hat{a}_\lambda(\tau) &= -\omega_\lambda \hat{a}_\lambda(\tau) \qquad \leftrightarrow \qquad \hat{a}_\lambda(\tau) = a_\lambda \, e^{-\omega_\lambda \tau} \end{aligned} \tag{C.35}$$

Using these and the fact that the bosonic operators have the commutation relation $\left[a_\lambda, a^\dagger_{\lambda'}\right] = \delta_{\lambda,\lambda'}$ and follow the Bose-Einstein statistics $\langle a^\dagger_\lambda a_\lambda \rangle_0 = n_B(\omega_\lambda) = \left(e^{\beta\omega_\lambda} - 1\right)^{-1}$, we get

$$\mathcal{D}_0(\lambda_b, \lambda_a; \tau) = \begin{cases} -\delta_{\lambda_b\lambda_a} \left(\left[n_B(\omega_{\lambda_a}) + 1 \right] \, e^{-\omega_{\lambda_a}\tau} + n_B(\omega_{\lambda_a}) \, e^{\omega_{\lambda_a}\tau} \right) & \tau > 0 \\ -\delta_{\lambda_b\lambda_a} \left(n_B(\omega_{\lambda_a}) \, e^{-\omega_{\lambda_a}\tau} + \left[n_B(\omega_{\lambda_a}) + 1 \right] \, e^{\omega_{\lambda_a}\tau} \right) & \tau < 0 \end{cases} \tag{C.36}$$

We can transform this function to bosonic Matsubara frequencies by

$$\mathcal{D}_0(\lambda_b, \lambda_a, iq_n) = \int_0^\beta d\tau \, \mathcal{D}_0(\lambda_b, \lambda_a; \tau) e^{iq_n\tau}, \qquad q_n = \frac{2n}{\beta}\pi \tag{C.37}$$

Performing the integral gives us

$$\begin{aligned} \mathcal{D}_0(\lambda_b, \lambda_a; iq_n) &= -\delta_{\lambda_b\lambda_a} \int_0^\beta d\tau \, \left(\left[n_B(\omega_{\lambda_a}) + 1 \right] \, e^{-\omega_{\lambda_a}\tau} + n_B(\omega_{\lambda_a}) \, e^{\omega_{\lambda_a}\tau} \right) e^{iq_n\tau} \\ &= -\delta_{\lambda_b\lambda_a} \int_0^\beta d\tau \, \left(\frac{e^{\beta\omega_{\lambda_a}} e^{-\omega_{\lambda_a}\tau} e^{iq_n\tau}}{e^{\beta\omega_{\lambda_a}} - 1} + \frac{e^{\omega_{\lambda_a}\tau} e^{iq_n\tau}}{e^{\beta\omega_{\lambda_a}} - 1} \right) \\ &= -\delta_{\lambda_b\lambda_a} \left[\frac{1}{iq_n - \omega_{\lambda_a}} \frac{e^{\beta\omega_{\lambda_a}} e^{-\omega_{\lambda_a}\tau} e^{iq_n\tau}}{e^{\beta\omega_{\lambda_a}} - 1} + \frac{1}{iq_n + \omega_{\lambda_a}} \frac{e^{\omega_{\lambda_a}\tau} e^{iq_n\tau}}{e^{\beta\omega_{\lambda_a}} - 1} \right]_0^\beta \\ &= -\delta_{\lambda_b\lambda_a} \left(\frac{1}{iq_n - \omega_{\lambda_a}} \frac{e^{iq_n\beta}}{e^{\beta\omega_{\lambda_a}} - 1} + \frac{1}{iq_n + \omega_{\lambda_a}} \frac{e^{\beta\omega_{\lambda_a}} e^{iq_n\beta}}{e^{\beta\omega_{\lambda_a}} - 1} \right. \\ &\quad \left. - \frac{1}{iq_n - \omega_{\lambda_a}} \frac{e^{\beta\omega_{\lambda_a}}}{e^{\beta\omega_{\lambda_a}} - 1} - \frac{1}{iq_n + \omega_{\lambda_a}} \frac{1}{e^{\beta\omega_{\lambda_a}} - 1} \right) \\ &= \delta_{\lambda_b\lambda_a} \left(\frac{1}{iq_n - \omega_{\lambda_a}} \left[\frac{e^{\beta\omega_{\lambda_a}}}{e^{\beta\omega_{\lambda_a}} - 1} - \frac{1}{e^{\beta\omega_{\lambda_a}} - 1} \right] + \frac{1}{iq_n + \omega_{\lambda_a}} \left[\frac{1}{e^{\beta\omega_{\lambda_a}} - 1} - \frac{e^{\beta\omega_{\lambda_a}}}{e^{\beta\omega_{\lambda_a}} - 1} \right] \right) \\ &= \delta_{\lambda_b\lambda_a} \left(\frac{1}{iq_n - \omega_{\lambda_a}} - \frac{1}{iq_n + \omega_{\lambda_a}} \right) = \delta_{\lambda_b\lambda_a} \frac{2\,\omega_{\lambda_a}}{(iq_n)^2 - \omega^2_{\lambda_a}} \end{aligned} \tag{C.38}$$

Where I have used that for bosonic Matsubara frequencies $e^{iq_n\beta} = e^{i\frac{2\pi n}{\beta}\beta} = 1$.

C.4 MAJORANA BASIS GREEN'S FUNCTION

The Hamiltonian in the Majorana basis (2.3), can be written as

$$H = \frac{i}{2} \sum_{nm} \Gamma^\alpha_n \chi^{\alpha\beta}_{nm} \Gamma^\beta_m = \frac{i}{2} \sum_{nm} \begin{pmatrix} \gamma_{A,n} & \gamma_{B,n} \end{pmatrix} \begin{pmatrix} 0 & L_{nm} \\ -L^\dagger_{nm} & 0 \end{pmatrix} \begin{pmatrix} \gamma_{A,m} \\ \gamma_{B,m} \end{pmatrix} \tag{C.39}$$

With

$$L_{nm} = -\frac{\mu}{2}\delta_{n,m} - \frac{t+\Delta}{4}\delta_{n,m+1} - \frac{t-\Delta}{4}\delta_{n+1,m} \tag{C.40}$$

In k-space, this function becomes

$$L(k) = \sum_{n,m} L_{nm} e^{-ik(n-m)} = \frac{1}{2}\left(-\mu - t\cos k + i\Delta \sin k\right) = \frac{1}{2}\left(\xi_k - \Delta_k\right) \tag{C.41}$$

Which was found in (2.39). The non-interacting Majorana GF can be defined as

$$\begin{aligned}\mathcal{B}_0^{\alpha\beta}(n,m;\tau) &= -\langle T_\tau\left(\Gamma_n^\alpha(\tau)\Gamma_m^\beta\right)\rangle_0 \doteq \begin{pmatrix}\mathcal{B}_0^{aa}(n,m;\tau) & \mathcal{B}_0^{ab}(n,m;\tau)\\ \mathcal{B}_0^{ba}(n,m;\tau) & \mathcal{B}_0^{bb}(n,m;\tau)\end{pmatrix}\\ &= \begin{pmatrix}-\langle T_\tau\left(\gamma_{A,n}(\tau)\gamma_{A,m}\right)\rangle_0 & -\langle T_\tau\left(\gamma_{A,n}(\tau)\gamma_{B,m}\right)\rangle_0\\ -\langle T_\tau\left(\gamma_{B,n}(\tau)\gamma_{A,m}\right)\rangle_0 & -\langle T_\tau\left(\gamma_{B,n}(\tau)\gamma_{B,m}\right)\rangle_0\end{pmatrix}\end{aligned} \tag{C.42}$$

By performing the EOM procedure as before, we get the differential equations for the Majorana basis Green's functions

$$\begin{aligned}\partial_\tau \mathcal{B}_0^{aa}(n,m;\tau) &= -2\delta(\tau)\delta_{nm} - 2i\sum_j L_{nj}\mathcal{B}_0^{ba}(j,m;\tau)\\ \partial_\tau \mathcal{B}_0^{ba}(n,m;\tau) &= 0 + 2i\sum_j L_{jn}\mathcal{B}_0^{aa}(j,m;\tau)\end{aligned} \tag{C.43}$$

Where the factor of two in the different terms, come from the anti-commutation relation for the Majorana operators $\{\gamma_{\alpha,n},\gamma_{\alpha',n'}\} = 2\delta_{\alpha,\alpha'}\delta_{n,n'}$. The equations of motion closes, and again we can write similar equations for $\mathcal{B}_0^{ab}(n,m;\tau)$ and $\mathcal{B}_0^{bb}(n,m;\tau)$, and collect everything into the matrix equation

$$\partial_\tau \mathcal{B}_0^{\alpha\beta}(n,m;\tau) = -2\delta(\tau)\delta_{nm}\delta^{\alpha\beta} - 2i\sum_{j\sigma}\begin{pmatrix}0 & L_{nj}\\ -L_{jn} & 0\end{pmatrix}^{\alpha\sigma}\mathcal{B}_0^{\sigma\beta}(j,m;\tau) \tag{C.44}$$

And by transforming to Matsubara frequencies, this equation becomes

$$2\delta_{nm}\delta^{\alpha\beta} = \sum_{j\sigma}\left(ik_n\delta^{\alpha\sigma}\delta_{nj} - 2i\chi_{nj}^{\alpha\sigma}\right)\mathcal{B}_0^{\sigma\beta}(j,m;ik_n) \tag{C.45}$$

With the solution

$$\mathcal{B}_0^{\alpha\beta}(n,m;ik_n) = \left[\left(\frac{1}{2}ik_n\mathbb{1}_{2N\times 2N} - i\underline{\underline{\chi}}\right)^{-1}\right]_{nm}^{\alpha\beta} \tag{C.46}$$

Again, this could be worked out using a path integral formalism as well. It is possible to write down a path integral for Majorana fields as [30]

$$\mathcal{Z} = \int \mathcal{D}\Gamma\; e^{-S\left[\Gamma^T,\Gamma\right]} \tag{C.47}$$

Where the free action is now

$$S_0\left[\Gamma^T,\Gamma\right] = \int_0^\beta d\tau \sum_{ij}\sum_{\sigma\rho}\left(\Gamma^T\right)_i^\sigma\left(\frac{1}{2}\delta^{\sigma\rho}\delta_{ij}\,\partial_\tau + i\chi_{ij}^{\sigma\rho}\right)\Gamma_j^\rho, \qquad \Gamma_j^\rho = \begin{pmatrix}\gamma_{A,j}\\ \gamma_{B,j}\end{pmatrix} \tag{C.48}$$

So there is a couple of differences to the fermionic path integral. There is no $\bar{\Gamma}$, so the path integral is only over Γ, and there is a factor $\frac{1}{2}$ on the imaginary time derivative. By repeating the same procedure as the one to find the Nambu GF, one can easily see that (C.46) is reproduced. Just set the factor $\frac{1}{2}$ on ik_n and replace $\mathcal{H}$ with $i\chi$ in (2.80).

C.5 MOMENTUM SPACE GREEN'S FUNCTION

For an infinite system, the momentum space GF is found as

$$\begin{aligned}\underline{\underline{\mathcal{G}_0}}(k, ik_n) &= (ik_n\mathbb{1} - \mathcal{H}(k))^{-1} \\ &= \left(ik_n\mathbb{1} - \xi_k\tau_z - i\Delta_k\tau_y\right)^{-1}\end{aligned} \tag{C.49}$$

Where we can use the following trick for inverting matrices containing the Pauli matrices

$$\left(a\mathbb{1} + b\tau_x + c\tau_y + d\tau_z\right)^{-1} = \frac{a\mathbb{1} - b\tau_x - c\tau_y - d\tau_z}{a^2 - b^2 - c^2 - d^2} \tag{C.50}$$

So the GF becomes

$$\underline{\underline{\mathcal{G}_0}}(k, ik_n) = \frac{ik_n\mathbb{1} + \xi_k\tau_z + i\Delta_k\tau_y}{(ik_n)^2 - \xi_k^2 - (i\Delta_k)^2} \tag{C.51}$$

Performing analytical continuation $ik_n \to \omega + i\eta$ gives us

$$\underline{\underline{\mathcal{G}_0}}(k, \omega) = \frac{\omega\mathbb{1} + \xi_k\tau_z + i\Delta_k\tau_y}{\omega^2 - \left[\xi_k^2 + |\Delta_k|^2\right]} \tag{C.52}$$

Which, as expected, has poles at $\omega = E_k$. We can also find the k-space Majorana GF as

$$\begin{aligned}\underline{\underline{\mathcal{B}_0}}(k, ik_n) &= \left(\frac{ik_n}{2}\mathbb{1} - i\chi(k)\right)^{-1} \\ &= \left(\frac{ik_n}{2}\mathbb{1} + \frac{i}{2}\Delta_k\tau_x + \frac{\xi_k}{2}\tau_y\right)^{-1} \\ &= \frac{2ik_n\mathbb{1} - 2\xi_k\tau_y - 2i\Delta_k\tau_x}{(ik_n)^2 - \xi_k^2 - |\Delta_k|^2}\end{aligned} \tag{C.53}$$

Which after analytical continuation becomes

$$\underline{\underline{\mathcal{B}_0}}(k, \omega) = \frac{2\omega\mathbb{1} + 2\left(t\cos k + \mu\right)\tau_y - 2\Delta\sin k\ \tau_x}{\omega^2 - E_k^2} \tag{C.54}$$

Also with poles at $\omega = E_k$.

D

ADDITIONAL MATERIAL ON MOMENTUM SPACE TOPOLOGY

D.1 THE SU-SCHRIEFFER-HEEGER MODEL

The famous SSH model describes as 1D system of N atoms on a chain, which has alternating hopping parameters t_1 and t_2 (which can happen if the system undergoes a Peierls transition). The Hamiltonian describing the spinless system is

$$H = \sum_n t_1 c_{2n-1}^\dagger c_{2n} + t_2 c_{2n}^\dagger c_{2n+1} + h.c \tag{D.1}$$

Which is depicted in figure 28 in the upper graphic. It turns out to be convenient to convert this Hamiltonian such that the chiral properties of the system is more prevalent, shown in the bottom part of the picture. We group the two atoms A and B into one unit cell, and describe the electrons with a new unit cell coordinate j and by the sublattice index A, B, such that the Hamiltonian becomes

$$\begin{aligned} H &= \sum_j t_1 c_{A,j}^\dagger c_{B,j} + t_2 c_{B,j}^\dagger c_{A,j+1} + h.c \\ &= \sum_{ij} \underline{C}_i^\dagger \, \underline{\underline{\mathcal{H}}}_{ij} \, \underline{C}_j \end{aligned} \tag{D.2}$$

Where in the last line we have written the Hamiltonian as a matrix in sublattice space with

$$\underline{\underline{\mathcal{H}}}_{ij} = \begin{pmatrix} 0 & T_{ij} \\ T_{ij}^\dagger & 0 \end{pmatrix} \qquad T_{ij} = t_1 \delta_{ij} + t_2 \delta_{i,j+1} \qquad \underline{C}_j = \begin{pmatrix} c_{A,j} \\ c_{B,j} \end{pmatrix} \tag{D.3}$$

This system exhibits zero energy states at the boundary for values of the hopping parameters t_1, t_2 which can be found by analysing the bulk topology. This means we want to analyse the bulk properties, which can be described in momentum space by

$$H = \sum_k \underline{C}_k^\dagger \, \underline{\underline{\mathcal{H}(k)}} \, \underline{C}_k \qquad \underline{\underline{\mathcal{H}(k)}} = \begin{pmatrix} 0 & T(k) \\ T^\dagger(k) & 0 \end{pmatrix} \tag{D.4}$$

and

$$T(k) = \sum_{ij} T_{ij} e^{-ik(i-j)} = \sum_{ij} \left(t_1 \delta_{ij} + t_2 \delta_{i,j+1} \right) e^{-ik(i-j)} = t_1 + t_2 e^{-ik} \tag{D.5}$$

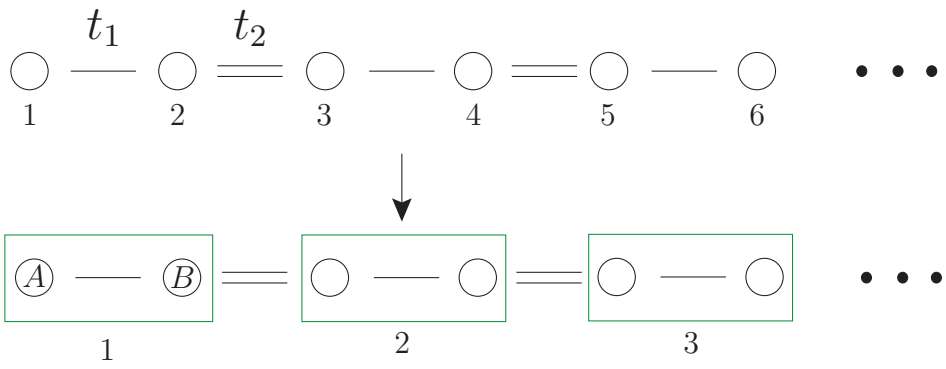

Figure 28

Similar to section 2.3, we can define a topological invariant N_1, describing the winding of $T(k)$ around the origin, as k sweeps the Brillouin zone. Similar analysis allows us to conclude that

$$N_1 = \begin{cases} 0 & |t_1| > |t_2| \ \textit{trivial} \\ -1 & |t_1| < |t_2| \ \textit{topological} \end{cases} \tag{D.6}$$

So an edge states exists if the bond that is broken at the edge (in this case t_2) is the largest.

D.2 TI AS A MAPPING BETWEEN BULK-MOMENTUM SPACE HAMILTONIAN AND THE UNIT SPHERE

The TI for the Kitaev model can also be understood from a more geometrical perspective. This is seen from the fact that the Hamiltonian is of the form $\mathcal{H}(k) = d(k) \cdot \tau$ with $d(k) = (0, \frac{\Delta \sin(k)}{E_k}, \frac{-t\cos(k)-\mu}{E_k})$ and $\tau = (\tau_x, \tau_y, \tau_z)$ [1]. The form of $\hat{d}(k)$ is restricted by the symmetries discussed earlier (TR, PH and Chiral), and we have

$$\begin{aligned} \Pi d_x(k)\tau_x\Pi^{-1} &= -d_x(k)\tau_x \rightarrow d_x(k) = 0 \\ \Xi d_y(k)\tau_y\Xi^{-1} &= -d_y(-k)\tau_y \rightarrow d_y(k) = -d_y(-k) \\ \Xi d_z(k)\tau_z\Xi^{-1} &= -d_z(-k)\tau_z \rightarrow d_z(k) = d_z(-k) \end{aligned} \tag{D.7}$$

If k is varied without the gap closing $|\hat{d}(k)| \neq 0$, in the interval $[0, \pi]$, then $\hat{d}(k)$ serves as a mapping between the Brillouin zone and the unit sphere. In figure 29 we see the contour that the vector $\hat{d}(k) = \frac{d(k)}{|d(k)|}$ sweeps as k covers this interval. Due to the restrictions on $d(k)$, we have at the endpoints

$$\hat{d}(0) = s_0\hat{z} \qquad\qquad \hat{d}(\pi) = s_\pi\hat{z} \tag{D.8}$$

Where $s_0, s_\pi = 1, -1$. We can thus define a TI

$$\nu = s_0 s_\pi = \frac{-(t+\mu)}{\sqrt{(t+\mu)^2}} \frac{(t-\mu)}{\sqrt{(t-\mu)^2}} = \begin{cases} -1 & |t| > |\mu| \text{ topological} \\ 1 & |t| < |\mu| \text{ trivial} \end{cases} \tag{D.9}$$

Which is $\nu = -1$ when the contour ends up at the opposite pole of the unit circle, and $\nu = 1$ when it returns to the same pole. This is visualized in figure 29.

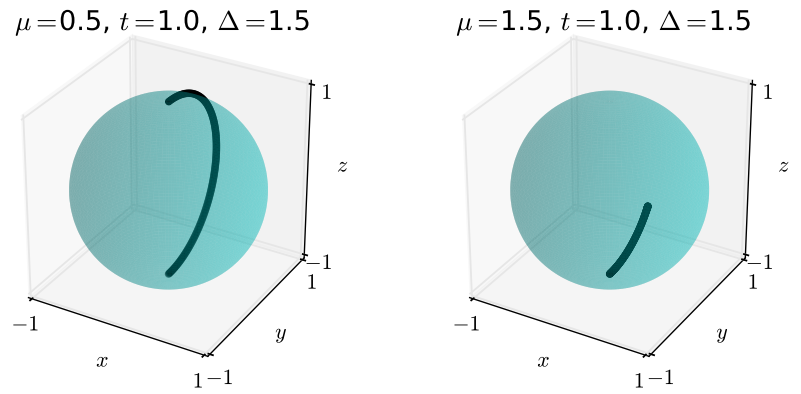

Figure 29: Plot of the contour $\hat{d}(k)$ makes on the unit sphere, when k sweeps from 0 to π. The topological phase is when the contour ends up on the opposite pole, and the trivial phase is when the contour goes out from the south pole, but returns. Again, the transition between these two scenarios happens at $|\mu| = |t|$

E

DETAILS FROM THE PERTURBATION THEORY OF ELECTRON-BOSON INTERACTIONS

E.1 FULL GF IN THE INTERACTION PICTURE

In this section we want to rewrite the full GF to the interaction picture. Quantitatively, the evolution of states and operators obey

$$\begin{aligned} |\hat{\psi}(\tau)\rangle &= e^{H_0\tau}|\psi(\tau)\rangle = e^{H_0\tau}e^{-H\tau}|\psi_0\rangle \\ \hat{A}(\tau) &= e^{H_0\tau}A\, e^{-H_0\tau} \\ |\hat{\psi}(\tau)\rangle &= \hat{U}(\tau,\tau_0)|\hat{\psi}(\tau_0)\rangle \end{aligned} \tag{E.1}$$

Where $\hat{U}(\tau,\tau_0)$ is a unitary operator. If the perturbation V is independent of τ, so the full Hamiltonian H is as well (which is true for systems in thermal equilibrium), this operator can be found by combining the defining equations

$$\begin{aligned} |\hat{\psi}(\tau)\rangle &= \hat{U}(\tau,\tau_0)|\hat{\psi}(\tau_0)\rangle \\ \updownarrow & \\ e^{H_0\tau}e^{-H\tau}|\psi_0\rangle &= \hat{U}(\tau,\tau_0)e^{H_0\tau_0}e^{-H\tau_0}|\psi_0\rangle \\ \updownarrow & \\ \hat{U}(\tau,\tau_0) &= e^{H_0\tau}e^{-H(\tau-\tau_0)}e^{-H_0\tau_0} \end{aligned} \tag{E.2}$$

Giving us the relations

$$\hat{U}(\tau,\tau')\hat{U}(\tau',\tau_0) = \hat{U}(\tau,\tau_0) \qquad\qquad \hat{U}(\tau_0,\tau_0) = 1 \tag{E.3}$$

Now we can achieve an equation for $\hat{U}(\tau,\tau_0)$ by taking the τ-derivative on both side of equation (E.2)

$$\begin{aligned} \partial_\tau\hat{U}(\tau,\tau_0) &= e^{H_0\tau}\,(H_0 - H)\,e^{-H(\tau-\tau_0)}e^{-H_0\tau_0} \\ &= e^{H_0\tau}\,V\,e^{-H_0\tau}e^{H_0\tau}e^{-H(\tau-\tau_0)}e^{-H_0\tau_0} = -\hat{V}(\tau)\hat{U}(\tau,\tau_0) \end{aligned} \tag{E.4}$$

Which can be solved by integration

$$\begin{aligned} \int_{\tau_0}^{\tau} d\tau'\partial_{\tau'}\hat{U}(\tau',\tau_0) &= -\int_{\tau_0}^{\tau} d\tau'\hat{V}(\tau')\hat{U}(\tau',\tau_0) \\ \updownarrow & \\ \hat{U}(\tau,\tau_0) - \hat{U}(\tau_0,\tau_0) &= -\int_{\tau_0}^{\tau} d\tau'\hat{V}(\tau')\hat{U}(\tau',\tau_0) \\ \updownarrow & \\ \hat{U}(\tau,\tau_0) &= 1 - \int_{\tau_0}^{\tau} d\tau'\hat{V}(\tau')\hat{U}(\tau',\tau_0) \end{aligned} \tag{E.5}$$

The τ-evolution operator can be solved for iteratively by inserting $\hat{U}(\tau,\tau_0)$ into the integral multiple times, keeping track of the τ ordering, giving us

$$\hat{U}(\tau,\tau_0)=\sum_{n=0}^{\infty}\frac{(-1)^n}{n!}\int_{\tau_0}^{\tau}d\tau_1\cdots\int_{\tau_0}^{\tau}d\tau_n T_\tau\left(\hat{V}(\tau_1)\dots\hat{V}(\tau_n)\right)=T_\tau e^{-\int_{\tau_0}^{\tau}d\tau_1\hat{V}(\tau_1)} \tag{E.6}$$

This is very useful, since we can now rewrite the density operator using that

$$\hat{U}(\beta,0)=e^{H_0\beta}e^{-H\beta}\leftrightarrow e^{-\beta H}=e^{-\beta H_0}\hat{U}(\beta,0) \tag{E.7}$$

We wanted to calculate the Green's function in equation (3.8) using the interaction picture, so we transform operators from the Heisenberg to the interaction picture by using

$$C^{\beta}_{\nu_b}(\tau_b)=e^{H\tau_b}C^{\beta}_{\nu_b}e^{-H\tau_b}=\underbrace{e^{H\tau_b}e^{-H_0\tau_b}}_{\hat{U}(0,\tau_b)}\underbrace{e^{H_0\tau_b}C^{\beta}_{\nu_b}e^{-H_0\tau_b}}_{\hat{C}^{\beta}_{\nu_b}(\tau_b)}\underbrace{e^{H_0\tau_b}e^{-H\tau_b}}_{\hat{U}(\tau_b,0)} \tag{E.8}$$

So the Green's function then becomes for $\beta>\tau_b>\tau_a>0$ (the case with $\tau_a>\tau_b$ gives the same result [4])

$$\begin{aligned}
&\mathcal{G}^{\beta\alpha}(\nu_b,\tau_b\,;\,\nu_a,\tau_a)\\
&=\frac{-\mathrm{Tr}\left[e^{-\beta H_0}\hat{U}(\beta,0)\hat{U}(0,\tau_b)\hat{C}^{\beta}_{\nu_b}(\tau_b)\hat{U}(\tau_b,0)\hat{U}(0,\tau_a)(\hat{C}^{\dagger})^{\alpha}_{\nu_a}(\tau_a)\hat{U}(\tau_a,0)\right]}{\mathrm{Tr}\left[e^{-\beta H_0}\hat{U}(\beta,0)\right]}\\
&=\frac{-\mathrm{Tr}\left[e^{-\beta H_0}\hat{U}(\beta,\tau_b)\hat{C}^{\beta}_{\nu_b}(\tau_b)\hat{U}(\tau_b,\tau_a)(\hat{C}^{\dagger})^{\alpha}_{\nu_a}(\tau_a)\hat{U}(\tau_a,0)\right]}{\mathrm{Tr}\left[e^{-\beta H_0}\hat{U}(\beta,0)\right]}\\
&=\frac{-\mathrm{Tr}\left[e^{-\beta H_0}T_\tau\left(\hat{U}(\beta,0)\hat{C}^{\beta}_{\nu_b}(\tau_b)(\hat{C}^{\dagger})^{\alpha}_{\nu_a}(\tau_a)\right)\right]}{\mathrm{Tr}\left[e^{-\beta H_0}\hat{U}(\beta,0)\right]}=\frac{-\langle T_\tau\left(\hat{U}(\beta,0)\hat{C}^{\beta}_{\nu_b}(\tau_b)(\hat{C}^{\dagger})^{\alpha}_{\nu_a}(\tau_a)\right)\rangle_0}{\langle\hat{U}(\beta,0)\rangle_0}
\end{aligned} \tag{E.9}$$

Where the τ-ordering operator has been reintroduced, and both the numerator and denominator has been devided by $Z_0=\mathrm{Tr}\left[e^{-\beta H_0}\right]$.

E.2 2ND ORDER EXPANSION - DIAGRAMMATICS

To illustrate the calculation in section 3.2 we can expand the numerator of $\mathcal{G}^{\beta\alpha}$ up to second order which gives the terms

$$\begin{aligned}
&\mathcal{G}_0^{\beta\alpha}(\nu_b,\tau_b\,;\,\nu_a,\tau_a)-\frac{1}{2}\int d\tau_1\int d\tau_2\sum_{\substack{\nu_1\nu_1'\lambda_1\\ \nu_2\nu_2'\lambda_2}}g_{\nu_1\nu_1'\lambda_1}g_{\nu_2\nu_2'\lambda_2}\langle T_\tau\left(\hat{\varphi}_{\lambda_1}(\tau_1)\hat{\varphi}_{\lambda_2}(\tau_2)\right)\rangle_0\\
&\times\langle T_\tau\left((\hat{C}^{\dagger})^{\sigma_1}_{\nu_1}(\tau_1)\tau_z^{\sigma_1\sigma_1'}\hat{C}^{\sigma_1'}_{\nu_1'}(\tau_1)(\hat{C}^{\dagger})^{\sigma_2}_{\nu_2}(\tau_2)\tau_z^{\sigma_2\sigma_2'}\hat{C}^{\sigma_2'}_{\nu_2'}(\tau_2)\hat{C}^{\beta}_{\nu_b}(\tau_b)(\hat{C}^{\dagger})^{\alpha}_{\nu_a}(\tau_a)\right)\rangle_0
\end{aligned} \tag{E.10}$$

So the zeroth order term is just the bare Green's function. Looking at the second order term, we use the bosonic Green's function to write it as

$$\frac{1}{2}\int d\tau_1 \int d\tau_2 \sum_{\substack{\nu_1\nu_1'\lambda\\ \nu_2\nu_2'}} g_{\nu_1\nu_1'\lambda} g_{\nu_2\nu_2'\lambda} \mathcal{D}_0(\lambda;\tau_1-\tau_2)$$
$$\times \tau_z^{\sigma_1\sigma_1'}\tau_z^{\sigma_2\sigma_2'}\langle T_\tau\left((\hat{C}^\dagger)^{\sigma_1}_{\nu_1}(\tau_1)\hat{C}^{\sigma_1'}_{\nu_1'}(\tau_1)(\hat{C}^\dagger)^{\sigma_2}_{\nu_2}(\tau_2)\hat{C}^{\sigma_2'}_{\nu_2'}(\tau_2)\hat{C}^{\beta}_{\nu_b}(\tau_b)(\hat{C}^\dagger)^{\alpha}_{\nu_a}(\tau_a)\right)\rangle_0 \tag{E.11}$$

Where the diagonality of the boson Green's function is used, and the dummy variable has been changed ($\lambda_1 \to \lambda$). The trick is now to use Wick's Theorem on the electron average, which can be stated using the concept of *contractions* [20] . Contractions are c-numbers defined by

$$\langle \overbracket{AB} \rangle = \langle T_\tau (AB)\rangle$$
$$\langle \overbracket{A\overbracket{BC}D} \rangle = \langle T_\tau (AC)\rangle\langle T_\tau (BD)\rangle \tag{E.12}$$

And Wick's theorem is

$$\begin{aligned}
&\langle T_\tau (ABCD)\rangle = \langle T_\tau (\text{sum of all possible contractions})\rangle \\
&= \langle T_\tau \left(\overbracket{AB}\overbracket{CD}\right)\rangle + \langle T_\tau \left(\overbracket{A\overbracket{BC}D}\right)\rangle + \langle T_\tau \left(\overbracket{A\overbracket{BC}D}\right)\rangle \\
&= \langle T_\tau (AB)\rangle\langle T_\tau (CD)\rangle \pm \langle T_\tau (AC)\rangle\langle T_\tau (BD)\rangle + \langle T_\tau (AD)\rangle\langle T_\tau (BC)\rangle
\end{aligned} \tag{E.13}$$

Note that for fermionic spinor operators, the minus signs should be accounted for when commuting (we have $\{C^\alpha_a, (C^\dagger)^\beta_b\} = \delta_{ab}\delta^{\alpha\beta}$ with a, b quantum numbers and α, β Nambu indices). This theorem allows us to write the 6-operator average as a sum of products of two operator Green's functions. Since we are calculating to second order in the interaction vertex with one bosonic Green's function $m = 1$, we have then $2 + 4m = 6$ operators in the electron average. Since each contracted pair needs to contain one C and one $C^\dagger$, the number of terms in the numerator for m boson lines will be equal to $(2m+1)!$. So $m = 1 \to 6$ terms and $m = 2 \to 120$ terms. As an example let us look at one of the terms in the numerator of equation (E.11)

$$\begin{aligned}
&\frac{1}{2}\int d\tau_1 \int d\tau_2 \sum_{\substack{\nu_1\nu_1'\lambda\\ \nu_2\nu_2'}} g_{\nu_1\nu_1'\lambda} g_{\nu_2\nu_2'\lambda} \mathcal{D}_0(\lambda;\tau_1-\tau_2)\tau_z^{\sigma_1\sigma_1'}\tau_z^{\sigma_2\sigma_2'} \\
&\times \langle T_\tau \left(\hat{C}^\beta_{\nu_b}(\tau_b)(\hat{C}^\dagger)^{\sigma_2}_{\nu_2}(\tau_2)\right)\rangle_0 \langle T_\tau \left(\hat{C}^{\sigma_2'}_{\nu_2'}(\tau_2)(\hat{C}^\dagger)^{\sigma_1}_{\nu_1}(\tau_1)\right)\rangle_0 \langle T_\tau \left(\hat{C}^{\sigma_1'}_{\nu_1'}(\tau_1)(\hat{C}^\dagger)^{\alpha}_{\nu_a}(\tau_a)\right)\rangle_0 \\
&= -\frac{1}{2}\int d\tau_1 \int d\tau_2 \sum_{\substack{\nu_1\nu_1'\lambda\\ \nu_2\nu_2'}} g_{\nu_1\nu_1'\lambda} g_{\nu_2\nu_2'\lambda} \mathcal{D}_0(\lambda;\tau_1-\tau_2) \\
&\times \mathcal{G}_0^{\beta\sigma_2}(\nu_b,\nu_2;\tau_b-\tau_2)\tau_z^{\sigma_2\sigma_2'}\mathcal{G}_0^{\sigma_2'\sigma_1}(\nu_2',\nu_1;\tau_2-\tau_1)\tau_z^{\sigma_1\sigma_1'}\mathcal{G}_0^{\sigma_1'\alpha}(\nu_1',\nu_a;\tau_1-\tau_a)
\end{aligned} \tag{E.14}$$

Or written out as matrix multiplication in Nambu space

$$-\frac{1}{2}\int d\tau_1 \int d\tau_2 \sum_{\substack{\nu_1\nu_1'\lambda \\ \nu_2\nu_2'}} g_{\nu_1\nu_1'\lambda} g_{\nu_2\nu_2'\lambda} \mathcal{D}_0(\lambda;\tau_1-\tau_2)$$
$$\times \underline{\underline{\mathcal{G}_0}}(\nu_b,\nu_2;\tau_b-\tau_2)\tau_z \underline{\underline{\mathcal{G}_0}}(\nu_2',\nu_1;\tau_2-\tau_1)\tau_z \underline{\underline{\mathcal{G}_0}}(\nu_1',\nu_a;\tau_1-\tau_a) \tag{E.15}$$

The negative sign will be absorbed in the Feynman rules, and the combinatorics of the diagrams will ensure that all the factors become unity, which we will se in a moment. This term is represented diagrammatically as

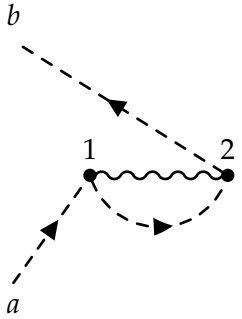

The diagrams we get for the numerator of $\mathcal{G}^{\beta\alpha}(\nu_b,\tau_b\ ;\ \nu_a,\tau_a)$ are (similar to [4])

$$-\langle T_\tau \left(\hat{U}(\beta,0)\hat{C}_{\nu_b\beta}(\tau_b)\hat{C}^\dagger_{\nu_a\alpha}(\tau_a)\right)\rangle_0 =$$

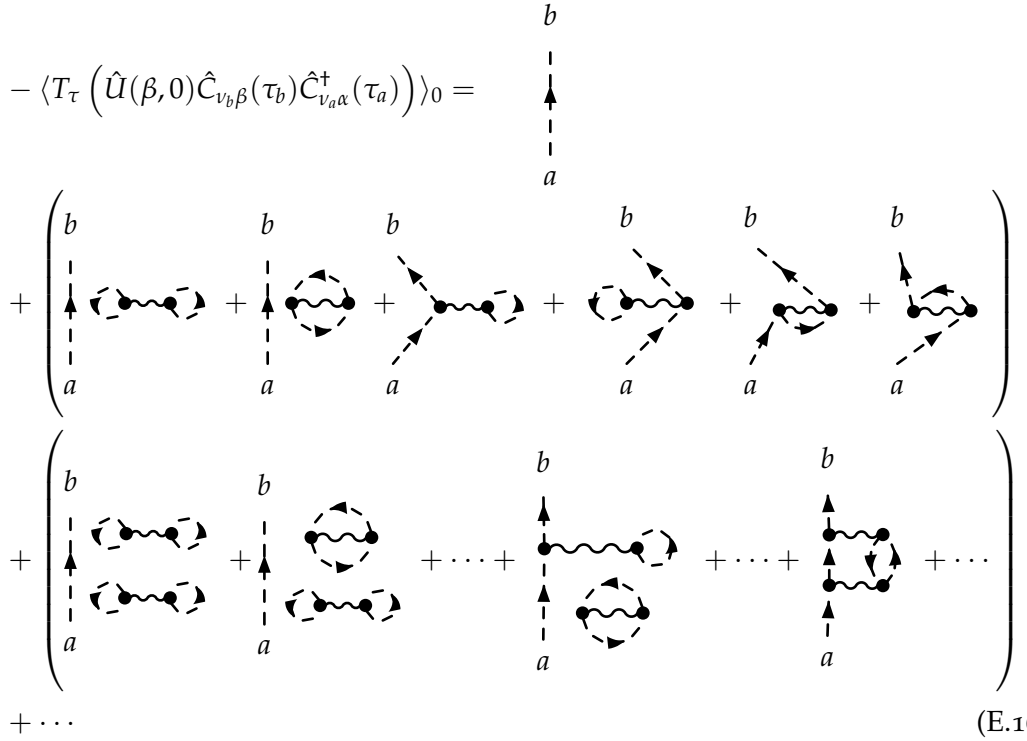

(E.16)

Where we note that the 3rd and 4th of the second order diagrams (in the interactions strength g), are topologically equivalent, which also goes for the 5th and 6th. These diagrams are identical in the sense that a $1 \leftrightarrow 2$ exchange leaves the integrals and summations invariant (e.g τ_1 and τ_2 are dummy variables in the

integrals, and can be exchanged). This takes care of the factor $\frac{1}{2}$ in (E.15), which will happen for all connected diagrams. Meanwhile, the denominator is

$$\langle \hat{U}(\beta,0)\rangle_0 = \Big(1 + \quad + \quad + \cdots\Big) \tag{E.17}$$

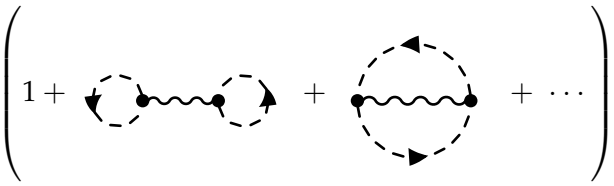

One thing we can do to simplify the expression for $\mathcal{G}^{\beta\alpha}(\nu_b,\tau_b\ ;\ \nu_a,\tau_a)$ is to factorize the numerator into connected diagrams (going from a to b via 1 and 2) and the disconnected, so-called vacuum diagrams like

$$\mathcal{G}^{\beta\alpha}(\nu_b,\tau_b\ ;\ \nu_a,\tau_a) = \frac{\Big(\quad + \quad + \quad + \cdots\Big)\Big(1 + \quad + \quad + \cdots\Big)}{\Big(1 + \quad + \quad + \cdots\Big)} \tag{E.18}$$

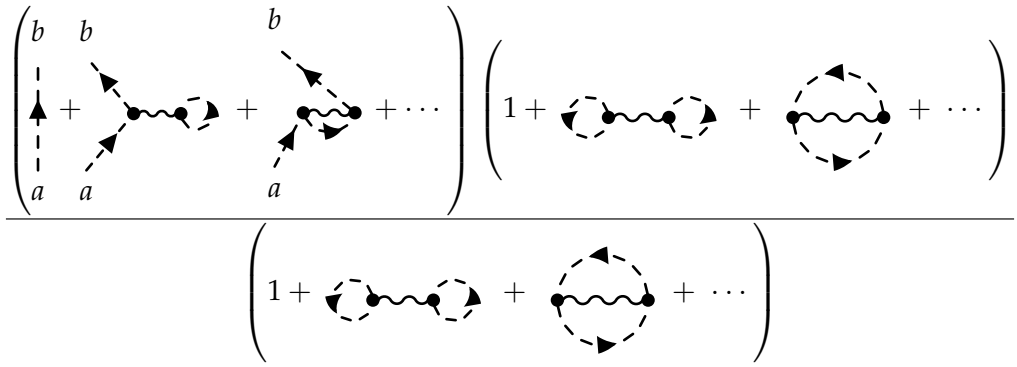

The denominator cancels the terms in the 2nd parenthesis in the numerator, leaving only the connected diagrams

$$\mathcal{G}^{\beta\alpha}(\nu_b,\tau_b\ ;\ \nu_a,\tau_a) = \Big(\quad + \quad + \quad + \quad + \cdots\Big) \tag{E.19}$$

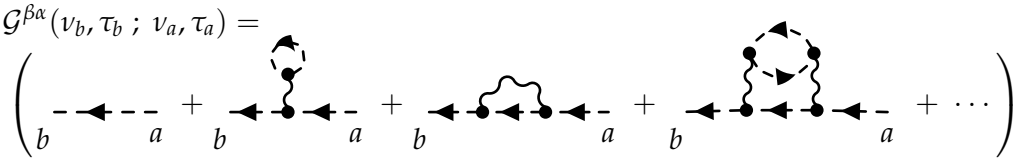

E.3 SELF-ENERGY EXAMPLES AND MATSUBARA FREQUENCY TRANSFORMATION

With the interaction in (3.18), the diagram in (3.16) (called $\underline{\underline{\mathcal{G}_H}}$ for the Hartree contribution to $\underline{\underline{\mathcal{G}}}$) would, using Nambu matrices, become

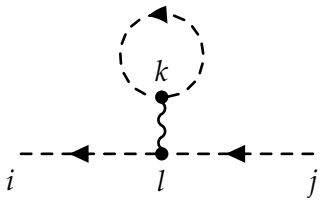

$$= \underline{\underline{\mathcal{G}_{\mathrm{H}}}}(i,j;\tau_i-\tau_j) =$$

$$\int d\tau_l \int d\tau_k \sum_{lkm} g_l g_k |V_m|^2 \mathcal{D}_0(m;\tau_k-\tau_l)\underline{\underline{\mathcal{G}_0}}(i,l;\tau_i-\tau_l)\tau_z\underline{\underline{\mathcal{G}_0}}(l,j;\tau_l-\tau_j)\mathrm{Tr}\left[\tau_z\underline{\underline{\mathcal{G}_0}}(k,k;0)\right]$$

Or by tranforming the Green's functions to Matsubara frequency

$$\begin{aligned}
&= \int d\tau_l \int d\tau_k \sum_{\substack{lkm\\ iq_n ik_n\\ ip_n is_n}} \frac{g_l g_k}{\beta^4} |V_m|^2 \mathcal{D}_0(m;iq_n)\underline{\underline{\mathcal{G}_0}}(i,l;ik_n)\tau_z\underline{\underline{\mathcal{G}_0}}(l,j;ip_n)\mathrm{Tr}\left[\tau_z\underline{\underline{\mathcal{G}_0}}(k,k;is_n)\right] \\
&\quad \times e^{-iq_n(\tau_k-\tau_l)} e^{-ik_n(\tau_i-\tau_l)} e^{-ip_n\left(\tau_l-\tau_j\right)} \\
&= \int d\tau_l \int d\tau_k \sum_{\substack{lkm\\ iq_n ik_n\\ ip_n is_n}} \frac{g_l g_k}{\beta^4} |V_m|^2 \mathcal{D}_0(m;iq_n)\underline{\underline{\mathcal{G}_0}}(i,l;ik_n)\tau_z\underline{\underline{\mathcal{G}_0}}(l,j;ip_n)\mathrm{Tr}\left[\tau_z\underline{\underline{\mathcal{G}_0}}(k,k;is_n)\right] \\
&\quad \times e^{-iq_n\tau_k} e^{-(ip_n-ik_n-iq_n)\tau_l} e^{-ik_n\tau_i} e^{ip_n\tau_j}
\end{aligned} \tag{E.20}$$

Now, the integral over τ_l and τ_k of the exponential functions become Kronecker delta functions

$$\begin{aligned}
&= \sum_{\substack{lkm\\ iq_n ik_n\\ ip_n is_n}} \frac{g_l g_k}{\beta^2} |V_m|^2 \mathcal{D}_0(m;iq_n)\underline{\underline{\mathcal{G}_0}}(i,l;ik_n)\tau_z\underline{\underline{\mathcal{G}_0}}(l,j;ip_n) \\
&\quad \times \mathrm{Tr}\left[\tau_z\underline{\underline{\mathcal{G}_0}}(k,k;is_n)\right] e^{-ik_n\tau_i} e^{ip_n\tau_j} \delta_{iq_n,0}\delta_{ip_n-ik_n-iq_n,0} \\
&= \frac{1}{\beta}\sum_{ik_n} \underbrace{\left[\sum_{\substack{lkm\\ is_n}} \frac{g_l g_k}{\beta} |V_m|^2 \mathcal{D}_0(m;0)\underline{\underline{\mathcal{G}_0}}(i,l;ik_n)\tau_z\underline{\underline{\mathcal{G}_0}}(l,j;ik_n)\mathrm{Tr}\left[\tau_z\underline{\underline{\mathcal{G}_0}}(k,k;is_n)\right]\right]}_{\underline{\underline{\mathcal{G}_{\mathrm{H}}}}(i,j;ik_n)} e^{-ik_n(\tau_i-\tau_j)}
\end{aligned} \tag{E.21}$$

We can also calculate the diagram (called $\underline{\underline{\mathcal{G}_F}}$ for the Fock contribution to $\underline{\underline{\mathcal{G}}}$)

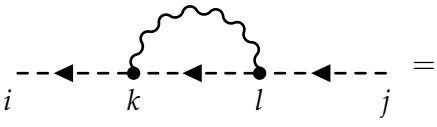

$$= \underline{\underline{\mathcal{G}_{\mathrm{F}}}}(i,j;\tau_i-\tau_j) = -\int d\tau_l \int d\tau_k \sum_{lkm} g_l g_k |V_m|^2$$

$$\times \mathcal{D}_0(m;\tau_k-\tau_l)\underline{\underline{\mathcal{G}_0}}(i,k;\tau_i-\tau_k)\tau_z\underline{\underline{\mathcal{G}_0}}(k,l;\tau_k-\tau_l)\tau_z\underline{\underline{\mathcal{G}_0}}(l,j;\tau_l-\tau_j) \tag{E.22}$$

Similarly, the Green's functions can be transformed to Matsubara frequency

$$\underline{\underline{\mathcal{G}_{\mathrm{F}}}}(i,j;\tau_i-\tau_j) = \frac{1}{\beta}\sum_{ik_n} e^{-ik_n(\tau_i-\tau_j)} \times \underbrace{\left[-\sum_{\substack{lkm\\ iq_n}} \frac{g_l g_k}{\beta}|V_m|^2 \mathcal{D}_0(m;iq_n)\underline{\underline{\mathcal{G}_0}}(i,k;ik_n)\tau_z\underline{\underline{\mathcal{G}_0}}(k,l;ik_n-iq_n)\tau_z\underline{\underline{\mathcal{G}_0}}(l,j;ik_n)\right]}_{\underline{\underline{\mathcal{G}_{\mathrm{F}}}}(i,j;ik_n)}$$

These two diagrams can be written in terms of *self energies* $\underline{\underline{\Sigma}}$

$$\begin{aligned}\underline{\underline{\mathcal{G}^{\mathrm{H}}}}(i,j;ik_n) &= \sum_{\substack{lkm\\ is_n}} \frac{g_l g_k}{\beta}|V_m|^2\mathcal{D}_0(m;0)\underline{\underline{\mathcal{G}_0}}(i,l;ik_n)\tau_z\underline{\underline{\mathcal{G}_0}}(l,j;ik_n)\mathrm{Tr}\left[\tau_z\underline{\underline{\mathcal{G}_0}}(k,k;is_n)\right]\\ &= \sum_l \underline{\underline{\mathcal{G}_0}}(i,l;ik_n)\underline{\underline{\Sigma_H}}(l,l;ik_n)\underline{\underline{\mathcal{G}_0}}(l,j;ik_n)\end{aligned} \tag{E.23}$$

Where

$\underline{\underline{\Sigma_H}}(l,l;ik_n) =$ 

$= \sum_{km,is_n} \frac{g_l g_k}{\beta}|V_m|^2\mathcal{D}_0(m;0)\mathrm{Tr}\left[\tau_z\underline{\underline{\mathcal{G}_0}}(k,k;is_n)\right]$

And for the Fock term

$$\begin{aligned}\underline{\underline{\mathcal{G}_{\mathrm{F}}}}(i,j;ik_n) &= -\sum_{\substack{lkm\\ iq_n}} \frac{g_l g_k}{\beta}|V_m|^2\mathcal{D}_0(m;iq_n)\underline{\underline{\mathcal{G}_0}}(i,k;ik_n)\tau_z\underline{\underline{\mathcal{G}_0}}(k,l;ik_n-iq_n)\tau_z\underline{\underline{\mathcal{G}_0}}(l,j;ik_n)\\ &= \sum_{lk}\underline{\underline{\mathcal{G}_0}}(i,k;ik_n)\underline{\underline{\Sigma_F}}(k,l;ik_n)\underline{\underline{\mathcal{G}_0}}(l,j;ik_n)\end{aligned} \tag{E.24}$$

With

$\underline{\underline{\Sigma_F}}(k,l;ik_n) =$ 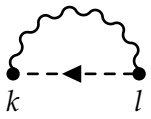

$= -\sum_{m,iq_n} \frac{g_l g_k}{\beta}|V_m|^2\mathcal{D}_0(m;iq_n)\tau_z\underline{\underline{\mathcal{G}_0}}(k,l;ik_n-iq_n)\tau_z$

(E.25)

E.4 NAMBU-GORKOV DIAGRAMS FOR ELECTRON-BOSON INTERACTION

The second order expansion in E.2, contains the following diagrams if one does not collect everything in Nambu formalism

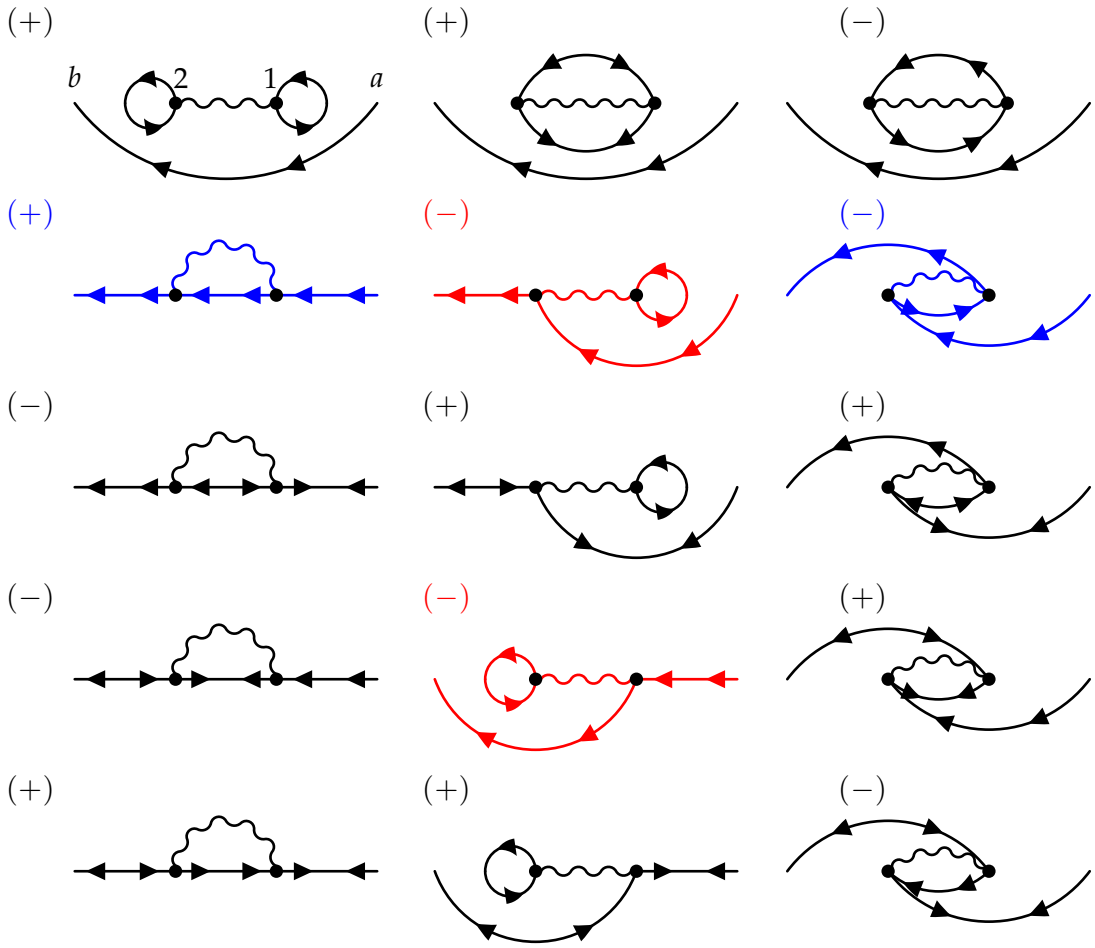

Where I have noted the signs required for the diagram rules. Since we are calculating the second order term for the *ee* Green's function, we always have to start and end with an electron operator. Looking from right to left, these are the ones pointing along this direction, so the first and last arrow has to point to the left. In between these, we can have vertices where we have a hole part, i.e. arrows go the other way from left to right. Every time we swap two operators for holes, for example comparing diagram 4 to 7: $\mathcal{G}^{ee}\mathcal{G}^{ee}\mathcal{G}^{ee} \to -\mathcal{G}^{ee}\mathcal{G}^{eh}\mathcal{G}^{he}$, we pick up a minus sign. This minus sign is the one absorbed into the hole component of the vertex Nambu matrix. The two diagrams in blue are topologically equivalent, and if we exchange the dummy variables in the integration over imaginary time $\tau_1 \leftrightarrow \tau_2$ and exchange two fermionic operators in the expression for the diagram on the right, the sign changes and it becomes the same expression as the diagram on the left. This gives a factor 2 thereby cancelling the factor $\frac{1}{2}$ we had in the numerator. This happens for the red diagrams as well, since one of them can be changed into the other by exchanging dummy variables, so we just count the diagram twice. The only

terms that have no partner to be combined with, and thus do not cancel the factors in front, is the disconnected diagrams, so for now, these factors will be contained in the diagrams.

F

CALCULATION OF INTEGRALS IN THE FOCK SELF-ENERGY

Let us calculate the last term in (3.56)

$$F_1(\epsilon)\,\mathcal{P}\int_0^\infty d\omega_b\,\frac{1}{\left(\omega_b^2+\omega_0^2\right)(\epsilon-\omega_b)} \tag{F.1}$$

The indefinite integral of this is

$$I=\int d\omega_b\,\frac{1}{\left(\omega_b^2+\omega_0^2\right)(\epsilon-\omega_b)} \tag{F.2}$$

First we would like to expand this using the partial fraction method

$$I=\int d\omega_b\,\frac{1}{\left(\omega_b^2+\omega_0^2\right)(\epsilon-\omega_b)}=\int d\omega_b\,\frac{x}{\omega_b^2+\omega_0^2}+\int d\omega_b\,\frac{y}{\epsilon-\omega_b} \tag{F.3}$$

Plus the condition that $x\,(\epsilon-\omega_b)+y\left(\omega_b^2+\omega_0^2\right)=1$, which is solved by $x=\frac{\epsilon+\omega_b}{\epsilon^2+\omega_0^2}$ and $y=\frac{1}{\epsilon^2+\omega_0^2}$ resulting in

$$\begin{aligned}
I&=\frac{1}{\epsilon^2+\omega_0^2}\left(\int d\omega_b\,\frac{\epsilon+\omega_b}{\omega_b^2+\omega_0^2}+\int d\omega_b\,\frac{1}{\epsilon-\omega_b}\right)\\
&=\frac{1}{\epsilon^2+\omega_0^2}\left(\int d\omega_b\,\frac{\epsilon}{\omega_b^2+\omega_0^2}+\int d\omega_b\,\frac{\omega_b}{\omega_b^2+\omega_0^2}+\int d\omega_b\,\frac{1}{\epsilon-\omega_b}\right)\\
&=\frac{1}{\epsilon^2+\omega_0^2}\left(\frac{\epsilon}{\omega_0^2}\int d\omega_b\,\frac{1}{\frac{\omega_b^2}{\omega_0^2}+1}+\int d\omega_b\,\frac{\omega_b}{\omega_b^2+\omega_0^2}+\int d\omega_b\,\frac{1}{\epsilon-\omega_b}\right)
\end{aligned} \tag{F.4}$$

Now we can solve them all by substitution. We define $s=\frac{\omega_b}{\omega_0}$, $u=\omega_b^2+\omega_0^2$ and $t=\omega_b-\epsilon$ which means $ds=\frac{1}{\omega_0}d\omega_b$, $du=2\omega_b\,d\omega_b$ and $dt=d\omega_b$ so that I becomes

$$\begin{aligned}
I&=\frac{1}{\epsilon^2+\omega_0^2}\left(\frac{\epsilon}{\omega_0}\int ds\,\frac{1}{s^2+1}+\frac{1}{2}\int du\,\frac{1}{u}-\int dt\,\frac{1}{t}\right)\\
&=\frac{1}{\epsilon^2+\omega_0^2}\left(\frac{\epsilon}{\omega_0}\arctan s+\frac{1}{2}\ln u-\ln t\right)+c\\
&=\frac{1}{\epsilon^2+\omega_0^2}\left(\frac{\epsilon}{\omega_0}\arctan\left(\frac{\omega_b}{\omega_0}\right)+\frac{1}{2}\ln\left(\omega_b^2+\omega_0^2\right)-\ln\left(\omega_b-\epsilon\right)\right)+c
\end{aligned} \tag{F.5}$$

So by simplifying a bit

$$I=\frac{1}{2\omega_0\epsilon^2+2\omega_0^3}\left(2\epsilon\ \arctan\left(\frac{\omega_b}{\omega_0}\right)+\omega_0\ln\left(\omega_b^2+\omega_0^2\right)-2\omega_0\ln\left(\omega_b-\epsilon\right)\right)+c \tag{F.6}$$

The definite integral can then be found using the definition of a principal value integral (3.54)

$$F_1(\epsilon)\ \mathcal{P}\int_0^\infty d\omega_b\ \frac{1}{(\omega_b^2+\omega_0^2)\,(\epsilon-\omega_b)} = F_1(\epsilon)\lim_{\Lambda\to\infty}\lim_{\delta\to 0}\left(I|_0^{\epsilon-\delta} + I|_{\epsilon+\delta}^{\Lambda}\right) \tag{F.7}$$

Where the cut-off Λ is introduced and subsequently sent to infinity. We insert the expression for I

$$\begin{aligned}\left[\frac{F_1(\epsilon)}{2\omega_0\epsilon^2+2\omega_0^3}\right]\lim_{\Lambda\to\infty}\lim_{\delta\to 0}(&2\epsilon\ \arctan\left(\frac{\epsilon-\delta}{\omega_0}\right)+\omega_0\ln\left((\epsilon-\delta)^2+\omega_0^2\right)-2\omega_0\ln\left(-\delta\right)\\ &-2\epsilon\ \arctan\left(\frac{0}{\omega_0}\right)-\omega_0\ln\left(\omega_0^2\right)+2\omega_0\ln\left(-\epsilon\right)\\ &2\epsilon\ \arctan\left(\frac{\Lambda}{\omega_0}\right)+\omega_0\ln\left(\Lambda^2+\omega_0^2\right)-2\omega_0\ln\left(\Lambda-\epsilon\right)\\ &-2\epsilon\ \arctan\left(\frac{\epsilon+\delta}{\omega_0}\right)-\omega_0\ln\left((\epsilon+\delta)^2+\omega_0^2\right)+2\omega_0\ln\left(\delta\right))\end{aligned} \tag{F.8}$$

This has to be simplified before it is safe to take the limits, so we collect terms

$$\begin{aligned}\left[\frac{F_1(\epsilon)}{2\omega_0\epsilon^2+2\omega_0^3}\right]\lim_{\Lambda\to\infty}\lim_{\delta\to 0}(&2\epsilon\left[\arctan\left(\frac{\epsilon-\delta}{\omega_0}\right)-\arctan\left(\frac{\epsilon+\delta}{\omega_0}\right)+\arctan\left(\frac{\Lambda}{\omega_0}\right)\right]\\ &+\omega_0\left[\ln\left((\epsilon-\delta)^2+\omega_0^2\right)-\ln\left((\epsilon+\delta)^2+\omega_0^2\right)+\ln\left(\Lambda^2+\omega_0^2\right)-\ln\left(\omega_0^2\right)\right]\\ &+2\omega_0\left[\ln\left(-\epsilon\right)-\ln\left(-\delta\right)+\ln\left(\delta\right)-\ln\left(\Lambda-\epsilon\right)\right])\end{aligned} \tag{F.9}$$

The last term can be rewritten as

$$\begin{aligned}2\omega_0\left[\ln\left(-\epsilon\right)-\ln\left(-\delta\right)+\ln\left(\delta\right)\right)-\ln\left(\Lambda-\epsilon\right)] &= 2\omega_0\left[\ln\left(\frac{\epsilon}{\delta}\right)+\ln\left(\frac{\delta}{\Lambda-\epsilon}\right)\right]\\ &= 2\omega_0\ln\left(\frac{\epsilon}{\Lambda-\epsilon}\right)\end{aligned} \tag{F.10}$$

Now it is okay to take the $\delta\to 0$ limit, and (F.9) then becomes

$$\begin{aligned}&\left[\frac{F_1(\epsilon)}{2\omega_0\epsilon^2+2\omega_0^3}\right]\lim_{\Lambda\to\infty}(2\epsilon\ \arctan\left(\frac{\Lambda}{\omega_0}\right)\\ &\quad+\omega_0\left[\ln\left(\Lambda^2+\omega_0^2\right)-\ln\left(\omega_0^2\right)\right]+2\omega_0\ln\left(\frac{\epsilon}{\Lambda-\epsilon}\right))\\ &=\left[\frac{F_1(\epsilon)}{2\omega_0\epsilon^2+2\omega_0^3}\right]\lim_{\Lambda\to\infty}(2\epsilon\ \arctan\left(\frac{\Lambda}{\omega_0}\right)+\omega_0\ln\left(\frac{\left[\Lambda^2+\omega_0^2\right]\epsilon^2}{\omega_0^2\left[\Lambda-\epsilon\right]^2}\right))\end{aligned} \tag{F.11}$$

Now we can perform the limit $\Lambda\to\infty$ and use that

$$\lim_{\Lambda\to\infty}\arctan\left(\frac{\Lambda}{\omega_0}\right)=\frac{\pi}{2} \tag{F.12}$$

And

$$\lim_{\Lambda\to\infty} \ln\left(\frac{\left[\Lambda^2+\omega_0^2\right]\epsilon^2}{\omega_0^2\left[\Lambda-\epsilon\right]^2}\right) = \lim_{x\to 0} \ln\left(\frac{\left[\frac{1}{x^2}+\omega_0^2\right]\epsilon^2}{\omega_0^2\left[\frac{1}{x}-\epsilon\right]^2}\right)$$
$$= \lim_{x\to 0} \ln\left(\frac{\left[1+x^2\omega_0^2\right]\epsilon^2}{\omega_0^2\left[1-x\epsilon\right]^2}\right) = \ln\left(\frac{\epsilon^2}{\omega_0^2}\right) \tag{F.13}$$

Finally, we get

$$F_1(\epsilon)\,\mathcal{P}\int_0^\infty d\omega_b\,\frac{1}{\left(\omega_b^2+\omega_0^2\right)\left(\epsilon-\omega_b\right)} = \left[\frac{F_1(\epsilon)}{2\omega_0\epsilon^2+2\omega_0^3}\right]\left(\pi\epsilon+\omega_0\ln\left(\frac{\epsilon^2}{\omega_0^2}\right)\right) \tag{F.14}$$

We can now collect (3.53), (3.56) and (F.14) so that

$$I_1 = -i\pi\alpha\,\frac{F_1(\epsilon)}{\epsilon^2+\omega_0^2} + \alpha\left[\frac{F_1(\epsilon)}{2\omega_0\epsilon^2+2\omega_0^3}\right]\left(\pi\epsilon+\omega_0\ln\left(\frac{\epsilon^2}{\omega_0^2}\right)\right) + \alpha\sigma_1 \tag{F.15}$$

G

3 SITE MANY-BODY HAMILTONIAN

Here we will see what physics this many-body Hamiltonian describes. Imagine a chain comprising of three sites 1, 2, and 3. The states are denoted in the occupation number basis as $|n_1 n_2 n_3\rangle$, where $n_1, n_2, n_3 = 0 \vee 1$, since we consider fermionic particles. For this small wire, the Hamiltonian, which is an operator in the $2^3 = 8$ dimensional Hilbert space, becomes

$$\begin{aligned} H_{N=3} = &- \mu(c_1^\dagger c_1 + c_2^\dagger c_2 + c_3^\dagger c_3) - \frac{t}{2}(c_1^\dagger c_2 + c_2^\dagger c_1 + c_2^\dagger c_3 + c_3^\dagger c_2) \\ &+ \frac{\Delta}{2}(c_1 c_2 + c_2^\dagger c_1^\dagger + c_2 c_3 + c_3^\dagger c_2^\dagger) + W(c_1^\dagger c_2^\dagger c_2 c_1 + c_2^\dagger c_3^\dagger c_3 c_2) \end{aligned} \tag{G.1}$$

We can interpret the different terms, by considering the following matrix elements

$$\begin{aligned} &\langle 100|H_{N=3}|100\rangle = -\mu \Rightarrow \text{E of having one site occupied (Chemical potential)} \\ &\langle 100|H_{N=3}|010\rangle = -\frac{t}{2} \Rightarrow \text{E of hopping between sites (Kinetic)} \\ &\langle 110|H_{N=3}|000\rangle = -\frac{\Delta}{2} \Rightarrow \text{E of creating (destroying) a cooper pair (Pairing)} \\ &\langle 110|H_{N=3}|110\rangle = W - 2\mu \Rightarrow \text{E of occupying two adjacent sites (Int. + Chem.)} \end{aligned} \tag{G.2}$$

Written in the basis $\{|000\rangle, |100\rangle, |010\rangle, |001\rangle, |110\rangle, |101\rangle, |011\rangle, |111\rangle\}$, $H_{N=3}$ is represented by the matrix

$$H_{N=3} = \begin{pmatrix} 0 & 0 & 0 & 0 & -\frac{\Delta}{2} & 0 & -\frac{\Delta}{2} & 0 \\ 0 & -\mu & -\frac{t}{2} & 0 & 0 & 0 & 0 & -\frac{\Delta}{2} \\ 0 & -\frac{t}{2} & -\mu & -\frac{t}{2} & 0 & 0 & 0 & 0 \\ 0 & 0 & -\frac{t}{2} & -\mu & 0 & 0 & 0 & -\frac{\Delta}{2} \\ -\frac{\Delta}{2} & 0 & 0 & 0 & W - 2\mu & -\frac{t}{2} & 0 & 0 \\ 0 & 0 & 0 & 0 & -\frac{t}{2} & -2\mu & -\frac{t}{2} & 0 \\ -\frac{\Delta}{2} & 0 & 0 & 0 & 0 & -\frac{t}{2} & W - 2\mu & 0 \\ 0 & -\frac{\Delta}{2} & 0 & -\frac{\Delta}{2} & 0 & 0 & 0 & 2W - 3\mu \end{pmatrix} \tag{G.3}$$

Transforming the basis to one which separates even and odd parity states is done by a transformation matrix U

$$U^\dagger \begin{pmatrix} 000 \\ 100 \\ 010 \\ 001 \\ 110 \\ 101 \\ 011 \\ 111 \end{pmatrix} = \begin{pmatrix} 000 \\ 110 \\ 101 \\ 011 \\ 100 \\ 010 \\ 001 \\ 111 \end{pmatrix} \tag{G.4}$$

In this new basis, the Hamiltonian becomes

$$\tilde{H}_{N=3} = U^\dagger H_{N=3} U = \begin{pmatrix} 0 & -\frac{\Delta}{2} & 0 & -\frac{\Delta}{2} & 0 & 0 & 0 & 0 \\ -\frac{\Delta}{2} & W-2\mu & -\frac{t}{2} & 0 & 0 & 0 & 0 & 0 \\ 0 & -\frac{t}{2} & -2\mu & -\frac{t}{2} & 0 & 0 & 0 & 0 \\ -\frac{\Delta}{2} & 0 & -\frac{t}{2} & W-2\mu & 0 & 0 & 0 & 0 \\ 0 & 0 & 0 & 0 & -\mu & -\frac{t}{2} & 0 & -\frac{\Delta}{2} \\ 0 & 0 & 0 & 0 & -\frac{t}{2} & -\mu & -\frac{t}{2} & 0 \\ 0 & 0 & 0 & 0 & 0 & -\frac{t}{2} & -\mu & -\frac{\Delta}{2} \\ 0 & 0 & 0 & 0 & -\frac{\Delta}{2} & 0 & -\frac{\Delta}{2} & 2W-3\mu \end{pmatrix} \tag{G.5}$$

Which is block-diagonal, showing that parity is still a conserved quantity. First we check the many-body spectrum, which is found by the eigenvalues to (G.5), in the case $W = 0, \mu = 0, \Delta = t$. As we saw in section 2.1.1, in this limit we can connect Majoranas according to figure 30.

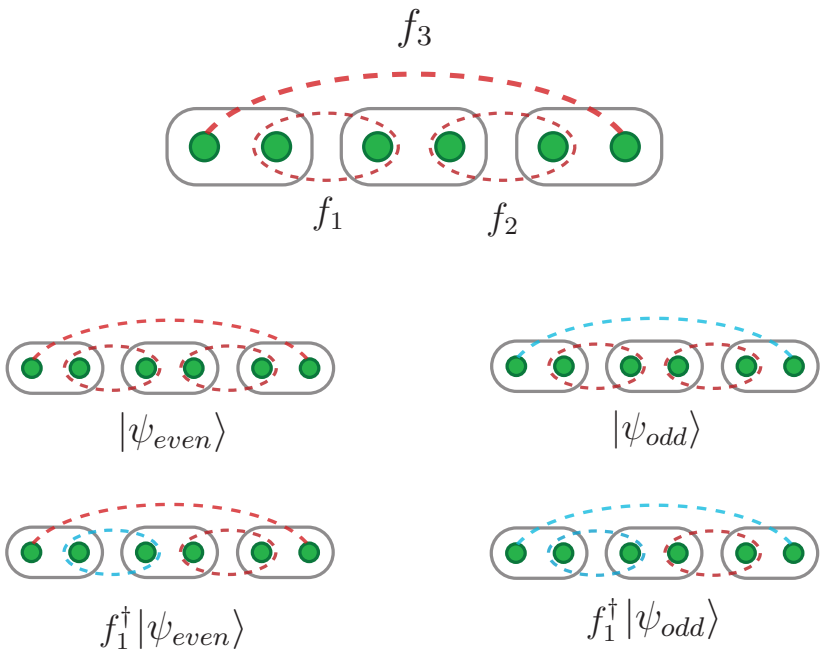

Figure 30: Visual description of some of the different states, where red means unoccupied and blue means occupied. The states are divided into two sectors of even and odd parity, determined by the occupation of the fermion f_3 consisting of the zero energy Majoranas.

The states determined by f_1, f_2, f_3 can be either occupied or unoccupied, giving us our 8 different states. The ground-state is degenerate since f_3 is constructed by zero energy Majoranas, so occupying this state cost no energy. From (2.5) the Hamiltonian in the diagonal basis is

$$H_{N=3} = t(f_1^\dagger f_1 + f_2^\dagger f_2) - t \tag{G.6}$$

So we can conclude there are two states with energy $-t$, four states with energy 0 and two with energy t. This is also what one gets from diagonalizing (G.3). This many-body spectrum is shown in figure 31, with a dashed line separating the even parity sector from the one with odd parity. By adding W this degeneracy is broken for this small chain, since the boundary modes WF overlap. For a long chain the ground states will still be degenerate and of opposite parity if we are in the topological regime seen in figure 18.

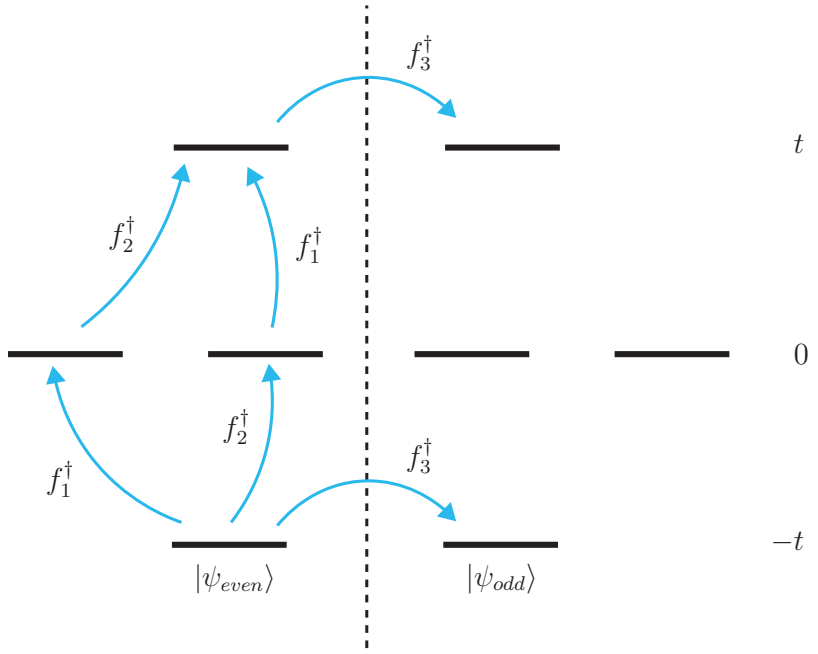

Figure 31: The many-body spectrum corresponding to the 3-site Kitaev chain, at the symmetric point without interactions. There are 8 states divided into an even and an odd parity sector. This degeneracy is due to the presence of the zero energy Majorana modes, and the fermion operator containing these (f_3) transforms between even and odd parity. This spectrum will change when departing from the highly idealised $\mu = W = 0, \Delta = t$ point.

BIBLIOGRAPHY

[1] J. Alicea. New directions in the pursuit of Majorana fermions in solid state systems. *Arxiv preprint arXiv:1202.1293*, 92697:36, 2012. ISSN 1361-6633. doi: 10.1088/0034-4885/75/7/076501. URL http://arxiv.org/abs/1202.1293. (Cited on pages 1 and 105.)

[2] A. Altland and B. Simons. *Condensed Matter Field theory*. Cambridge University Press, 2010. (Cited on page 2.)

[3] S. Blundell. *Magnetism in Condensed Matter*. Oxford University Press, 2001. (Cited on page 1.)

[4] H. Bruus and K. Flensberg. *Many-body Quantum Theory in Condensed Matter Physics*. Oxford Graduate Texts, 2016. (Cited on pages 23, 25, 29, 30, 47, 51, 52, 53, 56, 75, 81, 100, 108, and 110.)

[5] J. C. Budich and E. Ardonne. Equivalent topological invariants for one-dimensional Majorana wires in symmetry class D. *Physical Review B - Condensed Matter and Materials Physics*, 88(7):1–5, 2013. ISSN 10980121. doi: 10.1103/PhysRevB.88.075419. (Cited on page 43.)

[6] J. C. Budich and B. Trauzettel. Z2 Green's function topology of Majorana wires. *New Journal of Physics*, 15, 2013. ISSN 13672630. doi: 10.1088/1367-2630/15/6/065006. (Cited on page 41.)

[7] C. K. Chiu, J. C. Teo, A. P. Schnyder, and S. Ryu. Classification of topological quantum matter with symmetries. *Reviews of Modern Physics*, 88(3):1–63, 2016. ISSN 15390756. doi: 10.1103/RevModPhys.88.035005. (Cited on pages 12 and 13.)

[8] m. F. Dayi, M. Elbistan, and E. Yunt. Effective field theory of a topological insulator and the Foldy-Wouthuysen transformation. *Annals of Physics*, 327 (3):935–951, 2012. ISSN 00034916. doi: 10.1016/j.aop.2011.11.013. URL http://dx.doi.org/10.1016/j.aop.2011.11.013. (Cited on page 40.)

[9] P. Delplace, D. Ullmo, and G. Montambaux. Zak phase and the existence of edge states in graphene. *Physical Review B - Condensed Matter and Materials Physics*, 84(19):1–14, 2011. ISSN 10980121. doi: 10.1103/PhysRevB.84.195452. (Cited on page 43.)

[10] A. M. Essin and V. Gurarie. Bulk-boundary correspondence of topological insulators from their respective Green's functions. *Physical Review B - Condensed Matter and Materials Physics*, 84(12), 2011. ISSN 10980121. doi: 10.1103/PhysRevB.84.125132. (Cited on pages 1, 39, and 41.)

[11] L. Fidkowski and A. Kitaev. Effects of interactions on the topological classification of free fermion systems. *Physical Review B - Condensed Matter and Materials Physics*, 81(13), 2010. ISSN 10980121. doi: 10.1103/PhysRevB.81.134509. (Cited on pages 1, 3, 39, and 86.)

[12] L. Fidkowski and A. Kitaev. Topological phases in one dimension. *Presents*, 83 (7), 2011. ISSN 10980121. doi: 10.1103/PhysRevB.83.075103. (Cited on page 1.)

[13] N. M. Gergs, L. Fritz, and D. Schuricht. Topological order in the Kitaev/Majorana chain in the presence of disorder and interactions. *Physical Review B*, 93(7), 2016. ISSN 24699969. doi: 10.1103/PhysRevB.93.075129. (Cited on page 66.)

[14] M. Greiter, V. Schnells, and R. Thomale. The 1D Ising model and the topological phase of the Kitaev chain. *Annals of Physics*, 351:1026–1033, 2014. ISSN 1096035X. doi: 10.1016/j.aop.2014.08.013. URL http://dx.doi.org/10.1016/j.aop.2014.08.013. (Cited on page 6.)

[15] V. Gurarie. Single-particle Green ' s functions and interacting topological insulators. 085426(January):1–15, 2011. doi: 10.1103/PhysRevB.83.085426. (Cited on pages 1, 23, 33, 34, 38, 39, and 40.)

[16] T. H. Hansson, A. Karlhede, and M. Sato. Topological field theory for p-wave superconductors. *New Journal of Physics*, 14(2):1–6, 2012. ISSN 13672630. doi: 10.1088/1367-2630/14/6/063017. (Cited on page 86.)

[17] M. Z. Hasan and C. L. Kane. Colloquium: Topological insulators. *Reviews of Modern Physics*, 82(4):3045–3067, 2010. ISSN 00346861. doi: 10.1103/RevModPhys.82.3045. (Cited on page 1.)

[18] H. Katsura, D. Schuricht, and M. Takahashi. Exact ground states and topological order in interacting Kitaev/Majorana chains. *Physical Review B - Condensed Matter and Materials Physics*, 92(11):1–13, 2015. ISSN 1550235X. doi: 10.1103/PhysRevB.92.115137. (Cited on pages 3, 63, 64, 69, 71, 72, and 73.)

[19] A. Kitaev. Unpaired Majorana fermions in quantum wires. pages 130–136, 2000. ISSN 1468-4780. doi: 10.1070/1063-7869/44/10S/S29. URL http://arxiv.org/abs/cond-mat/0010440{%}0Ahttp://dx.doi.org/10.1070/1063-7869/44/10S/S29. (Cited on pages 2, 13, 15, and 17.)

[20] T. Lancaster and S. Blundell. *Quantum Field Theory for the gifted amateur*. Oxford Graduate Texts, 2016. (Cited on pages 40 and 109.)

[21] M. Leijnse and K. Flensberg. Introduction to topological superconductivity and Majorana fermions. *Semiconductor Science and Technology*, 27 (12):124003, 2012. ISSN 0268-1242. doi: 10.1088/0268-1242/27/12/124003. URL http://stacks.iop.org/0268-1242/27/i=12/a=124003?key=crossref.24c8187eaf71ff4bca950d5184462df5. (Cited on pages 1, 3, and 4.)

[22] Z. Li and Q. Han. Topological invariants in terms of Green's function for the interacting Kitaev chain. 2:1–5, 2018. (Cited on pages 3, 40, 63, 69, and 71.)

[23] S. R. Manmana, A. M. Essin, R. M. Noack, and V. Gurarie. Topological invariants and interacting one-dimensional fermionic systems. *Physical Review B - Condensed Matter and Materials Physics*, 86(20):1–14, 2012. ISSN 10980121. doi: 10.1103/PhysRevB.86.205119. (Cited on pages 39, 40, 41, and 86.)

[24] J.-J. Miao, H.-K. Jin, F.-C. Zhang, and Y. Zhou. Majorana zero modes and long range edge correlation in interacting Kitaev chains: analytic solutions and density-matrix-renormalization-group study. 2016. URL http://arxiv.org/abs/1608.08382. (Cited on pages 3, 63, and 69.)

[25] J. J. Miao, H. K. Jin, F. C. Zhang, and Y. Zhou. Exact Solution for the Interacting Kitaev Chain at the Symmetric Point. *Physical Review Letters*, 118(26):1–10, 2017. ISSN 10797114. doi: 10.1103/PhysRevLett.118.267701. (Cited on pages 63, 64, and 71.)

[26] X.-L. Qi, T. Hughes, and S.-C. Zhang. Topological Field Theory of Time Reversal Invariant Insulators. *KITP Workshop*, pages 1–25, 2008. doi: doi:10.1103/PhysRevB.78.195424. URL papers3://publication/uuid/724A8768-79DC-486E-A0F7-7071EFD87902. (Cited on pages 40 and 86.)

[27] K. F. Riley and M. P. Hobson. *Essential Mathematical Methods*. Cambridge University Press, 2011. (Cited on pages 42 and 58.)

[28] S. Ryu, A. P. Schnyder, A. Furusaki, and A. W. W. Ludwig. Topological insulators and superconductors: Tenfold way and dimensional hierarchy. *New Journal of Physics*, 12, 2010. ISSN 13672630. doi: 10.1088/1367-2630/12/6/065010. (Cited on pages 1 and 11.)

[29] M. J. Schmidt, D. Rainis, and D. Loss. Decoherence of Majorana qubits by noisy gates. *Physical Review B - Condensed Matter and Materials Physics*, 86(8):1–9, 2012. ISSN 10980121. doi: 10.1103/PhysRevB.86.085414. (Cited on pages 49 and 95.)

[30] R. Shankar. *Quantum Field Theory and Condensed Matter: An introduction*. Cambridge University Press, 2018. (Cited on pages 98 and 102.)

[31] Y. Wang, J.-J. Miao, H.-K. Jin, and S. Chen. Exact solution to an interacting dimerized Kitaev model at the symmetric point. pages 1–7, 2017. URL http://arxiv.org/abs/1707.08430. (Cited on page 70.)

[32] Y. Z. You, Z. Wang, J. Oon, and C. Xu. Topological number and fermion Green's function for strongly interacting topological superconductors. *Physical Review B - Condensed Matter and Materials Physics*, 90(6):1–5, 2014. ISSN 1550235X. doi: 10.1103/PhysRevB.90.060502. (Cited on page 40.)